N72-19876

OCTOBER, 1971

NASA CR-112024

FINAL REPORT

EARTH ORBITING SISYPHUS SYSTEM STUDY

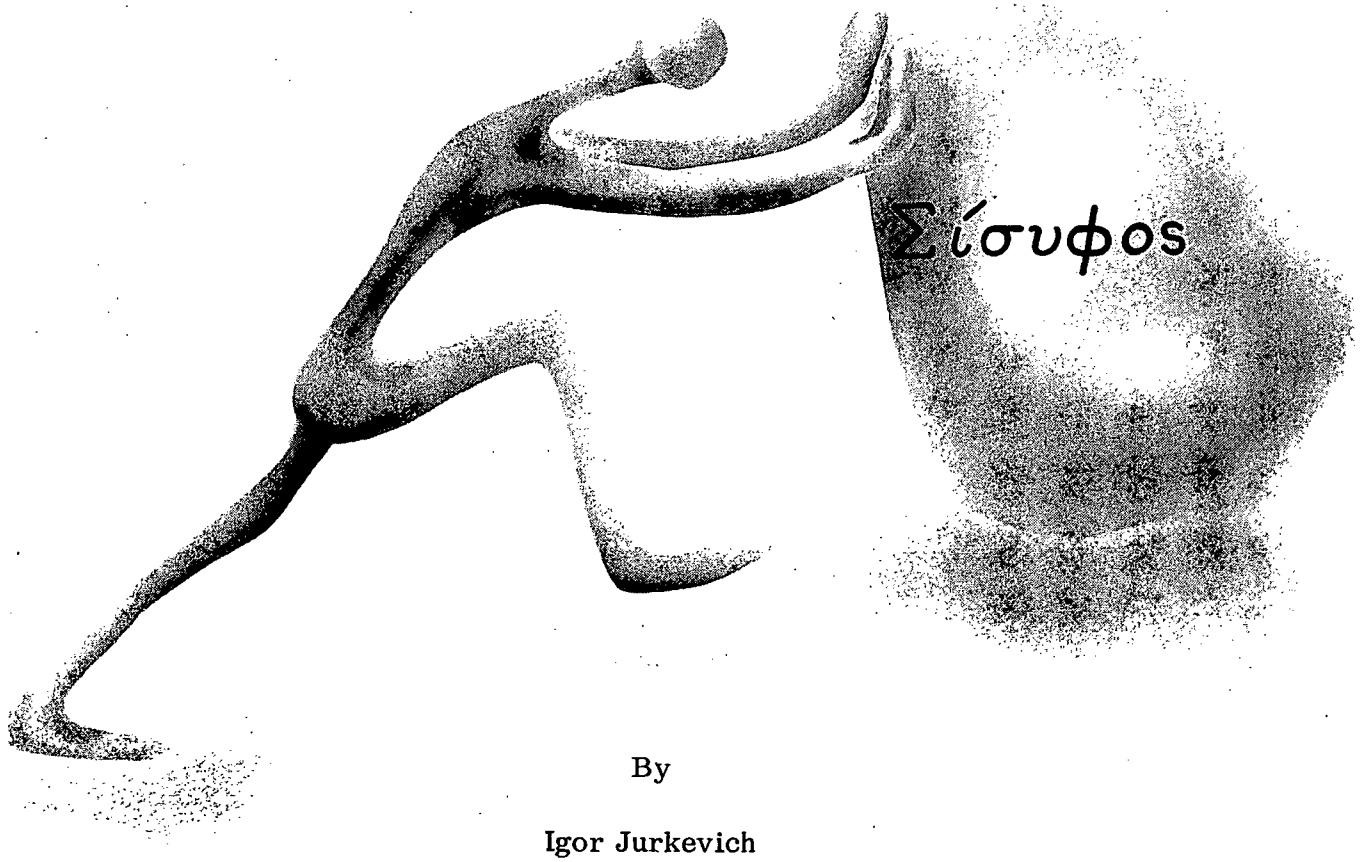

By

Igor Jurkevich
Kurt W. Krause
Sherman L. Neste
Robert K. Soberman

PREPARED UNDER CONTRACT NO. NAS1-10158

NATIONAL AERONAUTICS AND SPACE ADMINISTRATION

SPACE SCIENCES LABORATORY

GENERAL ELECTRIC
SPACE DIVISION

OCTOBER, 1971

NASA CR-112024

EARTH ORBITING SISYPHUS SYSTEM STUDY

By

Igor Jurkevich
Kurt W. Krause
Sherman L. Neste
Robert K. Soberman

Prepared under Contract No. NAS1-10158
GENERAL ELECTRIC COMPANY
Space Sciences Laboratory
Philadelphia, Pennsylvania

for

NATIONAL AERONAUTICS AND SPACE ADMINISTRATION

TABLE OF CONTENTS

TABLE OF CONTENTS (Continued)

ABSTRACT

Accurate knowledge of the near-Earth particulate environment has become extremely significant in view of the present plans to launch large long-life Earth orbiting space facilities. Preliminary estimates indicate that the naturally occuring particulate matter in the immediate vicinity of the Earth has already been exceeded by vehicle effluents and other debris left in space by man's activities. This man-made "space pollution" is generally in sizes too small to be detected from the ground and as yet it is still too sparce to be detected in space by currently available techniques. It is, however, of sufficient size and quantity to pose a hazard to large spacecraft. Assessment of this hazard and the measures to be taken to control and protect against it requires detailed knowledge of "pollution" particulate distribution in mass and velocity and the spatial and temporal variation of these distributions.

The purpose of this study is to establish feasibility of employing an optical meteoroid detecting system, known as Sisyphus, to measure the parameters mentioned above from an Earth orbiting vehicle. In contrast with all conventional meteoroid detectors, a Sisyphus system can discriminate between natural and man-made particles by virtue of the fact that the system measures orbital characteristics of particles.

A Sisyphus system which has been constructed for the Pioneer F/G missions to Jupiter is used as the baseline for the present study. A description of the Pioneer system is given in the present report.

The report contains two major sections. The first of these sections determines the amount of observing time which can be obtained by a Sisyphus instrument launched into various orbits. Observation time is lost when, (a) the Sun is in or near the field of view, (b) the lighted Earth is in or near the field of view, (c) the instrument is eclipsed by the Earth, and (d) the phase angle measured at the particle between the forward scattering direction and the instrument is less than a certain critical value.

Detailed considerations of the above factors show that for a nominal lifetime of one year the most cost effective system is an instrument in an eccentric orbit, whose attitude can be controlled either continuously or stepwise in such a manner that the optical axis points in the antisolar direction. For this case the observing time can exceed 90% of the nominal lifetime. In other less favorable cases it is still easy to achieve observing times greater than 50% of the nominal lifetime. A simpler attitude control system which constrains the optical axis to lie in the orbital plane and precess with it, yields total observing times in the range from 60 to nearly 80% of the nominal lifetime. With no attitude control capability whatever, available observing times are less satisfactory, falling generally to less than 40% of the nominal lifetime.

The second major section of the report is devoted to the selection of the launch system and the instrument platform. Since long observing times are desirable, the most effective operation is achieved with a dedicated, attitude controlled payload package. Examples of such systems are SATS and SOLRAD 10(C) vehicles, both compatible with

the SCOUT launch system. Other possibilities are AVCO Corp. S^4 system and the OWL system, the first of the so-called University Explorer Satellites. Also readily adaptable is the DELTA Payload Experiment Package (PEP). Since the space available on PEP and its operational characteristics are determined by the prime payload, the effectivenesses of a "piggy back" payload such as Sisyphus may be severely impaired.

Estimates of the anticipated event rates are made for the natural background and for the man-made debris. For the latter, the event rate is 0.16/day, for particles sizes in the range from 0.1 to 1.0 cm. For the natural particles the event rate is of the order of 1 per day with the bulk of the particles in the sub millimeter size range.

I. SUMMARY

Since 1967 the General Electric Space Sciences Laboratory has been working on a concept for particle detection and discrimination in space by optical means which has been called Sisyphus. The concept was first proved feasible in laboratory demonstrations under corporate funding. Under contract NAS 9-8104 with the NASA Manned Spacecraft Center, the concept was breadboarded in an approximation of a flight configuration. Using the breadboard and laboratory simulations a number of the problems associated with the flight development of the instrument were worked out. The results of these studies were documented in the final report on that contract (Chandra, et al 1970). In 1970 the Sisyphus experiment was selected to fly on the Pioneer F/G Missions through the asteroid belt to Jupiter. A contract was awarded to the General Electric Space Sciences Laboratory (NAS 2-5609) to fabricate the flight instruments for the Pioneer Missions. Under this contract with the NASA/Ames Research Center a lightweight, low power version of the instrument was developed and fabricated for flight. The hardware for the Pioneer F Mission scheduled for alunch in early 1972 has already been integrated with the spacecraft.

During 1970 the present contract, NAS 1-10158, with the NASA/Langley Research Center was awarded to study the optimum parameters for utilizing a Sisyphus configuration in an Earth orbiting satellite.

The work statement in the contract stated that the possibilities for utilizing Sisyphus in Earth orbit from both a manned workshop and an unmanned SCOUT launch satellite should be investigated. During the early phase of the study there appeared to be a possibility of getting a meteoroid and contaminant particle experiment on a Skylab B Mission. Toward that end an international consortium of investigators was organized and convened at NASA/Headquarters to examine a combined particle experiment using various sensors that could be placed on such a Skylab Mission. Some initial efforts were devoted to such a combination of sensors. With the tightening fiscal constraints and the dimming hope of a Skylab B Mission, the balance of the effort was devoted to the study of utilizing Sisyphus on an unmanned SCOUT launched vehicle. It should be noted, however, that a great deal of the effort reported herein is applicable to either a manned or unmanned earth orbiting vehicle. During the progress of the study it became apparent that the hazard to future space vehicles from "space pollution" exceeds that due to the natural meteoroid environment. This problem was treated in some detail.

On the basis of NASA Meteoroid Environment Model of 1969 one can estimate that a shell about the Earth of 3000 kilometer thickness contains at any time about 5 kilograms of natural meteoroid material. The larger bodies left in this space by man's activities are continuously tracked by the US Air Defense Command and are catalogued in the Space Defense Center Satellite Catalogue and Space Objects Identification Catalogue. Examination of these data indicates that the amount of man-made debris in the shell mentioned previously already far exceeds it's natural meteoroid content. If man-made material is assumed to be uniformly dispersed through the shell, a vehicle having a cross sectional area of 100 m^2 would experience, on average, two encounters per year

with particles having a mass of 1×10^{-2} gr or greater. At the present time these estimates are quite uncertain, but it is clear that the hazard due to "space pollution" is increasing with time, as more and more objects are orbited.

Currently, the Sisyphus instrument is the only known means for measuring space pollutants in the size range from sub-millimeter to multi-centimeter particles. Not only can they be detected by the instrument in concentrations far below those which would present a hazard to an orbiting spacecraft, but they can be distinguished from natural meteoroids by their orbits which in turn will also identify the polluting source. Using the limited available data and extrapolating to particle sizes which are undetectable by ground based radar, it was established that a Sisyphus instrument similar to the version that will be flown on the Pioneer F spacecraft would measure approximately one particle per week in the size range from one millimeter to one centimeter. For comparison purposes, the same instrument could expect to measure one natural meteoroid every three years in that same size range. It must be borne in mind that for meteoroids, the event rate increases rapidly with decreasing particle size. The total meteoroid event rate that could be anticipated would be approximately one per day.

Most present models of the near-Earth meteoroid environment are based on impact data obtained from satellites and on ground-based observations of meteors entering the earth's atmosphere. The masses of the meteoroids responsible for the impacts detected by the satellites must be estimated from empirical equations using assumed average velocities. The empirical equations relate the penetrated target thickness with the particle velocity, mass, density and shape. Data is obtained from laboratory experiments with simulated meteoroids. However, many of the meteoroid properties cannot be simulated in the laboratory (e.g. low density hypervelocity particles).

The ground-based meteor data consists of counts of the meteors detectable in the Earth's atmosphere and of measurements of the meteoroid entry velocity and deceleration. The masses of the meteoroids responsible for each observed meteor must be estimated from the brightness and ionization of the meteor. Here too, large uncertainties remain in the derived masses due to quantities which cannot be determined (e.g. the shape of the meteoroid). The two sets of data cover widely separated mass regions. Consequently, it is highly desirable to perform an experiment which can observe meteoroids over an extremely large mass range and thus attempt to provide a common tie for all meteoroid data. The Sisyphus experiment would yield statistically significant data for meteoroids with mass from 10^{-8} gm (similar to those measured by the Pegasus satellites) to 10^{-4} gm (similar to those measured by ground-based meteor radar detectors).

Section V of the report is concerned with the description of basic principles of the Sisyphus system and of their implementation for the Pioneer F/G missions. The major problem to which the instrument addresses itself is the measurement of the position and velocity of the detected particle with respect to an instrumental frame of reference. It is shown that the desired quantities can be deduced from measurements of entrance and exit times of illuminated particles into the crossed fields of view of several independent telescopes. Such a system is based in effect on a modification of the parallax

method of distance measurement. For a system consisting of three optical systems the parameters of interest are related to instrument characteristics via fifteen equations in fifteen unknowns. Although cumbersome, the solution of these equations is a straightforward computational problem. A transformation of the measured quantities from the instrument centered frame of reference to a geocentric or heliocentric one permits one to compute the orbital properties of the detected particles. In addition to orbital quantities, a Sisyphus instrument provides the particle counting rate and, subject to the assumption of its reflectivity an estimate of its size.

A brief description of the hardware implementation of these concepts for the Pioneer F/G missions is given. Since the weight, dimensions, power consumption and telemetry and communication requirements are essentially compatible with several small existing vehicles, the Pioneer version of the instrument has been taken as the basis for the present study.

Needless to say, certain operational aspects of this instrument are dictated by the interplanetary nature of the Pioneer mission. This is particularly true of the manner in which the calibration against known stars is achieved and the method by which false signals due to the interfering background are suppressed. The manner of handling these problems on an Earth orbiting mission need not be the same. However, similar problems will exist and, therefore, a description of the threshold estimation for the Pioneer instrument is given in Appendix IV. A computer code has been constructed to evaluate the threshold against the background sky brightness.

Section VI, the major section of the work, is concerned with the computation of the effective observing time achievable in an Earth's orbit. The nature of expected signals is such that to obtain meaningful observational material, long observation times are needed. Various interfering effects conspire to limit times available for observation. Aside from typical instrumental effects which determine the achievable signal to noise ratio, a Sisyphus fails to yield usable data under conditions such that, (a) the Sun is in or near the field of view, (b) the lighted Earth is in or near the field of view, (c) the instrument is in the Earth's shadow, (d) excessive sunlight is scattered by instrument surroundings into the field of view and (e) the illumination phase angle, measured between the forward scattering direction and the instrument, at the particle is less than approximately 90 degrees. A computer code was constructed to evaluate the influence of these factors. In its basic form, the code is concerned with a spin stabilized instrument. However, a straightforward modification permits one to study changes in the effective observing times when the attitude of the optical axis can be controlled according to simple laws.

The resulting computer program, described in this report in considerable detail, was then used to examine the available observing times for a number of typical orbits. All orbits considered are compatible with the payload capability of the SCOUT launch system. For all orbits the nominal lifetime was fixed at 1 year.

Computations show that for circular orbits having inclinations in the vicinity of the so-called critical one ($63.^{o}5$) and low perigees, say 100 to 200 nautical miles, a

spin stabilized vehicle cannot achieve reasonably long observing times. It is clear that for at least six months the Sun will be in the unfavorable position. Throughout the year intervals of continuous sunlight are very brief and, in general, satisfactory values of the illumination phase angle are likely to occur during the time when the useful observing interval is seriously limited by either the eclipses or Earth viewing or both.

If the eccentricity of the above orbit is increased to say, 0.25, without altering the perigee and inclination, one finds that the time when the vehicle is neither in the Earth's shadow nor viewing the Earth's surface increases to 54 to 60 percent of the orbital time. What makes such an orbit ultimately unsatisfactory is the briefness of time intervals during which the phase angle has acceptable values.

Circular orbits of low inclination, say 38^{o}, but high apogees, for example 1000 nautical miles, are found to be virtually useless because the maximum value of the phase angle does not exceed 104 degrees.

In the examples described above, the direction of the optical axis with respect to the spin axis was taken in the range from 30 to 45 degrees. The variation of this angle does not lead to better performance. The most important factor in the above examples is the fact that the direction of the spin axis once established, remains fixed in the inertial space. It is primarily this fact which ultimately results in a narrow range of satisfactory phase angles. Clearly, observing time can be increased if the direction of the spin axis can be changed according to a prescribed control law.

If, for instance, the spin axis is permanently fixed in the plane of the orbit, that is, it is made to precess at the orbital rate, one needs only a very simple control program. If, furthermore, a sun following orbit with eccentricities in the range 0.4 to 0.5 and perigee of 200 n.m. is taken, observing times in the order of 60 to 65% of the orbital lifetime can be achieved. Furthermore, if the angle between the spin axis and the optical axis is taken as 30 degrees and the field of view is set at 8 degrees, the minimum value reached by the phase angle is 82 degrees. For such conditions much of the loss of observing time can be ascribed to the advance of the line of apsides. In fact, if one would establish such an orbit at the critical inclination angle, the useful fraction of the observing time increases to about 80%. Nearly 60% of the time the phase angle is in excess of 90 degrees. Furthermore, if one were to decrease the angle between the optical and spin axis, the yearly fraction increases to 65 to 80 percent, depending on what is considered the minimum acceptable value of the phase angle.

Improvements achieved in the examples immediately preceding are sufficiently large to warrant the use of highly eccentric Sun following orbits having critical inclinations.

Even more dramatic improvement is possible with an attitude control which directs the optical axis in the antisolar direction. The use of such a control law in association with a critical inclination Sun following eccentric orbit yields observing times equal to nearly 95% of the nominal orbital lifetime. In fact, during a significant

portion of the year 100% of the orbital time is suitable for data acquisition. Since the instrument is pointing in the antisolar direction, the phase angle remains at the constant value of 180 degrees.

Examination of results for low inclination orbits indicates that the useful observing time is nearly the same whether one employs direct or retrograde orbits. For inclinations near 35^{o} and circular orbits with apogee altitudes in the neighborhood of 700 nautical miles, the total observing time constitutes 45 to 50 percent of the one year lifetime. The choice between the direct and retrograde orbits is then dictated by considerations other than the achievable observing time. In fact, the payload capability becomes one of the more important factors, since larger payloads can be launched into direct orbits.

From the studies, it is clear that the optimum performance is obtained in sun following, eccentric orbits, having critical inclination, and with the instrument axis being directed in the antisolar direction. The control need not be continuous. A periodic stepwise updating of the attitude is sufficient provided the drift in attitude is reasonably small.

The concluding section of the report is concerned with the selection of the instrument platform. The selection process is based on the premise that the platform must be an existing one, thus eliminating its development costs, and that it be reasonably readily available. Since only a small spacecraft is needed, the required launch system need not be anything more powerful or complex than the SCOUT system.

To achieve the longest possible observing times and, thereby, the most effective operation it would be desirable to employ an attitude controlled, payload dedicated package. The latter requirement is not a firm one, since a Sisyphus instrument could readily share a platform with other instruments whose requirements are not in conflict with particle detection. For instance, the Sisyphus system and instruments devoted to solar measurements would constitute such a set.

Various platforms considered for the present application are either spin stabilized or have simple semi-active attitude control systems of minimal weight and power consumption. The achievable precision in attitude is approximately 1.0 degree, a satisfactory figure for the present needs.

Five platforms were found suitable for operating Sisyphus in Earth's orbits. These are: (a) DELTA Payload Experiment Package (PEP), (b) The OWL System, (c) S^4 DELTA System, (d) Small Applications Technology Satellites (SATS), and (e) SOLRAD 10(C) spacecraft. It is to be noted that all costs stated subsequently are exclusive of the instrument costs. Present estimates indicate that a flight qualified instrument can be delivered in one year for approximately $525,000.

The SATS system is intended to be a quick reaction small, low cost dedicated spacecraft. This will be a standardized package so that it can be "called up", integrated and launched in minimum time. It will be compatible with the SCOUT launch system.

It appears that this spacecraft provides the degree of flexibility needed to deliver the optimal Sisyphus operation. The combined cost of the spacecraft, Sisyphus instrument, instrument integration, and the launch vehicle are estimated at approximately 4 million dollars. Ultimately, however, this system is likely to produce the lowest cost per observing hour. A preliminary layout shows that Pioneer F/G version of Sisyphus can easily be accomodated within the Scout shroud. No folding and subsequent deployment of a light shield is needed.

The DELTA PEP Spacecraft is designed to provide a stabilized platfrom in primarily circular orbits. It is a so-called "Piggyback" vehicle, that is, the specific DELTA will be devoted to some primary mission. However, since the second stage has excess payload capability, it can be utilized by secondary payloads such as Sisyphus. The second stage can accomodate 150 to 200 pounds of experiments, but the exact payload is dependent on the primary payload. Furthermore, the orbit is defined by the requirements of the primary mission. Finally, the nature of the envelope and the mode of its stabilization are such that a deployable light shield is unavoidable. The projected cost of this spacecraft is 2.8 million in non-recurring costs for PEP and 0.8 million per vehicle when in full production. Integration costs would add 0.2 million to the above figures. These costs can be shared between a number of experiments. From the Sisyphus point of view the unsatisfactory features are (a) no orbital and launch time flexibility, (b) the growth of the primary payload may, in fact, eliminate secondary payloads (c) operational conflicts with other instruments.

The S^4 system has been designed and ground tested by the AVCO Corporation. This spin stabilized scientific spacecraft is available at something like 1.0 million dollars exclusive of integration costs and launch vehicle cost. By present estimates, the latter would add 1.5 million to the overall cost.

The OWL System was the first of the so-called University Explorer satellites compatible with the SCOUT launch system. The original design called for three axis stabilization and a lifetime of one year. The spacecraft is sufficiently large to accomodate a typical Sisyphus system. Some of these spacecraft are owned by NASA and are stored at Wallops Island launch facility. Necessary data for this system were obtained too late in the program to permit detailed cost study.

Finally, the SOLRAD 10(C) spacecraft, designed by the Naval Research Laboratory for solar measurements, was considered. The spacecraft is compatible with the SCOUT launch system. This is a spinning spacecraft, and its longitudinal axis points to within ± 2 degrees of the sun line. The Sisyphus instrument could be mounted on the face of the spacecraft which points away from the sun. Electrical power is supplied by solar panels which provide the meteoroid detector with added shielding against stray sunlight. As in the case of OWL, insufficient details were available to carry out a cost study.

II. INTRODUCTION

An accurate knowledge of the near-Earth meteoroid environment has become extremely significant with the present plans for long-life Earth-orbiting space stations. A determination of the particle fluxes, mass, and velocity distributions is essential to the design of structural walls.

There also exists from the scientific viewpoint a desire to know the numbers of meteoroids present in space, their orbits, their physical properties, their origin, etc.

Most present models of the near-Earth meteoroid environment are primarily based on satellite penetration data and on ground-based observations of meteors in the Earth's atmosphere.

The masses of the meteoroids responsible for the penetrations detected by the satellites must be estimated from empirical equations using assumed average impact velocities. The empirical equations relate the penetrated target thickness with the particle velocity, mass, and other properties based on laboratory experiments.

The ground-based meteor data consists of counts of the meteors detectable in the earth's atmosphere and of measurements of the meteoroid entry velocity. The masses of the meteoroids responsible for each observed meteor must be estimated from the brightness of the meteor.

In addition to uncertainties due to lack of definite knowledge concerning velocities, masses and particle interaction with the target medium, there are other problems associated with both the penetration data and meteor data. Perhaps, the most critical one results from the fact that the two techniques yield data in narrow and at the same time widely separated mass regions.

It is highly desirable to perform an experiment which can observe meteoroids over an extremely large mass range and thus attempt to provide a common tie for all meteoroid data.

Since 1967 the General Electric Space Sciences Laboratory has been working on a concept for Optical Particle Detection in space which has been called Sisyphus. The concept was first proved feasible in laboratory demonstrations under corporate funding. Under contract NAS 9-8104 with the NASA Manned Spacecraft Center, the concept was breadboarded in an approximation of a flight configuration. Using the breadboard and additional laboratory simulations a number of the problems associated with the flight development of the instrument were worked out. The results of these studies were documented in the Final Report on that contract (Chandra, et al 1970). In 1970 the Sisyphus experiment was selected to fly on the Pioneer F/G Missions through the asteroid belt to Jupiter. A contract was awarded to the General Electric Space Sciences Laboratory (NAS 2-5609) to fabricate the flight instruments for the Pioneer Missions. Under

this contract with the NASA/Ames Research Center a lightweight, low power version of the instrument was developed and fabricated for flight. The hardware for the Pioneer F Mission scheduled for launch in early 1972 has already been integrated with the spacecraft. A description of the Sisyphus measurement concept and of the Pioneer F/G version of the hardware is given in Section V of this report.

During 1970 the present contract, NAS 1-10158, with the NASA/Langley Research Center was awarded to study the optimum parameters for utilizing a Sisyphus configuration from an Earth orbiting satellite.

The work statement in the contract stated that the possibilities for utilizing Sisyphus in Earth orbit from both a manned workshop and an unmanned SCOUT launch satellite should both be investigated. During the early phase of the study there appeared to be a possibility of getting a meteoroid experiment on a Skylab B Mission. Toward that end an international consortium of meteoroid investigators was organized and convened at NASA/Headquarters to examine a combined particle experiment using various sensors that could be placed on such a Skylab Mission. Some initial efforts were devoted to such a combination of sensors. With the tightening of fiscal constraints and the dimming hope of a Skylab B Mission, the balance of the effort was devoted to the study of utilizing Sisyphus on an unmanned SCOUT launched vehicle. It should be noted, however, that a great deal of the effort reported herein is applicable to either a manned or unmanned Earth orbiting vehicle. During the progress of the study it became apparent that the hazard to future space vehicles from pollution exceeds that due to the natural meteoroid environment. Section III of this report discusses the space debris problem. As shown in subsequent sections utilization of a small relatively inexpensive Sisyphus system on an unmanned satellite represents the most economic means of monitoring space debris and establishing the hazard level for Space Shuttle and Space Station.

The point of departure of the present study is the Pioneer F/G instrument which is designed for use on interplanetary missions. On such a mission, it is relatively easy to obtain long observation times for statistically significant data. Furthermore, the estimated nature of scattering functions for interplanetary particles of interest indicates that, at large phase angles, one obtains more intense signals. For our purpose, the phase angle is defined as the angle between the directions of propagation of the incident light (sunlight) and the scattered light.

It is pertinent to inquire whether sufficiently long observation times and suitable phase angles can be obtained from a Sisyphus system operating in an Earth orbit.

There are several restrictions which the orbit and the instrument orientation impose on the amount of remote optical observing time available. Observing time is lost when

a) the sun enters the field of view
b) the lighted Earth enters the field of view
c) the instrument is viewing the dark side of the Earth

d) the instrument is eclipsed by the Earth

In addition, it is desirable, but not essential, that

e) the phase angle at the illuminated particle should be as close to backscatter as possible. A typical value is in the neighborhood of 140^{o}. However, useful results are obtainable for phase angles as small as 90^{o}.

Detailed consideration of the above factors is presented in Section VI. It is shown that it is possible to select launch conditions, orbits, and attitude control, compatible with a typical SCOUT launch system to yield observing times in the range 50 to 90% of the one year system lifetime. EXAMPLE VII of Section VI.B, in which a SATS platform is used for pointing and attitude control, displays results for such a highly favorable orbit.

The detectivity of the Sisyphus system is background limited. A careful study of the background and its effect on the threshold detectivity is needed in order to estimate the performance of the instrument in terms of the expected rate of potentially measurable events. Appendix IV is devoted to these considerations. In Section VII, selection of the launch system and of the platform is given. For reasons of cost, maximum observing time, and the greatest flexibility, a SCOUT launched SATS platform is recommended.

The recommended system is designed to minimize cost. It will yield reasonable data return for natural particles in the size range of 20 microns to 1 millimeter. Man-made debris will be detectable from sub-millimeter range to particles up to 1 cm in radius. If the level of hazard is as projected, larger baseline could be used to measure range to larger particles. Such a version of the instrument was not considered for reasons of cost.

In conclusion, cost estimates show that a flight qualified instrument can be delivered in 1 year at a cost of $525,000. This will cover parts and subassemblies for a 4 sensor head and the associated electronics subsystem. This cost includes electrical and environmental tests similar to those performed for the Pioneer F/G instrument, excluding shock, acceleration, humidity, and non-vacuum thermal testing. Furthermore, the above figures does not cover design of the software necessary for data interpretation. It is felt, however, that this will have become available in connection with the Pioneer project.

III. SPACE DEBRIS

Since 1957 man has orbited about the Earth a large variety of objects. Along with satellite payloads and rocket bodies, a variety of smaller bodies and particulate matter have been left in orbit. The larger bodies are continuously tracked and cataloged by the US Air Defense Command. Information regarding these bodies is contained in the "Space Track Data Base". Information from the 1970 edition of this Data Base is shown in Figure 1. Very limited information exists regarding the bodies and particles too small to be measured by ground based radar. That even "clean" spacecraft leaves a large amount of particulate matter in orbit has been demonstrated (Grenda, et al 1969). There does not seem to be any good estimates for the total amount of small man-made particulate matter in orbit about the Earth. One paper which discusses the amount injected by individual manned spacecraft is that by Newkirk (1967). That such material will remain in orbit for a considerable length of time can be seen from Figures 2 and 3. The lifetimes are only approximate and are only considered for spherical particles of unit specific gravity. The information displayed in the above figures is based on the assumption of free molecular flow regime, the drag coefficient of 3 and a linear relation between the lifetime and the ballistic coefficient. The latter is the product of the drag coefficient C_D, by the cross sectional area of the particle A, divided by twice the particle mass. This quantity is important in describing the effect of air drag on the orbital elements of satellites.

From Figure 3 it can be seen that particles of millimeter size injected into orbits with perigee in excess of 600 st. m. will have lifetimes of the order of 800 days. Particle size need not be much larger to extend the lifetime to several tens of years at the same altitude. In fact, larger particles will have sufficiently long lifetimes even at lower perigees to present a hazard to future spacecraft which they may encounter.

To estimate the extent of the space debris problem, consider a shell about the Earth of 3,000 kilometer thickness. The 1970 Space Track Data Base indicates that 85% of the material currently being cataloged is in orbits included in this shell. The volume of such a shell is 2.1×10^{21} cubic meters. For comparative purposes, we can estimate the amount of natural meteoric material at any moment in this shell. From the NASA Meteoroid Environment Model 1969, the terrestrial influx of meteoroids with diameters greater than one millimeter can be shown to be approximately 5×10^{-14} grams per square meter per second. The lower limit was taken as presenting a hazard for present and future spacecraft. Assuming an average influx velocity of 20 kilometers per second, this would mean a space concentration of 2.5×10^{-18} grams per cubic meter. Multiplying this by the volume of the shell we conclude that only about 5 kilograms of natural meteoric material is present at any time within the shell. It is immediately obvious that this value has already been far exceeded by man-made debris. In Figure 4 we have plotted the 1970 Space Track Data. The number of debris bodies is shown as a function of size. The size is taken as the square root of the radar cross section. For sizes below one meter, the cumulative distribution departs from linearity on the log-log plot. It appears reasonable that this departure from linearity is due to instrumental limitations. This is the consequence of the fact that at a given wavelength the echo is

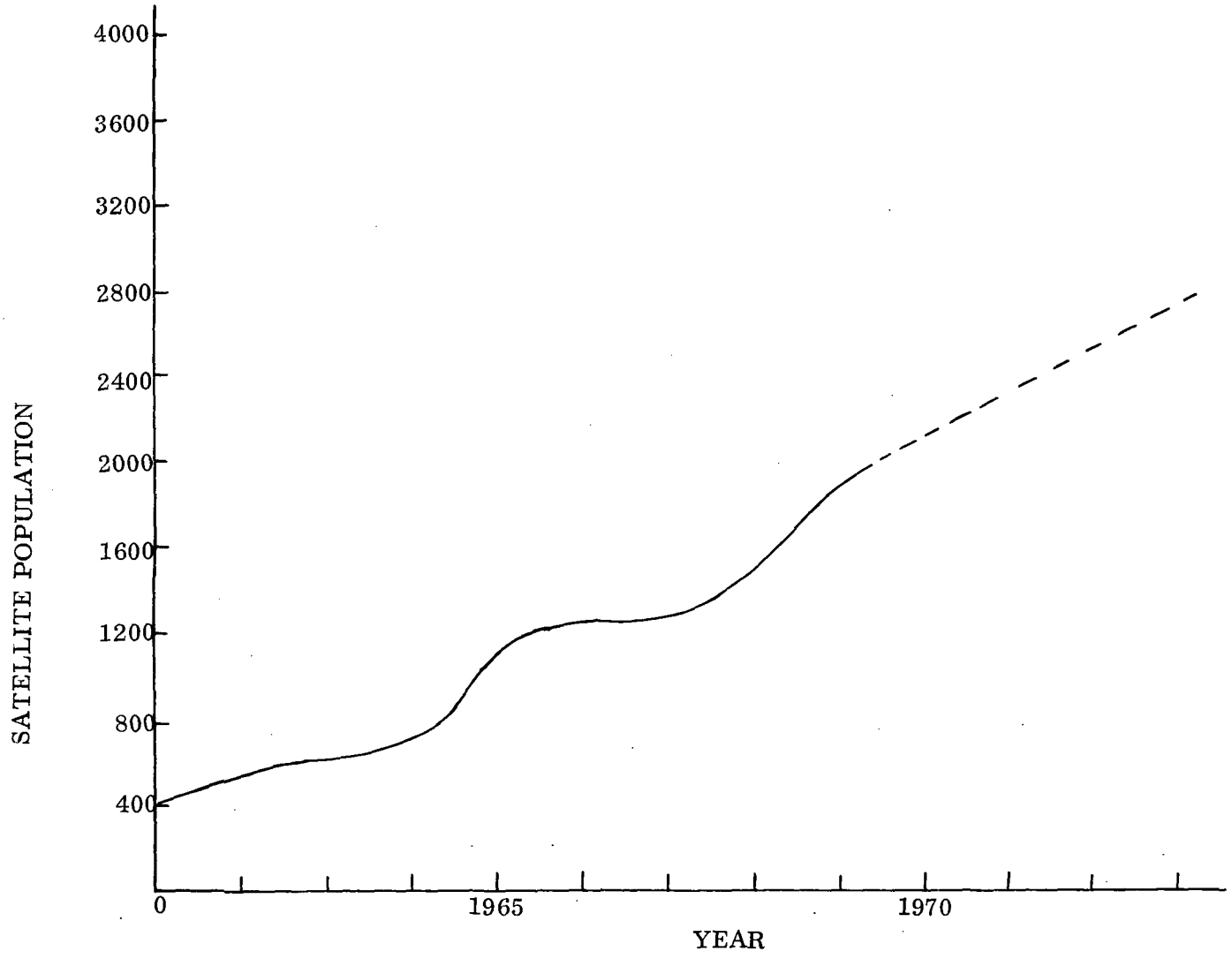

EXPECTED NUMBER OF SATELLITES (SPACE TRACK DATA BASE 1970)

Fig. 1

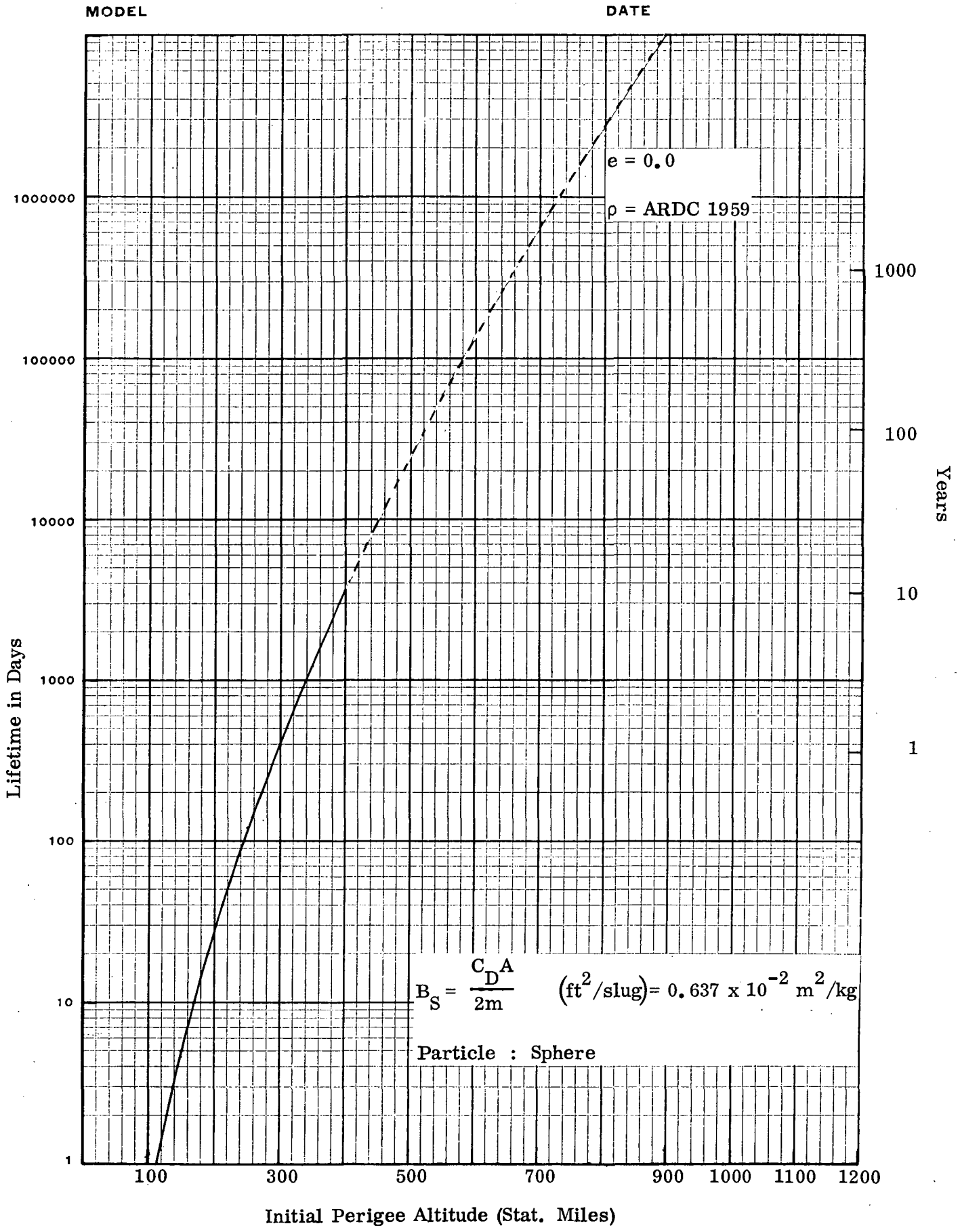
MODEL
DATE
e = 0.0
ρ = ARDC 1959
1000000
100000
10000
1000
100
10
1
Lifetime in Days
1000
100
10
1
Years
$B_S = \frac{C_D A}{2m}$ $(ft^2/slug) = 0.637 \times 10^{-2}\ m^2/kg$
Particle : Sphere
100
300
500
700
900
1000
1100
1200
Initial Perigee Altitude (Stat. Miles)

Fig. 2

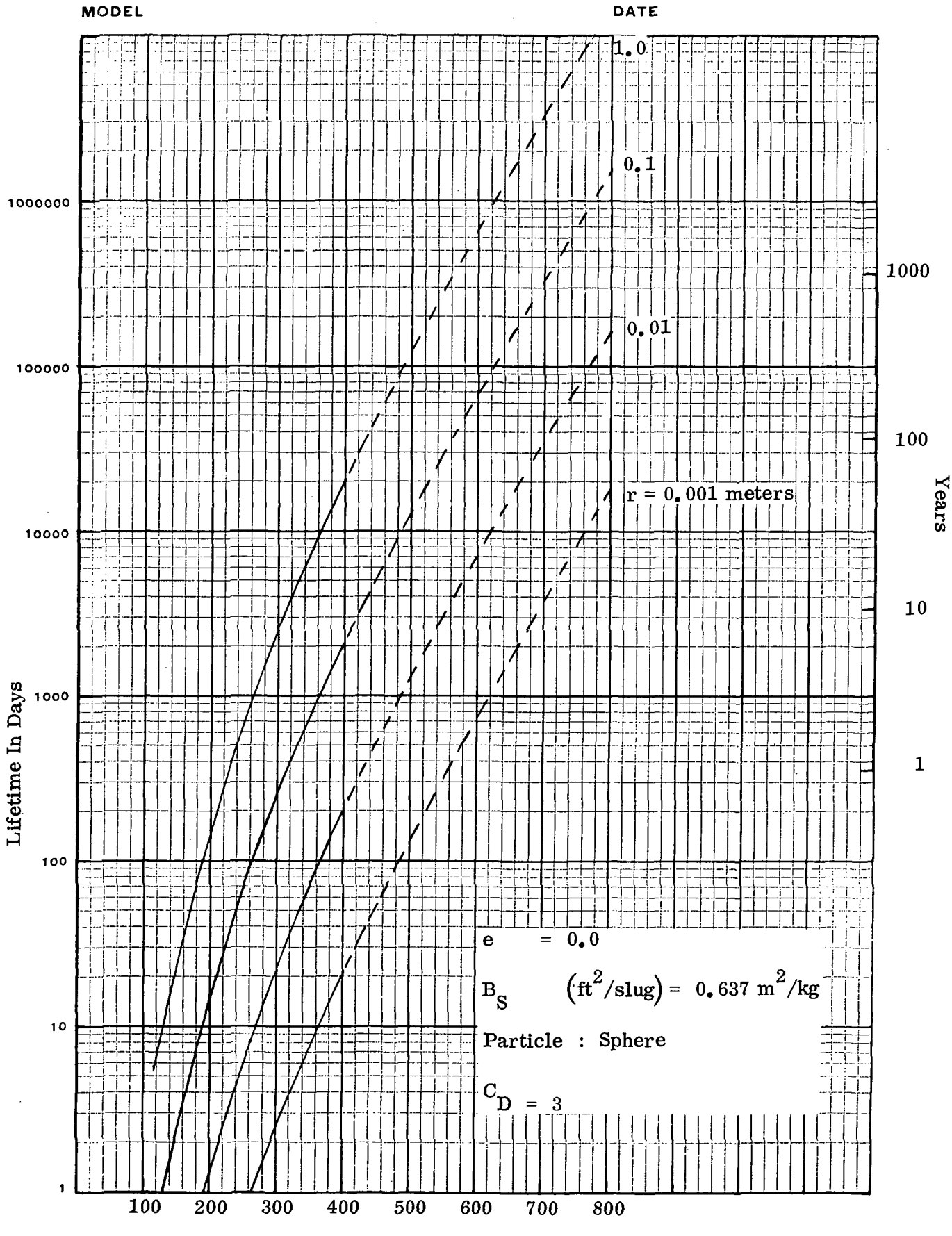
MODEL
DATE
1.0
0.1
0.01
r = 0.001 meters
1000000
100000
10000
1000
100
10
1
Lifetime In Days
1000
100
10
1
Years
e = 0.0
B_S $(ft^2/slug) = 0.637\ m^2/kg$
Particle : Sphere
$C_D = 3$
100
200
300
400
500
600
700
800
Perigee Altitude (Stat. Miles)

Fig. 3

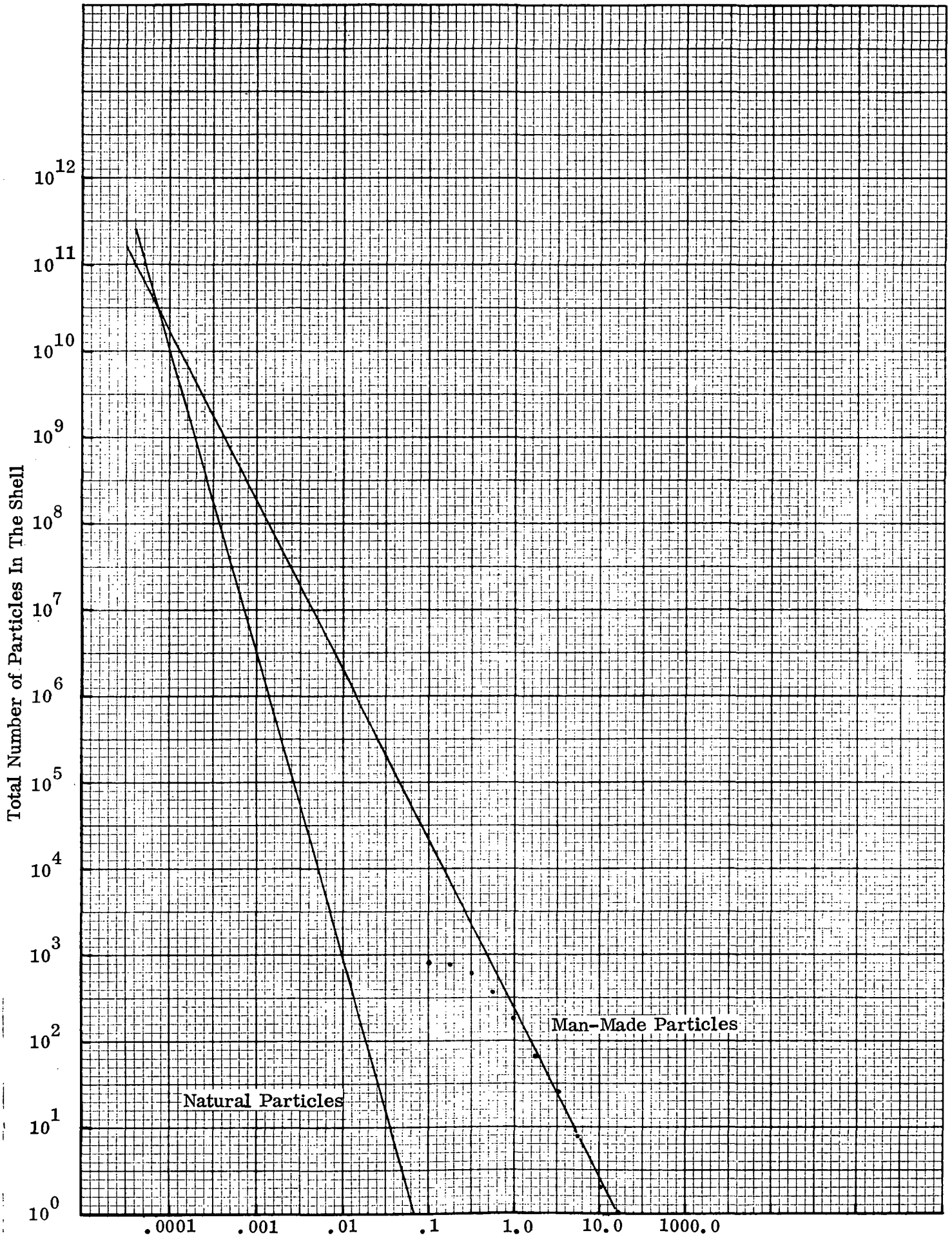
Total Number of Particles In The Shell
10^{12}
10^{11}
10^{10}
10^{9}
10^{8}
10^{7}
10^{6}
10^{5}
10^{4}
10^{3}
10^{2}
10^{1}
10^{0}
Man-Made Particles
Natural Particles
.0001
.001
.01
.1
1.0
10.0
1000.0
Particle Size In Meters

Fig. 4

proportional to the target cross section only for particles greater than or comparable to the wavelength. For particles much less than the wavelength the scattering cross section depends on a high power of the particle diameter. For instance, for spherical particles the echo depends on the sixth power of the diameter. Consequently, with the decreasing particle diameter, the desired signal is rapidly overpowered by various sources of noise.

We have extrapolated the linear portion of the distribution to smaller sizes. Such a procedure implies that the total mass also decreases linearly with size. The extrapolation is terminated at one millimeter below which atmospheric drag would insure a short lifetime for particles in low perigee orbits.

Admittedly, the reliability of such an extrapolation is low. Nevertheless, since debris such as, paint chips, remains of explosive squibs, thruster linings, etc., are left in orbits during every mission, estimates of debris population, however crude at the present time, are of practical importance. The natural meteoroid size distribution is shown for comparison in the same figure. This again was taken from the NASA Meteoroid Environment Model 1969. It is clear that for a reasonable extrapolation of the space debris curve, the likelihood of intercepting orbiting debris exceeds by orders of magnitude that for the natural meteoroids in size larger than one millimeter.

Assuming that the material is uniformly distributed through the shell (a conservative assumption), we can see from Figure 4 that a large spacecraft orbiting in the shell for a reasonable fraction of a year would have a high probability of colliding with such debris. For example, if the spacecraft had a cross section of 100 square meters, it could expect an average of two impacts per year with particles having mass in the order of 10^{-2} gr. It should be pointed out that while the impact velocity would on the average be less than that for a natural meteoroid this very likely would represent a more serious hazard. One would still anticipate relative velocities of the order of several kilometers per second, and at such a velocity, a meteoroid bumper would have little effectiveness. In fact, such a bumper may increase the damage from the interaction.

Apart from the uncertainties associated with the above calculations it should also be borne in mind that the hazard from space debris is one that is increasing as more and more objects are orbited. Figure 1 shows the history of the Space Track Data with an extrapolation to future years. From this figure one can see that the cataloged material is expected to double during the decade of the 1970's. Thus, it should be pointed out that while definite evidence does not exist to indicate a clear cut hazard at the present time, reasonable extrapolation of existing data show that such a hazard may already exist or could be reached in the foreseeable future.

In the next section an estimate is made of anticipated detection rates of both the natural and man created particles.

IV. ANTICIPATED EVENT RATE

The event count rate for an Earth orbiting Sisyphus depends, of course, on precise characteristics of the instrument as well as on the useful observing time available. For the present discussion a Pioneer F/G type instrument will be assumed moving in an orbit which permits 75% observing time. Description of the instrument is given in Section V. Observing time losses due to orbital and instrumental factors are discussed in Section VI.

The event count rate for an earth orbiting Sisyphus detector will be calculated for several assumptions regarding the natural meteoroid environment and the artificial debris type environment.

The event rate, as measured by the Sisyphus system can be written as

$$N = \int_{\Phi} \int_{A} d\,\Phi\,(a)\,dA = \int_{A_o(a)}^{A\,(a)} \Phi\,(a)\,dA \qquad (1)$$

where A is the effective surface area of the cone defined by the Sisyphus optics and Φ is the cumulative meteoroid flux. From Figure 5 the effective area can be approximated by

$$A = \frac{\pi^2 \alpha}{180} \left(R^2 - R_o^2\right) \qquad (2)$$

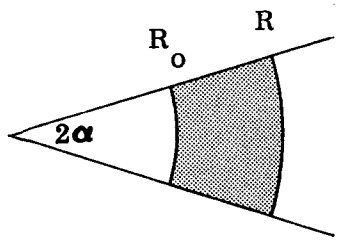

Fig. 5

where α is the half-angle of the detector field of view and R_o is the minimum effective range of the Sisyphus system at which the optics give sufficient overlap so that a real event will last at least 3.2 microseconds as required for noise discrimination. The range R is related to the particle radius via the equation

$$I = \frac{I_o r}{4 s^2} \left(\frac{a}{R}\right)^2 f\,(\lambda) \qquad (3)$$

where I is the intensity of the sunlight reflected by the particle onto the optics; I_o is the solar illumination at the object; r is the reflectivity coefficient of the object; a is the radius of the object; R is the distance from the object to the detector and s is the

heliocentric distance in astronomical units. The quantity f (λ) is a scattering function and its value for various scattering angles is given in Table 1. For the system as discussed above we have

$$\frac{R}{a} \sim 10^5. \tag{4}$$

A. Meteoroid Event Rate

The cumulative meteoroid flux distribution was obtained from NASA document NASA SP-8013 and its functional form is

$$\begin{aligned} \log_{10} \Phi &= -14.37 - 1.213 \log_{10} m, && 10^{-6} \le m \le 10^{0} \\ \log_{10} \Phi &= -14.339 - 1.584 \log_{10} m - .063 (\log_{10} m)^2, && 10^{-12} \le m \le 10^{-6} \end{aligned} \tag{5}$$

where Φ is the flux of cometary meteoroids of mass m grams and larger per square meter per second. Thus, if we assume that the meteoroids are approximately spherical with a mean density of 0.5 gm/cm^3, the event count rate can be determined using equations 1 - 5. The resulting event rates are shown in Figures 6 and 7 for reflectivities of 0.07 and 0.2 and for scattering angles of 135^o and 115^o respectively. These curves include an earth shielding factor of 0.5, while the earth defocusing factor is unity.

TABLE 1 - SCATTERING BY A WHITE, DIFFUSELY REFLECTING SPHERE, FOLLOWING LAMBERT'S LAW

γ	f (γ)	γ	f (γ)	γ	f (γ)
0^o	0	70^o	0.443	140^o	2.134
10^o	0.0015	80^o	0.630	150^o	2.349
20^o	0.0119	90^o	0.849	160^o	2.527
30^o	0.0395	100^o	1.093	170^o	2.628
40^o	0.0917	110^o	1.355	180^o	2.667
50^o	0.1742	120^o	1.624		
60^o	0.2907	130^o	1.888		

Using the values for the cumulative event rate shown in Figure 6 (scattering angle of 135^{o} and reflectivity of 0.07) we can calculate the uncertainity in the cumulative event rate. This uncertainty is converted to a percentage and shown (shaded area) on the NASA cumulative meteoroid flux distribution in Figure 8. It can be readily seen that the results from the earth orbiting Sisyphus experiment will span the existing gap between data from previous space experiments and data from earth based experiments (radar meteor and intensified video meteor). Thus, in addition to filling the gap, it will enable the intercomparison of these two disparate bodies of meteor data.

B. Debris Event Rate

The debris type environment was estimated using the data from the Space Track Data Base as of June 1969. From the data discussed in Section III, the cumulative number of particles in near earth orbit as a function of radius was calculated to be

$$\text{Total Number (debris)} \sim 50\, a^{-2} \tag{6}$$

where a is in meters.

The number per unit volume in a 3000 kilometer shell around the earth is, therefore,

$$\text{Number Density (debris)} = 2.4 \times 10^{-20}\, a^{-2}\, m^{-3} \tag{7}$$

Assuming a mean velocity of 8 km/sec for the debris, the flux equation for the debris becomes

$$\Phi = 1.9 \times 10^{-16}\, a^{-2}\, m^{-2} - \text{sec}^{-1} \tag{8}$$

Thus assuming a scattering angle of 135^{o} and performing calculations identical to those for the natural meteoroids, using equation (7) the event counting rate for debris becomes

$$N\,(\text{debris}) = 0.07\, \ell n\left(\frac{a}{a_o}\right) \text{day}^{-1} \tag{9}$$

If 1 cm and 1 mm are used for a and a_o respectively the debris counting rate is approximately 0.16 per day.

Figure 6. EVENTS PER YEAR ASSUMING 75 PERCENT OBSERVING TIME AND A SCATTERING ANGLE OF 135°.

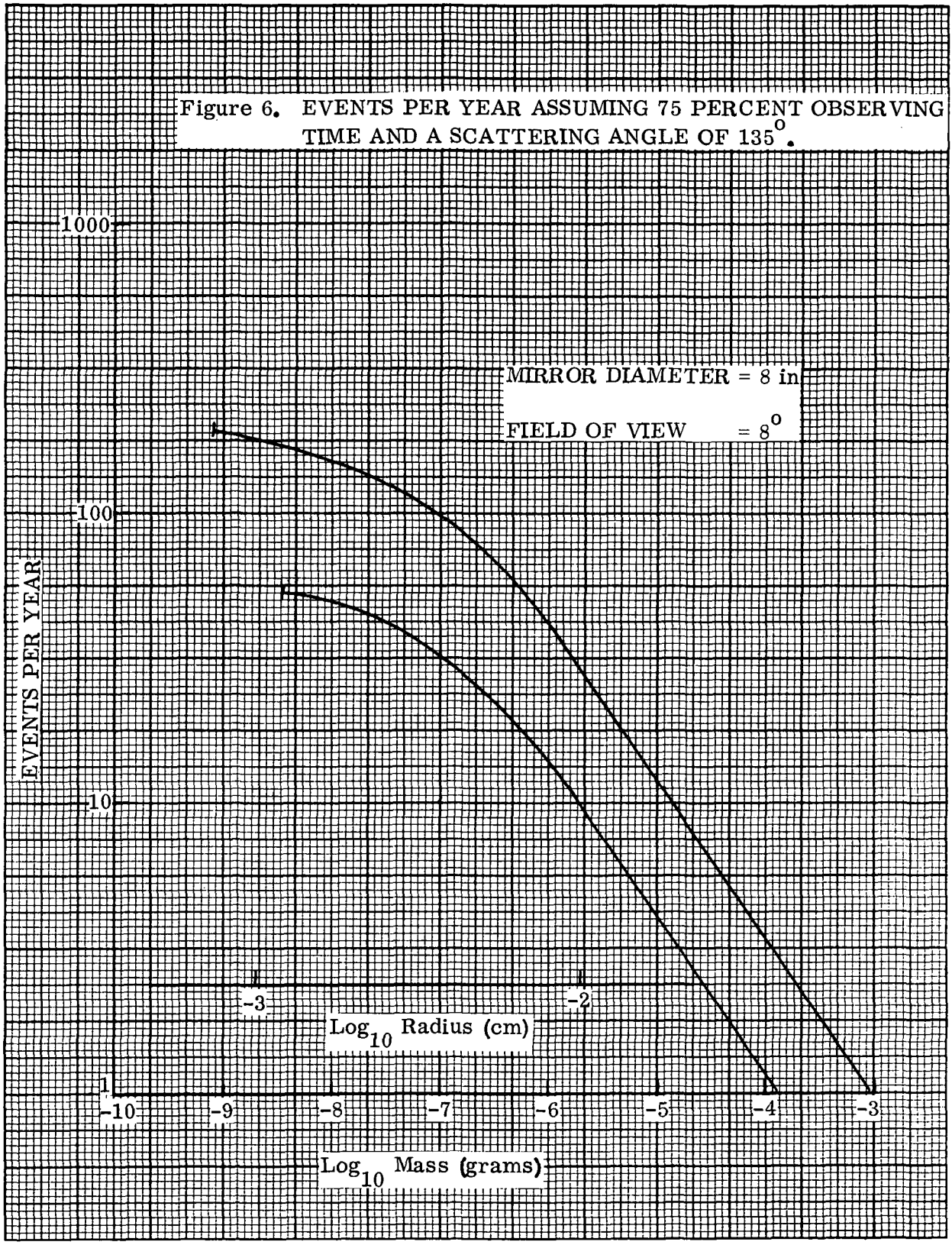

Figure 7. EVENTS PER YEAR ASSUMING 75 PERCENT OBSERVING TIME AND A SCATTERING ANGLE OF 115°.

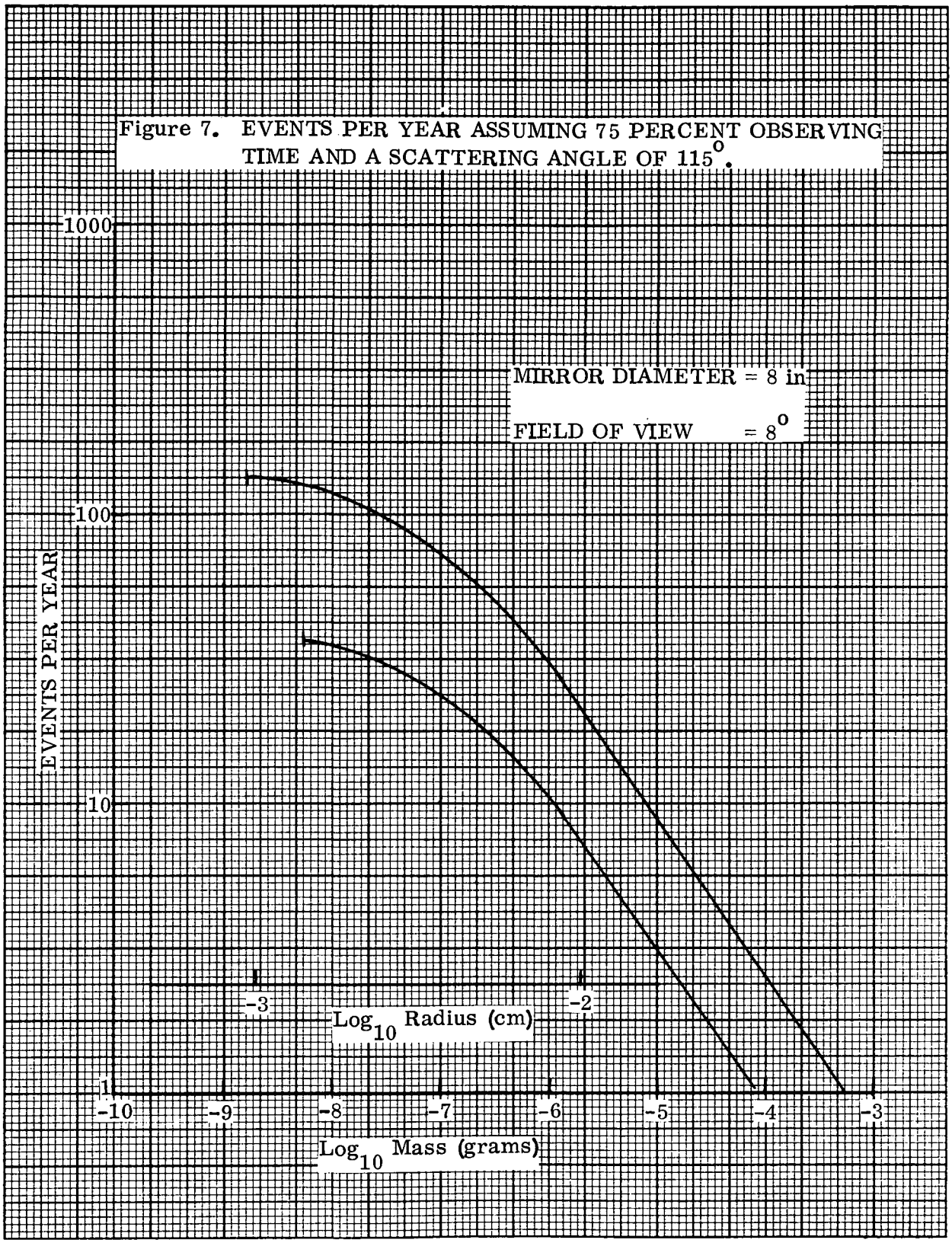

Figure 8. NASA CUMULATIVE METEOROID FLUX DISTRIBUTIONS WITH UNCERTAINTY LIMITS IN THE SISYPHUS DATA.

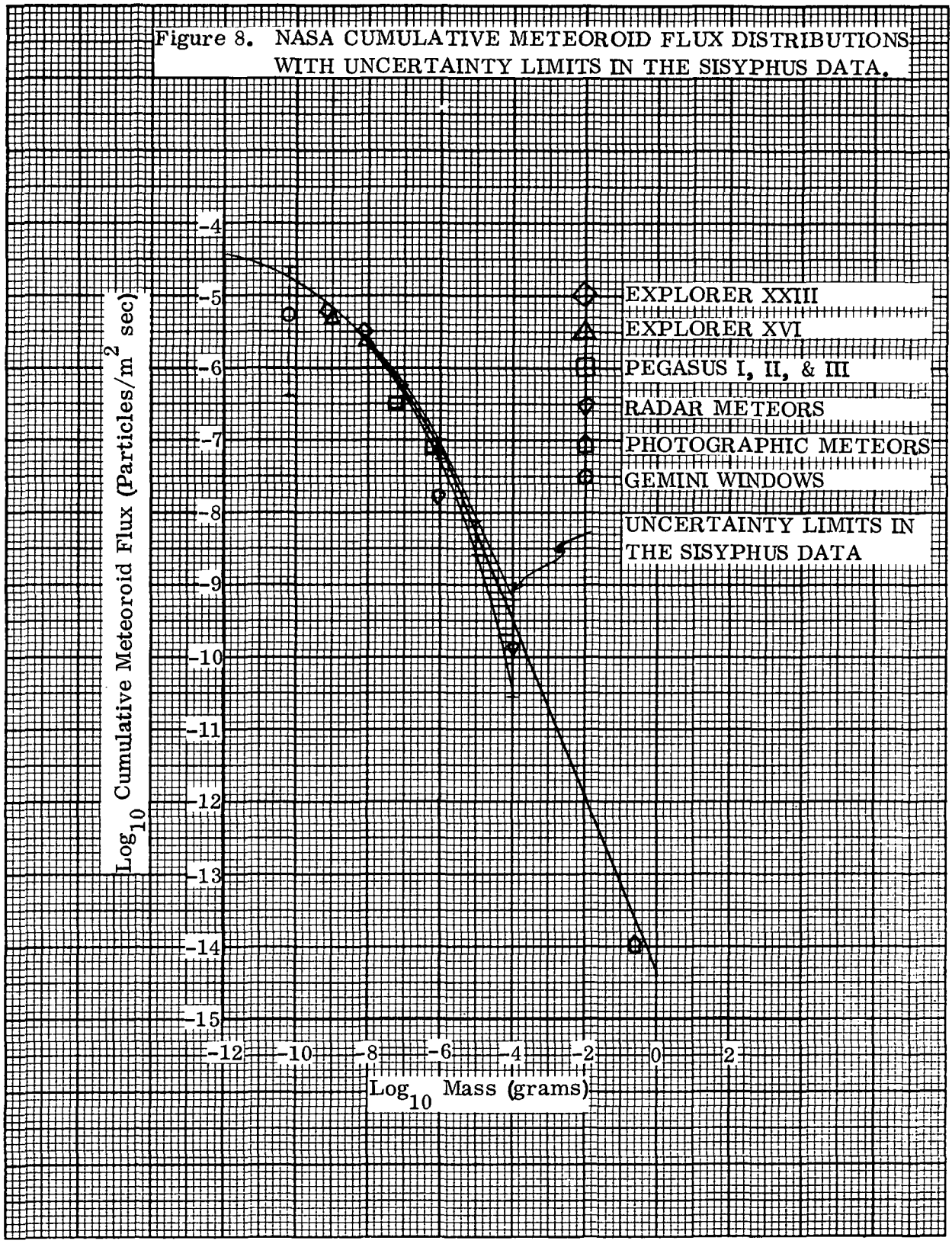

V. DESCRIPTION OF THE SISYPHUS INSTRUMENT

A. Concept of the Sisyphus Detection System

It is well known that a body in space will reflect sunlight by which it can be seen or detected. If an optical detector is oriented in space such that it looks away from the sun, we can approximate the amount of light incident on the aperture which results from the sunlight reflected by a spherical object by a relation of the form

$$I = \frac{I_0 \, r}{4 \, s^2} \left(\frac{a}{R} \right)^2 f(\lambda) \tag{10}$$

where I is the intensity of the reflected sunlight incident on the optics; I_0 is the solar illumination at the object; r is the reflectivity coefficient of the object; a is the radius of the object; R is the distance from the object to the detector; s is the distance from the sun and $f(\lambda)$ is the so-called scattering function.

The above relation is the result of the straightforward combination of inverse square law decrease with the distance of radiation flux,with the elementary reflection and scattering laws for spherical particles.

Using equation (10), one can calculate the size of an object that can be seen against a dark background. However, it is clear from the equation that a single detector would have no way of distinguishing different objects which had the same a/R ratio (i.e., a small object at close range from a large object far away). The Sisyphus system provides a means of determining the range and, hence, the size of the meteoroid.

Consider three optical subsystems as defining three parallel cones in space. Each subsystem consists of field optics (lenses, mirrors or a combination) and a photoelectric detector. If the optic subsystems are identical, then the edges of the field of view remain at a fixed distance from each other regardless of range. Any luminous object which crosses through the intersecting fields of view would then be detected by each of the optical systems. A model of the three optic Sisyphus system is shown in Figure 9. From the entrance and exit times in each field of view, one can completely calculate the trajectory of the body in space provided only that the body does not change its velocity during the transit time.

Mathematically, the Sisyphus problem is equivalent to finding the intersection of a straight line with three parallel cones. To demonstrate the mathematics of the system, we will choose a system of three identical cones with half angles α, as shown in Figure 10. Lines joining their apexes form an arbitrary triangle in the plane perpendicular to their axes. For purposes of convention, the vector from the base of the i^{th} cone

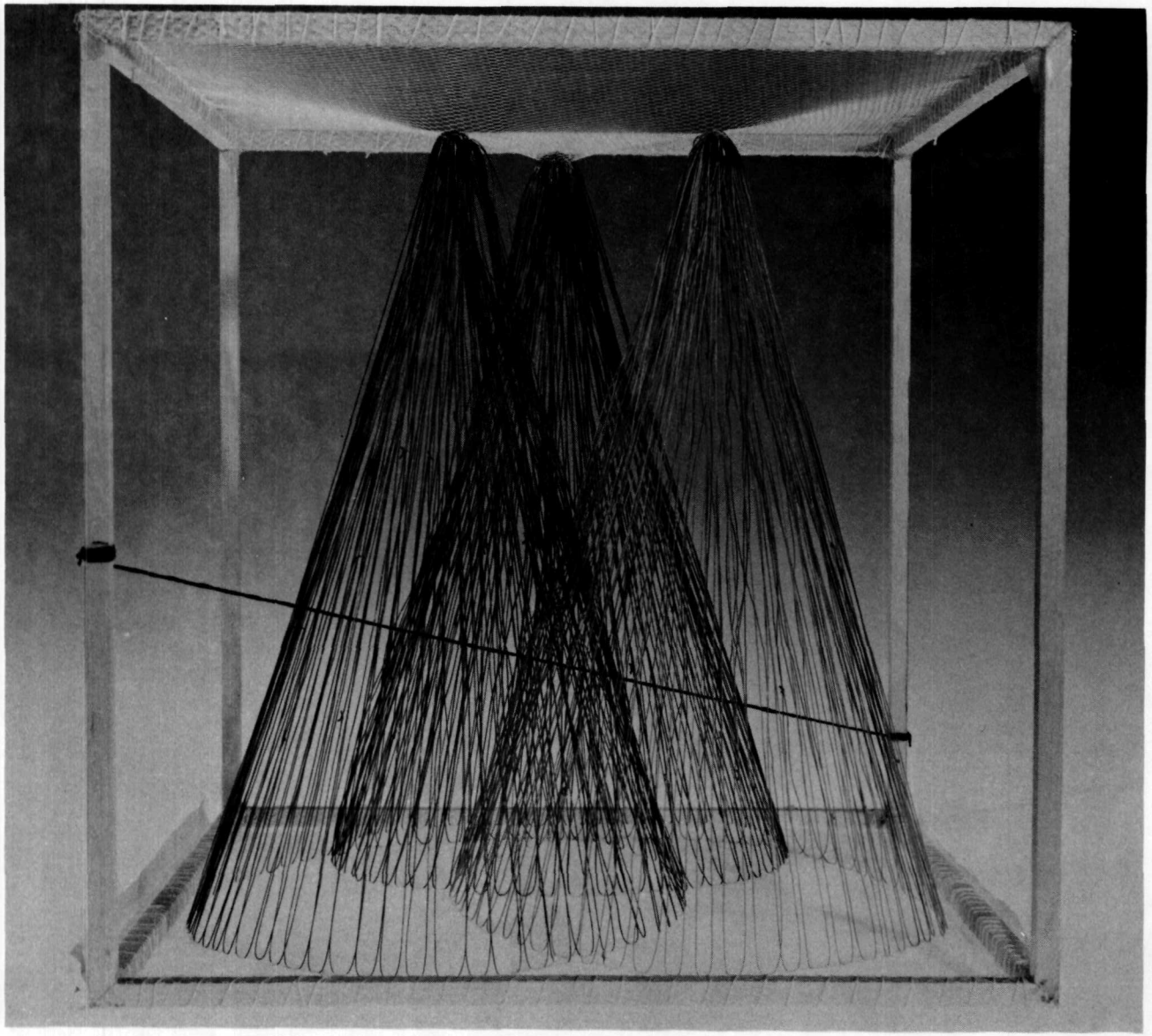

Figure 9. Geometrical Model of the Sisyphus System

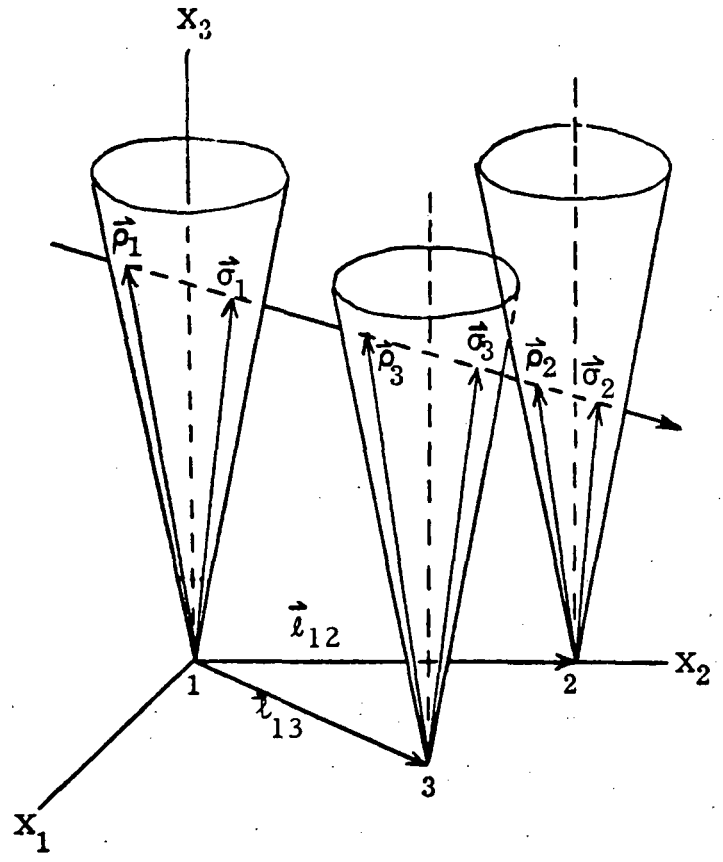

Figure 10. Sisyphus Geometry (For Convention Only)

to the particle's entrance into that cone is designated $\vec{\rho}_i$ and the vector to the particle's exit is $\vec{\sigma}_i$. The corresponding angles of entrance and exit in the plane of the apexes are φ_i and ψ_i. Times of entrance and exit at the i^{th} cone are designated τ_{ij}, where j is 1 for an entrance point or 2 for an exit point. The vector $\vec{v}$ is an arbitrary velocity vector.

Using this convention, five independent vector equations result:

$$
\begin{aligned}
\vec{\sigma}_1 &= \vec{\rho}_1 + (\tau_{12} - \tau_{11})\ \vec{v} \\
\vec{\rho}_2 &= \vec{\rho}_1 + (\tau_{21} - \tau_{11})\ \vec{v} - \vec{\ell}_{12} \\
\vec{\sigma}_2 &= \vec{\rho}_1 + (\tau_{22} - \tau_{11})\ \vec{v} - \vec{\ell}_{12} \\
\vec{\rho}_3 &= \vec{\rho}_1 + (\tau_{31} - \tau_{11})\ \vec{v} - \vec{\ell}_{13} \\
\vec{\sigma}_3 &= \vec{\rho}_1 + (\tau_{32} - \tau_{11})\ \vec{v} - \vec{\ell}_{13}
\end{aligned}
\qquad (11)
$$

By breaking these into components, we have 15 equations in 15 unknowns - ρ_i, σ_i, φ_i, ψ_i, and v_i - so a solution exists. The derivation for the aligned solution is presented in Reference 2. It has been programmed for computer use.

The above vector equations remain unchanged if the cone axes become misaligned for any reason. However, the 15 component equations are more complex since they involve two additional angles for each cone necessary to specify its orientation. This misaligned case has been reduced from the 15 original equations to 3 equations in 3 unknowns. Because of their complexity, further reduction appears impractical. Numerical solutions are obtained by computer iteration using the solution of the aligned case as a starting point. In this fashion, small misalignments due to thermal and mechanical stresses can be treated if the degree of misalignment is known. As we will show, this misalignment is periodically determined by using the background stars as a calibration source.

From the foregoing, it follows that independent of the amplitude of the signals detected by the individual optical systems, one can establish the three velocity components and the range of the luminous body. Using this calculated range, one can solve equation (10) for the product of the reflectivity and the cross-sectional area, and thus determine the mean radius of the body to an uncertainty of the square root of the reflectivity. For the reflectivity coefficient of meteoroids, two relatively widely differing values were selected to show the implications. The first is 0.2, which is a mean value for meteorites (Watson, 1938). The second is 0.07, which is the value quoted for the asteroids (Kuiper, 1961). It is to be noted that the difference in the size of the meteoroid derived using these two extreme values for the reflectivity coefficient would be a factor of 1.7. The mass difference would be a factor of 5. In current meteor

astronomy (earth based and spaceborne) such uncertainties are not considered large. Specular reflection may increase the albedo and introduce scintillations as the body rotates. Since several values of the range and intensity can be obtained, an average albedo cross section (analogous to the radar cross section) can be determined.

From the real time at which the event took place, the known position and orientation in space of the vehicle from which the measurement was made and the three velocity components of the body, the complete orbit of the body in the solar system can be determined.

B. Description of the Pioneer Instrument

The objective of the Pioneer Asteroid/Meteoroid Detector (AMD) is to determine the meteoroid and asteroid environment encountered in the region of the solar system beyond the Earth's orbit. Specifically, in one portion of the experiment, the cometary meteoroid environment believed to be responsible for the zodiacal cloud will be examined in these regions traversed by the Pioneer F/G vehicles.

In addition, the results from this experiment will also provide important engineering data since a prime consideration in the design of space vehicles is the possibility of damage caused by collisions with extraterrestrial debris. Depending upon the size, mass and velocity of the impinging particles, surface erosion, puncture or failure of the spacecraft can result.

The hardware implementation of the concept outlined in Section V.A for the Pioneer Mission is described in subsequent paragraphs.

The instrument consists of the optical and electronic subsystems.

1. Optical Sensor Assembly

The sensor subsystem includes four reflecting telescopes of Ritchey-Chrétien design, 8-inch aperture with 8-inch effective focal length. Each telescope is supported on a central "can" which houses a photomultiplier tube, dynode resistor assembly, and preamplifier. The photomultiplier tubes are RCA C7151Q, modified to include an S-20 photocathode. A "light tube" has been placed between the field stop (at the conical forward end of the housing) and the photomultiplier tube face. This light tube is a very thin 3/4-inch long, 1.2-inch diameter, stainless steel cylinder whose inside surface is gold coated to provide a reflectivity of 0.9 or better. By placing the photocathode away from the focal plane, the spot size is blurred to reduce the effect of local variations in photocathode sensitivity; the light tube reflects energy which would otherwise not reach the limited area of the photocathode.

The layout of a single unit is shown in Figure 11.

In the back of each housing, a preamplifier is located which serves as an impedance transformer as well as a means of varying bandwidth.

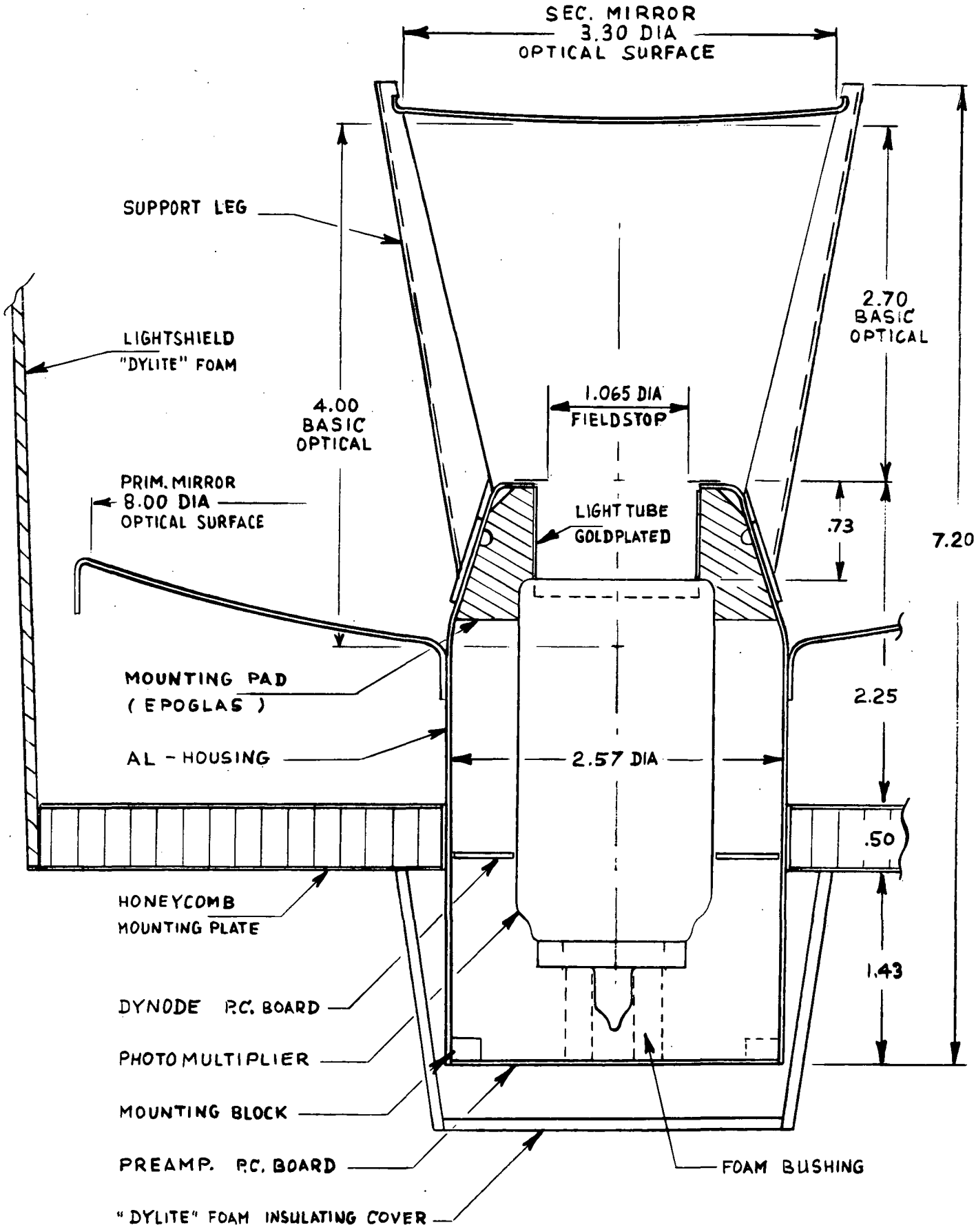
SEC. MIRROR
3.30 DIA
OPTICAL SURFACE
SUPPORT LEG
LIGHTSHIELD
"DYLITE" FOAM
4.00
BASIC
OPTICAL
2.70
BASIC
OPTICAL
1.065 DIA
FIELDSTOP
PRIM. MIRROR
8.00 DIA
OPTICAL SURFACE
LIGHT TUBE
GOLDPLATED
.73
7.20
MOUNTING PAD
(EPOGLAS)
AL - HOUSING
2.57 DIA
2.25
.50
HONEYCOMB
MOUNTING PLATE
1.43
DYNODE P.C. BOARD
PHOTOMULTIPLIER
MOUNTING BLOCK
PREAMP. P.C. BOARD
FOAM BUSHING
"DYLITE" FOAM INSULATING COVER

Fig. 11

Photomultiplier tube power is supplied to each dynode chain from a central 1700 volt supply, consisting of a transformer/voltage multiplier; this high voltage power supply receives its square wave drive from the basic dc-dc converter chopper in the electronics box. The gains of the photomultiplier tubes are equalized by adjustment of high voltage series dropping resistors.

Each preamplifier consists of an operational amplifier preceded by a dual field effect transistor, with another dual FET switching bandwidth to "wide", "medium", or "narrow" upon receipt of the appropriate commands. The three bandwidths are designed to accomodate signal rise times, τ_r of 0.7, 2.0, and 25.0 microseconds respectively. The preamplifiers have a quasi-logarithmic gain curve with two break-points to extend the dynamic range. The diodes which provide this non-linear function are matched over a wide range of temperatures (-70°F to + 150°F). In telescope "A", an additional matched diode has been added through which a constant current flows; the voltage drop across the junction is monitored via the AMD "temperature" analog channel of the Data Transmission Unit (DTU).

Four telescope assemblies, a high-voltage power supply, and a cable harness are mounted on a 17-1/2 inch square honeycomb panel. All assemblies, except the high-voltage power supply, are bonded to the panel using RTV sealant. To provide shielding against stray sunlight reflections, particularly from Radioactive Isotope Thermal Generators (RTG), a lightshield of 1/8-inch thick polystyrene foam is bonded to the honeycomb panel. A coating of 1-mil aluminized mylar protects the polystyrene against solar radiation during part of the S/C trajectory. Total weight of the Optical Sensor Subsystem is about 4.6 pounds (including panel). The layout of the overall sensor head is shown in Figure 12. Photographs of the actual hardware are shown in Figures 13 and 14.

2. Electronics Subsystem

The electronics subsystem is housed in a black-anodized aluminum box. Four multilayer boards are supported from a central "mother"-board which is squeezed between the two halves of the aluminum housing for rigidity. Two centrally located bosses provide additional support. Polyurethane foam is sandwiched between the boards for damping. The boards are fully conformally coated. Two connectors interface with the spacecraft and the optics, respectively. Total weight of the electronics box is 1.86 pounds. This subassembly is shown in Figure 15. The outputs of the four preamplifiers are processed by the electronics subsystem whose block diagram is shown in Figure 16.

3. Operation

A sunlit particle traverses the fields of view of the optical sensors. Its entrance times (into each of the sensor fields) and exit times (from these fields) are measured by counting clock pulses, and the results are stored for read-out by the DTU. The particle brightness (in each field of view) is measured in a peak detector, converted to digital form and stored for DTU read-out.

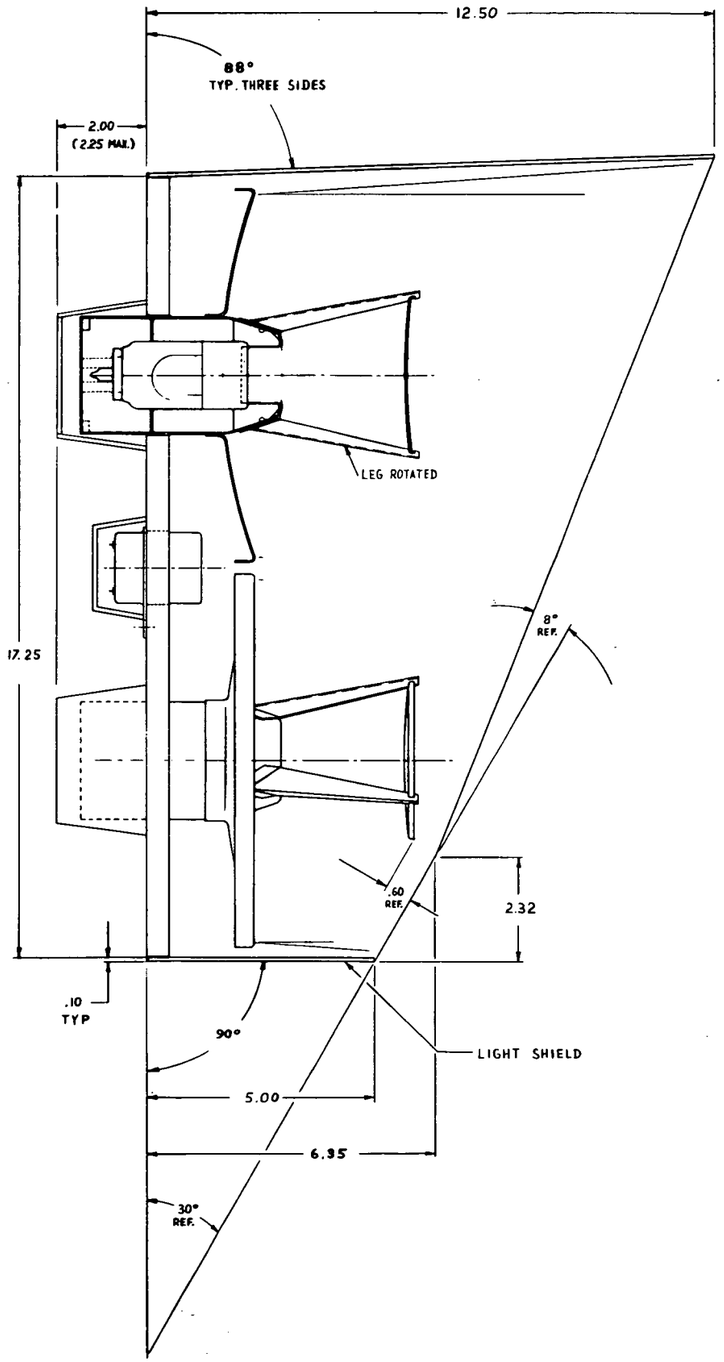

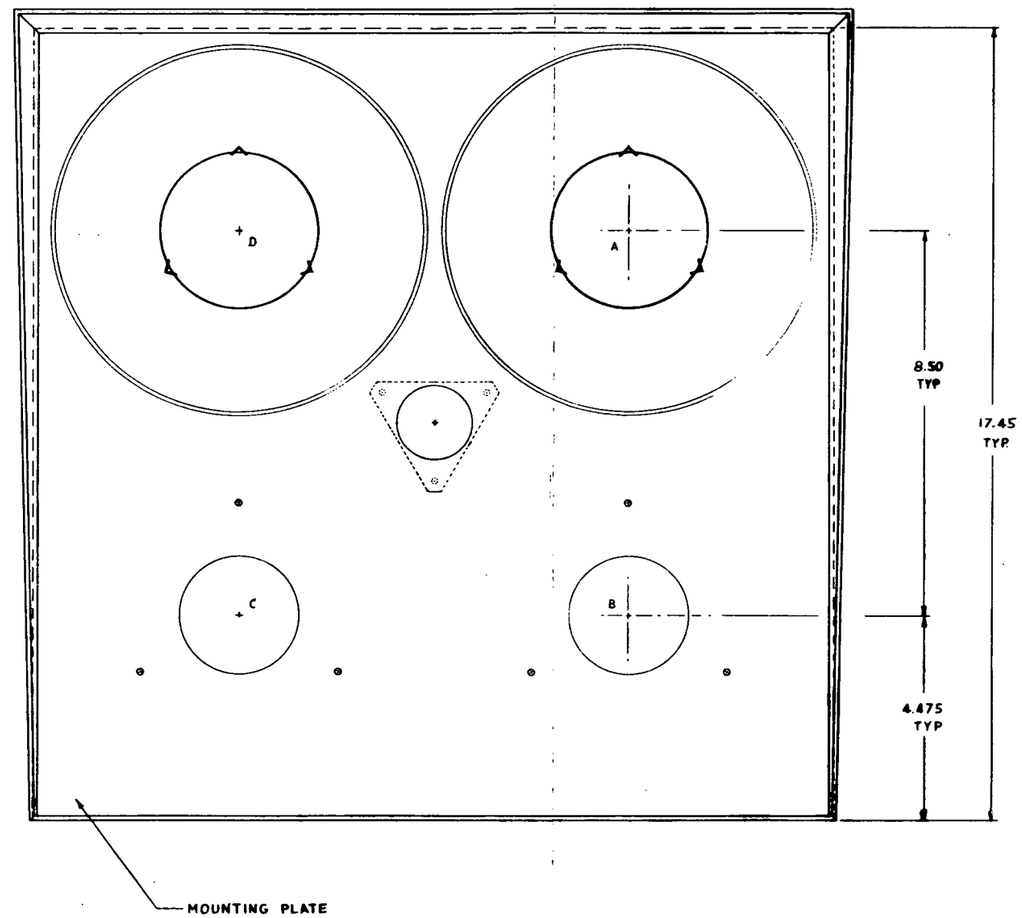

ATTACHMENT POINTS TO SPACECRAFT ARE NOT SHOWN

MATERIAL

SHIELD : EXPANDED POLYSTYRENE SHEET 6 LB/FT³
'DYLITE' FOAM .085 NOM. THICKNESS

MOUNTING PLATE : ALUMINUM HONEYCOMB 1.6 LB/FT³
CORE .50 THICK
FACE SHEET .008 THICK

Figure 12.

Figure 13.

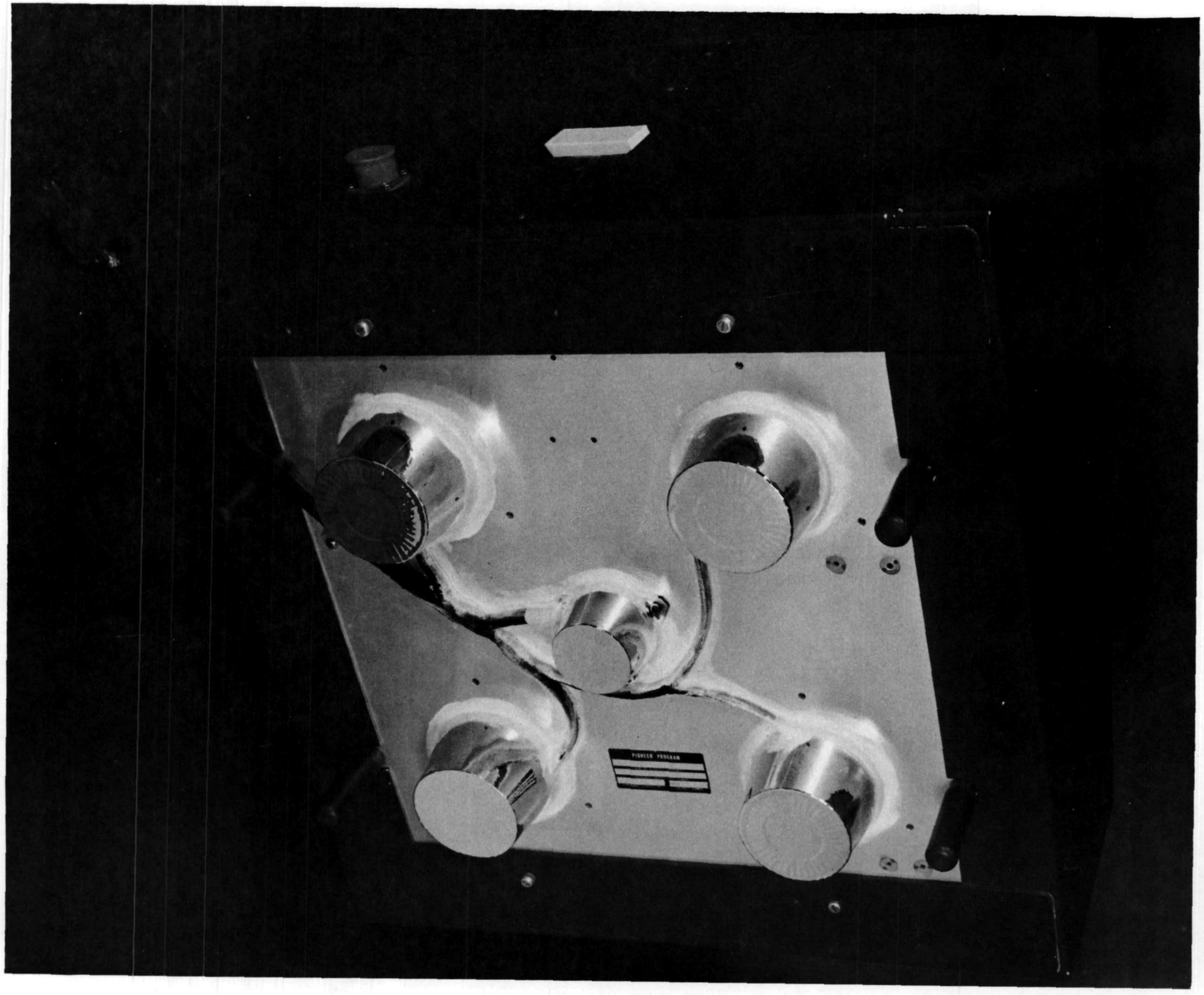

Figure 14.

Figure 15

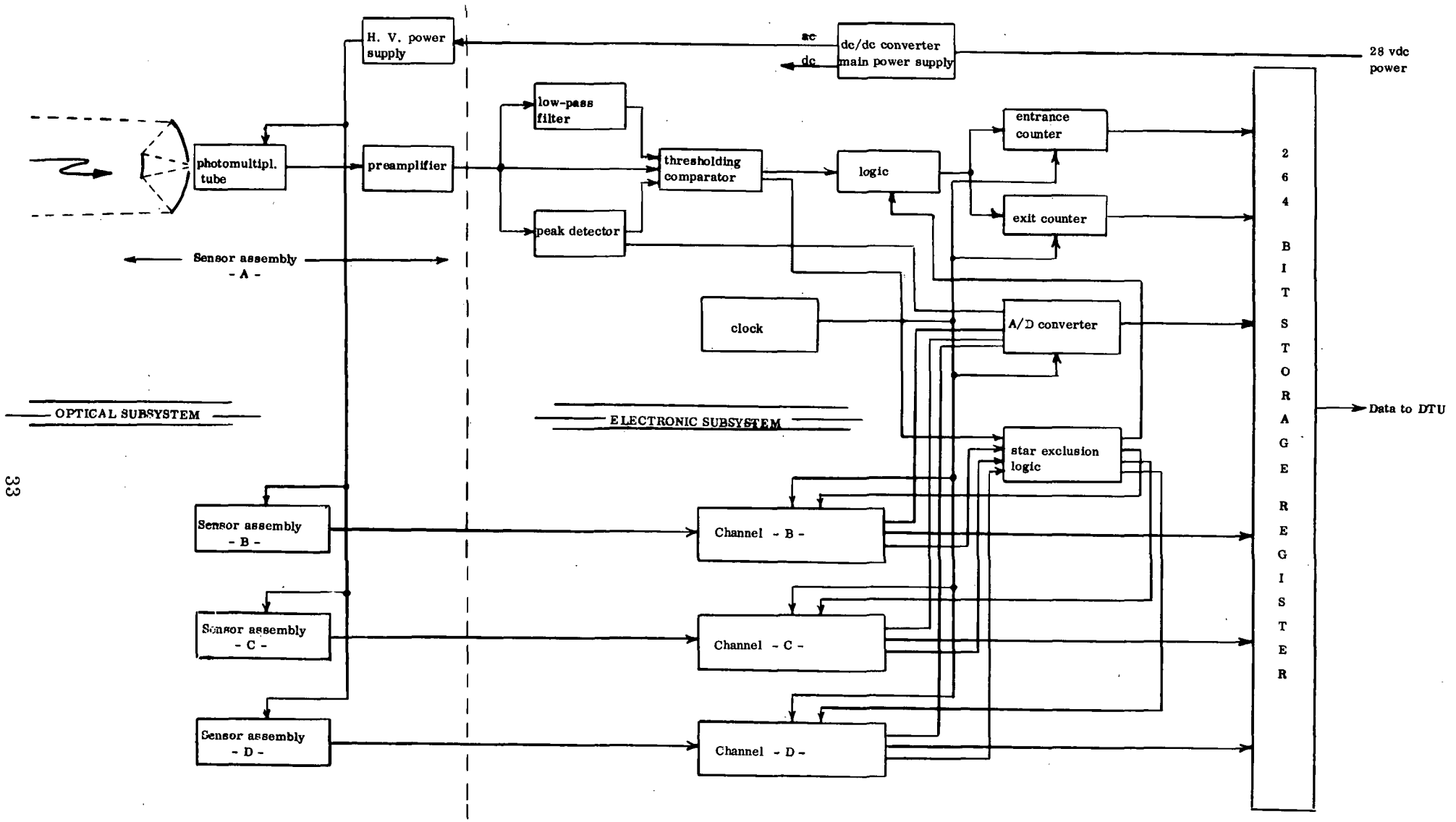

Figure 16. Block Diagram Asteroid/Meteoroid Detector

Threshold setting, described below, is specific to the spinning Pioneer F/G spacecraft. Procedural details will, in all likelihood, be different for an Earth orbiting instrument. Computations on which the subsequent discussion is based, are shown in Appendix IV.

The average dc background levels (each channel separately) are detected using a 47 millisecond time-constant to provide the BACKGROUND signal outputs. Four short time-constant peak detectors provide the PEAK signal outputs.

Since the input signals are very close to the noise levels, floating self-adaptive thresholding circuits (one per channel) are used. Threshold level is at 1.1 x dc background, plus 2 x noise peak, for "normal" setting and 1.2 x dc background plus 2 x noise peak for "high". As soon as the threshold is exceeded, the level is dropped to 1.1 x (or 1.2 x) dc background, only, by switching out the noise peak contribution. This hysteresis reduces signal dropout due to noise pulses.

When the signal in any channel exceeds the threshold, all entrance and exit counters are started. As the sunlit particle enters into (or exits from) a field of view, the corresponding entrance (or exit) counter is stopped. Note that the entrance counter of the channel which first saw the particle (and started all the counters) will be stopped immediately after starting. Thus, a typical event will find one entrance counter near zero, and the other entrance counters and the exit counters stopped at varying counts, depending on particle range, velocity and trajectory.

The digital data (position, entrance count, exit count), as well as the A-to-D converted background and peak signals, are stored in parallel-in/serial-out registers in 264 bits which are read out sequentially by the DTU. In order to meet the extreme constraints on power and weight, full use is made of complementary symmetry MOS integrated circuitry (COSMOS). The counters/registers are COSMOS hybrids.

As stated earlier, the system operates at a very low signal-to-noise ratio; this results in a large number of "false alarms" in each channel, due to the noise contribution of the background. In order to make sure that only "legitimate events" are registered in the counters, there is a three out of four coincidence circuit which further requires coincidence to be of at least 3.2 microsecond duration. A second logic circuit rejects signals which recur at the S/C spin rate. Such signals are attributed to stars, and, to limit the amount of data telemetered, are recorded only once. Nevertheless, since a set of selected stars will be used for calibration purposes, the star exclusion circuit can be disabled on command to permit repeated observation of a given star. Such observations are necessary to determine post launch misalignment of telescopes and the responsivity of the sensor system to sources of known brightness and spectral characteristics, the type of information important for the interpretation of zodiacal light measurements and the solution of system equations.

During the time when no "events" are registered, the system reads the background only. In order to provide a trajectory reference for "events", and to

permit "mapping" of the background, the Pioneer vehicle generates a spokewheel of 512 bits per revolution, referred to an index pulse. The AMD electronics divide the 512 bits by 4, and take a sample of this number at the time the data are taken; thus, position is recorded to an accuracy of $360^{o}/128$, i.e., about 2.8^{o}. In the normal "star exclusion enabled" mode, any event recurring at the vehicle spin rate, i.e., reappearing in the same 2.8^{o} (or adjacent) position sector in succession, is identified as a STAR and excluded from readout after the first time it is encountered. This circuit can be disabled upon command.

Finally, two basic thresholds are available on ground command; in addition, three preamplifier bandwidth settings can be commanded to improve signal-to-noise ratio under conditions of high ambient noise, for slower particles (expected farther from the sun), and during star calibration.

VI. COMPUTATION OF EFFECTIVE OBSERVING TIMES FOR A SPIN STABILIZED EARTH ORBITING SISYPHUS SYSTEM

A. Analysis

1. Introduction

In this section we consider the orbital and attitude parameters necessary to utilize the Sisyphus remote optical system in Earth's orbits.

A little reflection shows that Earth orbiting missions impose on the detection system a set of requirements which either do not exist on interplanetary missions or whose effect are not particularly pronounced.

As mentioned elsewhere, the nature of expected signals is such that to obtain meaningful observational material long observing times are needed. Various interfering effects conspire to limit times available for observation. Aside from typical instrumental effects which determine the achievable signal to noise ratio, we find that a Sisyphus system is rendered inoperable when

a) The Sun is in or near the field of view
b) The lighted Earth is in or near the field of view
c) The instrument is in the Earth's shadow
d) Excessive amount of sunlight is reflected by the surroundings into the field of view
e) The phase angle at the particle being detected is less than a certain critical value.

Items listed under a), b), c), and d) are self-explanatory. The requirement listed under e) stems from the nature of scattering functions for particles under consideration. According to these, the most significant fraction of incident energy is scattered in the direction of the illuminating source. If the illumination phase angle is defined as the angle at the particle between the forward scattering direction and the direction to the instrument then, ideally, this angle should be 180^{o}. In practice, good signals can be obtained for phase angles near 130^{o} to 140^{o} and acceptable signals for angles as small as 90^{o}.

It is clear that of the five conditions listed above, four depend totally and one partially on the geometrical and dynamical nature of the spacecraft orbit in relation to the Sun's position and on the direction of the field of view relative to the Sun, namely, the spacecraft attitude.

It is pertinent to inquire what effect the selection of a particular orbit and of instrument orientation has on achievable observing times.

The objective of the present study was then to construct a suitable computing scheme to estimate the available observing time as a function of orbital circumstances. In addition, a number of other parameters were to be evaluated, which would enable the mission planner to establish conditions necessary to obtain optimum performance and to effect attitude changes should these be desirable.

2. Assumptions

In order to make the problem tractable it is necessary to limit its scope. For this reason a number of mission constraints were imposed and several simplifying assumptions made. The factors in question are enumerated below:

a) The gravitational field of the Earth is assumed to be that of an oblate spheroid.

Since the precision of determination of observing time, necessary for design purposes, is only moderate, such a model is quite adequate. Furthermore, since for this model orbital inclination i, semimajor axis a, and eccentricity e exhibit only periodic disturbances of small amplitude, their average effect is ignored, e.g.

$$\overline{\Delta i} = \overline{\Delta a} = \overline{\Delta e} = 0$$

b) For any value of the Sun's longitude, $\lambda_\odot$, the orbital parameters are assumed fixed throughout one orbital period. Clearly, the validity of this assumption is least tenable for orbits having large secular rates in the line of the nodes, Ω, and the line of apsides, ω. However, such orbits are also of least interest for Sisyphus missions.

c) The instrument is assumed to be spin stabilized.

d) The direction of spin axis is assumed invariant with time. Ultimately the extent of the validity of this assumption will depend on the exact configuration of the platform used to mount the Sisyphus system.

e) Observing time is considered lost when,

1) The vehicle is eclipsed by the Earth

2) The field of view encounters the Earth, whether the hemisphere is sunlit or not. Furthermore, the entire spin cycle is considered lost, even though the Earth may be encountered only during a part of it.

This assumption will clearly lead to a somewhat conservative estimate of the available observing time because those times when the vehicle is in the sunlight and the phase angle is acceptable and yet the field encounters the dark hemisphere of the Earth, will not be counted. Times computed under these conditions are to be viewed as potentially useful. The actual effective observing time will further be limited by whatever phase angle circumstance exists at the moment. Finally, the present discussion makes no allowance for limitations which may arise from the geometrical configuration of the vehicle and the attendant stray light which must be contended with.

3. Principal Parameters of the Problem

The ultimate quantity of interest in the present problem is the effective observing time available to a Sisyphus system in a given Earth orbit.

To arrive at this estimate, however, it is necessary to compute the following parameters:

a) The angle between the direction to the Sun and the spin axis (SPINSUN). Clearly, this quantity is necessary to define the illumination phase angle.

b) The angle between the direction to the Sun and the orbit normal (ETA).

c) The angle between the direction to the Sun and the vehicle radius vector (SUNVEH).

The two parameters listed under (b) and (c) play the critical role in establishing eclipse limits. Furthermore, the angle under (b) is of independent interest should one desire to investigate Earth oriented systems in which one axis is always pointed along the nadir direction.

d) The angle between the spin axis and the direction of the vehicle radius vector (SPINVEH). This is the critical quantity in establishing Earth's viewing limits.

In the following paragraphs expressions are derived from which the above quantities will be computed. Symbols assigned to these angles are those eventually employed in the computer code.

To proceed with the computation we shall require a number of auxiliary relations between frequently occuring quantities. In this discussion it is assumed that the reader is familiar with the basic terminology of positional astronomy.

4. Auxiliary Relations

a) Distance (ψ) Between Two Points on the Celestial Sphere

Let the coordinates of points P1 and P2 in the celestial equatorial and ecliptic systems be given by pairs (α_1, δ_1), (α_2, δ_2) and (λ_1, β_1), (λ_2, β_2) respectively. The geometrical circumstance of the situation for the equatorial system is shown in the following sketch:

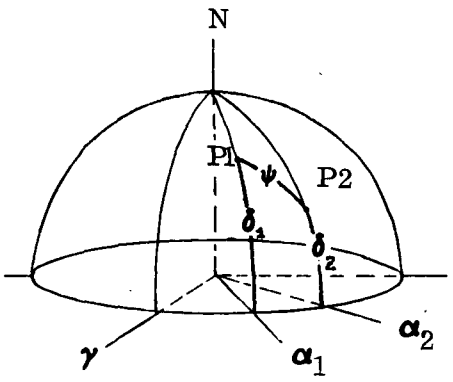

FIG. 17

The application of the cosine law to the triangle NP1P2 yields

$$\cos \psi = \sin \delta_1 \sin \delta_2 + \cos \delta_1 \cos \delta_2 \cos (\alpha_2 - \alpha_1) \qquad (12)$$

To express ψ in the ecliptic corrdinate system it is merely necessary to replace α's and δ's by the corresponding longitudes (λ's) and latitudes (β's).

b) Conversion of Coordinates Between the Equatorial and Ecliptic Systems

The relationship between the appropriate coordinates for a single point P is shown in Fig. 18.

By virtue of the three basic laws of spherical trigonometry applied to the triangle (EP) CNP (P) we have the following direct and inverse relations:

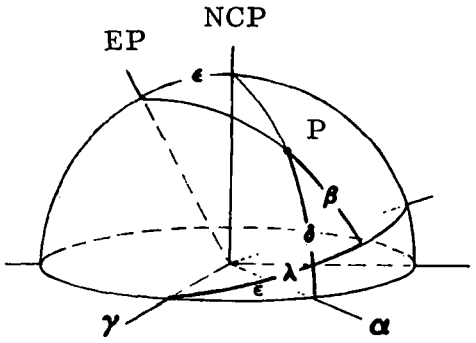

FIG. 18

$$\sin\beta = \sin\delta\cos\epsilon - \cos\delta\sin\epsilon\sin\alpha$$

$$\cos\beta\cos\lambda = \cos\delta\cos\alpha \qquad (13)$$

$$\cos\beta\sin\lambda = \sin\delta\sin\epsilon + \cos\delta\cos\epsilon\sin\alpha$$

$$\sin\delta = \sin\beta\cos\epsilon + \cos\beta\sin\epsilon\sin\lambda$$

$$\cos\delta\cos\alpha = \cos\beta\cos\lambda \qquad (14)$$

$$\cos\delta\sin\alpha = -\sin\beta\sin\epsilon + \cos\beta\cos\epsilon\sin\lambda$$

where ϵ is the obliquity of the ecliptic

c) Conversion of Orbital Orientation Elements Between the Equatorial and Ecliptic Coordinate Systems

Let the orientation of the orbit with respect to the equatorial system be described by the argument of the node, Ω, the argument of perigee, ω, and the orbital inclination, i. Let the corresponding elements in the ecliptic system be denoted by $\bar{\Omega}$, $\bar{\omega}$, and $\bar{i}$. Geometrical relationship between these two sets is shown in Fig. 19.

The required transformation expressions are obtained by applying the three fundamental laws of spherical trigonometry in either their basic or polar form to the triangle ABC of Fig. 19.

The resulting transformation of ecliptic elements into the equatorial ones are given by equations (15).

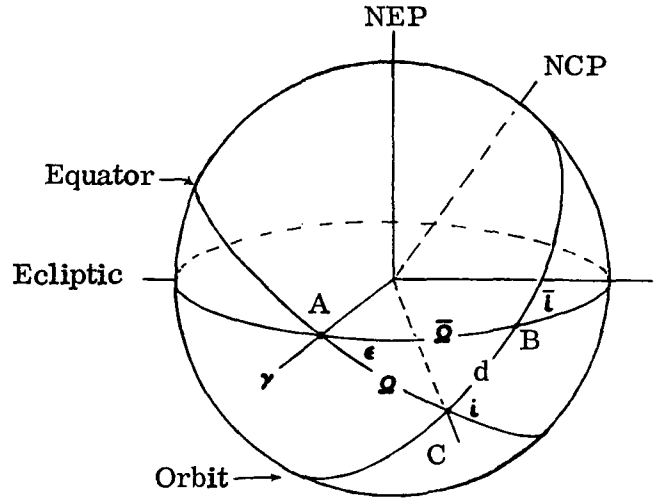

Fig. 19

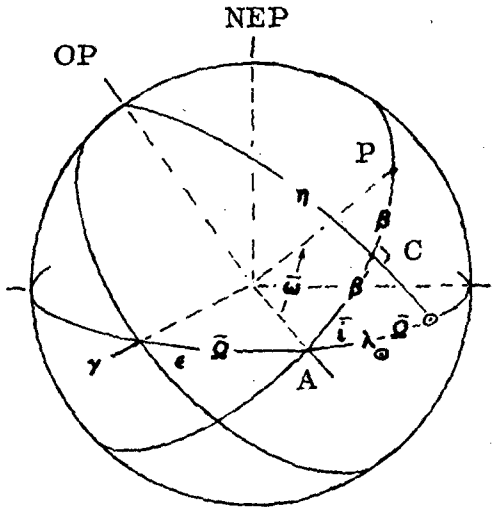

Fig. 20

$$\sin i \sin \Omega = \sin \bar{i} \sin \bar{\Omega},$$

$$\sin i \cos \Omega = \cos \bar{i} \sin \epsilon + \sin \bar{i} \cos \epsilon \cos \bar{\Omega}$$

$$\cos i = \cos \bar{i} \cos \epsilon - \sin \bar{i} \sin \epsilon \cos \bar{\Omega} \qquad (15)$$

$$\sin i \sin d = \sin \epsilon \sin \bar{\Omega},$$

$$\sin i \cos d = \sin \bar{i} \cos \epsilon + \cos \bar{i} \sin \epsilon \cos \bar{\Omega}$$

$$\omega = \bar{\omega} + d.$$

The inverse relations, that is, those transforming the equatorial quantities into their ecliptic counterparts are described by equations (16)

$$\sin \bar{i} \sin \bar{\Omega} = \sin i \sin \Omega$$

$$\sin \bar{i} \cos \bar{\Omega} = - \cos i \sin \epsilon + \sin i \cos \epsilon \cos \Omega$$

$$\cos \bar{i} = \cos i \cos \epsilon + \sin i \sin \epsilon \cos \Omega \qquad (16)$$

$$\sin \bar{i} \sin d = \sin \epsilon \sin \Omega$$

$$\sin \bar{i} \cos d = \sin i \cos \epsilon - \cos i \sin \epsilon \cos \Omega$$

$$\bar{\omega} = \omega - d.$$

d) Ecliptic Coordinates of the Vehicle as Functions of Position in Orbit

Let ν denote the true anomaly of the vehicle in the orbit and $\bar{u} = \nu + \bar{\omega}$, be the polar angle of the vehicle, measured in the orbital plane with respect to the ecliptic line of nodes. Consider now the right handed coordinate system whose positive x axis is directed to the First Point of Aries, z axis to the ecliptic pole, and y axis completes the required system. In such a system the rectangular and polar coordinates are given by

$$\begin{aligned} x_{ec} &= r(\cos \bar{u} \cos \bar{\Omega} - \sin \bar{u} \sin \bar{\Omega} \cos \bar{i}) = r \cos \beta v \cos \lambda v \\ y_{ec} &= r(\cos \bar{u} \sin \bar{\Omega} + \sin \bar{u} \cos \bar{\Omega} \cos \bar{i}) = r \cos \beta v \sin \lambda v \\ z_{ec} &= r \sin \bar{u} \sin \bar{i} \qquad\qquad = r \sin \beta v \end{aligned} \tag{17}$$

where βv, λv denote the celestial latitude and longitude of the vehicle.

e) Relations Between the Equatorial and Ecliptic Coordinates of the Sun

Let the right ascension, declination, celestial longitude, and celestial latitude of the Sun be denoted by $\alpha_\odot$, $\delta_\odot$, $\lambda_\odot$, and $\beta_\odot$. By definition $\beta_\odot = 0$.

By virtue of equations (3) we have then

$$\begin{aligned} \sin \delta_\odot &= \sin \lambda_\odot \sin \epsilon \\ \cos \alpha_\odot \cos \delta_\odot &= \cos \lambda_\odot \\ \sin \alpha_\odot \cos \delta_\odot &= \sin \lambda_\odot \cos \epsilon \end{aligned} \tag{18}$$

f) Angle, ψ, Between the Sun and an Arbitrary Point on the Celestial Sphere

If in equation (12) point P2 is identified with the Sun, and subscript 1 is dropped, we have

$$\cos \psi = \sin \delta \sin \delta_\odot + \cos \delta \cos \delta_\odot \cos (\alpha_\odot - \alpha) \tag{19}$$

The quadrant is uniquely determined by the algebraic sign of cos ψ, since $0 \leq \psi \leq \pi$.

As shown subsequently, it is convenient to carry out the requisite computations in terms of the Sun's longitude as the basic independent variable. In terms of this quantity cos ψ becomes

$$\cos \psi = (\sin \delta \sin \epsilon + \cos \delta \cos \epsilon \sin \alpha) \sin \lambda_{\odot} + \cos \delta \cos \alpha \cos \lambda_{\odot} \qquad (20)$$

5. Equations for Principal Parameters

a) Computation of ETA, The Angle Between The Sun and The Orbital Normal

A little reflection shows that the tip of the orbital normal has the following equatorial coordinates:

$$\begin{aligned} \alpha_N &= 3/2\ \pi + \Omega \\ \delta_N &= \pi/2 - i \end{aligned} \qquad (21)$$

Substituting α_N and δ_N into equation (20) and subsequently utilizing the second and third equations of (16) we obtain

$$\cos (\mathrm{ETA}) = -\sin \bar{i} \sin (\lambda_{\odot} - \bar{\Omega}) \qquad (22)$$

b) Computation of SPINSUN, the Angle Between the Sun and the Vehicle Spin Axis

Let the right ascension and declination of the spin axis, established at some point in the mission be α_s, δ_s. The desired angle is established by the use of equation (20) which yields

$$\cos (\mathrm{SPINSUN}) = (\sin \delta_s \sin \epsilon + \cos \delta_s \sin \alpha_s \cos \epsilon) \sin \lambda_{\odot} + \cos \delta_s \cos \alpha_s \times \cos \lambda_{\odot} \qquad (23)$$

c) Computation of SUNVEH, the Angle Between The Sun and the Radius Vector of the Vehicle.

Consider Fig. 21, showing positions of the Sun and the vehicle at some instant of time

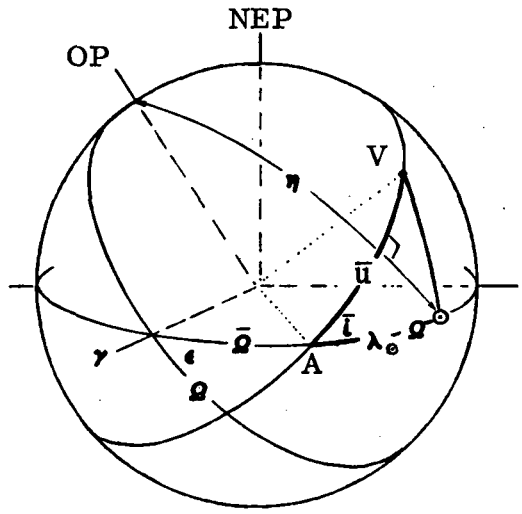

Fig. 21

The cosine law of spherical trigonometry, applied to the triangle AV⊙ yields

$$\cos (\text{SUNVEH}) = \cos \bar{u} \cos (\alpha_{\odot} - \bar{\Omega}) + \sin \bar{u} \sin (\alpha_{\odot} - \bar{\Omega}) \cos \bar{i} \qquad (24)$$

It is of some interest to establish conditions for which the Sun is on the vehicle's effective horizon. The geometrical aspects of this problem are illustrated in Figures 20 and 22.

The limiting value of SUNVEH, SUNVEH_{ℓ} is easily expressed as

$$\cos (\text{SUNVEH}_{\ell}) = \cos (90 + \eta_{\ell}) = - \sin \eta_{\ell} = -\sqrt{1 - \left(\frac{R_E}{R_{\ell}}\right)^2} \quad \text{and} \quad \cos \eta_{\ell} = \frac{R_E}{R_{\ell}}$$

where R_E is the Earth Radius and R_{ℓ} the magnitude of the vehicle's radius vector.

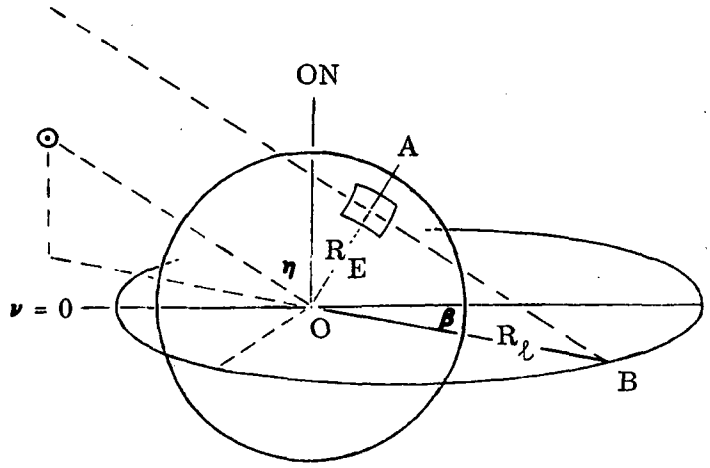

Fig. 22

It is reasonably easy to see that when

$$(\text{ETA} \equiv \eta) < \eta_\ell \qquad \text{or} \qquad \cos(\text{ETA}) > \cos \eta_\ell$$

the vehicle is in the Sunlight throughout the orbit. It is convenient to express this condition in terms of orbital parameters. To do this, project the Sun on the orbital plane and denote the angle between the perigee and the projected line by β. Furthermore, let β' represent the angle between the ecliptic line of nodes and the Sun's projection on the orbital plane. From the triangle ACO of Figure 20 we have, in general,

$$\cos(\lambda_\odot - \Omega) = \cos(\eta - 90^\circ)\cos\beta' + \sin(\eta - 90)\sin\beta'\cos 90^\circ$$

$$\therefore \quad \cos\beta' = \frac{\cos(\lambda_\odot - \bar{\Omega})}{\sin\eta} \tag{25}$$

Continued application of the laws of spherical trigonometry yields

$$\sin(\lambda_\odot - \bar{\Omega})\cos i = \cos(\eta - 90^\circ)\sin\beta' - \sin(\eta - 90^\circ)\cos\beta'\cos 90^\circ$$

$$\therefore \quad \sin\beta' = \frac{\sin(\lambda_\odot - \bar{\Omega})\cos i}{\sin\eta} \tag{26}$$

Clearly $\tan \beta' = \tan (\lambda_{\odot} - \bar{\Omega}) \cos \bar{i}$

From Fig. 20 we have

$$\beta = \omega - \beta'$$

Furthermore, it is convenient to define β as positive and always less than or equal to 180°.

For our purposes the general expression for the magnitude of the vehicle's radius vector is given with sufficient accuracy by

$$r = \frac{a(1 - e^2)}{1 + e \cos \nu} \tag{27}$$

The true anomaly, ν, corresponding to the limiting value of r, R_{ℓ} is given by $(\pi - \beta)$ so that

$$R_{\ell} = \frac{a(1 - e^2)}{1 + e \cos (\pi - \beta)} \tag{28}$$

6. General Remarks Concerning Eclipse Limits

When $\eta > \eta_{\ell}$ the vehicle will spend a fraction of its orbital period in the Earth's shadow. The instants of time at which the vehicle passes from the sunlit portion of the orbit into the eclipsed one can be obtained by noting that the quantity F_S, given by

$$F_S = \cos (\text{SUNVEH}) + \sqrt{1 - \left(\frac{R_E}{r}\right)^2} \tag{29}$$

changes the algebraic sign during this transition. In the sunlit part of the orbit $F_S > 0$ and in the shadow $F_S < 0$. The values of the appropriate times can be obtained analytically. In general, however, these times are defined by solutions of a quartic equation in true anomaly. Since ultimately the quartic in question lends itself only to numerical solution, it was found more convenient to treat this problem directly via equation (29). Details of this computation will be discussed later in the report.

7. General Remarks on Earth Viewing Limits

The essential geometrical situation of Earth viewing is shown in Fig. 23.

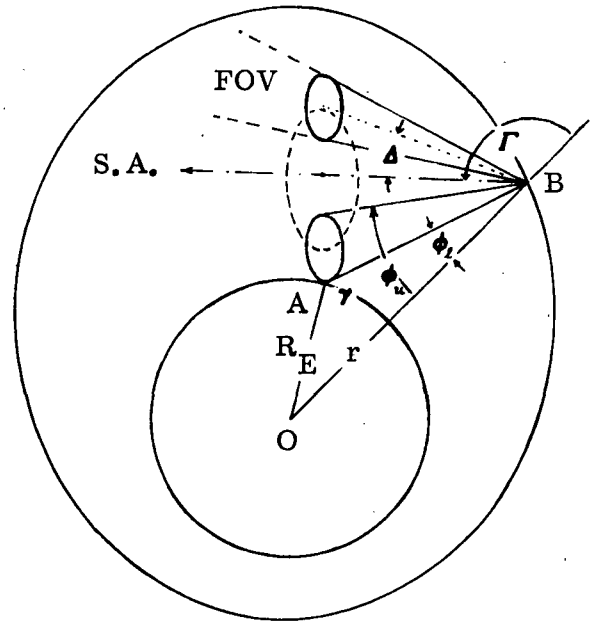

Fig. 23

In the above figure, φ_ℓ denotes the angle between the nadir of the vehicle and the edge of the field of view nearest the center of the Earth, φ_u -the corresponding angle of the edge farthest from the Earth's center, Γ represents the angle between the vehicle local vertical and the spin axis, and finally, Δ, is the angle between the spin axis and the optical axis.

From the triangle OAB it is evident that

$$\sin \varphi_\ell = \frac{R_E}{r} \sin \gamma$$

As the vehicle proceeds on its orbit, point A will travel along the surface of the Earth and eventually become tangent to if. At this point $\gamma = \pi/2$ and

$$\sin \varphi_\ell = \frac{R_E}{r}$$

Clearly, the quantity F_V, given by

$$F_V = \frac{R_E}{r} - \sin \varphi_\ell \tag{30}$$

is positive when the Earth is viewed, and vanishes when the lower edge of the field of view is tangent to the Earth's surface. With a further increase in true anomaly, φ_ℓ increases toward $\pi/2$ and R_E/r decreases relative to the value it had at tangency. Consequently at the point of tangency the function F_V changes its algebraic sign. A closer examination of the problem at hand shows that somewhere on the orbit φ_ℓ must necessarily approach the value of π. Consequently, there are other points on the orbit, not corresponding to the case when the field of view is tangent to the Earth, at which F_V alters its sign. Evidently then, the point of tangency is obtained, subject to the condition that $F_V = 0$ and $\varphi_\ell < \pi/2$.

8. Computation of the Shadow Interval

For our purposes the shadow interval is obtained with sufficient accuracy on the basis of umbra alone.

It is easy to see that for any orbit there are at most two points at which the vehicle enters and leaves the shadow. The time interval taken by a vehicle, moving in an elliptical orbit, to go from a point corresponding to the true anomaly ν_1 to that having true anomaly ν_2, is given by the well known Kepler's equation

$$M = E - e \sin E = n (t - T)$$

where M and E are, respectively, the mean and eccentric anomalies, n is the mean motion, and T is the time of perigee passage. From the above relation we have

$$M_2 - M_1 = n (t_2 - t_1) = (E_2 - E_1) - e (\sin E_2 - \sin E_1) \tag{31}$$

The required relations between the true and eccentric anomalies are given by

$$\sin E = \frac{(1 - e^2)^{1/2} \sin \nu}{1 + e \cos \nu} \qquad \cos E = \frac{e + \cos \nu}{1 + \cos \nu} \tag{32}$$

Finally $n = 2\pi/P$

where P is the orbital period.

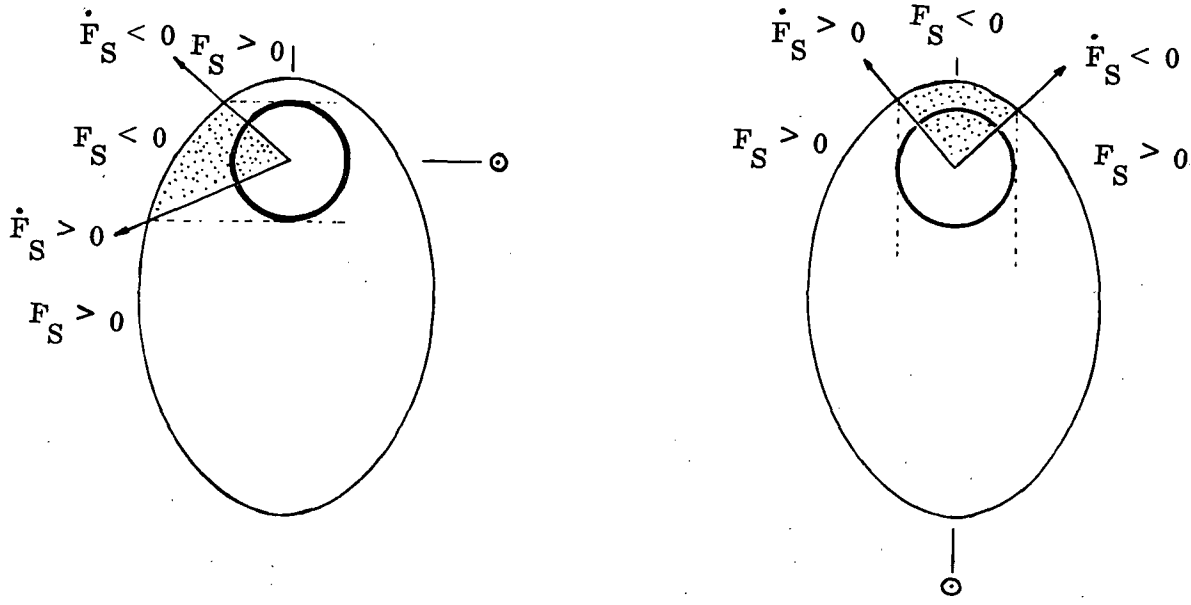

Fig. 24

From Fig. 24 it is easily seen that as long as $\Delta E = E_2 - E_1$ is less than 180°,

$$\Delta t = \Delta M/n \,. \tag{33}$$

If, however, ΔE exceeds π, the time interval in shadow is given by

$$\Delta t_s = P - \Delta t \tag{34}$$

where Δt is the value computed from equation (31). Another set of conditions which can be used to arrive at the proper value of Δt is based on the algebraic sign of the derivative of the function F_S with respect to true anomaly. As indicated in Fig. 24, if $F_{S1} < 0$ and $F_{S2} < 0$ the proper value of Δt is given directly by equation (31). If, on the other hand $F_{S1} > 0$ and $F_{S2} < 0$ the appropriate time interval is given by equation (34).

9. Computation of the Earth Viewing Intervals

The overall time interval during which the Earth could enter the field of view may consist either of a single interval or of two separate intervals. Which of these two possibilities obtains and what angular extent the intervals cover depends primarily on the angle between the spin axis and the major axis of the orbit, as well as on the angle between the optical axis and the spin axis. Typical geometrical configurations which may arise are shown in Figures 25 and 26.

Another complication in the computation of Earth viewing intervals is associated with the necessity of determining which edge of the field of view is nearer the Earth's center. A typical geometrical situation is shown in Fig. 26(D). Careful consideration of various configurations indicates that two possibilities exist.

When $\Gamma + \Delta > \pi$

$$\varphi_1 = \Gamma + \Delta - \pi - \rho/2 \qquad (35)$$

$$\varphi_2 = \Gamma + \Delta - \pi + \rho/2$$

When $\Gamma + \Delta < \pi$

$$\varphi_1 = \pi - \Gamma - \Delta + \rho/2 \qquad (36)$$

$$\varphi_2 = \pi - \Gamma - \Delta - \rho/2$$

where φ_1 and φ_2 represent the extreme edges of the field of view and ρ is the angular extend of the latter. The smaller of the two φ's is employed as φ_ℓ in equation (30). Note that whenever sign $(\varphi_1) =$ - sign (φ_2) the radius vector passes through the field of view and, in fact, if $\varphi_1 = -\varphi_2$, the optical axis lies along the radius vector. In actual computation it is found convenient to employ equations (36) to determine φ_1 and φ_2, but invert their sign whenever $(\Gamma + \Delta - \pi) > 0$. When $\Gamma + \Delta = \pi$, the proper value is obtained either from φ_1 or from $-\varphi_2$ of equation (36).

Having established the proper φ to employ in equation (30), we can use this equation to search numerically for the roots of $F_V = 0$. The roots for which $\varphi_\ell < \pi/2$ are the true anomalies at which the field of view is tangent to the Earth's surface. These in turn are used to obtain the necessary time intervals.

Unfortunately, due to the multiplicity of intervals the selection of central angles, ΔE, is not as straight-forward as it was in the case of a single shadow interval.

It is found that the most convenient way of computing Earth's viewing intervals is based on the behavior of the derivative, $\dot{F}_V$, of F_V with respect to true anomaly. Examination of Figures 25 and 26 reveals that, at the limiting values of φ_ℓ, the slope

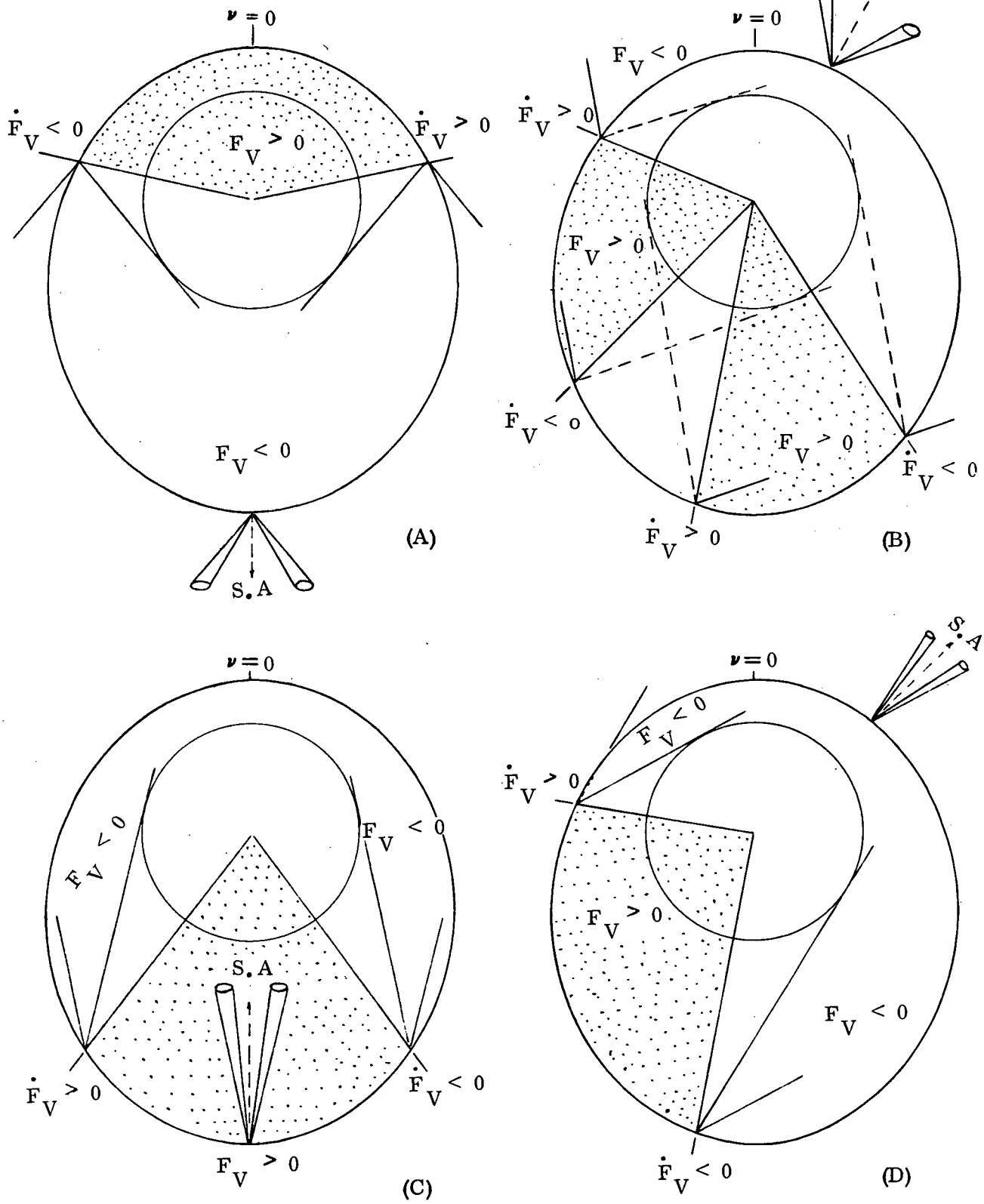
ν = 0
$\dot{F}_V < 0$
$\dot{F}_V > 0$
$F_V > 0$
$F_V < 0$
S.A
(A)
ν = 0
S.A
$F_V < 0$
$\dot{F}_V > 0$
$F_V > 0$
$\dot{F}_V < o$
$F_V > 0$
$\dot{F}_V < 0$
$\dot{F}_V > 0$
(B)
ν = 0
$F_V < 0$
$F_V < 0$
$\dot{F}_V > 0$
$\dot{F}_V < 0$
S.A
$F_V > 0$
(C)
ν = 0
S.A
$F_V < 0$
$\dot{F}_V > 0$
$F_V > 0$
$F_V < 0$
$\dot{F}_V < 0$
(D)

Fig. 25

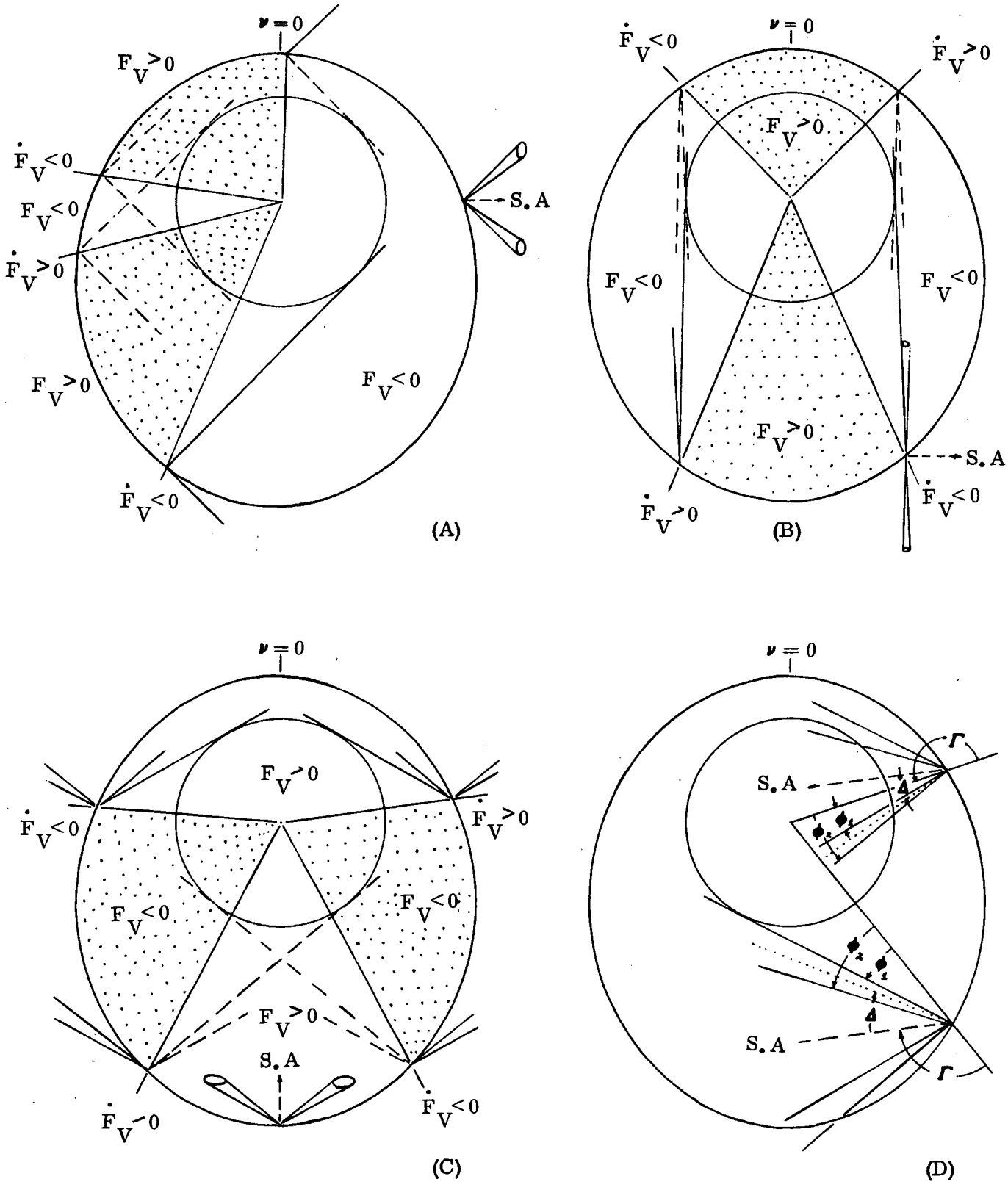
ν = 0
F_V > 0
Ḟ_V < 0
F_V < 0
Ḟ_V > 0
F_V > 0
F_V < 0
Ḟ_V < 0
S. A
(A)
ν = 0
Ḟ_V < 0
Ḟ_V > 0
F_V > 0
F_V < 0
F_V < 0
F_V > 0
S. A
Ḟ_V < 0
Ḟ_V > 0
(B)
ν = 0
F_V > 0
Ḟ_V < 0
Ḟ_V > 0
F_V < 0
F_V < 0
F_V > 0
S. A
Ḟ_V > 0
Ḟ_V < 0
(C)
ν = 0
Γ
S. A
Δ
S. A
Δ
Γ
(D)

Fig. 26

$\dot{F}_V$ can yield only the following two sequences of algebraic signs:

Sequence / φ_ℓ	I	II
	$\dot{F}_V$ Earth Not Viewed	$\dot{F}_V$ Earth Viewed
3	-	+
4	+	-
5	-	+
6	+	-

If the time instants corresponding to φ_ℓ's are denoted by t_3, t_4, t_5 and t_6, the overall intervals when the Earth is not viewed are given by

$$\Delta T = (t_4 - t_3) + (t_6 - t_5) \quad \text{for case I and} \tag{37-I}$$

$$\Delta T = P - (t_4 - t_3) - (t_6 - t_5)$$

$$= (t_5 - t_4) + P - (t_6 - t_3) \text{ for case II} \tag{37-II}$$

These relations continue to hold for the case when $\varphi_{\ell 5}$, $\varphi_{\ell 6}$ do not exist.

Details of the actual computation will be discussed later in the report.

10. Computation of the Effective Viewing Intervals

It is clear that within the assumed scheme of things observations are permitted only when the instrument is simultaneously not viewing the Earth and is not in the shadow; that is, when $F_S > 0$ and $F_V < 0$. A typical run of these two functions for a specific orbital geometry and instrument attitude is shown in the sketch below

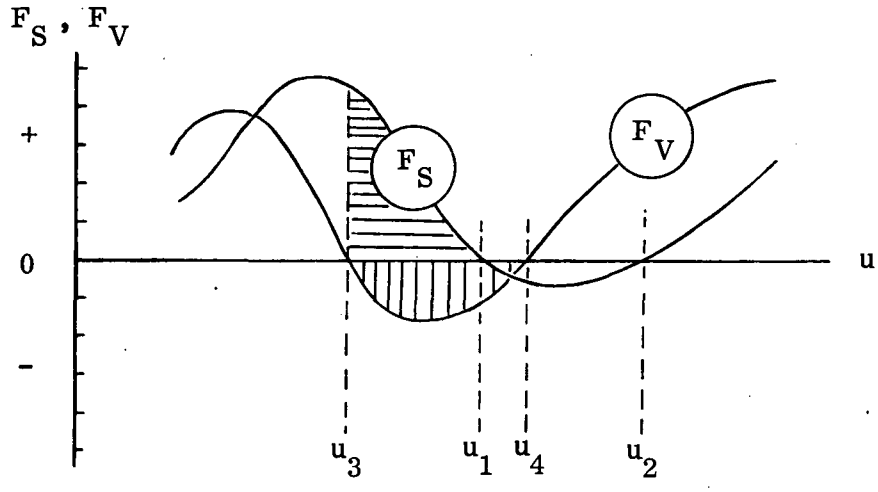

Fig. 27

where u_1,- u_4 are the values of the orbital polar angle at which either F_S or F_V vanish. For the indicated case the observing time corresponds to the interval between u_3 and u_1. Figure 27 indicates that in order to compute the available observing time it is necessary to establish relative phasing of the instants of time at which the functions F_S and F_V, measuring the shadowing and Earth viewing effects vanish. Furthermore, it is nesessary to keep track of the corresponding slopes, $\dot{F}_S$ and $\dot{F}_V$, in order to ascertain the order in which the vehicle passes from regions of one sign of F_S or F_V into the other.

Detailed consideration of possible geometries, one of which is displayed in Fig. 27, shows that observations are possible only during those intervals for which one of the following nine conditions obtains:

1) $F_S > 0$ and $F_V < 0$
2) $F_S > 0$ and ($/F_V/ \leq \epsilon$ and $\dot{F}_V < 0$)
3) ($/F_S/ \leq \epsilon$ and $\dot{F}_S < 0$) and $F_V < 0$ (38)
4) ($F_S > 0$ and $/F_V/ \leq \epsilon$) and $\dot{F}_V < 0$
5) ($/F_S/ \leq \epsilon$ and $\dot{F}_S < 0$) and ($/F_V/ \leq \epsilon$ and $\dot{F}_V < 0$)

6) $(/F_S/ \leq \epsilon$ and $\dot{F}_S > 0)$ and $(/F_V/ \leq \epsilon$ and $\dot{F}_V < 0)$

7) $(/F_S/ \leq \epsilon$ and $\dot{F}_S > 0)$ and $F_V < 0$

8) $(/F_S/ \leq \epsilon$ and $F_V > 0)$ and $(\varphi > \varphi_\ell)$ (38)

9) $(/F_S/ \leq \epsilon$ and $/F_V/ \leq 0)$ and $(\varphi > \varphi_\ell)$

where ϵ is the precision with which the roots of $F_S = 0$ and $F_V = 0$ have been computed. Evaluation of the required time instants is again carried out by Kepler's equation.

Details of the computational algorithm are discussed in the documentation of the computer program

11. Miscellaneous Orbital Parameters

a) Anomalistic Period

From the two body theory it is well known that the unperturbed anomalistic period is given by

$$P = \frac{2\pi}{\sqrt{\mu}} a^{3/2} \tag{39}$$

where μ is the Earth's gravitational constant whose value depends on the physical units employed. For instance, in cgs units $\mu = 3.98601 \times 10^{20}$ cm^3/sec^2. The exact value of this parameter depends on the values adopted for the radius and mass of the Earth and for the Universal Gravitational constant. However, within our adopted scheme of approximation such variations are unimportant. In this work, time will be expressed in hours and the semi-major axis in terms of the radius of the Earth ($R_E = 3441.8$ nautical miles). Under these conditions

$$P = 1.40835 \, (a/R_E)^{3/2} \quad \text{hours} \tag{40}$$

Perturbation of the motion due to the Earth's oblateness yields anomalistic periods which can be either longer or shorter than the unperturbed values, depending on whether the line of apsides advances or regresses. To the first order of approximation the perturbed and unperturbed periods are equal at inclinations of 54.7 and 125.3 degrees. However, since even in the most extreme case the differences between the periods do not exceed one part in a thousand, we shall not compute the perturbed period.

b) Nodal Time Rate of Change

As mentioned previously the first order analysis of perturbations due to Earth's oblateness yields secular changes only in the arguments of the node and perigee. The changes in the former are described by

$$\Delta\Omega = -\frac{3}{2} J_2 \left(\frac{R_E}{p}\right)^2 n \cos i \text{ radians/revolution}$$

where J_2 is the coefficient which represents a factor in the amplitude of the lowest zonal harmonic in the expansion of the Earth's potential and ρ is the semi-latus rectum of the orbit. If we adopt .001637 for $\frac{3}{2} J_2$ and express time in days, angular measure in degrees and p as a $(1 - e^2)$ we obtain

$$\dot{\Omega} = -10\left(\frac{R_E}{a}\right)^{3.5} (1 - e^2)^{-2} \cos i \text{ degrees/day} \qquad (41)$$

c) Aspidal Time Rate of Change

Similar considerations yield an expression for the secular change in the argument of perigee, ω. This change is given by

$$\Delta\omega = -\frac{3}{4} J_2 \left(\frac{R}{p}\right) n (1 - 5\cos^2 i) \text{ radians/revolution}$$

or

$$\dot{\omega} = 5.0\left(\frac{R_E}{a}\right)^{3.5} (1 - e^2)^{-2} (5\cos^2 i - 1) \text{ degrees/day} \qquad (42)$$

In principle, the semi-major axis, a, is the mean value with respect to true anomaly. However, since we have assumed no secular effect in this quantity such averaging need not be considered.

d) Sun Synchronous Orbits

From what has been said so far, one may suspect that the longest observing times would be obtained from vehicles following sun-synchronous orbits, that is, orbits which precess at the Sun's longitudinal rate and having inclination and perigee altitudes such that the vehicle never enters the Earth's shadow. Equation (41) can be used to strike such a compromise. For this purpose it is convenient to re-write this relation in the form

$$\cos i = -0.1\sqrt{2}\,\dot{\Omega}\left(\frac{r_a}{R_E}\right)^{3.5}\frac{\left(\frac{r_p}{r_a}\right)^2}{\left(1+\frac{r_p}{r_a}\right)^{1/2}}$$

where r_p and r_a are respectively the magnitudes of the radii vectors at perigee and apogee.

The above relation indicates that to obtain a sun following orbit, it is necessary to launch the vehicle into a retrograde orbit. Furthermore, for given perigee altitude and inclination, there exists a maximum apogee altitude for which the desired precession rate can be achieved. Extremal values of r_a and r_p are implicitly bounded by payload capabilities of available launch vehicles. Finally, it should be clear that the orbit cannot be a rigorously polar orbit because then the precession rate vanishes. Near polar orbits have other disadvantages as well. Thus, as i approaches 90^o, the only way to preserve $\dot{\Omega}$ at the solar rate value is to decrease either r_p or r_a. Both cases lead to a decrease of the semi-major axis and, therefore, of the period. In addition, too small a value of r_p may lead to unacceptably short lifetimes of the vehicle. Clearly, for a specific mission careful selection of these parameters is necessary if they are not to conspire to yield inadequate observing times.

e) Change of Independent Variable

Although the intrinsic independent variable of our problem is time (t) it is more convenient to compute various quantities of interest as functions of the Sun's position. The principal variables involved are α_o, Ω, and ω. Their variation with time is given by

$$\lambda_\odot = \lambda_{\odot in} + \dot{\lambda}_\odot t \tag{43}$$

$$\Omega = \Omega_{in} + \dot{\Omega} t$$

$$\omega = \omega_{in} + \dot{\omega} t \tag{44}$$

where $\lambda_\odot$ is the daily rate of change in Sun's longitude. This quantity is given to a sufficient precision by (360^o/365.25 days).

Elimination of time between (43) and each of (44) yields

$$\Omega = \Omega_{in} + (\dot{\Omega}/\dot{\lambda}_{\odot})(\lambda_{\odot} - \lambda_{\odot in})$$
$$\omega = \omega_{in} + (\dot{\omega}/\dot{\lambda}_{\odot})(\lambda_{\odot} - \lambda_{\odot in}) \qquad (45)$$

Since the time dependence of our problem is implicitly contained in variables ω and Ω and since, furthermore, the entire problem is sun dependent, it is convenient to employ Sun's longitude, $\lambda_{\odot}$, as the basic variable.

f) Location of Optical Axis as a Function of Time

The position of the optical axis for a spin stabilized instrument is computed by considering Figure 28, which displays the pertinent geometry. In this figure

ρ	=	angular separation of the optical and spin axes
$\nu = \omega t$	=	position angle of the optical axis measured from a reference meridian
β_o, β_s	=	Celestial latitudes of the optical and spin axis respectively
λ_o, λ_s	=	corresponding celestial longitudes
ω	=	spin rate
t	=	time

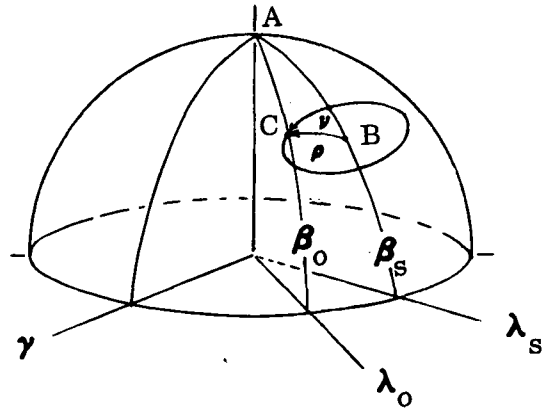

Fig. 28

Triangle ABC yields

$$\cos \beta_o \sin (\lambda_s - \lambda_o) = \sin \nu \sin \rho$$

$$\cos \beta_o \cos (\lambda_s - \lambda_o) = \cos \rho \cos \beta_s - \sin \rho \sin \beta_s \cos \nu \qquad (46)$$

$$\sin \beta_o = \cos \rho \sin \beta_s + \sin \rho \cos \beta_s \cos \nu$$

It must be realized that all arcs are parts of great circles.

All computations discussed in this section were programmed for the General Electric Time Sharing System. The listing of the program, its discussion and typical output are given in Appendix I. Representative results are given in the following examples.

B. Operational Examples

1. Example I.

This example has no other purpose than to show details of the program output for the case when all principal orbital parameters vary. To simplify the output, inclination, node, and argument of perigee are allowed to assume only two values. The longitude of the Sun is incremented in steps of 90^o until a range of 2π is covered.

Note that the quantity FF, corresponding to F_S or F_V, is less than the assigned tolerance, TOL, equal to 0.0001. In practice there is no need to print this quantity. The present form of the program retains FF because during the testing phase it was convenient to examine this quantity. Furthermore, for circular orbits RR, the radius vector corresponding to the eclipse and Earth's viewing limits, does not change and is always equal to the semi-major axis.

When the program has run through the complete cycle, determined by the number of inclination values to be used, a transfer is made to the beginning of the program. This condition is indicated by the printing of an equal sign. The program then halts and waits for a new set of input data. If no further computation is contemplated, the program execution is terminated in accordance with the procedure applicable to a given installation.

2. Example II.

Detailed examination of the available observing time was carried out for several randomly selected orbits. The first of these is a circular orbit having the following characteristics:

$e = 0$
$a = 3563.25$ n. m.
$h = 121.41$ n. m.
$i = i_{cr} = 63^{o}.4349$
ω = undefined
$P = 1.48$ hours

Since ω is undefined for a circular orbit, it is taken as zero in the computer input. The selected value of the inclination is equal to the critical value, for which the secular motion in the line of apsides vanishes. The initial value of the argument of the nodes is arbitrary and for a circular orbit its value does not affect the nature of long period results. Where appropriate, values of 0 and 90 degrees were examined. The initial direction of the spin axis is taken as $\alpha = 270^{o}$ and $i = -i_{cr}$ for all nodes. The field of view is nominally equal to 10^{o} and the angle between the spin and optical axes is 40^{o}. The initial value of the Sun's longitude is always taken as 0.0 degrees, that is, at the time when the Sun is in the First Point of Aries..

Under conditions specified, the angle between the Sun and the spin axis will be the same for all possible values of the initial node, and its variation throughout the year is shown in Figure 29. It is not too difficult to show that the maximum values attained by this angle are $180^{o} - (i - \epsilon)$ and $(i - \epsilon)$ respectively, where ϵ is the obliquity of the ecliptic. Figure 30 displays the yearly variation in the angle between the Sun and the orbit normal. The phasing of such a curve is clearly a function of the initial value of the node. Also shown on this curve are two envelopes of maximum and minimum values of the angle in question. These envelopes are given by $\eta_{max} = 90^{o} + i - \epsilon \operatorname{Sin} \lambda_{\odot}$ and $\eta_{min} = 90^{o} - i - \epsilon \operatorname{Sin} \lambda_{\odot}$. Recall that when $|\eta| > \eta_{cr}$ the vehicle is continuous sunlight. For a circular orbit this condition reduces to $|\cos \eta| > R_E/a$ which in the present case yields $\eta < 180^{o} - 15^{o} = 165^{o}$.

The dashed lines on Figure 30 are drawn at these levels. Thus, in our specific case, there will be four periods of approximately six days for each orbit when the vehicle is in continuous Sunlight. For the orbit specified by $\Omega_0 = 0^{o}.0$ these periods fall toward the end of April, the beginning of July, end of October and early January.

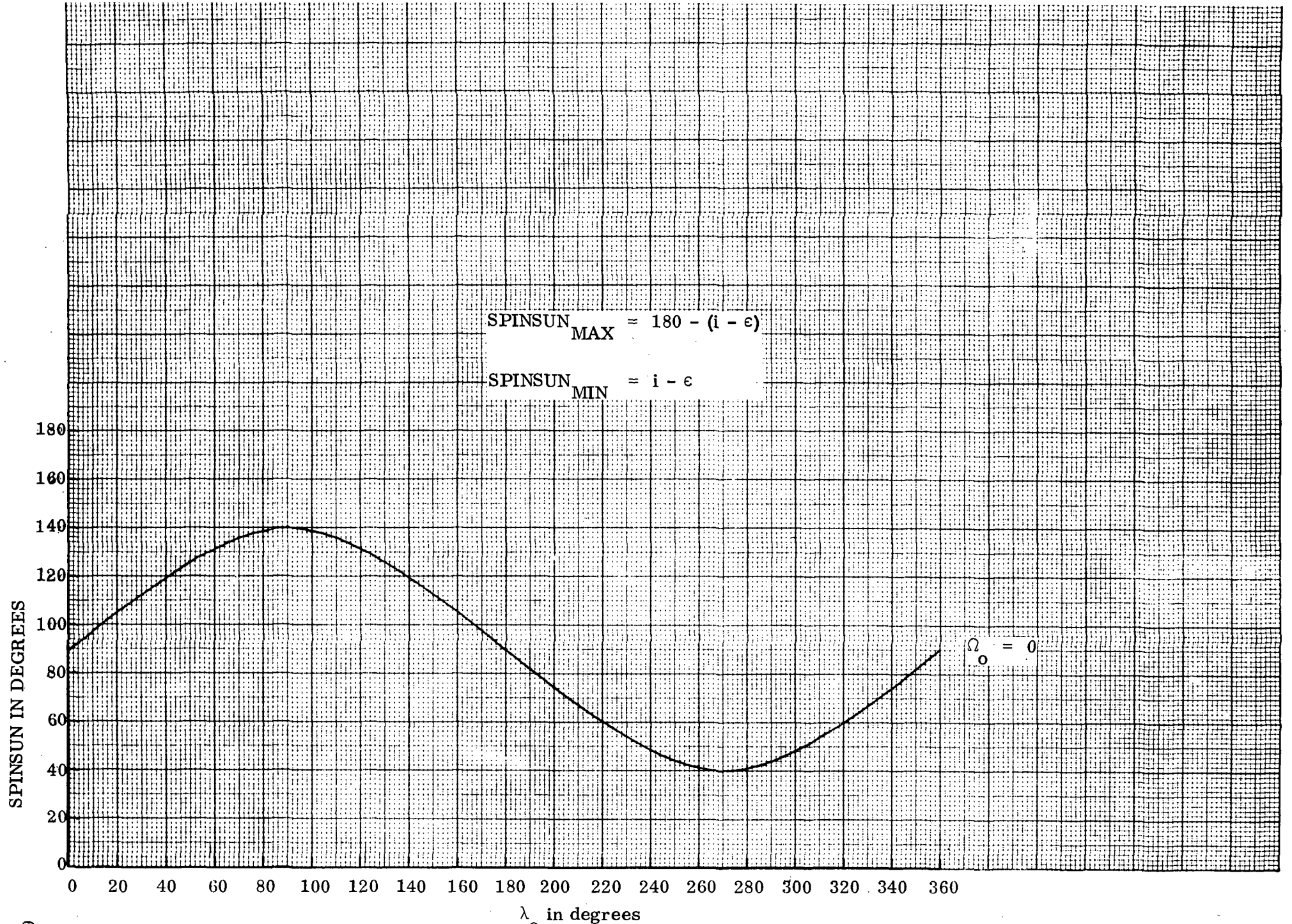
$SPINSUN_{MAX} = 180 - (i - \epsilon)$
$SPINSUN_{MIN} = i - \epsilon$
$\Omega_o = 0$
SPINSUN IN DEGREES
0
20
40
60
80
100
120
140
160
180
0 20 40 60 80 100 120 140 160 180 200 220 240 260 280 300 320 340 360
λ_Θ in degrees

Fig. 29

Fig. 30

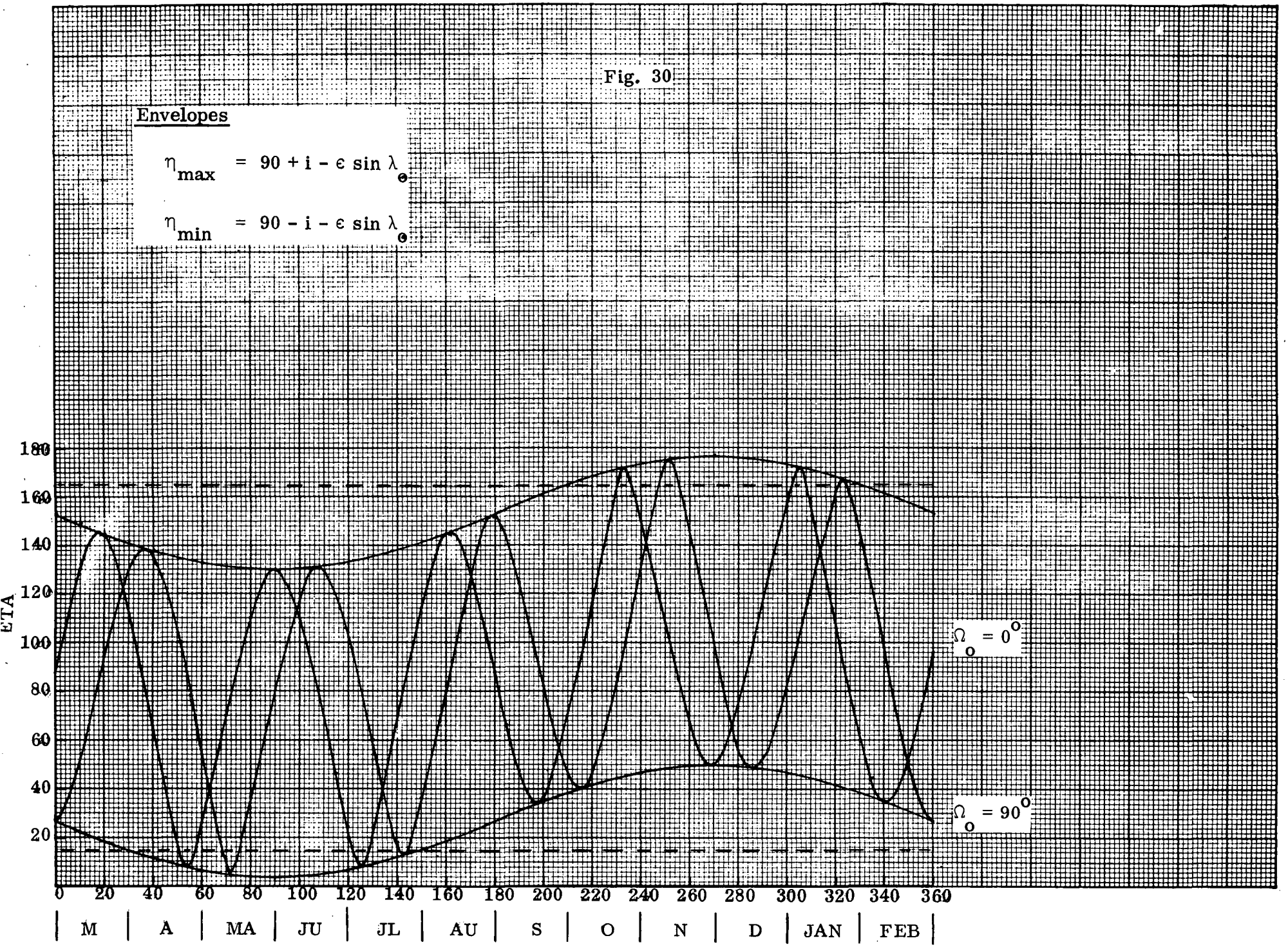
Envelopes
$\eta_{max} = 90 + i - \epsilon \sin \lambda_{\odot}$
$\eta_{min} = 90 - i - \epsilon \sin \lambda_{\odot}$
ETA
180
160
140
120
100
80
60
40
20
$\Omega_o = 0^o$
$\Omega_o = 90^o$
0 20 40 60 80 100 120 140 160 180 200 220 240 260 280 300 320 340 360
M A MA JU JL AU S O N D JAN FEB

This behavior is more clearly displayed in Figure 31, which shows the variation of time in shadow and the time when the Earth is not viewed. The narrow gaps in the former curve, in the vicinity of 51 to 58 degrees, 121 to 138 degrees, 221 to 226 degrees, and 301 to 308 degrees correspond to times when the vehicle will be in continuous Sunlight. Although Figure 31 also shows the time per period when the instrument may view the Earth, it contains no information on how the respective intervals are phased with respect to each other. Finally, Figure 32 shows the variation of time when the vehicle is neither in shadow nor viewing the Earth, that is the time potentially available to conduct observations. In the course of one year the above time constitutes about 19% of the orbital time. Should one consider only the interval from 160 to 360 degrees the fraction increases to about 35%.

It must be realized that the observing time is further limited by the illumination phase angle. For particles in question it is desirable that the angle at the particle between the direction to the Sun and the instrument be as small as possible or that the angle between the directions to the Sun and the optical axis of the instrument be as large as possible. It is easy to see that the corollary to these conditions is that

$$\text{SPINSUN} - \text{CAPDEL} \geq \theta^{\ell}$$

$$\text{SPINSUN} + \text{CAPDEL} \leq \theta^{u}$$

where SPINSUN and CAPDEL have been defined previously and θ^{ℓ} and θ^{u} are the acceptable lower and upper bounds which yield suitable phase angles. For instance, if the phase is not to be less than 90^{o}, then $\theta^{\ell} \sim 90^{o}$ and $\theta^{u} \sim 270^{o}$, and for the case under consideration $130^{o} \leq \text{SPINSUN} \leq 230^{o}$. This condition is satisfied between late April and early July. However, superposition of curves 29 and 32 indicates that this is the worst possible time for the orbit in question. This situation could be rectified somewhat by suitably altering parameters Ω_{o}, $\lambda_{\odot I}$, and (α_{s}, δ_{s}), namely, the launch time within a given day and year and the initial orientation of the spin axis.

3. Example III.

The purpose of this example is to investigate an eccentric orbit. Its characteristics, selected arbitrarily, are as follows:

$e = 0.2502$
$a = 4752.55$ n.m.
$h_p = 121.41$ n.m.
$h_a = 2500$ n.m.
$i = i_{cr}$
$\omega = 90$ degrees
$P = 2.29$ hours

The remaining parameters of the problem are the same as those for the previous example. Clearly, the variation of the angle SPINSUN will be the same as for

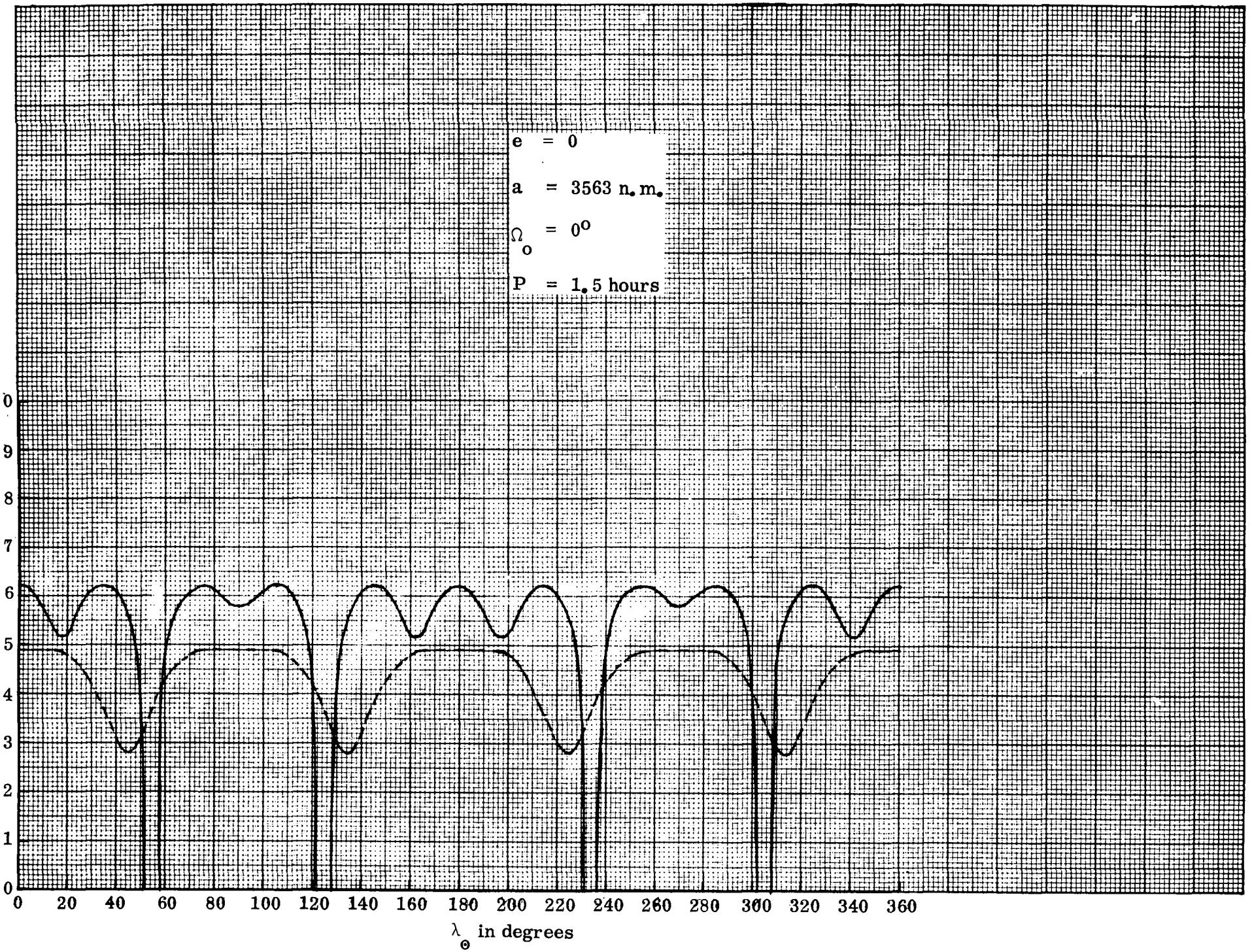
e = 0
a = 3563 n. m.
Ω_o = 0°
P = 1.5 hours
TIME IN SHADOW (HOURS) →
1.0
.9
.8
.7
.6
.5
.4
.3
.2
.1
0
0 20 40 60 80 100 120 140 160 180 200 220 240 260 280 300 320 340 360
λ_Θ in degrees
← TIME WHEN EARTH IS NOT VIEWED →

Fig. 31

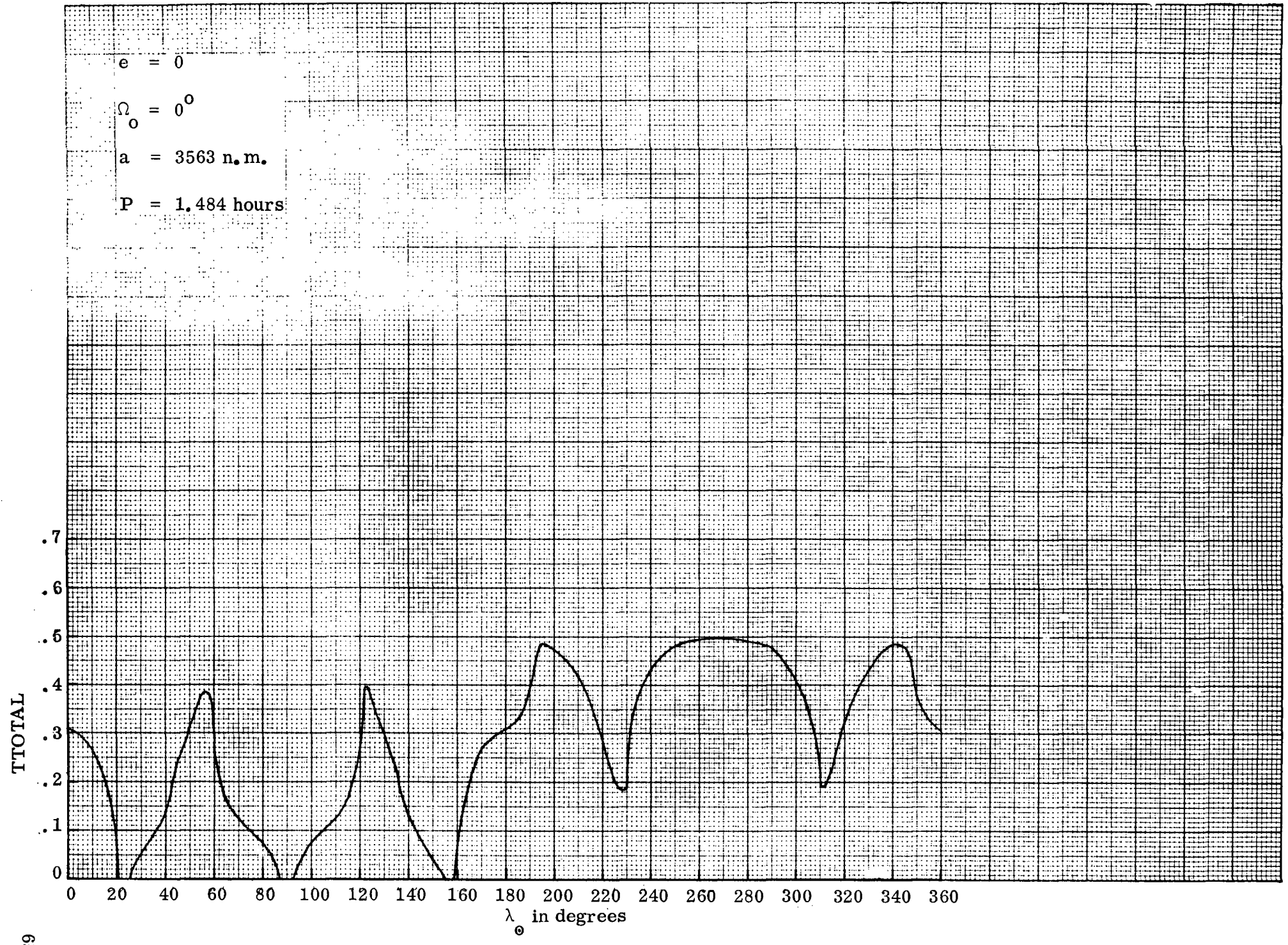
e = 0
Ω_o = 0°
a = 3563 n. m.
P = 1.484 hours
TTOTAL
.7
.6
.5
.4
.3
.2
.1
0
0 20 40 60 80 100 120 140 160 180 200 220 240 260 280 300 320 340 360
$\lambda_\odot$ in degrees

Fig. 32

the circular orbit of Example II, so that Figure 29 remains applicable to the present orbit. Other results are summarized in Figures 33, 34 and 35.

Figure 35 shows that the total fraction of the potentially useful observing time during the course of one year is 54%. During the first 6 months the fraction is 48%, during the second half of the year it increases to 60%. What makes this orbit ultimately unsatisfactory is the short duration during which acceptable phase angles obtain.

4. Example IV.

This example considers a circular orbit of relatively low inclination. The instrument package continues to be spin stabilized. System parameters are given by

$e = 0$
$a = 4441.84$
$h = 1000$ n.m.
$i = 38$ degrees
$\omega_0 = \Omega_0 = 0^o$
$P = 2.07$ hours
$\delta_s = 52^o$, $\alpha_s = 270^o$
$\Delta = 30^o$, FOV $= 10^o$

The results are shown in Figure 36. It is clear that the nature of phase angle variation makes this orbit virtually useless.

Note that in the examples given so far, the direction of spin axis once established, remains fixed in the inertial space. It is primarily this fact which leads to a narrow range of satisfactory phase angles. Observing time can be substantially increased if the spin axis direction is changed according to a pre-determined control law.

The next example treats such a situation.

5. Example V.

This example displays changes in the available observing time for a highly eccentric orbit in which a simple control law is used to position the spin axis of the instrument. The orbital elements selected for this computation are as follows:

$e = .4972$
$a = 7242.9$ n.m.
$h_p = 200$ n.m.
$h_a = 7401.9$ n.m.

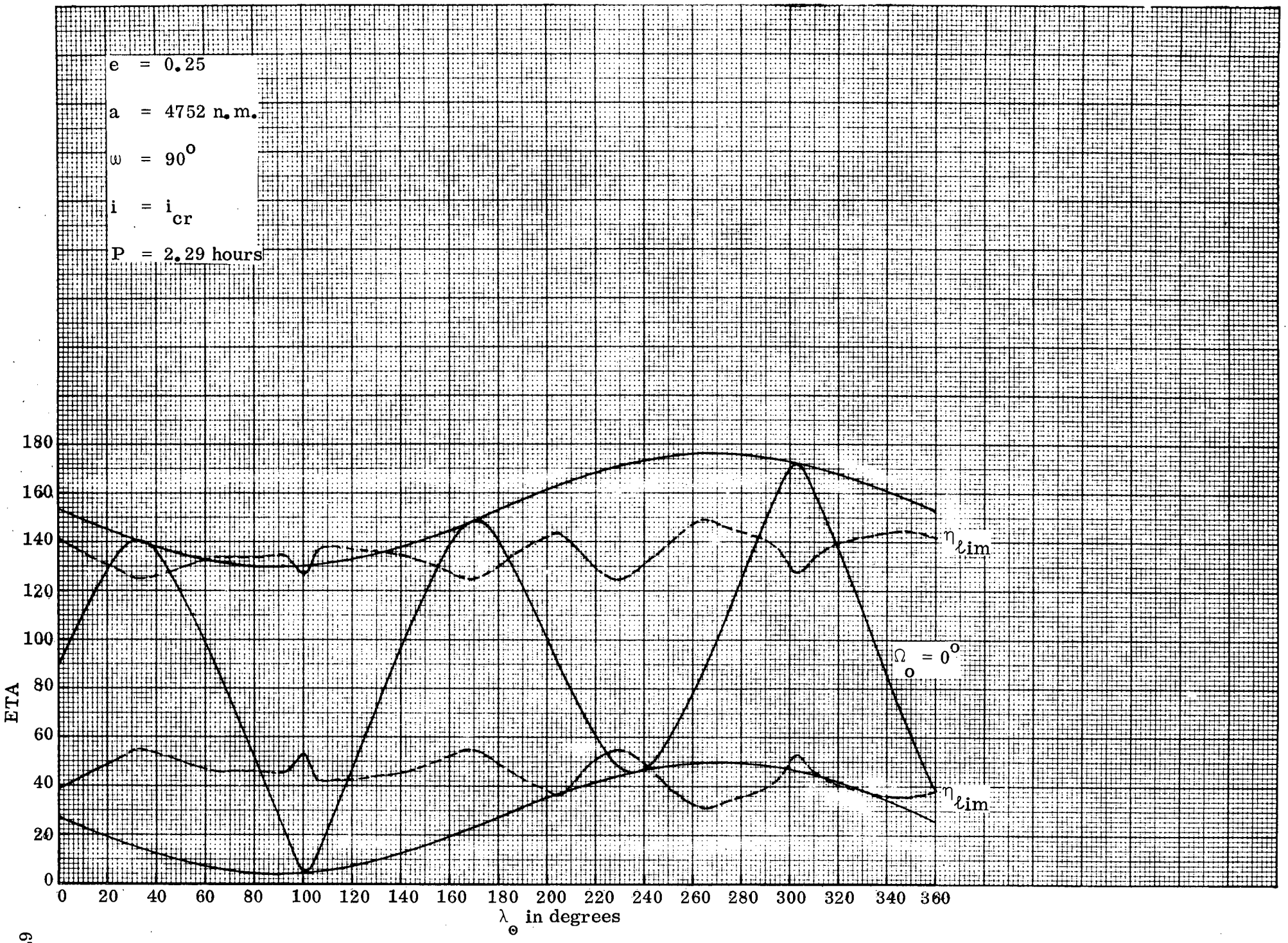
e = 0.25
a = 4752 n.m.
ω = 90°
i = i cr
P = 2.29 hours
ETA
180
160
140
120
100
80
60
40
20
0
0 20 40 60 80 100 120 140 160 180 200 220 240 260 280 300 320 340 360
λ Θ in degrees
η ℓim
Ω o = 0°
η ℓim

Fig. 33

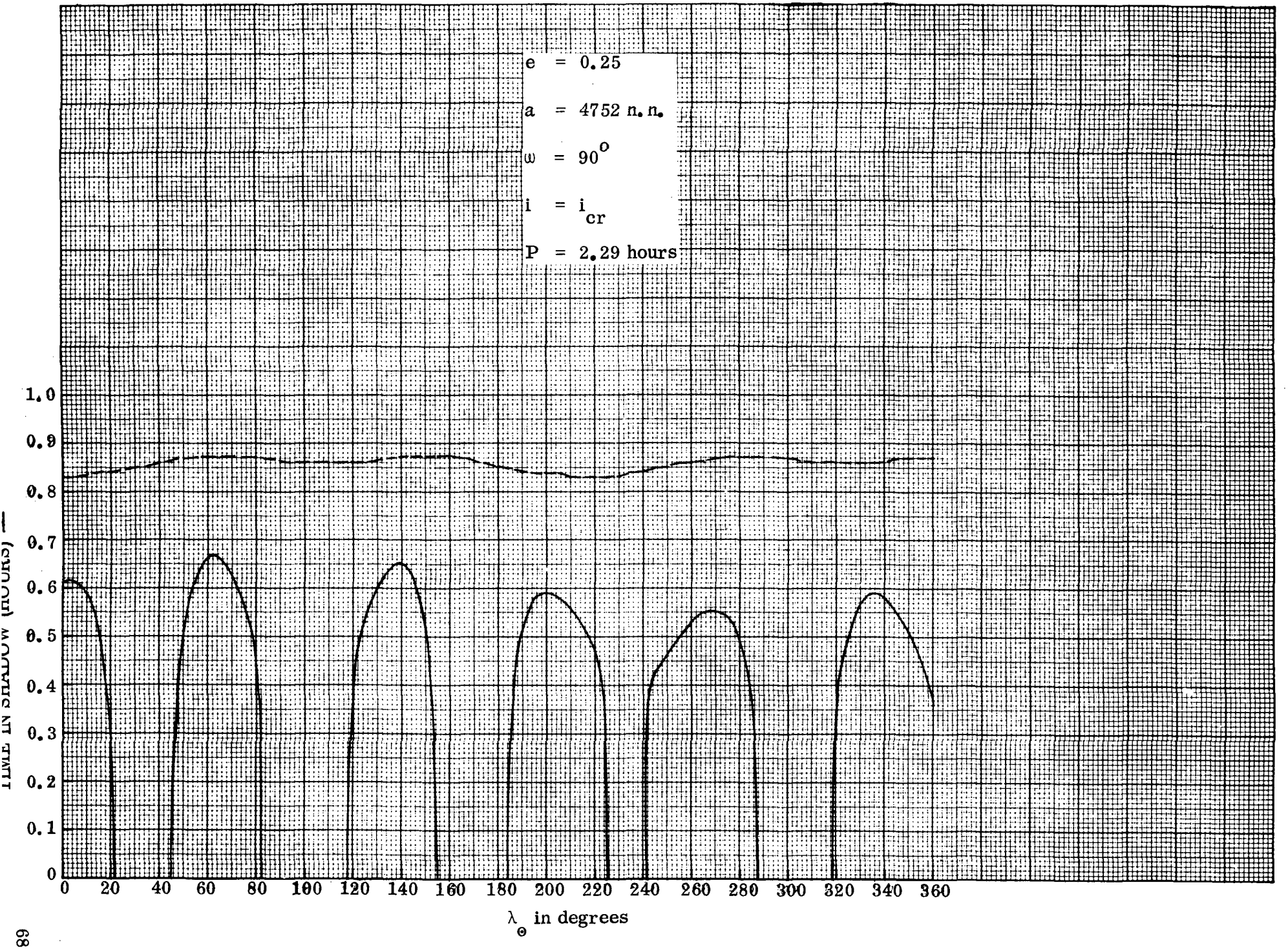
e = 0.25
a = 4752 n. m.
ω = 90°
i = i cr
P = 2.29 hours
TIME IN SHADOW (HOURS) —
TIME EARTH NOT VIEWED (HOURS) ---
1.0
0.9
0.8
0.7
0.6
0.5
0.4
0.3
0.2
0.1
0
0 20 40 60 80 100 120 140 160 180 200 220 240 260 280 300 320 340 360
λ Θ in degrees

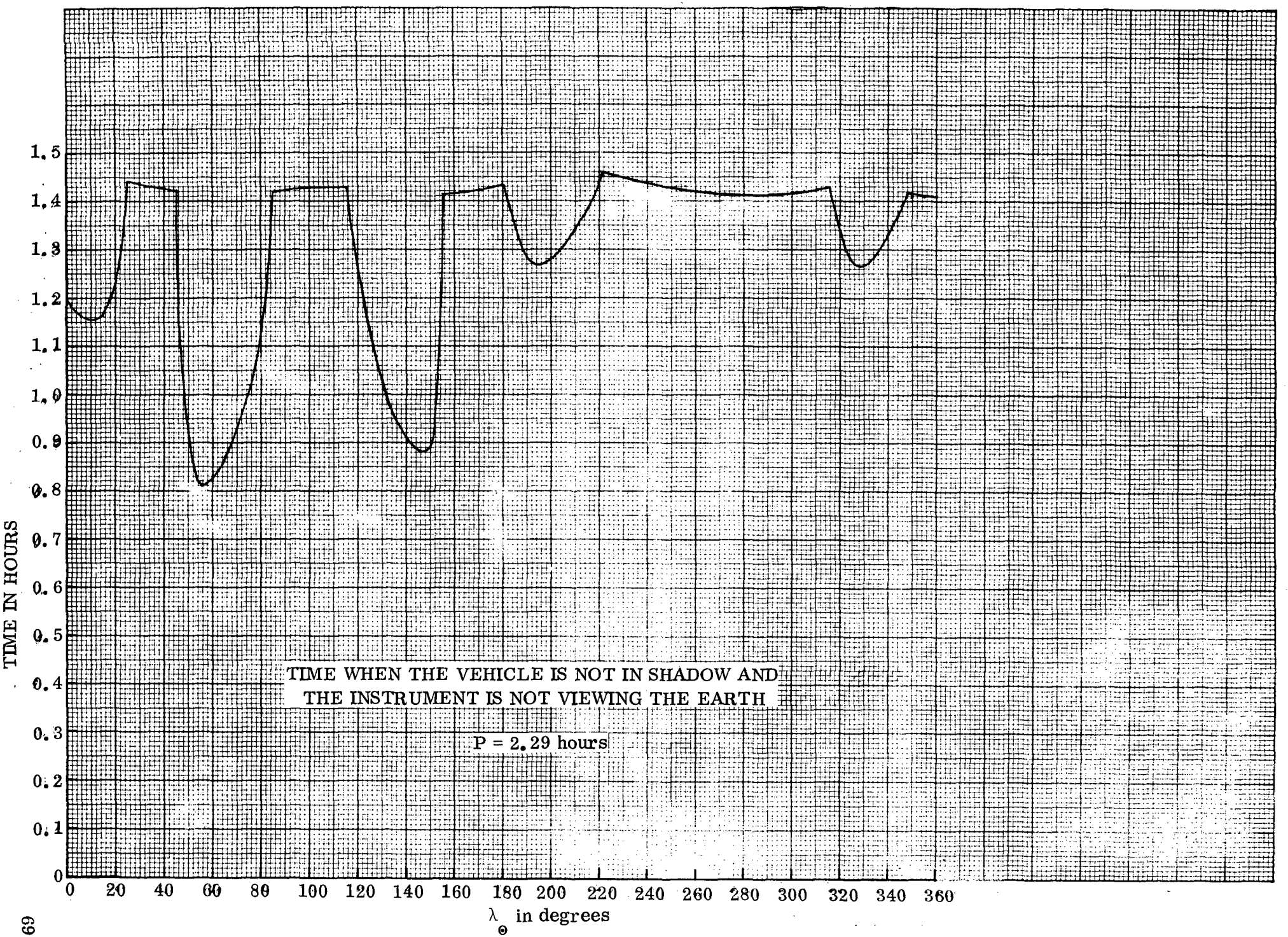
TIME IN HOURS
1.5
1.4
1.3
1.2
1.1
1.0
0.9
0.8
0.7
0.6
0.5
0.4
0.3
0.2
0.1
0
0 20 40 60 80 100 120 140 160 180 200 220 240 260 280 300 320 340 360
λ⊙ in degrees
TIME WHEN THE VEHICLE IS NOT IN SHADOW AND
THE INSTRUMENT IS NOT VIEWING THE EARTH
P = 2.29 hours

Fig. 35

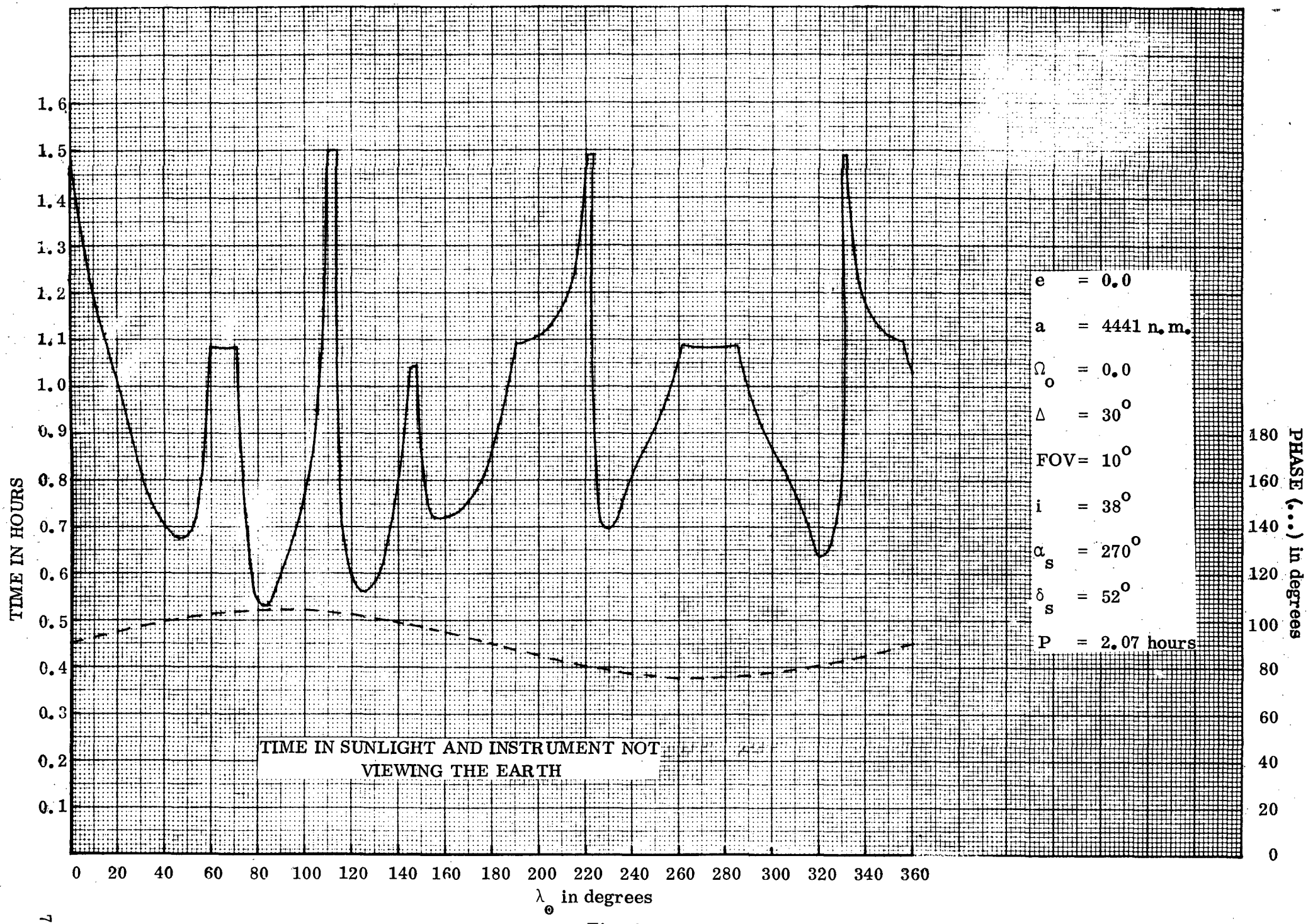
TIME IN HOURS
1.6
1.5
1.4
1.3
1.2
1.1
1.0
0.9
0.8
0.7
0.6
0.5
0.4
0.3
0.2
0.1
PHASE (...) in degrees
180
160
140
120
100
80
60
40
20
0
e = 0.0
a = 4441 n.m.
Ω_o = 0.0
Δ = 30°
FOV = 10°
i = 38°
α_s = 270°
δ_s = 52°
P = 2.07 hours
TIME IN SUNLIGHT AND INSTRUMENT NOT VIEWING THE EARTH
0 20 40 60 80 100 120 140 160 180 200 220 240 260 280 300 320 340 360
$\lambda_\odot$ in degrees

Fig. 36

$i = 140^{o}$
$\omega_o = 270^{o}$
$\Omega_o = 0^{o}$
$P = 4.299$ hours
$\delta_s = 40^{o}$
$\alpha_s = 270^{o} + \dot{\Omega}t$
$\lambda_{\odot I} = 90^{o}$

The payload capability of the SCOUT in such an orbit is approximately 100 pounds. The quantity α_s is the control law governing the position of the spin axis. Note that this is a sun following orbit and that the right ascension of the spin axis changes at 1^{o}/day at constant declination. The field of view is 10^{o} and the angle between the spin axis and the optical axis is 40^{o}. Results are summarized in Figure 37 which indicates that even in the worst case the phase angle is no smaller than 71^{o}.

If the spin angle is decreased to 30^{o} and the field of view to 8^{o}, the curve in Figure 37 is raised somewhat in the maxima and decreased in the minimum so that the total potential observing time is essentially unchanged. However, the minimum phase angle has now a more acceptable value of 82^{o}, occuring at the beginning and the end of the observing season. It is clear that the observing time could be increased further at the expense of more complexity in the control law by, for instance, positioning the spin axis in two directions.

6. Example VI.

Note that in Example V much of the loss of observing time between September and December is due to the advance of the line of apsides. Therefore, in the present example inclination is restored to its critical value. The orbit then is described by the following parameters:

$e = .3641$
$a = 5727.62$ n.m.
$h_p = 200$ n.m.
$h_a = 4371.2$ n.m.
$i = 116^{o}.56$
$\alpha_s = 270^{o}$ $\quad \delta_s = 40^{o}$
$\Delta = 30^{o}$, FOV $= 8^{o}$
$\Omega_o = 0^{o}$, $\quad \omega_o = 270^{o}$
$\lambda_{\odot I} = 90^{o}$
$P = 3.023$ hours
Payload $\approx$ 100 pounds

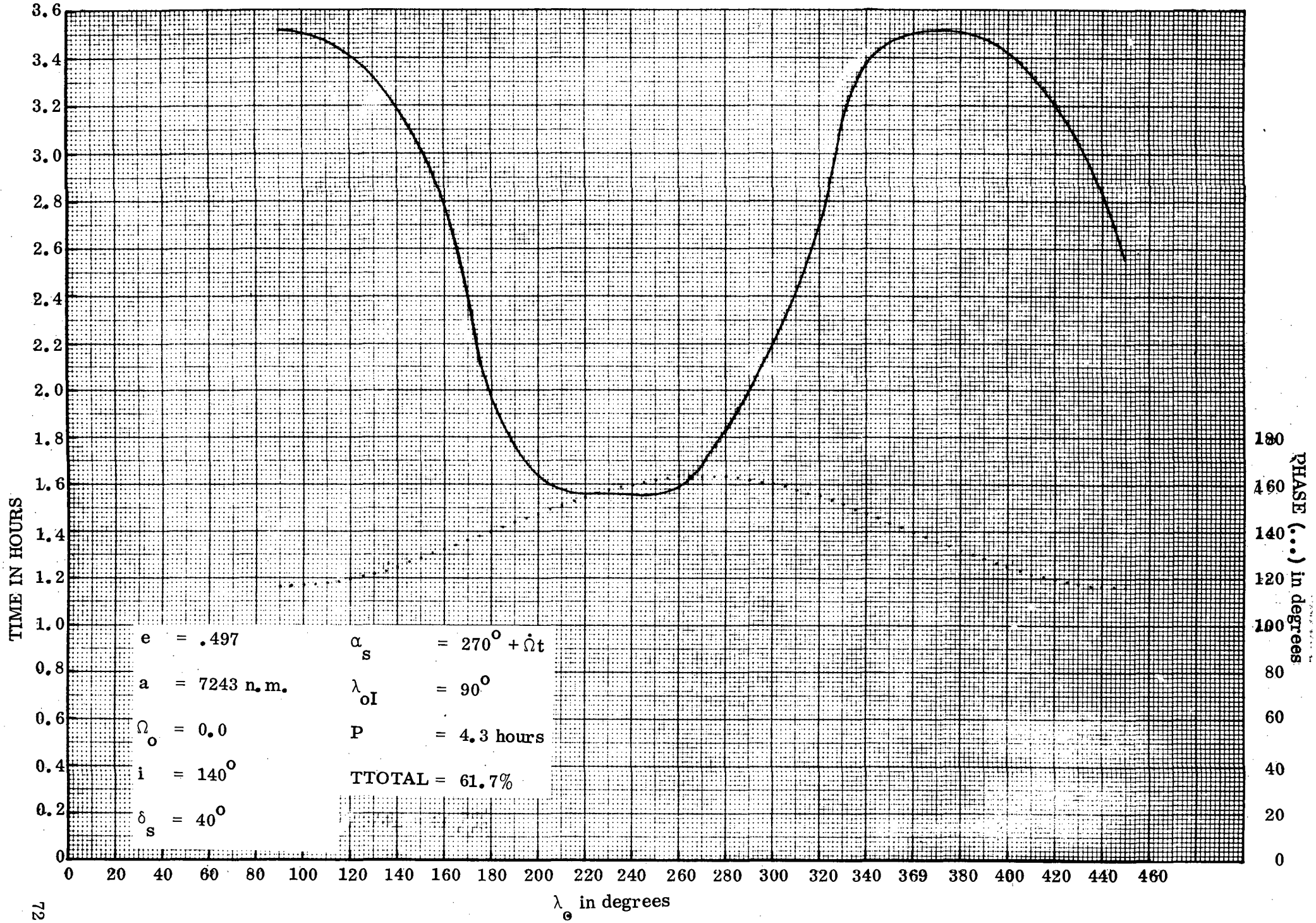
TIME IN HOURS
3.6
3.4
3.2
3.0
2.8
2.6
2.4
2.2
2.0
1.8
1.6
1.4
1.2
1.0
0.8
0.6
0.4
0.2
0
PHASE (...) in degrees
180
160
140
120
100
80
60
40
20
0
0 20 40 60 80 100 120 140 160 180 200 220 240 260 280 300 320 340 369 380 400 420 440 460
λ⊕ in degrees
e = .497
a = 7243 n.m.
Ω_o = 0.0
i = 140°
δ_s = 40°
α_s = 270° + Ω̇t
λ_oI = 90°
P = 4.3 hours
TTOTAL = 61.7%

Fig. 37

Furthermore, the orbit is a sun following orbit. With the parameters chosen, the vehicle is in continuous sunlight and the viewing time will be limited only by the encounters of the field of view with the Earth's surface. The variation of the angle between the Sun and the spin axis continues to be given by the curve shown in Figure 37.

Position of the spin axis is controlled in one axis only according to the same law as used in Example V.

Under conditions specified the effective observing time per orbit remains at a constant value of 2.32 hours throughout the year. If phase angles as low as 82^{o} are permitted then 77% of the total lifetime is available for observation. If the minimum allowable phase angle is 90^{o}, the above figure decreases to 57%. Another version of this experiment is not to spin the instrument, that is set $\Delta = 0^{o}$, but to continue controlling the position of the optical axis in the same way as above. In this case the useful time per orbit increases to 2.57 hours and the yearly percentages become 85% and 63% depending on the acceptable value of the phase angle.

Improvements achieved in this example are so large that the use of a highly eccentric sun following orbit at critical inclination is indicated.

7. Example VII.

Even a more dramatic improvement is possible if the stabilization system is used, such that the spin axis or the optical axis are continuously pointed in the antisolar direction.

The effect of the one axis control was studied by inserting at line 1200 the following statement

$$\alpha_{spin} = \alpha_{spinin} + \dot{\Omega}t.$$

The two axis control in the antisolar direction was simulated by inserting the following sequence of statements

01251 $\cos \delta_{spin} = (\cos^2 \lambda_{\odot} + \sin^2 \lambda_{\odot} \cos^2 \epsilon)^{1/2}$

01252 $\sin \delta_{spin} = - \sin \lambda_{o} \sin \epsilon$

01253 $\cos \alpha_{spin} = -\cos \lambda_{\odot} / \cos \delta_{spin}$

01254 $\sin \alpha_{spin} = - \sin \lambda_{\odot} \cos \epsilon / \cos \delta_{spin}$

The effect of changing the control law in the orbit of Example VI is shown in Figure 38. The total observing time is increased to 93% and, in fact, during a

significant portion of the vehicle lifetime 100% of the orbital time is available for observation. Clearly, since the instrument points in the antisolar direction, the phase angle has a constant value of 180^{o}, which is as desirable value as can possibly be achieved.

8. Examples VIII, IX and X.

Figure 39 shows the results for two retrograde circular orbits having the following parameters

	VIII	IX
e	= 0	
a	= 4141.84	4241.84
h_p	= 700 n.m.	800 n.m.
i	= 145^{o}	
Ω_o	= 0^{o}	
ω_o	= 0^{o}	
$\lambda_{\Theta I}$	= 90^{o}	$270.^{o}0$
P	= 1.859 hours	1.927
Δ	= 0^{o}	
FOV	= 8^{o}	

In both cases the optical axis is stabilized in the antisolar direction.

The total observing time is approximately equal to 44% of the orbital 1 year lifetime.

Results for example X are shown in Figure 40. This refers to a direct orbit with $i = 35^{o}$ and other parameters identical to those of EXAMPLE IX.

These examples indicate that for the low inclination orbits, observing time will be nearly the same whether one employs direct or retrograde orbits. The choice will then be dictated by the payload weight. Larger payloads can be launched into the direct orbits.

In conclusion,we point out that the orbits discussed above are compatible with the payload and orbital capabilities of the SCOUT launch system used either at WAFB or Wallops Island launch complexes.

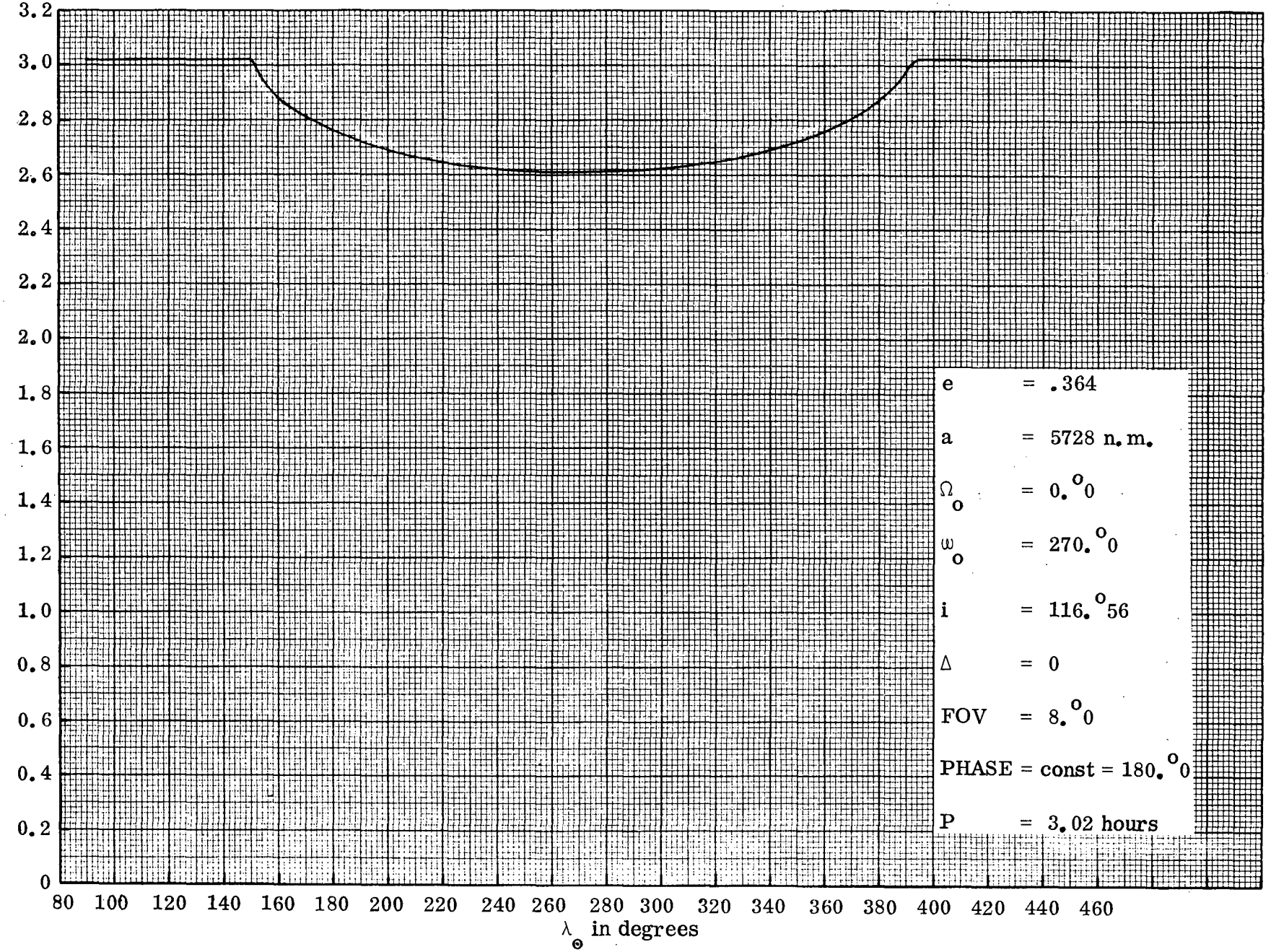
TIME/ORBIT IN HOURS
3.2
3.0
2.8
2.6
2.4
2.2
2.0
1.8
1.6
1.4
1.2
1.0
0.8
0.6
0.4
0.2
0
80 100 120 140 160 180 200 220 240 260 280 300 320 340 360 380 400 420 440 460
$\lambda_\odot$ in degrees
e = .364
a = 5728 n.m.
Ω_o = 0.°0
ω_o = 270.°0
i = 116.°56
Δ = 0
FOV = 8.°0
PHASE = const = 180.°0
P = 3.02 hours

Fig. 38

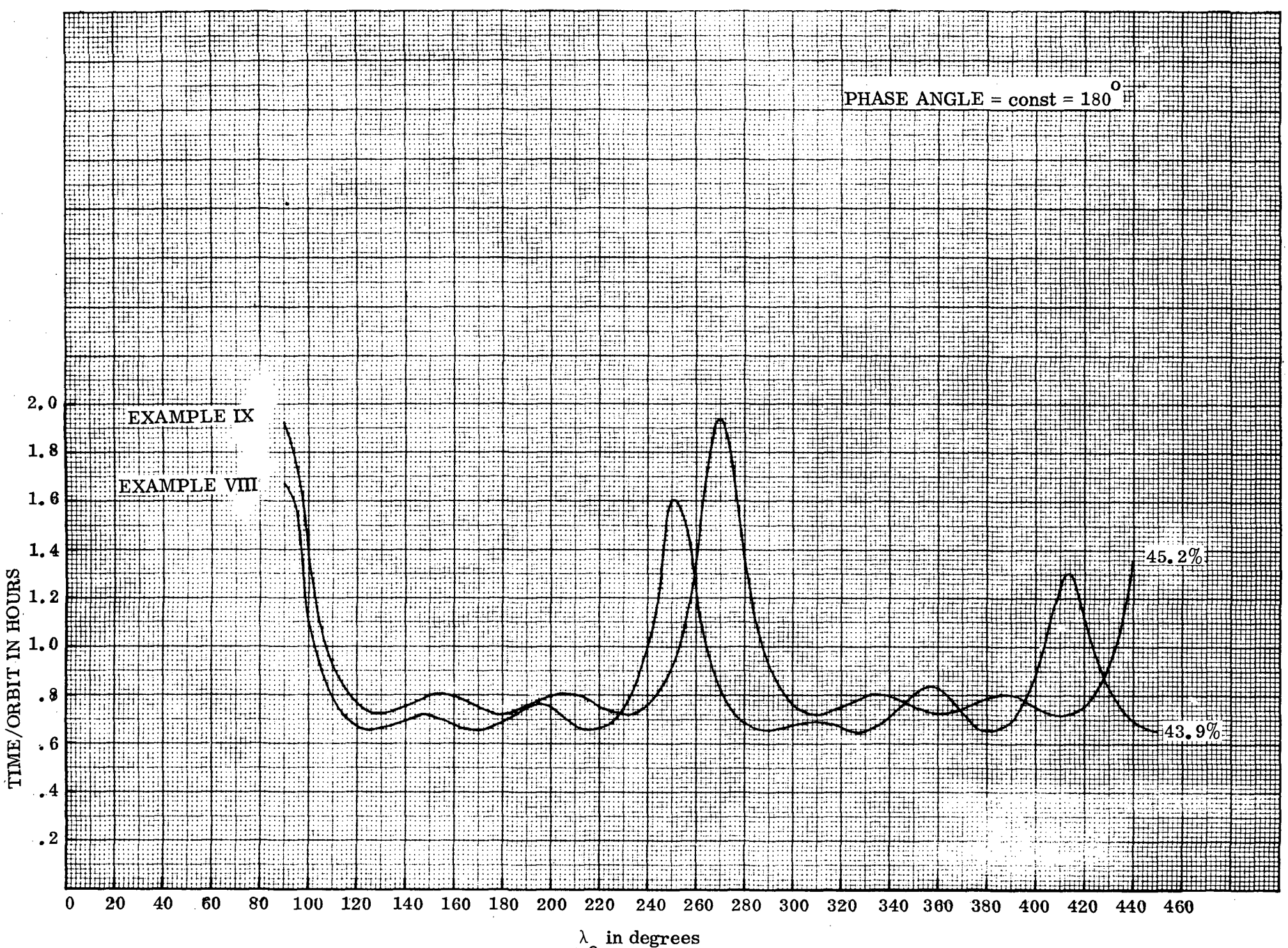
PHASE ANGLE = const = 180°
EXAMPLE IX
EXAMPLE VIII
45.2%
43.9%
TIME/ORBIT IN HOURS
2.0
1.8
1.6
1.4
1.2
1.0
.8
.6
.4
.2
0 20 40 60 80 100 120 140 160 180 200 220 240 260 280 300 320 340 360 380 400 420 440 460
λ⊙ in degrees

Fig. 39

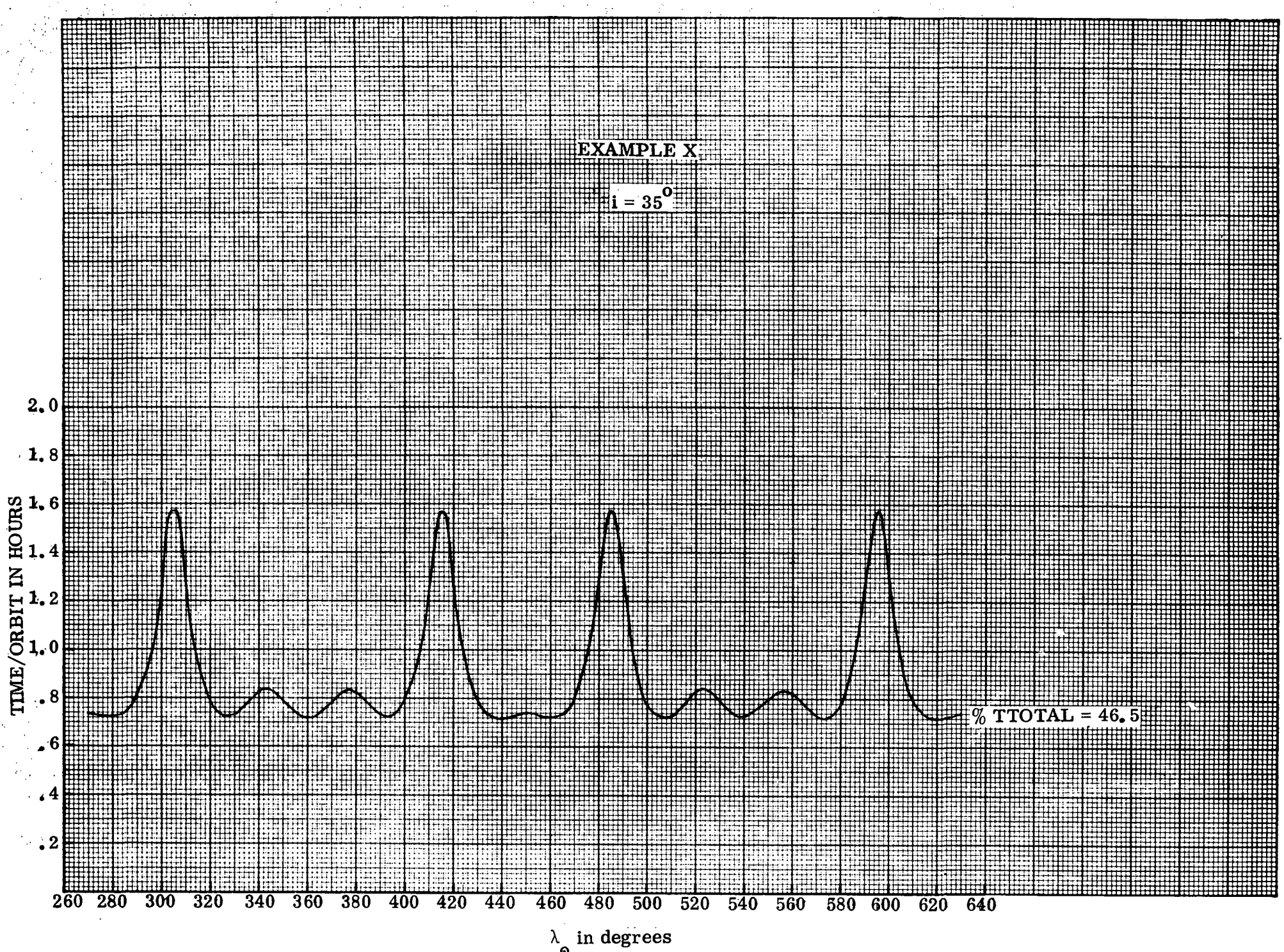
EXAMPLE X
i = 35°
TIME/ORBIT IN HOURS
2.0
1.8
1.6
1.4
1.2
1.0
.8
.6
.4
.2
% TTOTAL = 46.5
260 280 300 320 340 360 380 400 420 440 460 480 500 520 540 560 580 600 620 640
λ⊙ in degrees

Fig. 40

VII. PLATFORM SELECTION

A. General Considerations

The principal objective in selecting a platform for an Earth Orbiting Sisyphus is to achieve the lowest cost per unit of useful observing time. As shown in Section VI, the longest observing times are obtained for vehicles in Sun following orbits and for such attitudes, that the optical axis of the instrument is continuously pointing in the anti-solar direction. Stipulation of such conditions makes it abundantly clear that in order to achieve maximum observing time over a period as long as one year, the instrument must either represent a dedicated payload, or be combined with a payload whose instruments have similar requirements. Clearly, payloads devoted to solar measurements fall into the latter category. Launching a Sisyphus System in combination with instruments presenting mutually conflicting requirements will, of necessity, lead to losses in observing time. The amount of penalty incurred will depend on the nature of other instruments and, consequently, is difficult to estimate in advance.

One of the more important considerations in selecting a spacecraft for Sisyphus is the nature of the required shielding against stray light. Since the Sisyphus system measures sunlight reflected by a particle, the optical assembly must be protected from direct sunlight, Earth's reflected sunlight as well as light reflected by the spacecraft structure (booms, antennae, solar panels, etc.). This requirement imposes a severe constraint on the location of the instrument on the spacecraft. On sun synchronous, sun stabilized vehicles simple fixed baffles may provide full protection of the optics especially when the shading effect of spacecraft structures is utilized. Other kinds of attitude stabilization leads to serious complications. Detailed considerations of Earth oriented spacecraft, such as, Skylab, Payload Experiment Package (PEP), etc., show that the use of articulated, deployable sun shields is practically unavoidable. In fact, with such platforms it may be necessary to gimbal the whole instrument if reasonably long observing times are to be achieved.

In view of the generally simple structural arrangement of the Sisyphus instrument there seems to be insufficient justification to expend a large design effort on servo controlled gimbal mounts and articulated sun shields with their attendant high costs, increased weight and complications in the test, and checkout procedures. This is particularly so since the required observing times are achievable with much simpler systems.

The above factors were reviewed for a number of potential platforms with the intent of achieving cost effective designs.

B. Specific Platforms

A number of potential platforms were investigated for the present application. The platforms in question are either spin stabilized or have simple semi-active attitude control systems of minimal weight and power requirements. The achievable

precision in attitude angles is of the order of 1.°0, a satisfactory figure for the present needs. In the following paragraphs a brief description of each platform considered, is given.

It is to be noted that all costs stated subsequently are exclusive of the instrument costs. Present estimates indicate that a flight qualified instrument can be delivered in one year for approximately $525,000. This will cover parts and subassemblies for a 4 sensor head and the associated electronics subsystem. This cost includes electrical and environmental tests similar to those performed for the Pioneer F/G instrument, excluding shock, acceleration, humidity, and non-vacuum thermal testing. Furthermore, the above figure does not cover design of the software necessary for data interpretation. It is felt, however, that this will have become available in connection with the Pioneer project. Furthermore, the estimated cost does not include an elaborate sun shielding.

1. DELTA Payload Experiment Package (PEP)

Payload Experiment Package (PEP) is a subsystem module integrated with the DELTA vehicle designed to provide a stabilized platform in Earth's circular orbits. It is to be noticed that this is a so-called "Piggyback" vehicle, that is, the specific DELTA will be devoted to a primary mission, but since the second stage has excess payload capability, it can be utilized for other payloads. The platform based on the second stage is what will be known as the PEP. This platform will be stabilized by a Packaged Attitude Control System (PAC), and it will provide the necessary power, thermal control, command and communications interface, etc. A typical PAC is Semi-Active Gravity Gradient Systems (SAGS) of TRW. The current version provides stabilization about three axes with a precision of 2 to 6 degrees. It appears that with the addition of magnetic damping, stabilization accuracy of 1 degree can be achieved. The system can stabilize the final stage of the Delta Pac and an associated PEP in the attitude toward or away from the Earth, thus permitting Earth viewing or space viewing. It is not clear whether other attitudes can be called for. The SAGS system consumes 7 watts, weighs approximately 40 pounds, and occupies a 12 inch cube.

The PEP is to accomodate 150 to 200 pounds of experiments, but this is dependent upon the final weight of the primary payload. The shroud can accomodate payloads up to 5 feet in diameter. Total power capability would be approximately 170 watts for experiments. The minimum would be a total of 45 watts of which 27 - 28 watts are required for the vehicle. Power at 28 volts dc,regulated to ± 3 volts is to be available.

Continuous data logging with tape recorder storage and fast playback is anticipated.

Telemetry would employ 8 bit words, and a capability of approximately 128 commands is being considered. A launch rate of one per year is projected into circular orbits with altitudes between 200 to 900 n.m. Most launches will be into

the polar and near polar sun synchronous orbits from the Western Test Range. The Eastern Test Range would be used for launches into Earth Synchronous Orbits. The original feasibility study was conducted by the McDonnell Douglas Corporation. They are also involved in the design study which is to be completed in six month to one year. This corporation would also serve as the integrating contractor.

Preliminary cost figures are projected at 2.8 million in non-recurring costs for PEP and 0.8 million per vehicle when in full production. Integration costs would probably add another 0.2 million to the above figures.

At present it is not clear when to expect the first launch date. The most optimistic estimate would probably place it in the second half of 1973.

Examination of the projected PEP structure indicates that the current Sisyphus system can be accomodated in experiment bays 1 or 2. However, an arrangement would have to be made to cut the wall of the appropriate bay and hinge it so that it can be opened when the vehicle is in orbit. The hinged wall would then serve as the light shield against the Earth's shine.

The required power, command structure, data storage, and telemetry are compatible with the PEP package.

The most attractive feature of this arrangement is that the launch platform, and integration costs can be shared between a number of experiments. The most unsatisfactory aspect from Sisyphus point of view is the fact that (a) one has no orbital and launch time flexibility. These factors are defined solely by the prime payload, (b) the growth of the primary payload may use up the entire payload capability of the Delta, making projections for "Piggyback" operation nebulous, and, finally, (c) the presence of other experiments with the observing requirements different from those of Sisyphus could lead to an excessive loss of observing time.

Thus, PEP operation may yield the lowest cost per pound launched into orbit and yet for Sisyphus, this may be the least cost effective approach because the cost per observing hour may be too high. Since there is no way of saying what other instruments may be on board, it is not possible to estimate what the actual cost of PEP mounted Sisyphus may be.

In view of this, it is felt, that PEP has a restricted usefulness as a platform for an Earth Orbiting Sisyphus System.

2) The OWL System

This system was the first of the so-called University Explorer Satellites compatible with the SCOUT launch system. The original design called for three axis stabilization and a lifetime of one year.

The two flight units owned by NASA weigh about 180 pounds and are cylinders with a height of 33 inches and a diameter of about 30 inches. Power is obtained by approximately 2500 2 cm x 2 cm solar cells distributed on all sides and the average power available in the worst orbit is approximately 13 watts after radiation degradation corresponding to one year orbital lifetime. The solar cells trickle charge an array of nickel-cadmium batteries providing a general bus voltage of approximately 28 volts with an available tap at an unregulated 7 volts. Telemetry is pulse-code-modulated (PCM) at a radiated power of 2 watts. Data was to be transmitted in either real time or stored in one or both of two tape recorders for later transmission. The command system has the capacity of 70 commands.

Mechanically, the current Sisyphus could be integrated into this vehicle. The power, telemetry, etc. would be compatible with our requirements. The weakest aspect of the system is its stabilization system which employs magnetic interactions, consequently, its response is somewhat too slow to satisfy Sisyphus requirements.

Some of these vehicles are owned by NASA and are stored at Wallops Island launch facility. Necessary data for this system were obtained too late in the program to carry out a cost study.

3) S^4 DELTA System

This is a small spin stabilized scientific spacecraft designed to be carried "Piggyback" on the DELTA vehicle. It appears, however, that it could be launched by the SCOUT system.

The system has been designed and ground tested by AVCO Corporation. It is presumably available at a cost of something like 1 million excluding integration and launch costs. By present estimates these items would add about 1.3 million to the overall cost.

Since initially it appeared to be totally dependent on the DELTA launch system, it could not be justified as a dedicated platform. Furthermore, the prime payload would determine the allowable secondary payload and also define the orbit and launch time. For these reasons no further consideration was given to this system.

4) Small Applications Technology Satellite (SATS)

The SATS system is intended to be a quick reaction, multiple mission, small, low cost dedicated spacecraft, having orbital capability. The spacecraft will be standardized so that it can be "called-up", integrated, and launched in minimum time.

The concept has undergone extensive feasibility study at the Goddard Space Flight Center. Three operational possibilities have been considered in detail.

These are (a) a separate SCOUT launched mission, (b) a multiple SATS mission using DELTA launch system and (c) "piggyback" operation associated with the DELTA system.

The SATS spacecraft will be stabilized in three axes by some version of a semi-active attitude control system. Details of the control system have not yet been fixed. It appears, however, that a momentum wheel(s) in combination with horizon sensors will constitute the basic system. The system momentum vector can be precessed by either a magnetic torquing coil or by an auxiliary cold gas propulsion system. The latter would permit controlling the attitude of the spacecraft at will. The gas system would also be used in unloading the momentum wheels when the latter becomes saturated due to the accumulated disturbance momenta. The important fact is that such a system would provide nearly ideal attitude conditions for an Earth Orbiting Sisyphus system.

The spacecraft will be designed to accomodate power, communications, control, and data handling of a wide range of missions. Examination of the appropriate planning documents indicates that Sisyphus requirements would be compatible with SATS projections.

It is anticipated that in production the cost per spacecraft designed for 0.5 to 1.0 year lifetime would be between 2.0 to 2.5 million dollars. The estimated integration cost is about 0.2 million for the SCOUT launched system. It must be kept in mind, that for the latter system the current launch costs add approximately 1.3 to 1.6 million to the previous figures. The above expenditures are exclusive of the instrument cost. Finally, the current optimistic estimates indicate the first SATS spacecraft could be launched in mid to late 1974.

Clearly, the nominal cost of mating and launching a Sisyphus system with a SCOUT associated SATS is higher than that for a DELTA-Pack System. Nevertheless, the operational advantages are so striking that the cost per observing hour may in fact be lower. This is due to the fact that the system provides the flexibility needed to deliver the optimum Sisyphus operation. For these reasons a tentative mechanical layout was produced only for such a system.

a) SATS Configuration

The basic spacecraft design approach is shown in Figure 41. The configuration consists of five major subassemblies:

1. Experiment Module
2. Service Module
3. Experiment Adapter
4. Spacecraft Adapter
5. Solar Panels

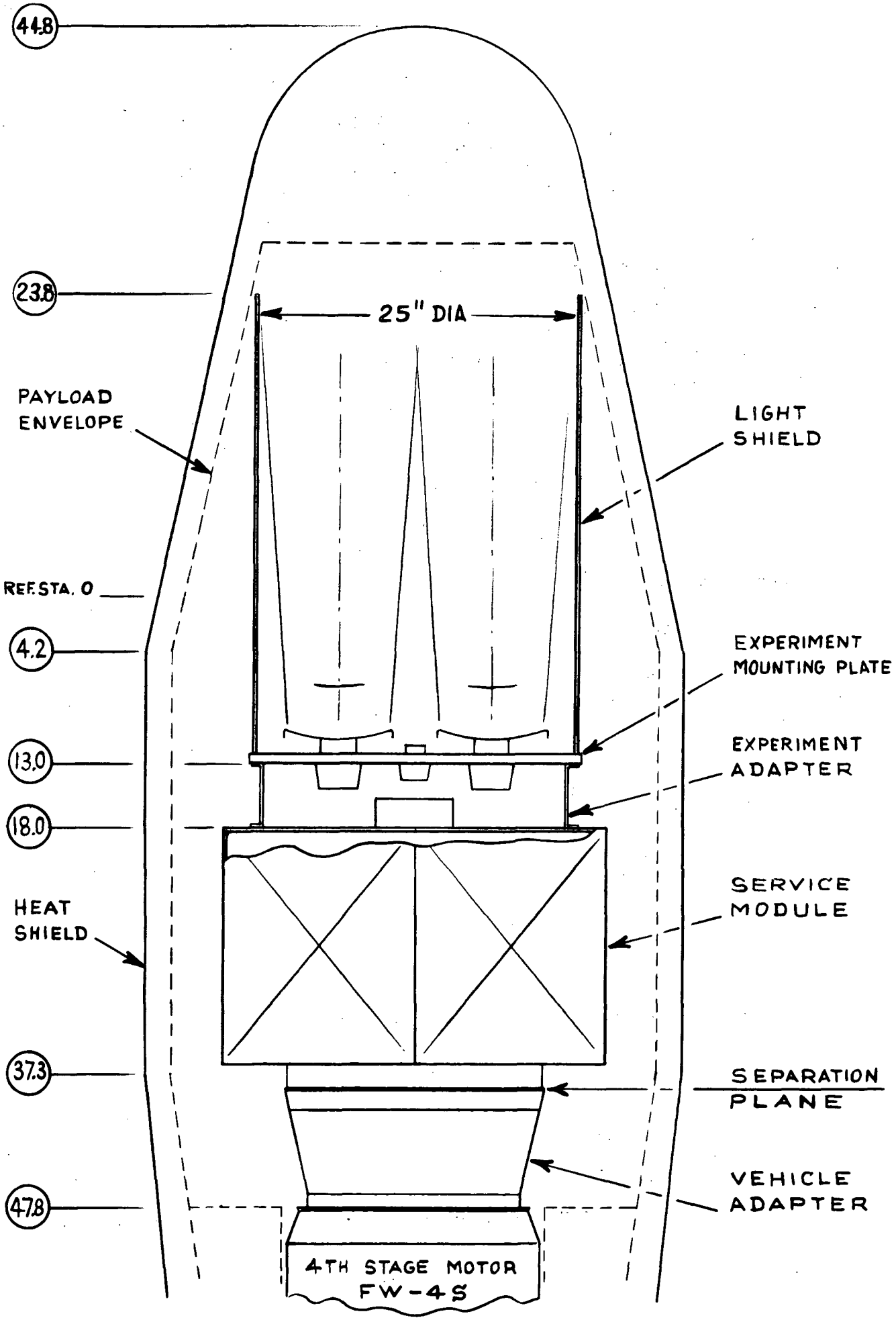
44.8
23.8
25" DIA
PAYLOAD ENVELOPE
LIGHT SHIELD
REF. STA. 0
4.2
EXPERIMENT MOUNTING PLATE
13.0
EXPERIMENT ADAPTER
18.0
SERVICE MODULE
HEAT SHIELD
37.3
SEPARATION PLANE
VEHICLE ADAPTER
47.8
4TH STAGE MOTOR FW-4S

Fig. 41

The experiment arrangement is similar to the Sisyphus design for Pioneer F/G. All components are attached to a 26" diameter 3/4" thick honeycomb mounting plate which is joined by an adapter ring to the service module top surface. Solar panels, attitude control system and antennas as part of the service module are not shown on the sketch. The length of the light shield is limited by the payload envelope and may be shortened depending on the service module size. The material (foamed Dylite) for the light baffle was selected based on tests performed for the Pioneer F spacecraft which showed adequate strength at minimum weight and cost. Due to the selected orbit and sun-earth oriented flight attitude a relatively simple fixed solar panel arrangement and related weight reduction of the power subsystem may be achieved. All experiment electronics are accommodated within the adapter ring and attached to the mounting plate allowing the experiment module to be tested and calibrated as a separate subsystem, which simplifies also the spacecraft checkout procedures resulting in low overall launch costs.

An approximate weight estimate is detailed in Table 2.

TABLE 2. SPACECRAFT WEIGHT

SERVICE MODULE

Structure	40.0	
Attitude Control	36.8	
Power	57.0	
Communications and Data	29.3	
		163.1

EXPERIMENT MODULE

Adapter	4.4	
Mounting Plate	2.4	
Lightshield	2.3	
Optics Assembly	4.5	
Electronics and Harness	3.1	
		16.7

SPACECRAFT ASSEMBLY TOTAL APPROXIMATELY - 180 POUNDS

5) SOLRAD Spacecraft

The SOLRAD series of spacecraft designed by the Naval Research Laboratory to measure various aspects of solar radiation is compatible with the SCOUT launch system. The latest spacecraft, SOLRAD 10(C), is a 12 sided "cylindrical" structure 30 inches in diameter, 24 inches high, weighing about 260 pounds. It employs four 6 x 12 inch solar cell panels which fold along the structure to fit into the SCOUT payload

envelope. The system employs two telemetry transmitters radiating about 3 watts. The data is stored in a 54 kilobit memory, which is read-out several times a day upon ground command.

The system employs an attractively simple attitude control system. The basic vehicle spins at 60 rpm. The spin axis attitude is controlled by an arrangement of 3 spin replenishment and four spin axis attitude control subsystems designed to maintain the spin rate at 60 rpm and the spin axis with $\pm 2^{o}$ of the sun line.

Solar sensors determine the angle to the sun and automatically apply control signals to the attitude spin subsystem. The spin rate is observed on the telemetry signal and is corrected by commanding a low-thrust ammonia or hydrazine gas system.

Attitude control subsystems 1 and 2 are redundant and share a common toroidal tank containing 9.5 pounds of liquid anhydrous ammonia. Each attitude control subsystem contains a solenoid valve, a latching valve and a nozzle. The latching valves and power for the solenoid valves are controlled by ground command and operation of the solenoid valves is controlled by solar sensor pulses. Upon receipt of the solar sensor pulses, ammonia vapor passes through the two sets of valves and nozzles and precesses the spin axis to within $\pm 2^{o}$ of the sun line.

Spin replenishment subsystems 1 and 2 are also redundant and share the same tank as attitude control subsystems 1 and 2. Each spin replenishment subsystem consists of a solenoid valve, a latching valve and a nozzle. Both the latching valves and the solenoid valves are controlled by ground command when spin replenishment is desired.

Attitude control subsystem 3 and spin replenishment subsystem 3 share a pair of spherical tanks containing five pounds of hydrazine and pressurized to 130 psi. Each subsystem contains a latching valve, a solenoid valve, a catalyst bed and a nozzle. The latching valve and power for the solenoid valve of attitude control subsystem 3 are controlled by ground command; operation of the solenoid valve is controlled by solar sensor pulses. Both the latching valve and the solenoid valve of spin replenishment subsystem 3 are controlled by ground command. The hydrazine system is being tested for future application in high-altitude follow-on SOLRAD satellites.

Characteristics of this spacecraft would, in principle, allow accomodating the current version of the Sisyphus system. Mounting the instrument to face out the back base, and launching the spacecraft into a Sun following orbit would provide Sisyphus with the necessary optimum observing conditions. Note, that the solar panels would provide added shielding against stray sunlight. Furthermore, observing requirements of solar instruments do not, in any way, conflict with those of the Sisyphus system. On the other hand, the spacecraft is small enough to serve as a dedicated platform.

At the present time insufficient details are available to establish costs associated with this platform.

VIII. CONCLUDING REMARKS

The present study indicates that a Sisyphus Optical Meteoroid Detector can be effectively employed on an Earth's Orbital mission. It is shown that for an instrument having a lifetime of approximately one year it is quite easy to obtain observing times of 50% of the orbital lifetime. Observing effectiveness of this order can be achieved without requiring special attitude control systems. Observing times approaching 90% of the orbital time can be reached for sun following orbits and relatively simple attitude control systems which would point the optical axis of the instrument in the anti-solar direction. Pointing need not be continuous, since the effectiveness of the instrument would not be impared by discrete adjustments in attitude at suitably selected instants of time.

It appears that at least three platforms can easily accomodate the Sisyphus instrument. These are, DELTA-PAC, SATS, and SOLRAD 10(C). Systems SATS and SOLRAD 10(C) are compatible with the SCOUT launch system and could be used as dedicated packages, thus providing nearly optimum conditions for Sisyphus operation. In principle the OWL and S^4 systems could also be used in the present application.

On the basis of our hardware experience with the Pioneer F/G instrument it is estimated that a flight qualified instrument designed for Earth orbital operation can be delivered at a cost of $525,000 in one year.

APPENDIX I.

COMPUTER PROGRAM

APPENDIX I

COMPUTER PROGRAM

A. GENERAL OUTLINE

The computations previously discussed were implemented on the General Electric Time Sharing System (DSCS) employing GE-605 central processor. In the present configuration the program requires 8000 storage locations of computer memory including I/O buffers. It was found that during peak loads, for reasons unknown, 16000 storage locations had to be requested.

The program is written in a modification of the FORTRAN IV language adapted for the GE Time Sharing System. In the present program, modifications concern primarily input/output statements. The adaptation to a different machine system are relatively straightforward.

The main program consists of eleven blocks each of which is introduced by a comment statement which is indicated by the asterisk. The main program employs three subroutines, QTEST, SPINVEH, and SUNVEH. Communication between the main program and these subroutines is via the COMMON area.

Input to the program consists of five statements (00400 to 00450). Each quantity appearing in these statements is defined at the beginning of the program. Note that the input is formatless, items being delimited by commas with the exception of the last item on the list.

The output has the general form

```
LONSUNØ  = XXXX.XX    ECC      = X.XXX     AØ = X.XXXXXXXXE+XX    CAPDEL = XXX.XX
      P  = XX.XXX     FOV      = XX.XX
NODEDOT  = XXXX.XX    PERDOT   = XXXX.XX   INC = XXX.XX
                      NODEREF  = XXX.XX
REFARPER = XXX.XX
```

```
LONSUN          ETA       SPINSUN     NODE        ARGPER  ETALIM
          JJ    ANU       RR          FF          AASPNV  AASUNV
          JJ    T(JJ)
XXXX.XX------XXX.XXXXXXXX.XXXXXXXX.XXXXXXXX.XXXXXXXX.XX
           1XXXXXX.XXXXXXXX.XXXXXXXX.XXXXXXXX.XXXXXXXX.XX
           2XXXXXX.XXXXXXXX.XXXXXXXX.XXXXXXXX.XXXXXXXX.XX
           3XXXXXX.XXXXXXXX.XXXXXXXX.XXXXXXXX.XXXXXXXX.XX
           4XXXXXX.XXXXXXXX.XXXXXXXX.XXXXXXXX.XXXXXXXX.XX
           1XXXXXX.XX
           2XXXXXX.XX
TTOTAL = X.XXXXXXXE+XX
```

Some of the quantities in the output have already been defined, and those that have not, have the following meaning.

ETA = Angle between the Sun and the orbit Normal
SPINSUN = Angle between the Sun and the Spin axis
NODE = Argument of the node with respect to the equator
ARGPER = Argument of Perigee with respect to the equator
ETALIM = The value of ETA for which the Sun is on the Vehicle's horizon
ANU = Value of the orbital polar angle for which F_s or F_v vanish
RR = Magnitude of the vehicle's radius vector when F_s or F_v are zero
FF = Values of F_s or F_v corresponding to ANU
AASPNV = Angle between the radius vector and spin axis
AASUNV = Angle between the radius vector and the Sun
TTOTAL = Total observing time
T(JJ) = Time intervals in shadow or time intervals of Earth viewing

Quantities corresponding to JJ = 1, 2 refer to eclipse computations; those for JJ = 3,...6 refer to Earth's viewing computations. The quantity T(1) gives the time in shadow; T(2) or T(3) give the intervals during which the Earth is viewed.

The normal output is defined by format statements, lines 00460, 00470, 00670, 00680, 00810, 00820, 00870, 00880, 00910, 00920, 00940, 00950, 00960, 00970, 00980, 00990, 01000, 03640, 03650, 03660, 03670, 03680, 03690, 03700, 03740, 04780.

Deviations from the normal form of the output may occur during the execution of the program. In such cases special messages, defined by lines 01610, 01630, 03010, 03040, 03590 and 03610, appear in the output.

B. DETAILS OF THE PROGRAM

The first block in the program (lines 00450 to 00620) defines various auxiliary quantities frequently used in the remainder of the program. These quantities are:

PI = π
PI2 = $\pi/2$
TWOPI = 2π
RE = Radius of the Earth in n.m.
RECSUNRT = Reciprocal in the Sun's daily rate in days/degree
CONV = Conversion factor from degrees to radians
EPS = Obliquity of the ecliptic
ACAPDEL and AFOV are CAPDEL and one half FOV expressed in radians
SNEPS, CSEPS = sine and cosine of the obliquity of the ecliptic
INC is defined at this stage as the assigned initial value of the orbital inclination

Statements associated with line numbers 00640 through 00660 complete the orbital period in units of hours.

The computer program contains four major nested DO loops. The innermost of these, starting at line 01010, steps the computation through the assigned range of the Sun's longitude. The outermost loop, starting at line 00690 controls the incrementing of orbital inclination. The loops with their beginning at lines 00860 and 00900 control the variation in the orbital node and the argument of perigee respectively.

Statement lines 00700 through 00730 define the following quantities:

ARGINC = Running value of the inclination (in radians)
SNINC, CSINC = Sine and cosine of inclination
DECNORM = Declination of the orbital normal

The function of lines 00750 through 00800 is to compute the nodal and apsidal rates as defined by equations (41) and (42). At this point DENECC and TEMP denote $(1 - e^2)$ and $-10\,(R_E/a)^{3.5}$ respectively. Lines 00790 and 00800 define $\dot{\Omega}$ and $\dot{\omega}$.

Lines 00830 and 00840 define factors $(\dot{\Omega}/\dot{\lambda}_\odot)$ and $(\dot{\omega}/\dot{\lambda}_\odot)$ in equations (45). Lines 00850 and 00890 assign initial values to Ω_{in} and ω_{in} in equations (45).

With the execution of line 01000, the appropriate input quantities have been printed and the heading for the main output has been produced.

Lines 01020 through 01080 establish quantities

DSUNLON = $\lambda_{\odot} - \lambda_{in}$
EQNODE = Equatorial argument of the node given by equations (33)
ARGPER = Equatorial argument of perigee given by equations (33)
RADNODE and RADARPER are the node and perigee expressed in radians
ALFNORM = Right ascension of the orbital normal
ARSUNLON = Sun's longitude expressed in radians

Statements associated with line numbers 01100 through 01180 produce the angle between the Sun and the orbit normal (ETA) according to equation (20). All symbols on the left hand sides of the expressions are self-explanatory. Angle ETA is expressed in degrees.

An identical procedure is employed on lines 01200 through 01280 to compute the angle between the Sun and the Spin axis (SPINSUN). The quantities SPINALF and SPINDEC denote ALFSPIN and DECSPIN converted to degrees. Lines 01260 and 01270 represent the FORTRAN version of equation (23). Angle SPINSUN is converted to degrees on line 01280.

Equatorial orientation elements of the orbit are converted to the corresponding ecliptic elements by the set of statements listed on lines 01310 through 01430. Quantity CSIBAR denotes cos i, and is computed from the third equation of (16).

Lines 01380 and 01390 produce sin $\overline{\Omega}$ and cos $\overline{\Omega}$, given by the first two equations of set (16). Subroutine QTEST is then entered to return the value of $\overline{\Omega}$ on line 01370.

Lines 01380 and 01390 produce sind and cosd from the fourth and fifth relations of equations (16). Subroutine QTEST yields the required value of angle d. Finally, line 01410 represents the FORTRAN counterpart of the last relation of (16).

It is convenient to define $\overline{\omega}$ as always positive and not exceeding 360 degrees. However, since there is no guarantee that the computed value is positive, the condition is tested at statement 46 (line 01420) and, should $\overline{\omega}$ turn out to be negative, it is re-defined as $(2\pi - \overline{\omega})$ on line 01430. Finally, statement 45 (line 01450) defines the value of the quantity UCOMP which represents the upper limit of the polar angle which will be used to compute eclipse and viewing limits.

The computation of eclipse and Earth's viewing limits begins on line 01470. The lines 01470 through 01550 produce the limiting value of the angle ETA. Line 01470 represents the numerator of equation on (27) or (28). Quantity XX (line 01480) denotes $(\lambda_{\odot} - \overline{\Omega})$. Variable CSBETPR contains the quantity cos β' computed according to equation (14). Line 01510 produces angle β according to the equation on $\beta = |\beta' - \overline{\omega}|$. Line 01520 defines the angle $(180^{\circ} - \beta)$ which is then used to produce the limiting radius vector of the vehicle (line 01530) from equation (28). Statements on lines 01540 and

01550 generate the limiting value of ETA in degrees.

If $\cos \eta > \cos \eta_\ell$ the program transfers to statement 52 and the message: "VEHICLE INCONTINUOUS SUNLIGHT" is printed. If $\cos \eta = \cos \eta_\ell$ the program transfers control to statement 51 and the message: "SUN ON VEHICLE'S HORIZON AT |ETA - 90|. " is printed. In either case there is no need to search for eclipse limits since the vehicle essentially does not enter the Earth's shadow. Should this situation be encountered the control passes to statement 53 and the program proceeds to search for the Earth's viewing limits. If, however, $\cos \eta < \cos \eta_\ell$ the program control passes to statement 50 where the computation of the eclipse limits begins.

1) Computation of Eclipse Limits

The general outline of this computation is as follows. Starting at the point of perigee, the function F_S from equation (29) is computed for various values of the polar angle u. The interval Δu between computations is defined in the input. At each computed point the value of F_S is compared with its previous value and, if a change in sign occurs, an iterative search is made for the value of u at which F_S vanishes. This process is repeated until two values have been found. Since the computational algorithm includes in it the computation of viewing limits as well, considerable logic is needed to keep track of which of the two cases is being processed. Further logical complication arises from the fact that the signs of the derivatives of F_S and F_V, needed later in the program, are being computed simultaneously with the zeroes of F_S and F_V. Since either function can vanish at $u = \overline{\omega}$, thereby indicating a solution, it is necessary to set up a way which produces measures of $\dot{F}_S$ and $\dot{F}_V$ despite the fact that no iteration for zeroes is needed. To achieve this, the actual computation is started at $\nu = -\Delta u$ and it is incremented twice. Note that if eclipse limits exist, the procedure of computing these three initial values need not be repeated for the viewing limits. If, however, no eclipse limits exist, the procedure must be followed for the computation of the viewing limits. If the three initial values are to be computed the parameter CONST is set equal to -1.0. If not it is redefined to be equal to 1.0 on the line 02910.

Various limits and the associated quantities are filed in the appropriate arrays defined by the lines 02700 to 02810.

The computation of eclipse limits starts at statement 50, where the value of parameter KK is defined. It is set equal to zero for the computation of eclipse limits. Since the eclipse limits exist, CONST is defined as -1.0. Finally, the parameter KKK, which designates the sequential order of the computed limits, is initially set equal to zero. The control is then transferred to statement 15, where the initial value of $u = \overline{\omega} - \Delta u$ is defined. The parameters ITEST and INDF indicate which of the three initial values of F_S and F_V are to be computed. At this stage they are set equal to 1. Further, line 01690 defines the initial content of the running

counter ANUCOUNT, which will keep track of the last value of u which was incremented by DELU. The purpose of this counter is discussed later in the program. Since CONST = -1.0, line 01700 transfers control to line 01710 where the value of parameter INDF is defined.

Statements on the lines 01720 to 01780 redefine the value of DELU as DEL, define the sine and cosine values of the angle u, define the value of true anomaly (TRUANOM), compute the value of the vehicle radius vector (R), establish the value of the first term in equation (30), and lastly, compute the quantity PHILIM which represents the value of the angle between the nadir and the lower edge of the field of view if the latter were tangent to the Earth Surface.

The lines 01790 and 01800 are calls to the appropriate subroutines which return values of angles SUNVEH and SPINVEH.

At this point the value of F_S from equation (29) can be evaluated. This is done on the line 01810.

To determine the value of F_V we must decide whether condition (35) or (36) applies. This computation is accomplished by a set of statements starting on the line 01820 and concluding with the line 01940. The quantity PHIS represents the first three terms on the right hand side of equations (36). Variables PHI1 and PHI2 contain the current values of φ_1 and φ_2 defined by (36). Statement on the line 01850 tests whether condition (24) applies and, if so, reverses the signs of φ_1 and φ_2 in the next two statements. When $\Gamma + \Delta = \pi$ we choose to compute φ from PHI2 and this is done by statement 40. The purpose of statements on the lines 01900 to 01930 is to determine which of the two φ's is the smaller one. The appropriate φ is then used to compute F_V on the line 01940 from equation (30).

Statements on the lines 01950 to 02490 have the purpose of establishing values of F_S, F_V and the signs of $\dot{F}_S$ and $\dot{F}_V$ for the arguments $\nu = -\Delta u$, 2π or 0, and Δu. Their further objective is to save these quantities for future use and to establish various temporary variables required by the computation.

Since initially ITEST = 1 and INDF = 1 control passes to statement 96 where the current values of F_S and F_V are assigned names F1S and F1V. Statements on the lines 02010 to 02030 advance the value of INDF to 2, increment u by Δu, advance ANUCOUNT counter and transfer control to statement 3. This produces values of F_S and F_V for $\nu = 0$ by the procedure already described. Since ITEST = 1 and INDF = 2 control is transferred to statement 98. Statements 02050 to 02100 define the values of FSTWOPI = $F_S(0)$, FVTWOPI = $F_V(0)$, FSDTTPI = $F(0) - F_S(-\Delta u)$, FVDTTPI = $F_V(0) - F_V(-\Delta u)$, PHITWOPI = $\varphi(0)$, PHILTWPI = $\sin^{-1}(R_E/r(0))$ where all arguments refer to values of the true anomaly. Note, that the third and fourth of these quantities represent a measure of the sign of the gradient of the respective functions in the interval $-\Delta u \leq \nu \leq 0$.

At this stage the value of 3 is assigned to INDF and the program branches to statement 91. As above, u and ANUCOUNT are incremented, the control returns to statement 3 and the entire procedure of computing F_S and F_V is repeated.

Since ITEST = 1 and INDF = 3 the program will branch to statement 99. The statements on the lines 02130 to 02180 define values for FSØ = $F_S(0)$, FSDOTØ = $F_S(\Delta u) - F_S(0)$, FVØ = $F_V(0)$, FVDOTØ = $F_V(\Delta u) - F_V(0)$, PHIØ = $\varphi(0)$, and PHILØ = $\sin^{-1}(R_E/r\ (0))$.

The outcome of cycling through the above procedure three times has been to generate values of F_S and F_V at $\nu = \Delta u$, 0 or 2π, and Δu, their first differences, as well as the values of φ and $\sin^{-1}(R_E/r)$ at $\nu = 0$ and Δu.

The four statements beginning on the line 02190 simply re-define $F_S(0)$, $F_V(0)$, $F_V(\Delta u)$, and $F(\Delta u)$ as new running variables F1S, F1V, FS, and FV which will be used to search for zeroes of the functions F_S and F_V. At this point INDF is assigned value 4.

Since INDF = 4 and DEL = DELU, the logical statement 95 transfers control to statement 97. The next four statements define the running values for the first differences SLS = $F_S(\Delta u) - F_S(0)$, SLV = $F_V(\Delta u) - F_V(0)$ and place the current values of F_S and F_V into temporary storage at TEMPFS and TEMPFV.

Since KK = 0, that is, eclipse limits are being computed,the logical statement 29 sends the program to statement 24 where the current and the previous values of F_S are re-defined as F and F1. The current value of the first difference is also assigned a new name, SL. Since ITEST = 1, statement 73 transfers control to those on the lines 02390 and 02400. The purpose of these two statements is to ascertain whether there may be a zero of F_S in the immediate neighborhood of $u = \varpi$ (or $\nu = 0$). This condition is indicated by (a) $F_S(0) < \epsilon$ and both $F_S(0)$ and $F_S(\Delta u)$ are positive, (b) $F_S(0) < \epsilon$ and both $F_S(0)$ and $F_S(\Delta u)$ are negative, (c) F_S changes sign between $\nu = 0$ and $\nu = \Delta u$.

Cases (a) and (b) are tested on the lines 02390 and 02400. If either (a) or (b) are satisfied control transfers to statement 56. At this point U, ANUCOUNT, F, TEMPFS, TEMPFV are all shifted back to correspond to values existing at $\nu = 0$. Index ITEST is set equal to 2 and the control is transferred to statement 3 which leads to the re-computation of $F_S(0)$, $F_V(0)$, PHI, PHILIM, etc. This appears to be lost motion, since these quantities have been computed before. However, it must be realized that in computing F_S and F_V at $\nu = \Delta u$, other quantities such as, angles ASPINVEH, ASUNVEH, U, PHI, PHIL, etc. apply to $\nu = \Delta u$. Those applicable at $\nu = 0$ were destroyed and the only way to restore them is to re-compute them. Statement on the line 01950 transfers control to statement 55 where ITEST is set equal to 3 and the computation is then directed to statement 1. This, and

and the next statement are the concluding statements of the testing procedure for zeroes of F_S and F_V. Both statements are used for F_V whereas only statement 1 need be employed for F_S. Since KK = 0 the program branches to statement 2 where the counter KKK is assigned the value of 1 and all quantities of interest corresponding to the present eclipse limit are saved in the appropriate arrays. These are

AASPNV = Angle between the spin axis and vehicle radius vector
AASUNV = Angle between the sun and the vehicle
ANU = Orbital polar angle u
RR = Magnitude of the vehicle radius vector
FF = Value of function F
SLOPE = Numerator of the slope of F
FSHAD = Value of F_S
FDOTS = Value of the numerator of $\dot{F}_S$
FVIEW = Value of F_V
FDOTV = Value of the numerator of $\dot{F}_V$
PHIT = Value of the angle φ
PHIL = Value of $\sin^{-1}(R_E/r)$

Having done this, the program increments the angle u as well as the counter ANUCOUNT and on the line 02840 tests whether the resulting u is greater than UCOMP = $2\pi + \omega$, that is,whether ν has been stepped through its full period of 2π. If this is not the case and, if furthermore, KKK $\neq$ 2 which would indicate that all eclipse limits have been obtained, the program proceeds to 02860 and 02870. These will store in FIS and FIV the last values of F_S and F_V found prior to the search for zeroes. Control then passes to statement 6.

The values of F_S and F_V corresponding to the incremented value of u are computed as before. Since ITEST = 3 and INDF = 4 the program branches to statement 95 which, as before, sends the program to statement 97 whose function has already been described. As in the previous cycle the program ends up at statement 73. Now, however, this statement transfers control to statement 18.

Statement 18 assigns the value of 1 to the quantity MFLAG. The purpose of this quantity is to indicate whether statements on the lines 02510 and 02530 were used in the course of computation. The latter statements detect a change in sign between successive values of F_S or F_V. If there is no change in sign, it is still possible that the current value is near zero within the assigned tolerance. Test for this condition is made on the line 02540. Should this be the case a zero has been located and the control passes to statement 1 which, in the present case,transfers control to statement 2 whose function has already been described. If statements on the lines 02510 and 02530 indicate no change in sign of the function under consideration,either of these statements will send the program to statement 7. Since at this stage DEL = DELU,control is transferred to statement 47, where U is incremented, F_S and F_V are assigned their current

values. Lines 02660 and 02670 contain statements whose purpose is to detect whether a zero may exist at $u = \bar{\omega} + 2\pi$ and whether u may have been incremented beyond this value. In the former case control is transferred to statement 1 whose function has been discussed earlier. In the latter case control goes to statement 8. If neither is the case,control is transferred to statement 3, new current values of F_S and F_V are computed and the whole cycle repeates until a change in sign is indicated and statement on the line 02540 is satisfied. The procedure in the latter case has been already described. However, if the latter statement is not satisfied, the implication is that a zero occurs between two successive values of u.

In the latter case the statement on the line 02540 transfers control to statement 19 if F_S is under consideration. For F_V this occurs only if $\varphi \leq \pi/2$.

The search for zero proceeds by successive approximations in which the increment in U is successively halved from its previous value until the condition on the line 02540 is satisfied.

The procedure starts with the statement 19 where the normal increment is halved and assigned a negative sign. Since DEL becomes less than DELU control passes to statement 47 and,as before,U is incremented by -DELU/2, and F_S and F_V are assigned their current values and the whole cycle repeats. Note that as long as DEL < DELU counter ANUCOUNT is not advanced. This preserves the last value of U which had existed just before the procedure for locating zero has begun. As soon as a new change of sign is detected, but $|F| >$ TOL,the procedure repeats in the opposite direction with an increment in Δu = DEL/4. The computation proceeds in this manner until statements on the lines 02540, 02590, and 02600 send the program to statement 2. The function of statements on the lines 02700 through 02810 has already been discussed.

Note that at this point, U and ANUCOUNT are incremented from that value which was preserved at the initiation of zero search. Furthermore, the input value of DELU is again used.

In any event,the above procedure is followed until two zeroes for F_S have been found.

At this stage of the computation, regardless of which of the statements on the lines 02840 and 02850 is satisfied,the program is sent to statement 8. Note that for F_S, ν will not be allowed to go through its complete cycle of 2π, because in any event only two zeroes are possible and so there is no need to continue examining this function once the second zero has been located.

In the latter case statement 8 tests the value of KK. After both F_S and F_V have been scanned for zeroes,statements on the lines 02840 and 02890 send the program to statement 27. If only F_S has been examined for zeroes, statement 8 is not satisfied,

KK is assigned value of 1, CONST is re-defined as 1, DEL is restored to DELU, and control is transferred to statement 15. Note that there is no need to repeat the computation of F_S and F_u at $\nu = -\Delta u$, 0, Δu because this was done for computation of zeroes of F_S. However, if F_S has either no zeroes at all, or only one zero, statements on the lines 01610 through 01630 would force the computation of the initial three values for the computation of zeroes of F_V. In the latter case the procedure would be identical to that followed in the first stages of locating zeroes of F_S. The only difference is that F1 and the running values of F and SL refer now to function F_V. These are defined by statements on the lines 02310 through 02330. Furthermore, since KK = 1 the statement on the line 02600 will always be used. In all other respects the computation of zeroes of F_V is the same as that for those of F_S.

When all zeroes of F_S and F_V have been determined, statement 8 transfers control of the program to statement 27 at which time the computation of shadow and Earth viewing intervals begins.

2) Computation of Shadow and Earth Viewing Intervals

(a) Computation of Eccentric Anomalies

Note that u's and all other computed quantities corresponding to zeroes of F_S and F_V are stored in their respective arrays so that KKK = 1, 2 refer to F_S whereas those referring to F_V are located at 3 through 6. In order to compute the intervals in question it is necessary to identify the number and kinds of zeroes.

This is accomplished in the sequence of statements between 02950 through 03160.

Statement 27, not really part of this computation, defines the vehicle mean motion, n. The parameter NFLAG is eventually used in combination with MFLAG to control printing of either the normal output or of special messages. Initially NFLAG is set equal to zero. The statement listed on the line 02960 is identical to that on the line 01560 and it has the same purpose. It is implied that if the condition listed under 02960 is satisfied, there are two eclipse limits. In such a case, statement 60 assigns the value of one to the parameter NX, which will eventually serve as the lower index of the DO loop employed in the computation of the appropriate intervals. If, on the other hand, there is only one or no eclipse limits, NX is set equal to 3 on the line 02970. In either case a search is made for the number of F_V zeroes and, depending on what is found, the upper limit of the DO loop index, NY, is defined. The procedure begins at statement 64. If it is found that KKK = 6, that is, F_V has four zeroes, control is transferred to statement 61 where NY is set equal to 6. If, however, KKK $\neq$ 6, the possibility of KKK = 4 is examined. If such is the case, F_V has two zeroes, that is two Earth viewing limits and NY is set equal to 4 by statement 63. If KKK $\neq$ 6, or 4, the possibility remains that the field is tangent to the Earth's surface when the vehicle is at perigee.

In this case KKK = 3 and this condition is tested by the statement listed on the line 03000. Note, that such a sequence of events cannot yield a positive value of (KKK - 3) and, therefore, the upper address of the IF statement in question is, in effect, a dummy statement 26. If KKK = 3 the appropriate message is printed at statement 80 and control is transferred to statement 82. If at this stage KKK < 3, it is possible that the Earth is either not viewed at all,in which case there was no change of sign of any kind in F_V and, therefore, MFLAG has the value of 0. The Earth is not viewed at all on this orbit and the message to this effect is written by statement 89. If, on the other hand, MFLAG is 1, this means that F_V is positive throughout the orbit so that there is partial Earth's viewing at all times.

In any of these cases the program ends up at Statement 82. If F_S has two zeroes this statement, via statement 83, sets NY = 2 and control is transferred to statement 70. If, however, NX $\neq$ 1, the parameter NFLAG is set equal to 1 and the program proceeds to statement 71.

This, and the subsequent statement examine values of NFLAG and MFLAG. If NFLAG = 1, then regardless of the value of MFLAG,normal output is expected as specified by statements 86 and 23 and the associated FORMAT statements 23 and 33. If, however, NFLAG = 1 and MFLAG = 1, the vehicle is essentially in the sun throughout the orbit and F_V is always positive, which implies that the Earth is viewed partially throughout the orbit. This message is flashed on the line 03590, with the subsequent transfer to statement 103. Consequently, within our definitions, there is no useful observing time on such an orbit. If, on the other hand, NFLAG = 1 (that is NX = 3) and MFLAG = 0 we have a situation when the vehicle is continuously in sunlight and the field of view never encounters the Earth's surface. Consequently, the potentially useful observing interval is equal to the orbital period. Statement 90 produces a message to this effect. The total observing interval TTOTAL is assigned the value of P on the line 03620 and control is transferred to statement 106.

In any event, should either F_S or F_V have at least two zeroes, there exists a corresponding shadow or Earth viewing interval and the program ends up at statement 70.

The sequence of statements beginning on the line 03170 and concluding with the line 03260 employs equations (32) to produce eccentric anomalies corresponding to those values of U at which the functions F_S and F_V possess zeroes, that is, points on the orbit corresponding to the eclipse and the Earth viewing limits. The meaning of symbols employed is reasonably self explanatory. The eccentric anomaly is placed within its correct quadrant by the subroutine QTEST. The indices of the DO loop, spanning statements 70 to 20 represent the total number of appropriate zeroes of F_S and F_V.

(b) Computation of Intervals

Each eclipse and Earth viewing limit is associated with a definite position of the vehicle in its orbit and therefore, with the corresponding time in orbit. Furthermore, it should be clear that the number of intervals during which the vehicle is not in shadow or during which the Earth is not viewed is equal to one half the number of the respective limits. Consequently the computation starts with defining this number on the line 03290. Next, the value of NX is examined. If there are eclipse periods, indicated by NX = 1, the program sets the parameter NXX equal to 1. Thus,in this case we have one eclipse interval and one or two Earth viewing intervals, depending on the value of NY. If NX = 3, the parameter NXX is set equal to 2 by the statement on the line 03310. In this case we shall be concerned only with the Earth viewing intervals whose number continues to be defined by the value of NYY. The computation proper, according to equation (31), is contained wholly with the DO loop between the statements 85 and 21. Within this DO loop, we have included the logic designed to determine which of the expressions (33), (34) and (37) I, II are to be used.

Assume for the moment that NXX = 1. In this case the logical statement on the line 03350 transfers control to statement 65 where parameters M and MM are assigned values of 2 and 1. These parameters are the precise counterparts of the subscripts used in equations (31) and (37). Statements on the lines 03470 to 03490 produce the difference in the true anomalies of interest which,in this particular case, is the right hand side of equation (31). Statement on the line 03500 sends the program to statement 25, whose purpose is to examine the signs of slopes, F_{S1} and F_{S2}. If F_{S1} = SLOPE (1) < 0 and F_{S2} = SLOPE (2) > 0 control is transferred to statement 21 and the interval $(t_2 - t_1)$ is computed directly from equation (31) or (33). If, however, the slopes have signs opposite to those indicated above, equation (34) is employed, represented by statements on the lines 03540 and 03550.

As the DO loop advances, JJ becomes equal to 2 and the statement on the line 03350 transfers control to the statement immediately following it. The form and the meaning of this statement is exactly the same as those of statement 25, but it applies to the Earth viewing limits. If the condition is satisfied, the subsequent procedure becomes identical to that for the eclipse interval until statement on the line 03500 is reached. Since in the present case JJ = 2 control passes to the next statement at which the program takes one of two possible branches, depending on whether there is one or two viewing intervals. In the former case control passes to statement 25 and the subsequent course of action is the same as for eclipse limits. Should there be a second interval, the computation proceeds exactly as for the first one until the statement on the line 03510 is reached. In this case the program continues to the next statement and since JJ = 3, control is transferred to statement 21. As a consequence of this sequence of computation, the two terms on the right hand side of equation (37) - I have been produced.

The situation alters considerably if the slopes of F_V do not satisfy the condition on the line 03660. In this case equation (37) - II is used to determine intervals in question. Statement on the line 03360 transfers control to that on the line 03370 and since JJ = 2, the program is sent to statement 66. If, at this point, we have only one Earth viewing interval, NYY = 2, and the program continues to the following two statements where M and MM are set equal to 5 and 4 respectively. The subsequent calculation is as described earlier. Since in this case JJ = 2 and NYY = 2, the program branches to statement 25 and, because the indicated relation between the slope signs is not satisfied, it proceeds to calculate the quantity $[P - (t_4 - t_3)]/n$ in equation (26)-II. If, however, there should be two intervals, that is, NYY = 3, the combination of statements on the lines 03370 and 03410 will, for JJ = 2, define M = 5 and MM = 4. As a consequence, the subsequent logic will produce the quantity $(t_5 - t_4)/n$ in equation (37) - II. For JJ = 3, lines 03380 and 03390 assign values of 6 and 3 to parameters M and MM. The subsequent flow of computations starting at statement 67, ultimately yields the quantity $[P - (t_6 - t_3)]$ in the same equation.

Finally, the statement on the line 03560 tests for the number of Earth viewing intervals and, if it is found that there are more than two of these, the overall interval , T(4), during which the Earth is not viewed on the orbit,is computed.

The function of statements listed on the lines 03570 through 03680 has been described earlier. As part of the normal output the individual intervals are printed under control of statements on the lines 03690 and 03700. Furthermore, should there be two Earth viewing periods, their sum is printed via statement 87 and the statement immediately following it. In either event control is transferred to statement 103, which is the beginning of the computation of the overall potentially useful observing time.

3) Computation of the Total Time When the Vehicle is Simultaneously in Sunlight and the Instrument is not Viewing the Earth

(a) Sequencing of Limiting Values of F'S and $\dot{F}$'S.

In order to compute the quantity TTOTAL, it will be necessary to establish whether any of the conditions (38) are satisfied. To do this it is necessary to arrange all limiting values of F_S, $\dot{F}_S$, F_V, $\dot{F}_V$, φ, and φ_ℓ according to the ascending order of the appropriate u's or ν's. This could be accomplished in a relatively straight-forward manner if the necessary quantities were stored sequentially according to some index running from 1 to an appropriate maximum value. However, at this stage of the computation this is not so. Recall, for instance, that if no eclipses exist, the count NX starts at 3. The count, NY, ends at either 4 or 6, depending on how many viewing intervals there may be. Furthermore, the respective values of F_S, F_V, and measures of their slopes at $\nu = 0$ and 2π are not even part of the arrays defined on the lines 02700 to 02810. In short, then, the required quantities must be suitably resequenced. The resequenced arrays have in the first position values corresponding to

$\nu = 0$, and in the last one those corresponding to $\nu = 2\pi$.

Resequencing is accomplished by a series of statements starting on the line 03760 and ending on the line 04070. Note that NX can have values 1 or 3, and NY values 2, 4, and 6. To examine the procedure consider the simplest case when NX = 1 and NY = 2, that is, we have an eclipse period, but the earth is not viewed on this orbit. The eccentric anomaly, E, will be taken as the controlling variable.

During the first pass through the DO loop (lines 03760 through 03890), JJ = 1, and since NX = 1, control passes to statement 37 where parameters JJJ and JJJJ are assigned values of 2 and 3 respectively. Statement 38 shifts the value of E, currently in the second position in the array, to the third position which, of course, is empty since NY = 2. Expressions through the statement 36 do the same for other variables of interest. During the second pass through the loop, JJ = 2 and expressions on the lines 03810 and 03820 yield JJJ = 1 and JJJJ = 2. Consequently, statement 38 shifts the present E(1) value to the second position previously occupied by E(2) which, however, is no longer needed since it has been shifted to the third position on the previous pass. Since the DO loop in question has completed its function the program continues to statement on the line 03900 where E($\nu = 0$) is assigned value of zero. Statements on lines 03910 to 03690 store the corresponding quantities in first positions of their respective arrays. Since NX = 1, the logical statement on the line 03970 sends the program to statement 39. At this point JJ is assigned the value of 4 and statement 48 sets E(4) = E($\nu = 2\pi$) equal to 2π. Statements through the line 04070 establish the corresponding values of F_S, F_V, $\dot{F}_S$, $\dot{F}_V$, φ, and φ_ℓ.

The procedure can be traced in a similar manner for every allowable combination of NX and NY. The important aspect is to make sure that various quantities be shifted into their proper positions before being overlaid by the quantity following it.

At the end of this procedure, the required data is arranged in the form

$E(1) = 0$	$F_S(0)$	$F_V(0)$	$\dot{F}_S(0)$	$\dot{F}_V(0)$	$\varphi(0)$	$\varphi_\ell(0)$
$E(u_1)$	$F_S(U_1)$	$F_V(U_1)$	$\dot{F}_S(U_1)$	$\dot{F}_V(U_1)$	$\varphi(U_1)$	$\varphi_\ell(U_1)$
	...					
$E(\text{last}) = 2\pi$	$F_S(U_n)$	$F_B(U_n)$	$\dot{F}_S(U_n)$	$\dot{F}_V(U_n)$	$\varphi(U_n)$	$\varphi_\ell(U_n)$

where $U_n = 2\pi + \bar{\omega}$.

The next step is to arrange all limiting u's or ν's, regardless of whether they are associated with F_S or F_V, in the ascending order.

(b) Sorting Data In The Ascending Order

The sorting routine begins on the line 04090 and continues through the line 04420. Details of this routine have been described by D. L. Shell in an article published in Comm. ACM, 2, No. 7, July 1959, pp. 30-32.

For the present purposes we shall outline its principal features.

The array to be sorted is divided into halves. Corresponding quantities in each half are compared and exchanged should the item in the lower half exceed that in the upper half.

The array is then divided into four parts. First, elements in the first quarter are compared with those in the second quarter and then those in the second quarter with those in the third quarter, etc. When an element is transferred from the third quarter to the second quarter, it is subsequently compared with the corresponding item in the first quarter to ascertain whether it should be shifted again. Generally, when an element is shifted from one section to another, it is compared with the corresponding item in the next higher section until no further move is required or until the element reaches the highest section.

One continues to divide the array and follow the above procedure until a point is reached at which adjacent elements are compared.

In our program eccentric anomaly continues to serve as the principal variable. All other quantities simply follow its moves.

When sorting has been completed the program reaches statement 900.

4) Computation of the Total Observing Interval

The computation starts by assigning the parameter LL value of 0. This parameter has a dual function. When all the required data has been tested for conditions (38), the highest value of LL indicates the number of E's to be used in the computation of the total observing interval, TTOTAL. However, during the intermediate phases, LL is employed to arrange all E's satisfying conditions (38) in sequential order.

Tests whether the data satisfies (38), incrementing LL, and re-sequencing the appropriate E's are accomplished by the DO loop starting on the line 04470 and concluding with statement 35. Note, that the first statement of this loop tests whether eclipse limits exist. If not, the value of F_S is set equal to TOL, the tolerance employed in computing zeroes of F_S and F_V. This is done to avoid numerical problems found to arise occasionally in the subsequent statements due to truncation and roundoff errors

involved in storing TOL and the computation of zeroes. Typical variation of F_S and F_V and phasing of their zeroes is shown in figures 42 through 46.

If no data is found to satisfy conditions (38), the program proceeds to the statement listed on the line 04700, which stores zero in TTOTAL. The next statement evaluates the number of consecutive pairs of E's found to satisfy (38). Clearly, if there are no pairs, LL = 0 and, therefore, LLL = 0. The logical statement on the line 04720 sends the program to statement 106, which prints TTOTAL. If, on the other hand, LL $\neq$ 0, then the statement TTOTAL = 0, merely sets the initial value for the summation procedure for all intervals, indicated in statement 22. In this case the program proceeds to the statement on the line 04730. The DO loop starting on this line and ending at statement 22, evaluates the time intervals when the Earth is not viewed and the vehicle is not in the shadow and sums them up. The computation employs Kepler's equation, whose form is shown in equation (31). As before, the result is printed by statement 106.

At this stage, one pass through the innermost loop of the program has been completed. At statement 400, the Sun's longitude is incremented, the program returns to the statement on the line 01020 and the entire procedure repeats until NSUNLON values of the Sun's longitude have been used. At this point the program proceeds to statement 300 which increments the argument of perigee, and the computation is returned to the statement on the line 00900. The entire sequence of computations is then repeated for as many values of the argument of perigee as specified in the input by NARGPER. Analogously, all values of the argument of the node and inclination are used via the DO LOOPS terminating at statement 200 and 100 respectively. Statements on the lines 04830 and 04840 are added to provide blank lines between the major blocks of output.

The program as currently constituted does not terminate via a program stop, but returns to statement 30 and waits for a new set of input data.

5) Subroutines

a) Subroutine QTEST (CSD, SND)

The purpose of this subroutine is to insure that all angles whose range is 2π or more are placed within their proper quadrant. This is accomplished in a straightforward manner by examining the algebraic signs and, when appropriate, the magnitude of sine (SND), cosine (CSD) functions of the angles in question.

b) Subroutine SUNVEH (ASUNVEH)

This subroutine evaluates the angle between the Sun and the vehicle by means of equation (24). Since this angle cannot exceed 180 degrees, the proper quadrant is automatically established by the standard library ARCOS subroutine. The computed

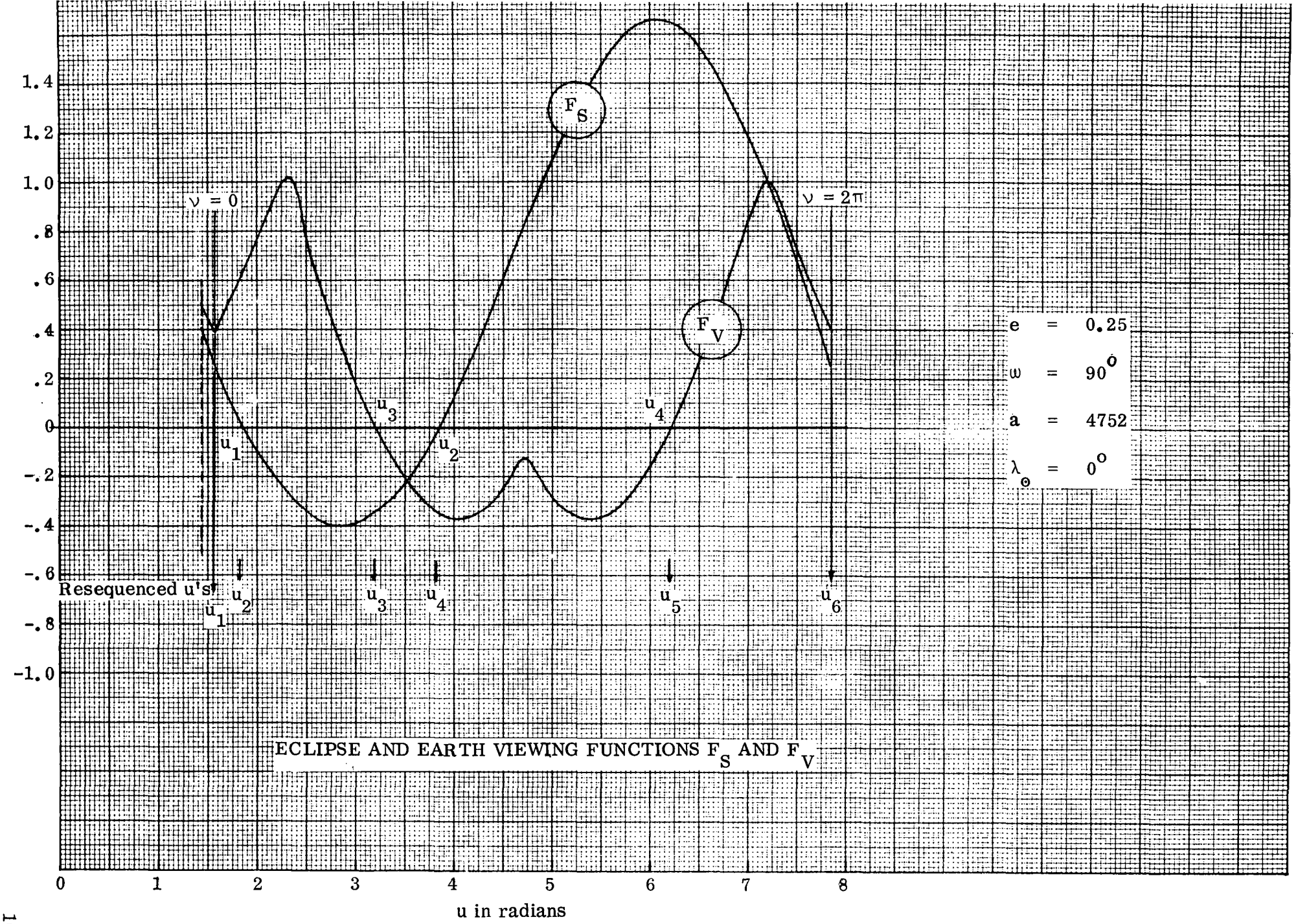

ECLIPSE AND EARTH VIEWING FUNCTIONS F_S AND F_V

Fig. 42

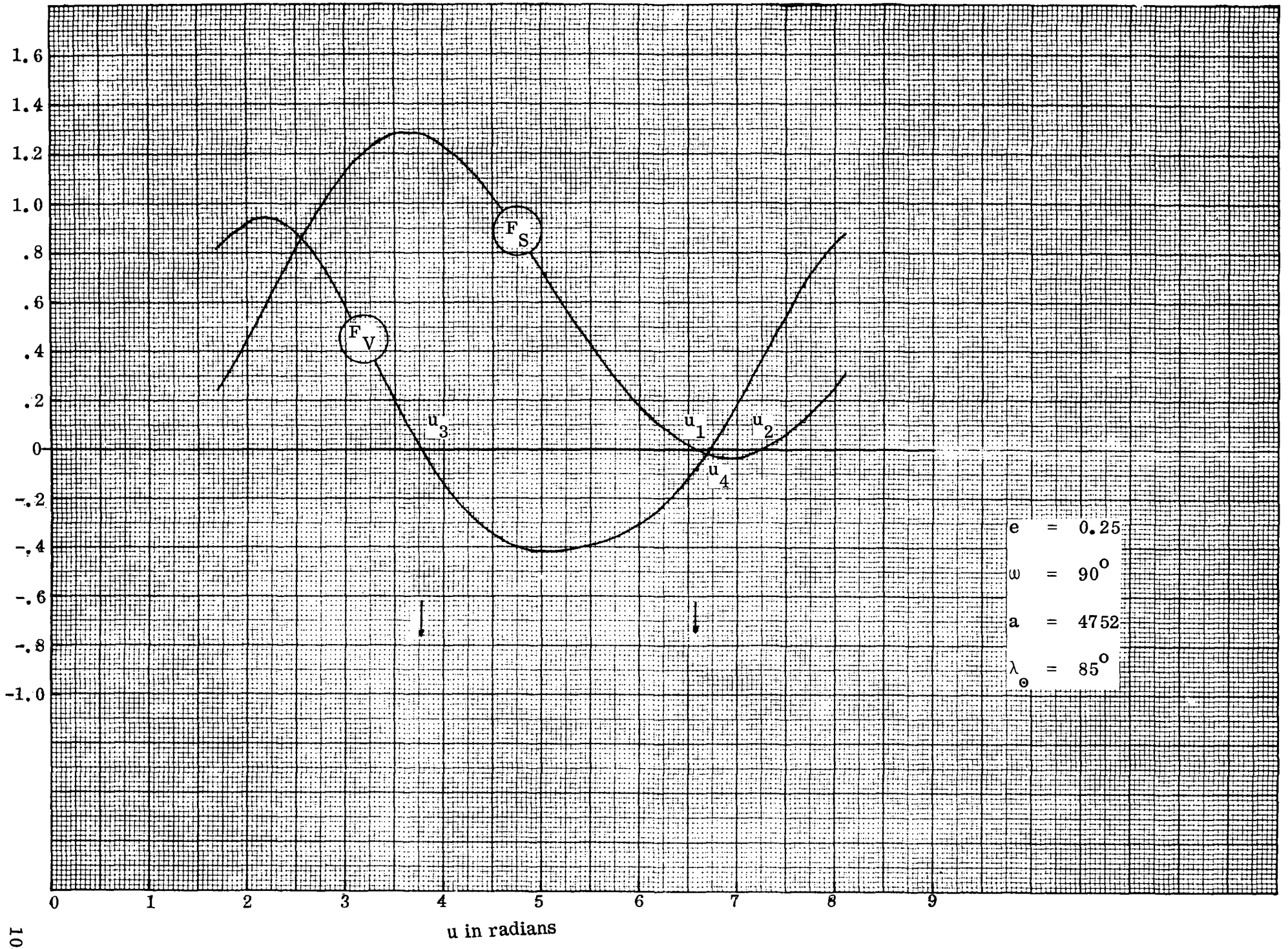
1.6
1.4
1.2
1.0
.8
.6
.4
.2
0
-.2
-.4
-.6
-.8
-1.0
0
1
2
3
4
5
6
7
8
9
u in radians
F_S
F_V
u_1
u_2
u_3
u_4
e = 0.25
ω = 90°
a = 4752
$\lambda_\odot$ = 85°

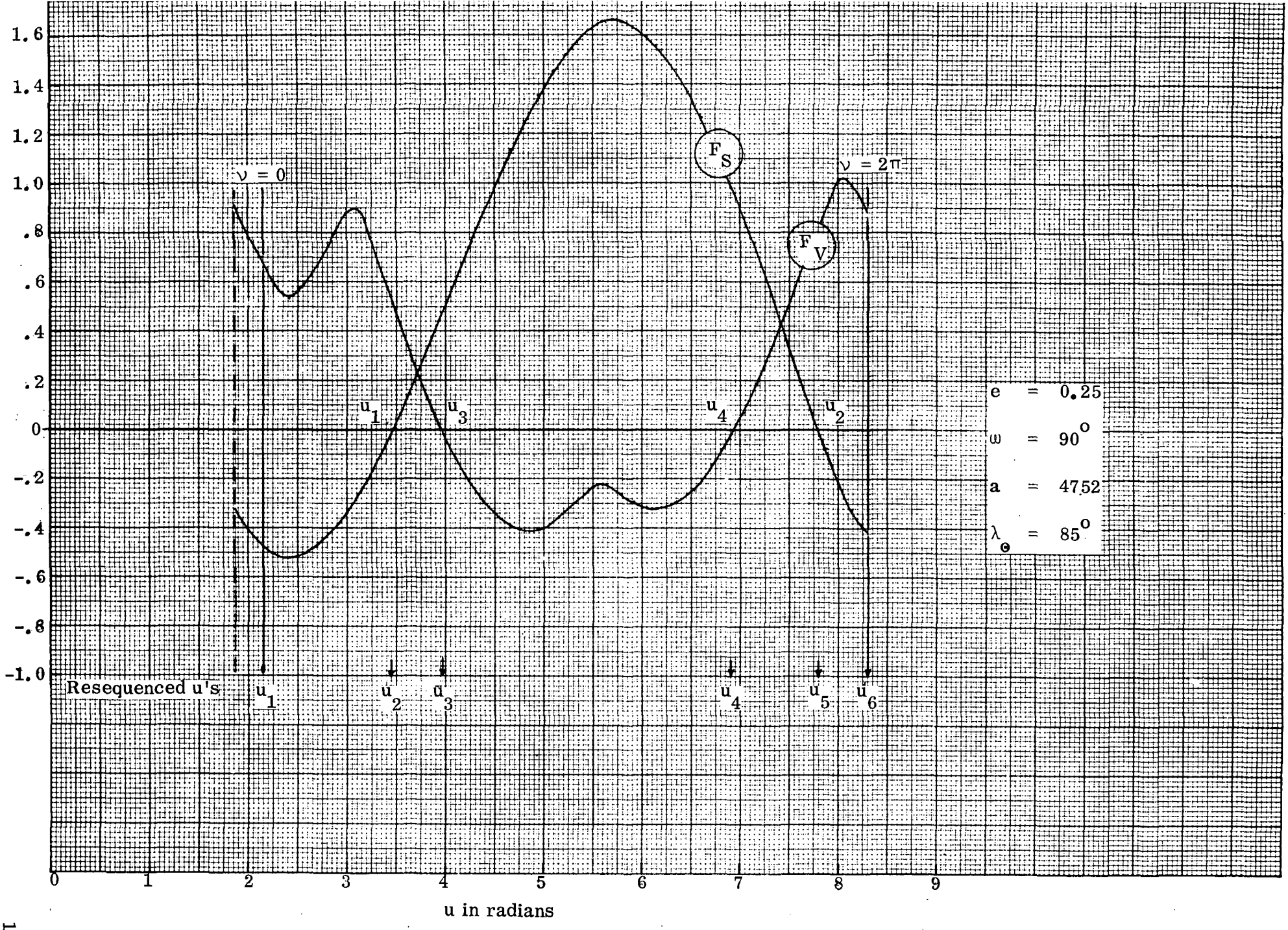
1.6
1.4
1.2
1.0
.8
.6
.4
.2
0
-.2
-.4
-.6
-.8
-1.0
ν = 0
ν = 2π
F_S
F_V
u_1
u_3
u_4
u_2
e = 0.25
ω = 90°
a = 4752
λ_Θ = 85°
Resequenced u's
u_1
u_2
u_3
u_4
u_5
u_6
0
1
2
3
4
5
6
7
8
9
u in radians

Fig. 44

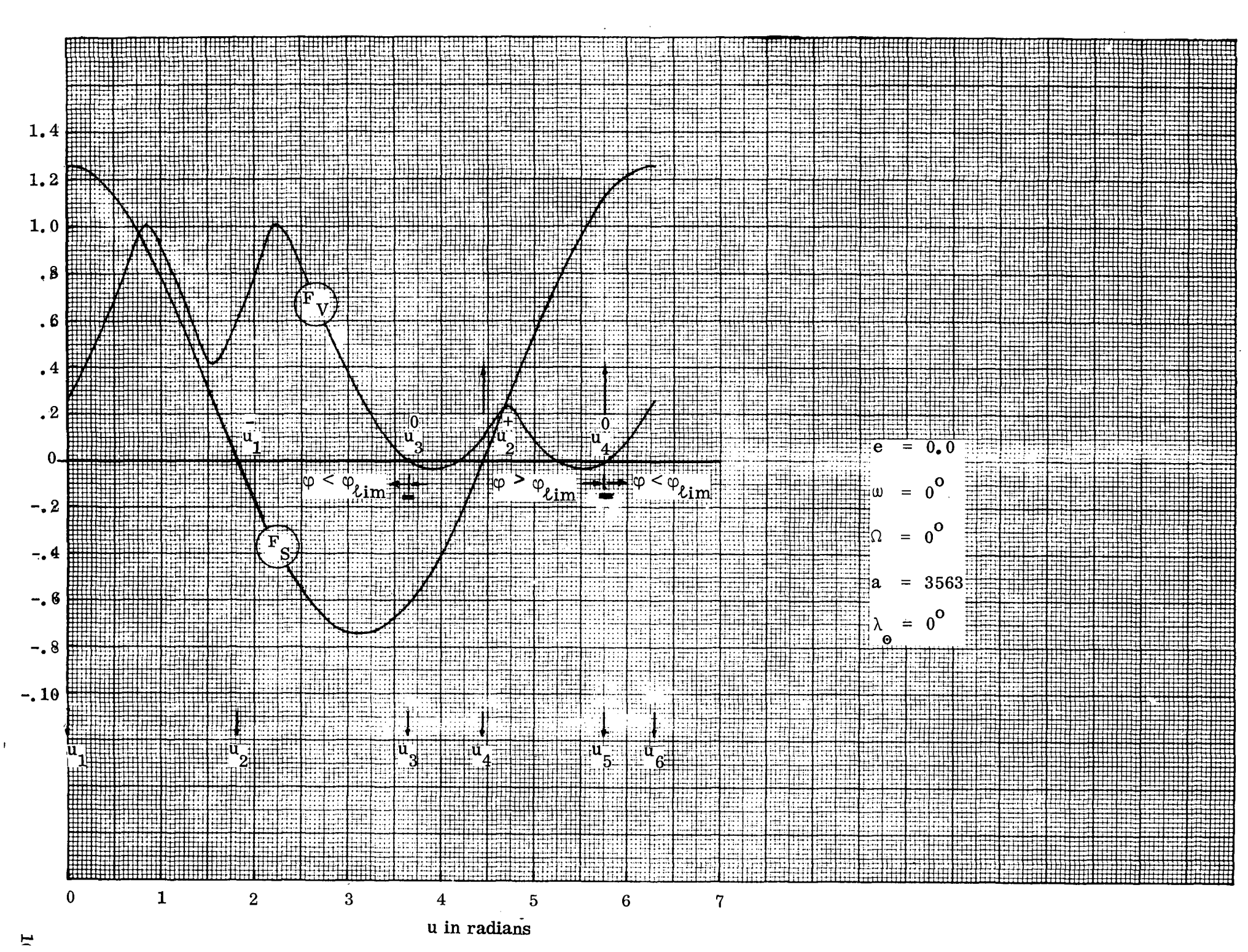
1.4
1.2
1.0
.8
.6
.4
.2
0
-.2
-.4
-.6
-.8
-.10
F V
F S
$\bar{u}_1$
0_{u_3}
$+_{u_2}$
0_{u_4}
$\varphi < \varphi_{\ell im}$
$\varphi > \varphi_{\ell im}$
$\varphi < \varphi_{\ell im}$
e = 0.0
ω = 0°
Ω = 0°
a = 3563
$\lambda_\odot$ = 0°
u_1 u_2 u_3 u_4 u_5 u_6
0 1 2 3 4 5 6 7
u in radians

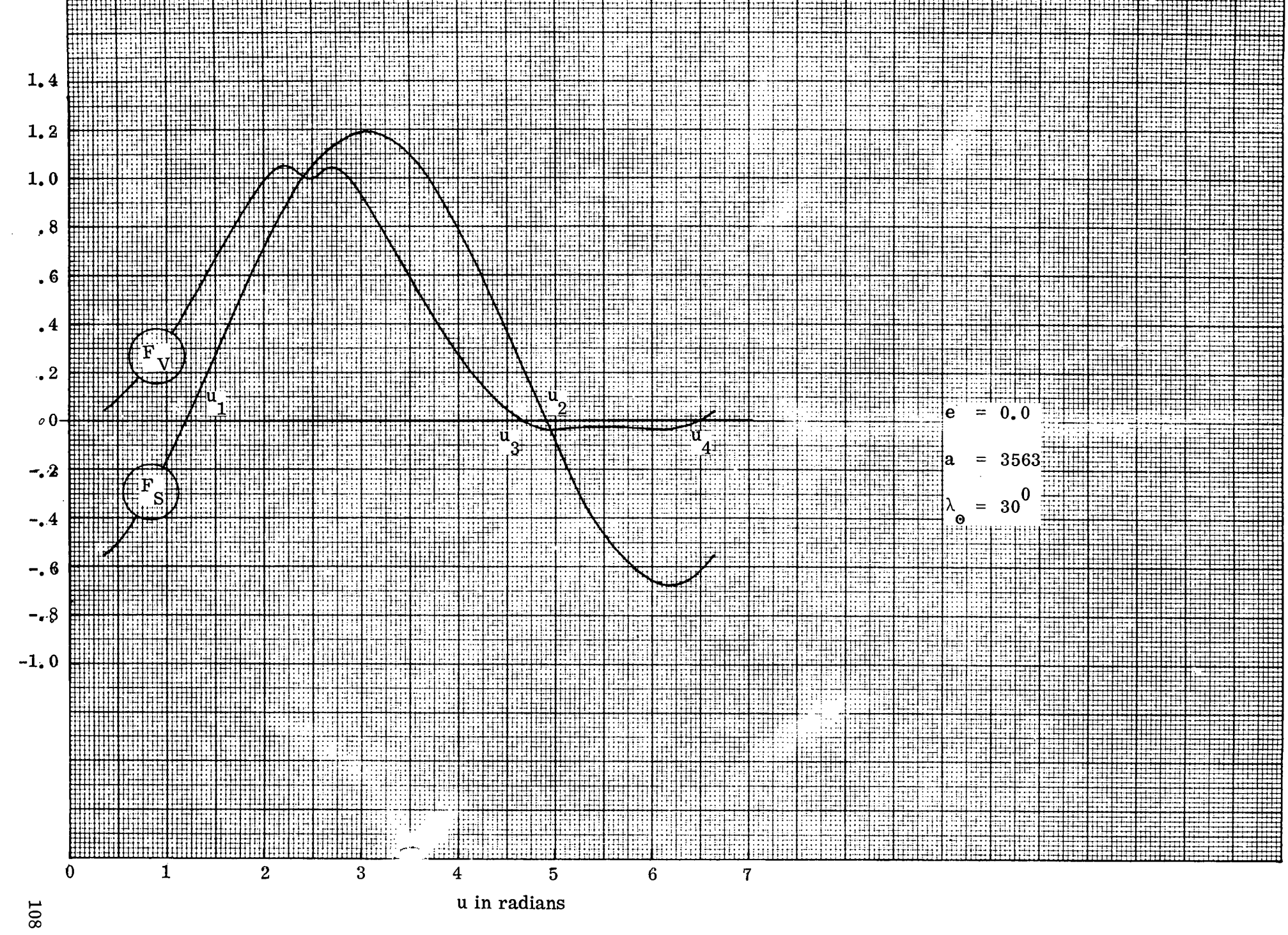
1.4
1.2
1.0
.8
.6
.4
.2
0
-.2
-.4
-.6
-.8
-1.0
0
1
2
3
4
5
6
7
u in radians
F_V
F_S
u_1
u_2
u_3
u_4
e = 0.0
a = 3563
$\lambda_\Theta = 30^0$

Fig. 46

angle is returned to the main program via the variable contained in the calling statement.

c) Subroutine SPINVEH (ASPINVEH)

This subroutine contains three parts. The first, evaluates the celestial longitude and latitude of the vehicle from equations (17). Names of various variables are mnemonically close to those used in equations (17) so that their meaning should not be too difficult to identify. Since the latitude β_v normally falls in the range of $\pm 90^o$, the library ARSIN subroutine will place β_v in the proper quandrant. For the longitude, λ_v, this is not the case, and therefore, a call is made to the QTEST function. Note that the computation in its present form will break down should β_v attain a value of 90^o. Furthermore no tests are made for such a condition.

The second section converts the right ascension and declination of the spin axis to the corresponding celestial longitude and latitude. This conversion employs equations (13). The latitude itself is not evaluated because in the third section only its sine and cosine are needed. The longitude, however, must be evaluated explicitely. As in the first section mnemonics of symbols should make them easily identifiable in terms of equations (13). The computation would break down if the latitude should be equal to 90^o. No diagnostic tests of this condition are included.

The final section develops the angle between the spin axis and the radius vector of the vehicle. Equation (12) is used for this purpose, expressed in the ecliptic coordinate system. The return to the main program is through the argument defined in the name of the subroutine.

APPENDIX II

LISTING OF THE PROGRAM

APPENDIX II

```
$LIST SISYPHUS

4/16/71


00010 *     COMPUTATION OF EFFECTIVE OBSERVING TIMES FOR EARTH ORBITING
00020 *     SISYPHUS SYSTEM
00030 *     DEFINITIONS:
00040 *     LONSUN  =SUN'S CELESTIAL LONGITUDE
00050 *     DLONSUN =INCREMENT IN SUN'S LONGITUDE
00060 *     NLONSUN =NUMBER OF INCREMENTS IN SUN'S LONGITUDE
00070 *     LONSUNIN=INITIAL VALUE OF SUN'S LONGITUDE
00080 *     LONSUN0 =REFERENCE VALUE OF SUN'S LONGITUDE
00090 *     INC     =ORBITAL INCLINATION WITH RESPECT TO THE EQUATOR
00100 *     DELINC  = INCREMENTS IN INCLINATION
00110 *     NINC    =NUMBER OF INCREMENTS IN INCLINATION
00120 *     INCIN   =INITIAL VALUE OF INCLINATION
00130 *     NODREFIN=INITIAL VALUE OF THE EQUATORIAL NODE
00140 *     DELNODE =INCREMENT IN THE INITIAL VALUE OF THE NODE
00150 *     NNODE   =NUMBER OF INCREMENTS IN THE NODE
00160 *     ARGPERIN=INITIAL VALUE OF THE EQUATORIAL ARGUMENT OF PERI-
00170 *     GEE
00180 *     DELARPER=INCREMENT IN THE INITIAL VALUE OF THE ARGIMENT OF
00190 *     PERIGEE
00200 *     NARGPER =NUMBER OF INCREMENT IN ARGUMENT OF PERIGEE
00210 *     ALFSPIN =RIGHT ASCENSION OF THE SPIN AXIS
00220 *     DECSPIN =DECLINATION OF THE SPIN AXIS
00230 *     DELU    =INCREMENT IN ORBITAL POLAR ANGLE
00240 *     ECC     =ORBITAL ECCENTRICITY
00250 *     A0      =ORBITAL SEMI-MAJOR AXIS
00260 *     TOL     =TOLERANCE ON COMPUTING EARTH VIEWING AND ECLIPSE
00270 *     LIMITS
00280 *     CAPDEL  =ANGLE BETWEEN SPIN AXIS AND OPTICAL AXIS IN DEGREES
00290 *     FOV     =FIELD OF VIEW IN DEGREES
00300 *     UNITS: INPUT-ALL ANGLES IN DEGREES,A0 IN NAUTICAL MILES
00310 *            OUTPUT-P,TOTAL,T(JJ) IN HOURS,ANU,AASPNV,AASUNV IN
00320 *            RADIANS,ALL OTHER ANGLES IN DEGREES
00330       COMMON PI,LONSUN,NODEBAR,SNIBAR,CSIBAR,SNU,CSU,CONV,SNEPS,CSE
00340 &PS,SNSPINAL,CSSPINAL,SNSPINDE,CSSPINDE
00350       DIMENSION ANU(6),ECCAN(8),SNE(6),RR(6),FF(6),T(4),AASPNV(6)
00360       DIMENSION AASUNV(6),E(8),SLOPE(6),FSHAD(8),FDOTS(8)
00370       DIMENSION FVIEW(8),FDOTV(8),PHIT(8),PHIL(8)
00380       REAL LONSUN,LONSUNIN,LONSUN0,INC,INCIN,NODEREF,NODREFIN,NODE,
00390 &NODEBAR,NODEDOT
00400    30 READ:LONSUN0,LONSUNIN,DLONSUN,NLONSUN
00410       READ:INCIN,DELINC,NINC,NODREFIN,DELNODE,NNODE,ARGPERIN,DELARP
00420 &ER,NARGPER
00430       READ:ALFSPIN,DECSPIN
00440       READ:ECC,A0
00450       READ:DELU,TOL,CAPDEL,FOV
00460       PRINT 9,LONSUN0,ECC,A0,CAPDEL
00470     9 FORMAT(//1X8HLONSUN0=F7.2,3X4HECC=F5.3,3X3HA0=F14.8,3X7HCAPDE
00480 &L=F6.2)
00490 *     MISCELLANEOUS DATA
```

```
00500       PI=3.1415926
00510       PI2=1.5707963
00520       TWOPI=2.*PI
00530       RE=3441.84
00540       RECSUNRT=365.25/360.
00550       CONV=PI/180.
00560       EPS=23.452*CONV
00570       DELU=DELU*CONV
00580       ACAPDEL=CAPDEL*CONV
00590       AFOV=FOV*CONV/2.
00600       SNEPS=SIN(EPS)
00610       CSEPS=COS(EPS)
00620       INC=INCIN
00630 *     ANOMALISTIC PERIOD
00640       B=A0/RE
00650       B=B*SQRT(B)
00660       P=1.4083542*B
00670       PRINT 28,P,FOV
00680    28 FORMAT(1X8H       P=F6.3,4X4HFOV=F5.2)
00690       DO 100 I=1,NINC
00700       ARGINC=INC*CONV
00710       SNINC=SIN(ARGINC)
00720       CSINC=COS(ARGINC)
00730       DECNORM=PI2-ARGINC
00740 *     NODAL AND APSIDAL RATES
00750       B=(RE/A0)**3.5
00760       DENECC=1.-ECC*ECC
00770       TEMP=-10.*B
00780       DEN=DENECC*DENECC
00790       NODEDOT=TEMP*CSINC/DEN
00800       PERIGDOT=5.*B*(5.*CSINC*CSINC-1.)/DEN
00810       PRINT 11,NODEDOT,PERIGDOT,INC
00820    11 FORMAT(/1X8HNODEDOT=F7.2,2X7HPERDOT=F7.2,2X4HINC=F6.2)
00830       AK=NODEDOT*RECSUNRT
00840       AKK=PERIGDOT*RECSUNRT
00850       NODEREF=NODEFIN
00860       DO 200 J=1,NNODE
00870       PRINT 12,NODEREF
00880    12 FORMAT(/15X8HNODEREF=F6.2)
00890       REFARPER=ARGPERIN
00900       DO 300 K=1,NARGPER
00910       PRINT 13,REFARPER
00920    13 FORMAT(/1X9HREFARPER=F6.2)
00930       LONSIN=LONSUNIN
00940       PRINT 14
00950    14 FORMAT(2X6HLONSIN,6X3HETA,5X7HSPINSUN,3X4HNODE,5X6HARGPER,3X6
00960      &HETALIM)
00970       PRINT 31
00980    31 FORMAT(9X2HJJ,3X3HANU,5X2HRR,8X2HFF,7X6HAASPNV,3X6HAASUNV)
00990       PRINT 32
01000    32 FORMAT(9X2HJJ,3X5HT(JJ))
01010       DO 400 L=1,NLONSUN
01020       DSUNLON=LONSUN-LONSUN0
01030       EQNODE=NODEREF+AK*DSUNLON
01040       ARGPER=REFARPER+AKK*DSUNLON
01050       RADNODE=EQNODE*CONV
01060       RADARPER=ARGPER*CONV
01070       ALFNORM=3.*PI2+RADNODE
01080       ARSUNLON=LONSUN*CONV
01090 *     ANGLE BETWEEN THE SUN AND THE ORBIT NORMAL (ETA)
01100       SNDECNOR=SIN(DECNORM)
01110       CSDECNOR=COS(DECNORM)
01120       SNALFNOR=SIN(ALFNORM)
01130       CSALFNOR=COS(ALFNORM)
01140       SNSUNLON=SIN(ARSUNLON)
```

```
01150       CSSUNLON=COS(ARSUNLON)
01160       CSETA=(SNDECNOR*SNEPS+CSDECNOR*CSEPS*SNALFNOR)*SNSINLON
01170       CSETA=CSETA+CSDECNOR*CSALFNOR*CSSUNLON
01180       ETA=ARCOS(CSETA)/CONV
01190 *     ANGLE BETWEEN THE SPIN AXIS AND THE SUN
01200       SPINALF=ALFSPIN*CONV
01210       SPINDEC=DECSPIN*CONV
01220       SNSPINAL=SIN(SPINALF)
01230       CSSPINAL=COS(SPINALF)
01240       SNSPINDE=SIN(SPINDEC)
01250       CSSPINDE=COS(SPINDEC)
01260       CSSPNSIN=(SNSPINDE*SNEPS+CSSPINDE*CSEPS*SNSPINAL)*SNSUNLON
01270       CSSPNSUN=CSSPNSUN+CSSPINDE*CSSPINAL*CSSUNLON
01280       SPINSUN=ARCOS(CSSPNSUN)/CONV
01290 *     CONVERSION OF EQUATORIAL ORBIT ORIENTATION ELEMENTS TO THE
01300 *     ECLIPTIC ELEMENTS
01310       CSNODE=COS(RADNODE)
01320       SNNODE=SIN(RADNODE)
01330       CSIBAR=CSEPS*CSINC+SNEPS*SNINC*CSNODE
01340       SNIBAR=SQRT(1.-CSIBAR*CSIBAR)
01350       SND=SNINC*SNNODE/SNIBAR
01360       CSD=(SNINC*CSEPS*CSNODE-CSINC*SNEPS)/SNIBAR
01370       NODEBAR=QTEST(CSD,SND)
01380       SND=SNEPS*SNNODE/SNIBAR
01390       CSD=(SNINC*CSEPS-CSINC*SNEPS*CSNODE)/SNIBAR
01400       SMALLD=QTEST(CSD,SND)
01410       ARPERBAR=RADARPER-SMALLD
01420    46 IF(ARPERBAR.GE.0.0)GO TO 45
01430       ARPERBAR=TWOPI-ABS(ARPERBAR)
01440       GO TO 46
01450    45 UCOMP=TWOPI+ARPERBAR
01460 *     COMPUTATION OF EARTH VIEWING AND ECLIPSE LIMITS
01470       SLRECT=A0*DENECC
01480       XX=ARSUNLON-NODEBAR
01490       CSBETPR=COS(XX)/SIN(ETA*CONV)
01500       BETPR=ARCOS(CSBETPR)
01510       BETA=ABS(BETPR-ARPERBAR)
01520       XXX=PI-BETA
01530       RLIMIT=SLRECT/(1.+ECC*COS(XXX))
01540       CSETALIM=RE/RLIMIT
01550       ETALIM=ARCOS(CSETALIM)/CONV
01560       IF(ABS(CSETA)-CSETALIM)50,51,52
01570    50 KK=0
01580       CONST=-1.
01590       KKK=0
01600       GO TO 15
01610    51 PRINT:"SUN ON VEHICLE'S HORIZON AT /ETA-90./"
01620       GO TO 53
01630    52 PRINT:"VEHICLE IN CONTINUOUS SUNLIGHT"
01640    53 KK=1
01650       CONST=-1.
01660       KKK=2
01670    15 U=ARPERBAR+CONST*DELU
01680       ITEST=1
01690       ANUCOUNT=U
01700       IF(CONST.EQ.1.)GO TO 92
01710       INDF=1
01720     6 DEL=DELU
01730     3 SNU=SIN(U)
01740       CSU=COS(U)
01750       TRUANOM=U-ARPERBAR
01760       R=SLRECT/(1.+ECC*COS(TRUANOM))
01770       RATIO=RE/R
01780       PHILIM=ARSIN(RATIO)
01790       CALL SUNVEH(ASUNVEH)
```

```
01800       CALL SPINVEH(ASPINVEH)
01810       FS=SQRT(1.-RATI)*RATI))+COS(ASUNVEH)
01820       PHIS=PI-ASPINVEH-ACAPDEL
01830       PHI1=PHIS+AFOV
01840       PHI2=PHIS-AFOV
01850       IF(-PHIS)40,41,42
01860    42 PHI1=-PHI1
01870       PHI2=-PHI2
01880       GO TO 40
01890    41 PHI2=-PHI2
01900    40 IF(PHI1.LE.PHI2)GO TO 43
01910       PHI=PHI2
01920       GO TO 44
01930    43 PHI=PHI1
01940    44 FV=RATI)-SIN(PHI)
01950       GO TO(54,55,54),ITEST
01960    55 ITEST=3
01970       GO TO 1
01980    54 GO TO(96,98,99,95),INDF
01990    96 FIS=FS
02000       FIV=FV
02010       INDF=2
02020    91 U=U+DELU
02030       ANUCOUNT=ANUCOUNT+DELU
02040       GO TO 3
02050    98 FSTWOPI=FS
02060       FVTWOPI=FV
02070       FSDTTPI=FS-FIS
02080       FVDTTPI=FV-FIV
02090       PHITWOPI=PHI
02100       PHILTWPI=PHILIM
02110       INDF=3
02120       GO TO 91
02130    99 FS0=FSTWOPI
02140       FSDOT0=FS-FS0
02150       FV0=FVTWOPI
02160       FVDOT0=FV-FV0
02170       PHI0=PHITWOPI
02180       PHIL0=PHILTWPI
02190    92 FIS=FS0
02200       FIV=FV0
02210       FS=FSDOT0+FS0
02220       FV=FVDOT0+FV0
02230       INDF=4
02240    95 IF((INDF.EQ.4).AND.(ABS(DEL).EQ.DELU))GO TO 97
02250       GO TO 29
02260    97 SLS=FS-FIS
02270       SLV=FV-FIV
02280       TEMPFS=FS
02290       TEMPFV=FV
02300    29 IF(KK.EQ.0)GO TO 24
02310       F=FV
02320       FI=FIV
02330       SL=SLV
02340       GO TO 73
02350    24 F=FS
02360       FI=FIS
02370       SL=SLS
02380    73 IF(ITEST.EQ.3)GO TO 18
02390       IF((ABS(FI).LE.TOL).AND.((FI.GT.0.0).AND.(F.GT.0.0)))GO TO 56
02400       IF((ABS(FI).LE.TOL).AND.((FI.LT.0.0).AND.(F.LT.0.0)))GO TO 56
02410       ITEST=3
02420       GO TO 18
02430    56 U=ARPERBAR
02440       ANUCOUNT=U
```

```
02450       F=F1
02460       TEMPFS=FS0
02470       TEMPFV=FV0
02480       ITEST=2
02490       GO TO 3
02500    18 MFLAG=1
02510       IF((F1.GT.0.0).AND.(F.GT.0.0))GO TO 7
02520       MFLAG=0
02530       IF((F1.LT.0.0).AND.(F.LT.0.0))GO TO 7
02540       IF(ABS(F).LE.TOL)GO TO 1
02550       IF(KK.NE.1)GO TO 19
02560       IF(PHI.GT.PI2)GO TO 7
02570    19 DEL=-DEL/2.
02580       GO TO 7
02590     1 IF(KK.NE.1)GO TO 2
02600       IF(PHI.LT.PI2)GO TO 2
02610     7 IF(ABS(DEL).LT.DELU)GO TO 47
02620       ANUCOUNT=ANUCOUNT+DELU
02630    47 U=U+DEL
02640       FIS=FS
02650       FIV=FV
02660       IF((U.EQ.UCOMP).AND.(ABS(F).LE.TOL))GO TO 1
02670       IF(U.GT.UCOMP)GO TO 8
02680       GO TO 3
02690     2 KKK=KKK+1
02700       AASPNV(KKK)=ASPINVEH
02710       AASUNV(KKK)=ASUNVEH
02720       ANU(KKK)=U
02730       RR(KKK)=R
02740       FF(KKK)=F
02750       SLOPE(KKK)=SL
02760       FSHAD(KKK)=FS
02770       FDOTS(KKK)=SLS
02780       FVIEW(KKK)=FV
02790       FDOTV(KKK)=SLV
02800       PHIT(KKK)=PHI
02810       PHIL(KKK)=PHILIM
02820       U=ANUCOUNT+DELU
02830       ANUCOUNT=ANUCOUNT+DELU
02840       IF(U.GT.UCOMP)GO TO 8
02850       IF(KKK.EQ.2)GO TO 8
02860       FIS=TEMPFS
02870       FIV=TEMPFV
02880       GO TO 6
02890     8 IF(KK.EQ.1)GO TO 27
02900       KK=1
02910       CONST=1.
02920       DEL=DELU
02930       GO TO 15
02940    27 SMALLN=TWOPI/P
02950       NFLAG=0
02960       IF(ABS(CSETA).LT.CSETALIM)GO TO 60
02970       NX=3
02980    64 IF(KKK.EQ.6)GO TO 61
02990       IF(KKK.EQ.4)GO TO 63
03000       IF(KKK-3)81,80,26
03010    80 PRINT:"FIELD TANGENT TO EARTH AT PERIGEE"
03020       GO TO 82
03030    81 IF(MFLAG)26,89,88
03040    89 PRINT:"EARTH IS NOT VIEWED ON THIS ORBIT"
03050       GO TO 82
03060    88 PRINT:"PARTIAL EARTH VIEWING THROUGHOUT THIS ORBIT"
03070    82 IF(NX.EQ.1)GO TO 83
03080       NFLAG=1
03090       GO TO 71
```

```
03100    83 NY=2
03110       GO TO 70
03120    60 NX=1
03130       GO TO 64
03140    63 NY=4
03150       GO TO 70
03160    61 NY=6
03170    70 DO 20 JJ=NX,NY
03180       TRUAN0M=ANU(JJ)-ARPERBAR
03190       CSTRUAN=COS(TRUAN0M)
03200       SNTRUAN=SIN(TRUAN0M)
03210       DEN=1.+ECC*CSTRUAN
03220       TT=SQRT(DEN*ECC)
03230       CSD=(CSTRUAN+ECC)/DEN
03240       SND=TT*SNTRUAN/DEN
03250       SNE(JJ)=SND
03260    20 E(JJ)=QTEST(CSD,SND)
03270 *             COMPUTATION OF LIMITING TIMES, SHADOW AND EARTH
03280 *             VIEWING INTERVALS
03290       NYY=NY/2
03300       IF(NX.EQ.1)GO TO 84
03310       NXX=NX-1
03320       GO TO 85
03330    84 NXX=NX
03340    85 DO 21 JJ=NXX,NYY
03350       IF(JJ.EQ.1)GO TO 65
03360       IF((SLOPE(2*JJ-1).LT.0.0).AND.(SLOPE(2*JJ).GT.0.0))GO TO 65
03370       IF(JJ.EQ.2)GO TO 66
03380       M=2*JJ
03390       MM=JJ
03400       GO TO 67
03410    66 IF(NYY.NE.3)GO TO 65
03420       M=2*JJ+1
03430       MM=M-1
03440       GO TO 67
03450    65 M=2*JJ
03460       MM=M-1
03470    67 DIFF=E(M)-E(MM)
03480       TEMP=ECC*(SIN(E(M))-SIN(E(MM)))
03490       T(JJ)=DIFF-TEMP
03500       IF(JJ.EQ.1)GO TO 25
03510       IF(NYY.EQ.2)GO TO 25
03520       IF(JJ.NE.3)GO TO 21
03530    25 IF((SLOPE(2*JJ-1).LT.0.0).AND.(SLOPE(2*JJ).GT.0.0))GO TO 21
03540       T(JJ)=TWOPI-T(JJ)
03550    21 T(JJ)=T(JJ)/SMALLN
03560       IF(NYY.EQ.3)T(4)=T(2)+T(3)
03570    71 IF(NFLAG.EQ.0)GO TO 86
03580       IF(MFLAG.EQ.0)GO TO 90
03590       PRINT:"NO SHADOW,BUT PARTIAL EARTH VIEWING FOR ENTIRE ORBIT"
03600       GO TO 103
03610    90 PRINT:"NO SHADOW AND NO EARTH VIEWING ON THIS ORBIT"
03620       TTOTAL=P
03630       GO TO 106
03640    86 PRINT 23,LONSUN,ETA,SPINSUN,EQNODE,ARGPER,ETALIM
03650    23 FORMAT(1XF7.2,6XF6.2,4F9.2)
03660       PRINT 33,(JJ,ANU(JJ),RR(JJ),FF(JJ),AASPNV(JJ),AASUNV(JJ),JJ=
03670 &NX,NY)
03680    33 FORMAT(9X12,5F9.2)
03690       PRINT 34,(JJ,T(JJ),JJ=NXX,NYY)
03700    34 FORMAT(9X12,F9.2)
03710       IF(NYY.EQ.3)GO TO 87
03720       GO TO 103
03730    87 JJ=4
03740       PRINT 34,JJ,T(JJ)
```

```
03750 *          RESEQUENCING OF LIMITING F'S AND FDOT'S
03760  103 DO 36 JJ=NX,NY
03770      IF(NX.EQ.1)GO TO 37
03780      JJJ=JJ
03790      JJJJ=JJ-1
03800      GO TO 38
03810   37 JJJ=NY+1-JJ
03820      JJJJ=JJJ+1
03830   38 E(JJJJ)=E(JJJ)
03840      PHIT(JJJJ)=PHIT(JJJ)
03850      PHIL(JJJJ)=PHIL(JJJ)
03860      FSHAD(JJJJ)=FSHAD(JJJ)
03870      FDOTS(JJJJ)=FDOTS(JJJ)
03880      FVIEW(JJJJ)=FVIEW(JJJ)
03890   36 FDOTV(JJJJ)=FDOTV(JJJ)
03900      E(1)=0.
03910      FSHAD(1)=FS0
03920      FDOTS(1)=FSDOT0
03930      FVIEW(1)=FV0
03940      FDOTV(1)=FVDOT0
03950      PHIT(1)=PHI0
03960      PHIL(1)=PHIL0
03970      IF(NX.EQ.1)GO TO 39
03980      JJ=NY
03990      GO TO 48
04000   39 JJ=NY+2
04010   48 E(JJ)=TWOPI
04020      FSHAD(JJ)=FSTWOPI
04030      FDOTS(JJ)=FSDTTPI
04040      FVIEW(JJ)=FVTWOPI
04050      FDOTV(JJ)=FVDTTPI
04060      PHIT(JJ)=PHITWOPI
04070      PHIL(JJ)=PHILTWPI
04080 *          SORTING SUBROUTINE
04090      M=JJ
04100  101 M=M/2
04110      IF(M.EQ.0)GO TO 900
04120      KS=JJ-M
04130      II=1
04140  102 IS=II
04150  105 IM=IS+M
04160      IF(E(IS).LE.E(IM))GO TO 104
04170      TEMP1=E(IS)
04180      TEMP2=FSHAD(IS)
04190      TEMP3=FDOTS(IS)
04200      TEMP4=FVIEW(IS)
04210      TEMP5=FDOTV(IS)
04220      TEMP6=PHIT(IS)
04230      TEMP7=PHIL(IS)
04240      E(IS)=E(IM)
04250      FSHAD(IS)=FSHAD(IM)
04260      FDOTS(IS)=FDOTS(IM)
04270      FVIEW(IS)=FVIEW(IM)
04280      FDOTV(IS)=FDOTV(IM)
04290      PHIT(IS)=PHIT(IM)
04300      PHIL(IS)=PHIL(IM)
04310      E(IM)=TEMP1
04320      FSHAD(IM)=TEMP2
04330      FDOTS(IM)=TEMP3
04340      FVIEW(IM)=TEMP4
04350      FDOTV(IM)=TEMP5
04360      PHIT(IM)=TEMP6
04370      PHIL(IM)=TEMP7
04380      IS=IS-M
04390      IF(IS.GE.1)GO TO 105
```

```
04400  104 II=II+1
04410      IF(II.GT.KS)GO TO 101
04420      GO TO 102
04430 *            EVALUATION OF TOTAL TIME WHEN THE VEHICLE IS NOT IN
04440 *            THE SHADOW AND DOES NOT VIEW THE EARTH, THAT IS, TOTAL
04450 *            POTENTIAL OBSERVING TIME
04460  900 LL=0
04470      DO 35 II=1,JJ
04480      IF(ABS(CSETA).GE.CSETALIM)FSHAD(II)=TOL
04490      IF((FSHAD(II).GT.0.0).AND.(FVIEW(II).LT.0.0))GO TO 16
04500      IF((FSHAD(II).GT.0.0).AND.((FVIEW(II).LE.TOL).AND.(FDOTV(II).
04510 &LT.0.0)))GO TO 16
04520      IF(((ABS(FSHAD(II)).LE.TOL).AND.(FDOTS(II).LT.0.0)).AND.(FVIE
04530 &W(II).LT.0.0))GO TO 16
04540      IF((FSHAD(II).GT.0.0).AND.((ABS(FVIEW(II)).LE.TOL).AND.(FDOTV
04550 &(II).GT.0.0)))GO TO 16
04560      IF(((ABS(FSHAD(II)).LE.TOL).AND.(FDOTS(II).LT.0.0)).AND.((ABS
04570 &(FVIEW(II)).LE.TOL).AND.(FDOTV(II).GT.0.0)))GO TO 16
04580      IF(((ABS(FSHAD(II)).LE.TOL).AND.(FDOTS(II).GT.0.0)).AND.((ABS
04590 &(FVIEW(II)).LE.TOL).AND.(FDOTV(II).LT.0.0)))GO TO 16
04600      IF(((ABS(FSHAD(II)).LE.TOL).AND.(FDOTS(II).GT.0.0)).AND.(FVIE
04610 &W(II).LT.0.0))GO TO 16
04620      IF((ABS(FSHAD(II)).LE.TOL).AND.((FVIEW(II).GE.0.0).AND.(PHIT(
04630 &II).GT.PHIL(II))))GO TO 16
04640      IF((ABS(FSHAD(II)).LE.TOL).AND.((ABS(FVIEW(II)).LE.TOL).AND.(
04650 &PHIT(II).GT.PHIL(II))))GO TO 16
04660      GO TO 35
04670   16 LL=LL+1
04680      ECCAN(LL)=E(II)
04690   35 CONTINUE
04700      TTOTAL=0.
04710      LLL=LL/2
04720      IF(LL.EQ.0)GO TO 106
04730      DO 22 JJ=1,LLL
04740      DIFF=ECCAN(2*JJ)-ECCAN(2*JJ-1)
04750      TEMP=ECC*(SIN(ECCAN(2*JJ))-SIN(ECCAN(2*JJ-1)))
04760      TIMEINT=(DIFF-TEMP)/SMALLN
04770   22 TTOTAL=TTOTAL+TIMEINT
04780  106 PRINT:"TTOTAL=",TTOTAL
04790  400 LONSIN=LONSUN+DLONSUN
04800  300 REFARPER=REFARPER+DELARPER
04810  200 NODEREF=NODEREF+DELNODE
04820  100 INC=INC+DELINC
04830      PRINT 26
04840   26 FORMAT(///)
04850      GO TO 30
04860      END
```

```
$LIST QTEST

4/16/71

00010 *    THIS ROUTINE TESTS QUADRANTS OF ANGLES
```

```
00020       FUNCTION QTEST(CSD,SND)
00030       COMMON PI
00040       IF(CSD)21,22,21
00050    22 CS=1.E-36
00060       GO TO 54
00070    21 CS=CSD
00080    54 QTEST=ATAN(SND/CS)
00090       IF(CSD)31,32,32
00100    31 QTEST=QTEST+PI
00110       RETURN
00120    32 IF(SND)33,34,34
00130    33 QTEST=QTEST+2.*PI
00140    34 RETURN
00150       END
```

$LIST SPINVEH

4/16/71

```
00010 *     SUBROUTINE TO COMPUTE THE ANGLE BETWEEN THE SPIN AXIS AND
00020 *     THE VEHICLE RADIUS VECTOR
00030       SUBROUTINE SPINVEH(ASPINVEH)
00040       COMMON PI,DUM2,NODEBAR,SNIBAR,CSIBAR,SNU,CSU,CONV,SNEPS,CSEPS
00050 &,SNSPINAL,CSSPINAL,SNSPINDE,CSSPINDE
00055       REAL NODEBAR
00060 *         CELESTIAL LONGITUDE AND LATITUDE OF THE VEHICLE
00070       SNBETV=SNU*SNIBAR
00080       CSBETV=SQRT(1.-SNBETV*SNBETV)
00090       SNNODBAR=SIN(NODEBAR)
00100       CSNODBAR=COS(NODEBAR)
00110       SNLAMDV=(CSU*SNNODBAR+SNU*CSNODBAR*CSIBAR)/CSBETV
00120       CSLAMDV=(CSU*CSNODBAR-SNU*SNNODBAR*CSIBAR)/CSBETV
00130       SND=SNLAMDV
00140       CSD=CSLAMDV
00150       BETV=ARSIN(SNBETV)
00160       ALAMDV=QTEST(CSD,SND)
00170 *         CONVERSION OF SPIN AXIS RIGHT ASCENSION AND DECLINATION
00180 *         TO CELESTIAL LONGITUDE AND LATITUDE
00190       SNBETSPN=SNSPINDE*CSEPS-CSSPINDE*SNEPS*SNSPINAL
00200       CSBETSPN=SQRT(1.-SNBETSPN*SNBETSPN)
00210       CSLAMSPN=CSSPINDE*CSSPINAL/CSBETSPN
00220       SNLAMSPN=(SNSPINDE*SNEPS+CSSPINDE*CSEPS*SNSPINAL)/CSBETSPN
00230       SND=SNLAMSPN
00240       CSD=CSLAMSPN
00250       ALAMDSPN=QTEST(CSD,SND)
00260 *         ANGLE BETWEEN THE SPIN AXIS AND THE RADIUS VECTOR
00270       CSSPNVEH=CSBETSPN*CSBETV*COS(ALAMDV-ALAMDSPN)
00280       CSSPNVEH=CSSPNVEH+SNBETSPN*SNBETV
00290       ASPINVEH=ARCOS(CSSPNVEH)
00300       RETURN
00310       END
```

```
$LIST SUNVEH


4/16/71



00010 *     SUBROUTINE TO COMPUTE THE ANGLE BETWEEN THE SUN AND
00020 *     THE VEHICLE
00030       SUBROUTINE SUNVEH(ASUNVEH)
00040       COMMON DUM1,LONSUN,NODEBAR,SNIBAR,CSIBAR,SNU,CSU,CONV
00045       REAL LONSUN,NODEBAR
00050       ANG=LONSUN*CONV-NODEBAR
00060       CSSUNVEH=CSU*COS(ANG)+SNU*CSIBAR*SIN(ANG)
00070       ASUNVEH=ARCOS(CSSUNVEH)
00080       RETURN
00090       END
```

APPENDIX III

OUTPUT FOR EXAMPLE I

APPENDIX III

```
SD  22 10:08 EST 20 AUG 71
USER CODE= 2R100238
VALUE '70'S -- AEROSPACE TIMESHARING


READY


$FORT SISYPHUS,QTEST,SUNVEH,SPINVEH

=0.,0.,90.,5
=60.,5.,2,0.,90.,2,0.,90.,2
=270.,-60.
=0.,3563.
=8.,.0001,40.,10.




LONSUN0=    0.      ECC=0.       A0=0.35630000E+04   CAPDEL= 40.00
      P= 1.483     FOV=10.00

NODEDOT=  -4.43   PERDOT=    1.11   INC= 60.00

               NODEREF=  0.

REFARPER=  0.
 LONSUN        ETA       SPINSUN     NODE       ARGPER     ETALIM
         JJ    ANU       RR          FF         AASPNV     AASUNV
         JJ    T(JJ)
   0.           90.00      90.00       0.         0.       14.98
          1      1.83    3563.00       0.00       2.88      1.83
          2      4.45    3563.00       0.00       0.26      1.83
          3      3.67    3563.00       0.00       1.05      2.62
          4      5.76    3563.00       0.00       1.05      0.52
          1      0.62
          2      0.49
TTOTAL=   3.0897118E-01
  90.00         111.58     143.45    -404.49     101.12     14.98
          1      4.59    3563.00      -0.00       0.89      1.83
          2      7.17    3563.00      -0.00       1.69      1.83
          3      4.43    3563.00       0.00       1.05      1.69
          4      6.52    3563.00      -0.00       1.05      2.41
          1      0.61
          2      0.49
TTOTAL=   3.6891028E-02
```

```
 180.00        30.02     90.00   -808.99    202.25     14.98
          1     7.26   3563.00      0.00      1.50      1.83
          2     9.31   3563.00     -0.00      2.55      1.83
          3     4.78   3563.00     -0.00      1.05      1.08
          4     6.75   3563.00      0.00      1.05      1.59
          1     0.49
          2     0.47
TTOTAL=    4.6522715E-01
 270.00       138.22     36.55  -1213.48    303.37     14.98
          1     8.51   3563.00     -0.00      2.30      1.83
          2    10.85   3563.00     -0.00      1.19      1.83
          3     6.32   3563.00      0.00      1.05      0.86
          4    11.11   3563.00      0.00      1.05      1.67
          1     0.55
          2     0.35

TTOTAL=    3.5333115E-01
PARTIAL EARTH VIEWING THROUGHOUT THIS ORBIT
 360.00        91.75     90.00  -1617.98    404.49     14.98
          1     1.31   3563.00     -0.00      2.07      1.83
          2     4.97   3563.00      0.00      1.06      1.83
          1     0.62
TTOTAL=    0.

REFARPER= 90.00
 LONSUN        ETA       SPINSUN     NODE      ARGPER    ETALIM
          JJ   ANU       RR          FF        AASPNV    AASUNV
          JJ   T(JJ)
    0.          90.00     90.00       0.       90.00     14.98
          1     1.83   3563.00      0.00      2.88      1.83
          2     4.45   3563.00      0.00      0.26      1.83
          3     3.67   3563.00      0.00      1.05      2.62
          4     5.76   3563.00      0.00      1.05      0.52
          1     0.62
          2     0.49
TTOTAL=    3.0897119E-01
  90.00       111.58    143.45   -404.49    191.12     14.98
          1     4.59   3563.00     -0.00      0.89      1.83
          2     7.17   3563.00     -0.00      1.69      1.83
          3     4.43   3563.00      0.00      1.05      1.69
          4     6.52   3563.00     -0.00      1.05      2.41
          1     0.61
          2     0.49
TTOTAL=    3.6891040E-02
 180.00        30.02     90.00   -808.99    292.25     14.98
          1     7.26   3563.00      0.00      1.50      1.83
          2     9.31   3563.00     -0.00      2.55      1.83
          3     6.75   3563.00      0.00      1.05      1.59
          4    11.06   3563.00     -0.00      1.05      1.08
          1     0.49
          2     0.47
TTOTAL=    1.0181427E+00
 270.00       138.22     36.55  -1213.48    393.37     14.98
          1     2.23   3563.00     -0.00      2.30      1.83
          2     4.57   3563.00     -0.00      1.19      1.83
          3     4.83   3563.00      0.00      1.05      1.67
          4     6.32   3563.00      0.00      1.05      0.86
          1     0.55
          2     0.35
TTOTAL=    3.5333056E-01
 360.00        91.75     90.00  -1617.98    494.49     14.98
```

```
          1      4.97   3563.00      0.00      1.06      1.83
          2      7.59   3563.00     -0.00      2.07      1.83
          3      4.74   3563.00     -0.00      1.05      1.60
          4      4.74   3563.00     -0.00      1.05      1.60
          1      0.62
          2     -0.00
TTOTAL=   1.4071806E-08

                NODEREF= 90.00

REFARPER=  0.
 LONSUN        ETA      SPINSUN    NODE      ARGPER    ETALIM
         JJ    ANU       RR        FF        AASPNV    AASUNV
         JJ    T(JJ)
   0.           30.00     90.00     90.00      0.       14.98
          1      6.36   3563.00     -0.00      2.52      1.83
          2      8.42   3563.00     -0.00      1.53      1.83
          3      8.96   3563.00      0.00      1.05      1.57
          4     10.93   3563.00      0.00      1.05      1.09
          1      0.49
          2      0.46
TTOTAL=   4.6406795E-01
  90.00       110.97    143.45   -314.49    101.12     14.98
          1      2.24   3563.00     -0.00      1.70      1.83
          2      4.82   3563.00      0.00      0.89      1.83
          3      2.89   3563.00     -0.00      1.05      2.42
          4      4.98   3563.00      0.00      1.05      1.68
          1      0.61
          2      0.49
TTOTAL=   3.7856916E-02
 180.00        90.88     90.00   -718.99    202.25     14.98
          1      4.95   3563.00     -0.00      0.26      1.83
          2      7.57   3563.00      0.00      2.88      1.83
          3      3.64   3563.00      0.00      1.05      0.52
          4      5.74   3563.00      0.00      1.05      2.62
          1      0.62
          2      0.49
TTOTAL=   3.0897097E-01
 270.00        67.82     36.55  -1123.48    303.37     14.98
          1      7.71   3563.00      0.00      2.24      1.83
          2     10.29   3563.00     -0.00      1.46      1.83
          3      6.51   3563.00      0.00      1.05      0.74
          4     10.71   3563.00     -0.00      1.05      1.45
          1      0.61
          2      0.49
TTOTAL=   9.9097338E-01
 360.00       149.94     90.00  -1527.98    404.49     14.98
          1      4.08   3563.00      0.00      1.67      1.83
          2      6.14   3563.00      0.00      0.56      1.83
          3      4.77   3563.00     -0.00      1.05      2.06
          4      6.75   3563.00      0.00      1.05      1.54
          1      0.49
          2      0.47
TTOTAL=   1.4453853E-01

REFARPER= 90.00
 LONSUN        ETA      SPINSUN    NODE      ARGPER    ETALIM
         JJ    ANU       RR        FF        AASPNV    AASUNV
         JJ    T(JJ)
   0.           30.00     90.00     90.00     90.00     14.98
          1      2.13   3563.00     -0.00      1.53      1.83
          2      6.36   3563.00     -0.00      2.52      1.83
```

```
          3      2.68   3563.00      0.00      1.05      1.57
          4      4.64   3563.00      0.00      1.05      1.09
          1      0.49
          2      0.46
TTOTAL=   4.6406821E-01
  90.00       110.97    143.45   -314.49    191.12     14.98
          1      4.82   3563.00      0.00      0.89      1.83
          2      8.52   3563.00     -0.00      1.70      1.83
          3      4.98   3563.00      0.00      1.05      1.68
          4      9.18   3563.00     -0.00      1.05      2.42
          1      0.61
          2      0.49
TTOTAL=   3.7856899E-02

 180.00        90.88    90.00   -718.99    292.25     14.98
          1      7.57   3563.00      0.00      2.88      1.83
          2     11.84   3563.00     -0.00      0.26      1.83
          3      5.74   3563.00      0.00      1.05      2.62
          4      9.93   3563.00      0.00      1.05      0.52
          1      0.62
          2      0.49
TTOTAL=   3.0897077E-01
 270.00        67.82    36.55  -1123.48    393.37     14.98
          1      1.43   3563.00      0.00      2.24      1.83
          2      4.01   3563.00     -0.00      1.46      1.83
          3      4.42   3563.00     -0.00      1.05      1.45
          4      6.51   3563.00      0.00      1.05      0.74
          1      0.61
          2      0.49
TTOTAL=   4.9239647E-01
 360.00       149.94    90.00  -1527.98    494.49     14.98
          1      4.08   3563.00      0.00      1.67      1.83
          2      6.14   3563.00      0.00      0.56      1.83
          3      4.77   3563.00     -0.00      1.05      2.06
          4      6.75   3563.00      0.00      1.05      1.54
          1      0.49
          2      0.47
TTOTAL=   1.4453853E-01

NODEDOT=  -3.74  PERDOT=  -0.47  INC= 65.00

              NODEREF=  0.

REFARPER=  0.
 LONSUN        ETA       SPINSUN     NODE       ARGPER     ETALIM
         JJ    ANU       RR          FF         AASPNV     AASUNV
         JJ    T(JJ)
   0.          90.00     90.00       0.         0.         14.98
          1      1.83   3563.00      0.00      2.87      1.83
          2      4.45   3563.00      0.00      0.28      1.83
          3      3.67   3563.00      0.00      1.05      2.62
          4      5.76   3563.00      0.00      1.05      0.53
          1      0.62
          2      0.49
TTOTAL=   3.0845608E-01
  90.00       188.47    143.45   -341.89    -43.27     14.98
          1      5.39   3563.00     -0.00      1.02      1.83
          2      9.21   3563.00     -0.00      1.45      1.83
          3      5.42   3563.00     -0.00      1.05      1.81
          4      9.61   3563.00      0.00      1.05      2.13
          1      0.58
          2      0.49
```

```
TTOTAL=   6.5670164E-03
 180.00       122.37     90.00   -683.79    -86.54     14.98
          1     6.92   3563.00      0.00      2.83      1.83
          2    10.68   3563.00     -0.00      0.31      1.83
          3     5.13   3563.00      0.00      1.05      2.39
          4     9.32   3563.00     -0.00      1.05      0.75
          1     0.59
          2     0.49
TTOTAL=   3.2055964E-01
 270.00       71.53     36.55  -1025.68   -129.80     14.98
          1     5.24   3563.00     -0.00      1.36      1.83
          2     7.83   3563.00     -0.00      2.33      1.83
          3     4.92   3563.00     -0.00      1.05      1.53
          4     9.12   3563.00      0.00      1.05      0.64
          1     0.61
          2     0.49
TTOTAL=   9.9045841E-01
 360.00       30.23     90.00  -1367.57   -173.07     14.98
          1     7.01   3563.00      0.00      2.88      1.83
          2     9.08   3563.00      0.00      0.97      1.83
          3     4.78   3563.00     -0.00      1.05      1.05
          4     9.00   3563.00     -0.00      1.05      1.87
          1     0.49
          2     0.49
TTOTAL=   4.6883293E-01

REFARPER= 90.00
 LONSUN        ETA       SPINSUN     NODE       ARGPER    ETALIM
          JJ   ANU       RR          FF         AASPNV    AASUNV
          JJ   T(JJ)
   0.          90.00     90.00       0.         90.00     14.98
          1     1.83   3563.00      0.00      2.87      1.83
          2     4.45   3563.00      0.00      0.28      1.83
          3     3.67   3563.00      0.00      1.05      2.62
          4     5.76   3563.00      0.00      1.05      0.53
          1     0.62
          2     0.49
TTOTAL=   3.0845607E-01
  90.00      128.47    143.45   -341.89     46.73     14.98
          1     2.92   3563.00     -0.00      1.45      1.83
          2     5.39   3563.00     -0.00      1.02      1.83
          3     3.33   3563.00      0.00      1.05      2.13
          4     5.42   3563.00     -0.00      1.05      1.81
          1     0.58
          2     0.49
TTOTAL=   6.5669884E-03

 180.00       122.37     90.00   -683.79      3.46     14.98
          1     6.92   3563.00      0.00      2.83      1.83
          2    10.68   3563.00     -0.00      0.31      1.83
          3     9.32   3563.00     -0.00      1.05      0.75
          4    11.42   3563.00      0.00      1.05      2.39
          1     0.59
          2     0.49
TTOTAL=   3.2055959E-01
 270.00       71.53     36.55  -1025.68    -39.80     14.98
          1     5.24   3563.00     -0.00      1.36      1.83
          2     7.83   3563.00     -0.00      2.33      1.83
          3     9.12   3563.00      0.00      1.05      0.64
          4    11.20   3563.00     -0.00      1.05      1.53
          1     0.61
          2     0.49
TTOTAL=   4.9291135E-01
```

```
 360.00        30.23     90.00 -1367.57    -83.07     14.98
          1     7.01   3563.00     0.00      2.88      1.83
          2     9.08   3563.00     0.00      0.97      1.83
          3     4.78   3563.00    -0.00      1.05      1.05
          4     9.00   3563.00    -0.00      1.05      1.87
          1     0.49
          2     0.49
TTOTAL=    4.6883292E-01

                NODEREF= 90.00

REFARPER=   0.
 LONSUN         ETA       SPINSUN    NODE       ARGPER    ETALIM
          JJ    ANU       RR         FF         AASPNV    AASUNV
          JJ    T(JJ)
    0.          25.00     90.00     90.00      0.        14.98
          1     6.50   3563.00     0.00      2.64      1.83
          2     8.32   3563.00     0.00      1.66      1.83
          3     8.98   3563.00     0.00      1.05      1.57
          4    10.99   3563.00     0.00      1.05      1.18
          1     0.43
          2     0.47
TTOTAL=    4.7385410E-01
  90.00         64.75    143.45  -251.89    -43.27     14.98
          1     8.01   3563.00    -0.00      1.94      1.83
          2    10.57   3563.00     0.00      0.75      1.83
          3     9.06   3563.00     0.00      1.05      2.65
          4    10.96   3563.00     0.00      1.05      1.48
          1     0.60
          2     0.45
TTOTAL=    9.1809306E-02
 180.00        136.99     90.00  -593.79    -86.54     14.98
          1     4.51   3563.00    -0.00      0.93      1.83
          2     8.43   3563.00     0.00      1.66      1.83
          3     4.70   3563.00    -0.00      1.05      1.71
          4     9.25   3563.00     0.00      1.05      2.26
          1     0.56
          2     0.41
TTOTAL=    4.3522481E-02
 270.00        147.52     36.55  -935.68   -129.80     14.98
          1     5.06   3563.00     0.00      1.21      1.83
          2     7.20   3563.00    -0.00      2.32      1.83
          3     4.78   3563.00     0.00      1.05      1.68
          4     9.57   3563.00     0.00      1.05      1.03
          1     0.50
          2     0.35
TTOTAL=    3.5075565E-01
 360.00        74.12     90.00 -1277.57   -173.07     14.98
          1     5.00   3563.00     0.00      1.07      1.83
          2     7.59   3563.00    -0.00      2.21      1.83
          3     3.75   3563.00     0.00      1.05      0.65
          4     4.93   3563.00     0.00      1.05      1.77
          1     0.61
          2     0.28
TTOTAL=    2.7967711E-01


REFARPER=  90.00
 LONSUN         ETA       SPINSUN    NODE       ARGPER    ETALIM
          JJ    ANU       RR         FF         AASPNV    AASUNV
          JJ    T(JJ)
    0.          25.00     90.00     90.00      90.00     14.98
```

```
          1      2.04   3563.00      0.00      1.66      1.83
          2      6.50   3563.00      0.00      2.64      1.83
          3      2.70   3563.00      0.00      1.05      1.57
          4      4.70   3563.00      0.00      1.05      1.18
          1      0.43
          2      0.47
TTOTAL=    4.7385434E-01
  90.00        64.75    143.45   -251.89     46.73     14.98
          1      1.73   3563.00     -0.00      1.94      1.83
          2      4.29   3563.00      0.00      0.75      1.83
          3      2.77   3563.00      0.00      1.05      2.65
          4      4.68   3563.00      0.00      1.05      1.48
          1      0.60
          2      0.45
TTOTAL=    9.1809299E-02
 180.00       136.99     90.00   -593.79      3.46     14.98
          1      8.43   3563.00      0.00      1.66      1.83
          2     10.80   3563.00     -0.00      0.93      1.83
          3      9.25   3563.00      0.00      1.05      2.26
          4     10.98   3563.00     -0.00      1.05      1.71
          1      0.56
          2      0.41
TTOTAL=    4.3522493E-02
 270.00       147.52     36.55   -935.68    -39.80     14.98
          1      7.20   3563.00     -0.00      2.32      1.83
          2     11.35   3563.00      0.00      1.21      1.83
          3      9.57   3563.00      0.00      1.05      1.03
          4     11.06   3563.00      0.00      1.05      1.68
          1      0.50
          2      0.35
TTOTAL=    3.5075506E-01
 360.00       74.12     90.00  -1277.57    -83.07     14.98
          1      5.00   3563.00      0.00      1.07      1.83
          2      7.59   3563.00     -0.00      2.21      1.83
          3      4.93   3563.00      0.00      1.05      1.77
          4     10.03   3563.00      0.00      1.05      0.65
          1      0.61
          2      0.28
TTOTAL=    2.7967763E-01


=\

READY


$STATUS CONTINUE

ACCOUNT FOR 2R100238

TERMINAL HOURS:  0.57
C P U  SECONDS: 62.10
I/O   REQUESTS: 16
13 OF 25 LINKS USED

22 DISCONNECTED AT 10:43
```

APPENDIX IV

SISYPHUS THRESHOLD ESTIMATION

APPENDIX IV. SISYPHUS THRESHOLD ESTIMATION

A. INTRODUCTION

If the Sisyphus system is mounted on a spinning spacecraft, the sky background viewed by the telescopes is continuously varying. The threshold in each telescope is designed to "follow" the background and high frequency noise. Since the telescopes remain approximately aligned, the background and, consequently, the thresholds of all four telescopes should remain approximately equal. The background is averaged through a comparatively long time constant circuit which has the effect of introducing a delay in the background response. The relative threshold for each telescope at any instant t is designed to be self-setting at a value of

$$T_{rel} = K_1\, i_n(t) + K_2\, i_B(t) - i_B\,(t - \Delta t).$$

The change in the relative threshold over a complete spacecraft rotation as a function of the orientation of the spacecraft spin axis for the Pioneer mounted instrument is calculated by means of a program called THRESH1. The present section discusses this program and the results it yields.

The program first reads the sky sector at which the vehicle spin axis is pointed (galactic longitude and latitude) and a reference angle from which the vehicle is spinning. This latter angle is taken with respect to the galactic pole (see Figure 47). Also as input data, the program reads the bandwidth (in Hz) at which the instrument is operating, the roll rate of the vehicle (in degrees per second), the active filter time constant, the multiplication factor by which the high frequency noise is multiplied, the multiplication factor by which the background is multiplied, and finally the angular increments for the rotation of the vehicle. The program has a minimum increment of 3^{o}; for coarser information, these increments can be set at any value.

The program first calculates the galactic longitude and latitude at which the telescopes are pointed. It then calls a subroutine which calculates the mean sky brightness in tenth magnitude stars (visual) per square degree for that position in the sky. The subroutine has as input data a complete sky mapping (see Figure 48). The subroutine interpolates linearly to obtain the sky brightness. The interpolation in two dimensions is a modification of a one dimensional routine in Reference 4.

The main program then uses the mean sky brightness to calculate the background for two cases: (a) the instantaneous background, and (b) the background which the instrument saw at a time equal to the present time minus the active filter time constant. The instantaneous noise for the background limited condition (i.e., photon noise) is then computed.

Corresponding to the operation of the threshold setting logic of the instrument, the relative threshold is then calculated for a multiple of the instantaneous noise plus a multiple of the delayed slower varying background minus the instantaneous background.

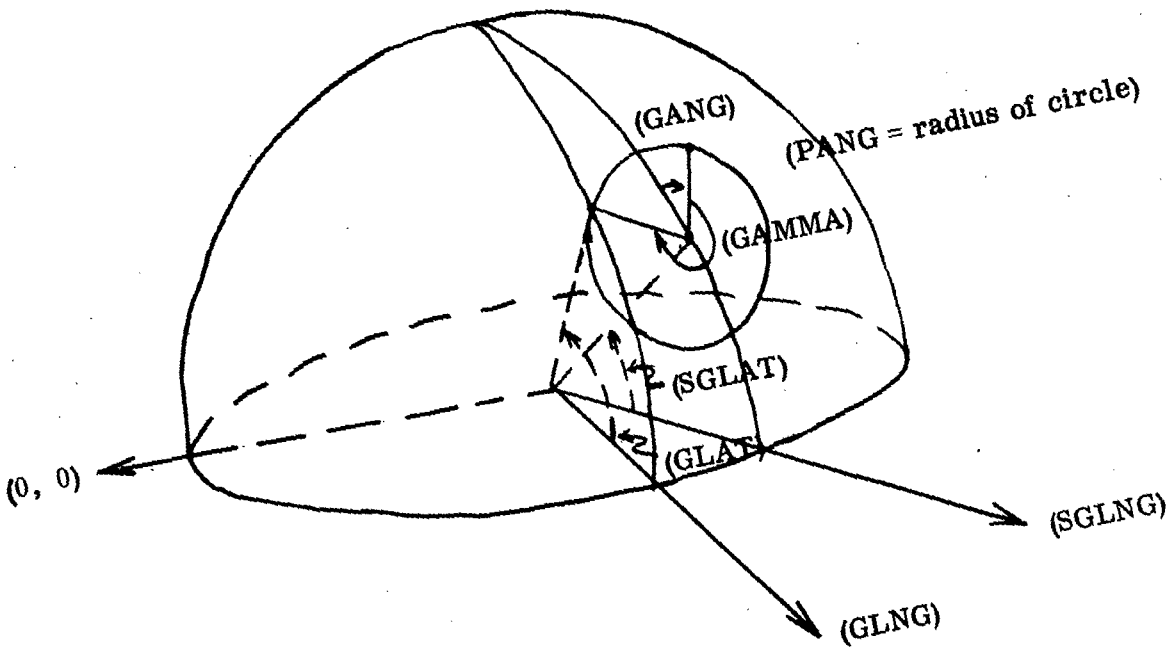

Figure 47. Galactic Coordinate Reference (THRESH1)

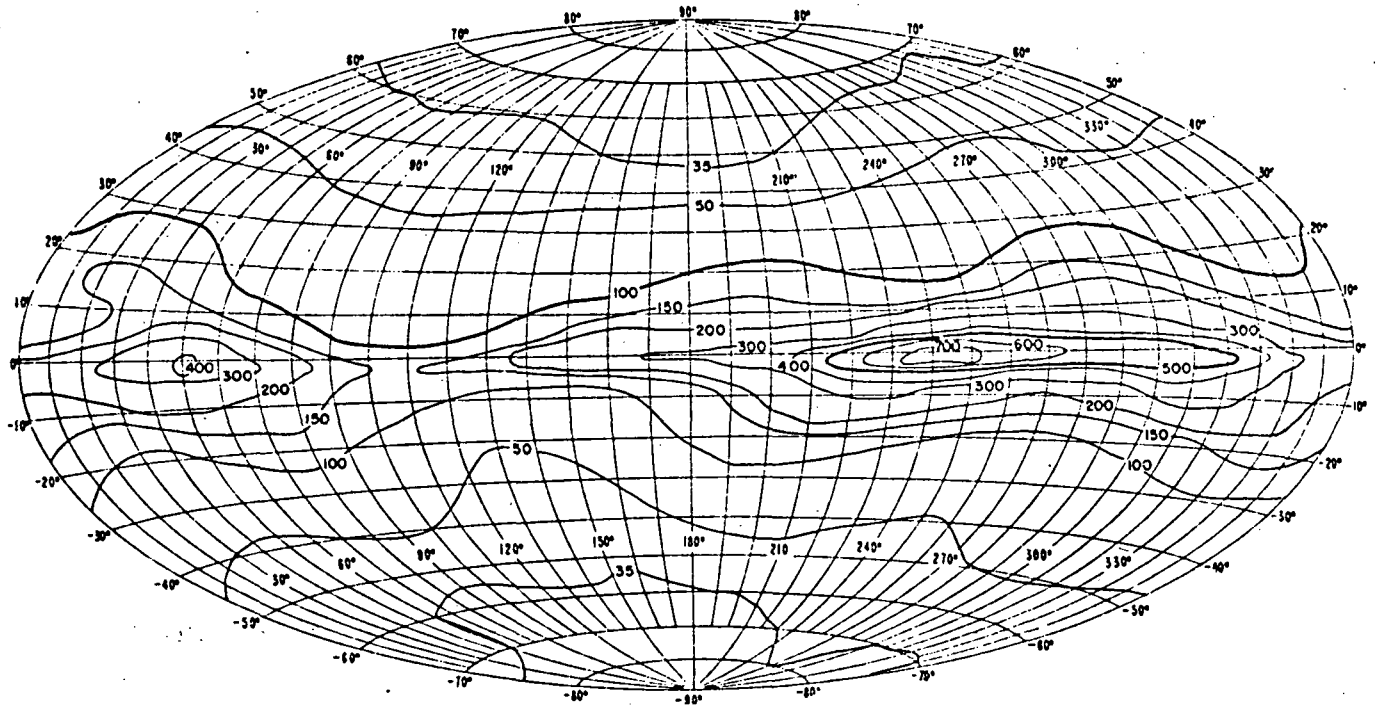

Figure 48. Total integrated starlight in number of tenth magnitude (visual) stars per square degree in galactic co-ordinates (after Reference 8).

This threshold then corresponds to the instantaneous relative threshold of the system. It is calculated in photocathode amperes, in watts per square centimeter (solar spectrum equivalent) illumination of the telescope, and in equivalent stellar visual magnitudes. These values are printed out, along with the instantaneous background photocathode current in amperes and the rotation angle. The program then steps around the spin axis by the preset increment and repeats the calculations above. When all values for a complete revolution are stored in the memory and printed out, a graph is plotted of the instantaneous relative threshold and the instantaneous mean peak noise (taken as $\sqrt{2}$. rms noise). The plotting routine is a modification of one also given in Reference 4. The values are plotted in visual stellar magnitude as a function of rotation angle. Finally, for cross reference, plotting calibration of stars and events, a table of the rotation angle versus galactic longitude and latitude are printed.

B. COMPUTER PROGRAM AND ITS OUTPUT

The program was written in FORTRAN IV for the GE Deskside Computer System which utilizes a GE 605 computer. A listing of the code and the associated flow chart (Fig. 49) are given on the following pages. In addition, six examples of the results are included for various modes of the Sisyphus detector. Three of these cases correspond to the star exclusion circuit disabled and are shown for comparison with three hand calculated curves. Variations are due to the fact that the hand calculated version used approximations for the sky brightness. The three cases run with the star exclusion circuit enabled are for corresponding sky sectors as the previous three cases; however, in each of these latter three, variations were made in the input data to show the difference in sensitivity as the instrument is commanded to change bandwidth.

The program constants and variables are as follows:

GANG	=	starting angle with respect to the galactic equator (see Figure 47)
GAMMA	=	the rotation angle with respect to reference (0 to 360^0)
DELTAF	=	the bandwidth for signal acceptance of the instrument
SGLNG	=	the galactic longitude to which the spin axis of the vehicle is pointed
SGLAT	=	the galactic latitude to which the spin axis of the vehicle is pointed
PANG	=	the pointing angle of the telescopes with respect to the spin axis
CHARGE	=	the unit electron charge
ETA	=	the conversion constant for the photomultiplier photocathode from total illuminated watts to photocathode output current
BRITE	=	the brightness of a tenth magnitude star (visual) in watts/cm^2
DIAM	=	the effective aperture of the telescopes
ALPHA	=	the half viewing angle of the telescopes
BKGND	=	the photocathode background in amperes (two values - instantaneous and delayed)
NOISE	=	photon photocathode noise in amperes
ROLRTE	=	the rotation of the vehicle in degrees/second
TCONST	=	the active filter time constant
THDAMP	=	the threshold in photocathode amperes
THDWAT	=	the threshold illumination in watts/cm^2

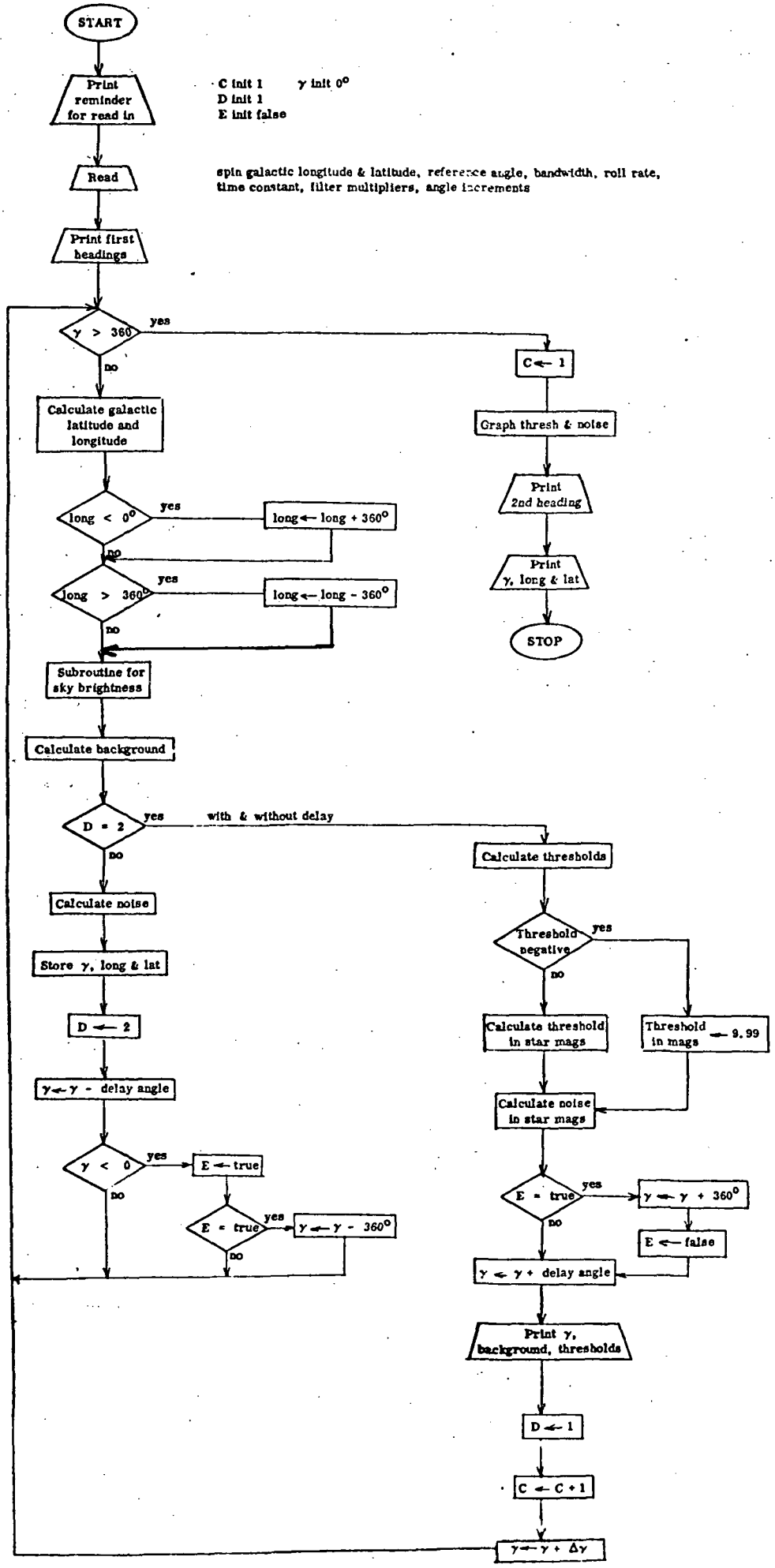
START
Print reminder for read in
C init 1
D init 1
E init false
γ init 0°
Read
spin galactic longitude & latitude, reference angle, bandwidth, roll rate, time constant, filter multipliers, angle increments
Print first headings
γ > 360
yes
no
C ← 1
Graph thresh & noise
Print 2nd heading
Print γ, long & lat
STOP
Calculate galactic latitude and longitude
long < 0°
yes
long ← long + 360°
no
long > 360°
yes
long ← long - 360°
no
Subroutine for sky brightness
Calculate background
D = 2
yes
with & without delay
no
Calculate thresholds
Calculate noise
Threshold negative
yes
no
Store γ, long & lat
Calculate threshold in star mags
Threshold in mags ← 9.99
D ← 2
Calculate noise in star mags
γ ← γ - delay angle
γ < 0
yes
E ← true
no
E = true
yes
γ ← γ - 360°
no
E = true
yes
γ ← γ + 360°
no
E ← false
γ ← γ + delay angle
Print γ, background, thresholds
D ← 1
C ← C + 1
γ ← γ + Δγ

Figure 49.

M1	=	the multiplication factor for the instantaneous noise
M2	=	the multiplication factor for the delayed background (active filter)
THDMAG	=	the instantaneous threshold in stellar magnitudes (visual)
NOIMAG	=	the instantaneous noise in stellar magnitudes (visual)
DELTAG	=	the incremental angle for stepping around the circle in degrees (minimum 3^{o})
GLNG	=	the galactic longitude at which the telescopes are pointed
GLAT	=	the galactic latitude at which the telescopes are pointed
SIGMA	=	the sky brightness corresponding to those galactic latitudes and longitudes

(these latter three are common to the subroutine, called SKY)

GAMMAS	=	storage location for the rotation angle
GLNGS	=	storage location for corresponding galactic longitude
GLATS	=	storage location for corresponding galactic latitude

Also used in the program are a number of indices, print out words and one logic word:

C	=	index corresponding to a fixed value of gamma (max value 121)
D	=	takes the value 1 or 2 depending upon whether one is looking instantaneously or with the delayed time constant
E	=	logic word
LINE	=	array used for graphing
DOT	=	" . "
X	=	" X "
BLANK	=	space
O	=	O
MARK	=	a storage location for reference dots used in plotting
J	=	graphing index
K	=	tabulation index

The subroutine (SKY) uses the following additional indices for location of the sky brightness of the sky map:

M	=	stepping longitude index
N	=	stepping latitude index
MM	=	one side of the bracketed value of galactic longitude
NN	=	one side of the bracketed value of galactic latitude

```
 00010 *      SISYPHUS THRESHOLDS (THRESH1)
00020        REAL GANG, GAMMA, DELTAF, SGLNG,
00030 &      SGLAT, PANG, CHARGE, ETA, BRITE, DIAM, ALPHA,
00040 &      BKGND(121,2), NOISE(121), ROLRTE, TCONST,
00050 &      THDAMP(121), THDWAT(121), M1, M2, THDMAG(121),
00060 &      NOIMAG(121),DELTAG,GAMMAS(121),GLNGS(121),GLATS(121)
00070        INTEGER C, D
00080        LOGICAL E
00090        ASCII LINE(51), DOT, X, BLANK, O, MARK
00100        COMMON GLNG, GLAT, SIGMA
00110        DATA C, D, GAMMA, CHARGE/ 1, 1, 0.0, 1.60E-19/
00120        DATA E/.FALSE./
00130        DATA ETA, BRITE/ 0.046, 1.34E-16/
00140        DATA DOT, X, BLANK, O/".", "X", " ", "O"/
00150        DATA DIAM, ALPHA, PANG/ 18., 3.9, 45./
00160        PRINT: "SGLNG, SGLAT, GANG, DELTAF, ROLRTE, TCONST,
00170 &      M1,M2,DELTAG .GE. 3."
00180        PRINT 30
00190     30 FORMAT (1H )
00200        READ: SGLNG,SGLAT,GANG,DELTAF,ROLRTE,TCONST,M1,M2,DELTAG
00210 *      HEADINGS
00220        PRINT 12
00230     12 FORMAT (4X, "ANGLE", 3X, "BACKGROUND", 3X, "RMS NOISE",
00240 &      8X, "RELATIVE THRESHOLDS" /5X, "DEG.", 6X, "AMPS.", 7X,
00250 &      "AMPS.", 7X, "AMPS.", 5X, "W/SQ CM", 5X, "MAGS." //)
00260 *      EXIT FROM LOOPS
00270      1 IF (GAMMA .GT. 360.) GO TO 3
00280 *      CALC. GALACTIC LAT. & LONG.
00290        GLAT=ARSIN(COS(.0175*PANG)*SIN(.0175*SGLAT)+
00300 &      SIN(.0175*PANG)*COS(.0175*SGLAT)*
00310 &      COS(.0175*(GAMMA+GANG)))/.0175
00320        GLNG=SGLNG+
00330 &      (ARSIN(SIN(.0175*(GAMMA+GANG))*
00340 &      SIN(.0175*PANG)/COS(.0175*GLAT)))/.0175
00350 *      CORRECT IF LONG .LT. 0 OR .GT. 360
00360        IF(GLNG.LT.0.0) GLNG=360.+GLNG
00370        IF(GLNG.GT.360.) GLNG=GLNG-360.
00380 *      FIND SKY BRIGHTNESS
00390        CALL SKY (GLNG, GLAT, SIGMA)
00400 *      CALC. SKY BACKGROUND
00410        BKGND(C,D) =SIGMA*BRITE*ETA*(3.14*ALPHA*DIAM/2.)**2
00420 *      ARE WE LOOKING NOW OR WITH DELAY
00430        IF (D .EQ. 2) GO TO 2
00440 *      WITHOUT DELAY, CALC. NOISE
00450        NOISE(C) = SQRT(2. * BKGND(C,1)* CHARGE * DELTAF)
00460 *      STORE VALUES FOR LATER
00470        GAMMAS(C)=GAMMA
00480        GLNGS(C)=GLNG
00490        GLATS(C)=GLAT
00500 *      RESET FOR DELAY
00510        D = 2
00520        GAMMA = GAMMA - ROLRTE * TCONST
00530 *      AVOID NEG. ANGLE
```

```
00540         E=GAMMA .LT. 0.0
00550         IF(E) GAMMA=GAMMA+360.
00560         GO TO 1
00570 *       CALC. THRESHOLDS & NOISE IN AMPS, W/SQ CM, & STAR MAGS.
00580    2    THDAMP(C)=M1*NOISE(C)+M2*BKGND(C,2)-BKGND(C,1)
00590         THDWAT(C) = 4. * THDAMP(C)/(ETA * 3.14 * DIAM **2)
00600 *       AVOID NEGATIVE VALUES FOR LOGARITHMS
00610         IF(THDWAT(C) .GT. 1.36E-16) GO TO 6
00620         THDMAG(C) = 9.99
00630         GO TO 7
00640    6    THDMAG(C)=2.5/2.3*ALOG(BRITE*1.0E+04/THDWAT(C))
00650    7    NOIMAG(C)=2.5/2.3*ALOG(BRITE*1.0E+04*3.14
00660 &       *ETA*DIAM**2/(4.*1.41*NOISE(C)))
00670 *       RESET VALUES
00680         IF(E) GAMMA=GAMMA-360.
00690         E=.FALSE.
00700 *       TAKE OUT DELAY
00710         GAMMA = GAMMA + ROLRTE * TCONST
00720         PRINT 14, GAMMA, BKGND(C,1), NOISE(C), THDAMP(C),
00730 &       THDWAT(C), THDMAG(C)
00740     14  FORMAT(4X, F5.0, 4(3X, 1PE9.2), 4X,0PF5.2)
00750 *       RESET INDEXES & LOOP
00760         GAMMA=GAMMA+DELTAG
00770         D = 1
00780         C = C + 1
00790         GO TO 1
00800 *       SKIP SOME LINES & GRAPH RESULTS
00810    3    C = 1
00820         PRINT 19
00830    19   FORMAT(1H-/1H-)
00840 *       PRINT DOTS FOR REFERENCE
00850         DO 5 J=1,51
00860     5   LINE(J)=BLANK
00870         DO 4 J=1,51,10
00880     4   LINE(J)=DOT
00890         PRINT 25, BLANK, LINE
00900 *       SET UP LINE OF DOTS
00910    20   DO 21 J=1, 51
00920    21   LINE(J) = DOT
00930 *       CALC. INPUTS (THRESHOLD & PEAK NOISE)
00940 *       J = 51 IS 0, J = 1 IS + 5.0
00950    22   J = 51 - IFIX(10.*THDMAG(C))
00960 *       PUT IN X FOR THRESHOLD, IGNORE OUT OF BOUNDS
00970         IF(J .GT. 51) GO TO 23
00980         IF(J .LT. 1) GO TO 23
00990         LINE(J) = X
01000    23   J = 51 - IFIX(10. * NOIMAG(C))
01010 *       PUT IN O FOR NOISE, IGNORE OUT OF BOUNDS
01020         IF(J .GT. 51) GO TO 24
01030         IF(J .LT. 1) GO TO 24
01040         LINE(J) = O
01050 *       SET UP REFERENCE DOTS IN OTHER DIRECTION
01060    24   IF(((C-1)/10)*10 .EQ. (C-1)) MARK = DOT
```

```
01070          IF(((C-1)/10)*10 .NE. (C-1)) MARK = BLANK
01080 *        PRINT LINE WITH DOTS & VALUES
01090          PRINT 25, MARK, LINE
01100    25    FORMAT(10X, 52A1)
01110 *        BLANK THE LINE
01120          DO 26 J = 1, 51
01130    26    LINE(J) = BLANK
01140 *        PUT A DOT AT 1 & 51
01150          LINE(1) = DOT
01160          LINE(51) = DOT
01170 *        INDEX & CONDITION
01180          C = C + 1
01190          IF(C-IFIX(360./DELTAG+1.)) 22,20,27
01200 *        PRINT TABLE OF COORDINATES
01210    27    PRINT 19
01220          PRINT 31
01230    31    FORMAT(4X,"ANGLE",3X,"GAL. LONG.",3X,"GAL. LAT." //)
01240          DO 32 K=1,121
01250          IF(K.EQ.C) STOP
01260    32    PRINT 33,GAMMAS(K),GLNGS(K),GLATS(K)
01270    33    FORMAT(4X,F5.0,5X,F6.1,6X,F6.1)
01280          END
01290          SUBROUTINE SKY (GLNG, GLAT, SIGMA)
01300          REAL STARS (37, 24), LNG (37), LAT (24)
01310          DATA LNG /0.0, 10., 20., 30., 40., 50., 60., 70.,
01320 &        80., 90., 100., 110., 120., 130., 140., 150., 160.,
01330 &        170., 180., 190., 200., 210., 220., 230., 240.,
01340 &        250., 260., 270., 280., 290., 300., 310., 320., 330.,
01350 &        340., 350., 360./
01360          DATA LAT /90., 80., 70., 60., 50., 40., 30., 20.,
01370 &        15., 10., 5., 0.0, -2., -5., -10., -15., -20.,
01380 &        -30., -40., -50., -60., -70., -80., -90./
01390          DATA STARS/37*27., 30., 2*29., 7*28., 2*29.,
01400 &        2*30., 29., 2*28., 3*27., 28., 29., 4*30.,
01410 &        4*29., 2*30., 3*31., 2*30., 2*32., 2*31.,
01420 &        3*30., 29., 30., 6*31., 2*29., 3*27., 29.,
01430 &        30., 31., 5*32., 31., 2*32., 33., 2*34., 2*33.,
01440 &        32., 3*36., 3*35., 34., 33., 5*34., 33.,
01450 &        32., 2*30., 3*29., 30., 31., 33., 34., 35.,
01460 &        36., 4*37., 3*38., 2*37., 2*36., 42., 4*43.,
01470 &        42., 2*41., 2*40., 2*39., 2*38., 36., 35.,
01480 &        4*33., 34., 35., 37., 39., 41., 43., 45.,
01490 &        3*46., 45., 44., 2*43., 3*42., 56., 58., 60.,
01500 &        59., 57., 55., 52., 49., 47., 3*45., 44., 43., 44.,
01510 &        3*43., 42., 2*43., 44., 47., 49., 51., 54.,
01520 &        57., 59., 2*58., 56., 53., 2*51., 52., 54.,
01530 &        56., 80., 86., 90., 88., 83., 74., 66., 60., 56.,
01540 &        54., 53., 2*54., 55., 57., 58., 59., 61.,
01550 &        63., 2*64., 62., 2*63., 66., 72., 77., 82.,
01560 &        84., 81., 75., 69., 2*65., 67., 73., 80.,
01570 &        104., 127., 146., 149., 132., 109., 89.,
01580 &        75., 69., 68., 70., 72., 2*73., 72., 74.,
01590 &        79., 89., 101., 110., 112., 106., 96., 86.,
```

```
01600 &     85., 92., 107., 128., 145., 147., 132., 109.,
01610 &     90., 79., 78., 86., 104., 113., 138., 165.,
01620 &     173., 158., 131., 105., 87., 77., 2*74., 77., 79.,
01630 &     81., 84., 88., 97., 112., 129., 141., 144.,
01640 &     135., 122., 111., 109., 119., 141., 172.,
01650 &     200., 206., 185., 149., 117., 95., 89., 94.,
01660 &     113., 109., 120., 136., 155., 165., 162.,
01670 &     141., 115., 92., 76., 67., 66., 71., 83.,
01680 &     102., 124., 145., 157., 162., 159., 158., 163.,
01690 &     173., 189., 207., 231., 251., 263., 266.,
01700 &     258., 237., 207., 172., 139., 118., 108., 109.,
01710 &     124., 128., 148., 179., 218., 236., 217.,
01720 &     173., 127., 95., 78., 73., 81., 104., 140.,
01730 &     183., 218., 228., 214., 202., 204., 229.,
01740 &     277., 333., 383., 412., 406., 388., 364.,
01750 &     344., 326., 296., 254., 202., 159., 133.,
01760 &     124., 208., 212., 246., 308., 367., 402.,
01770 &     369., 293., 215., 161., 133., 126., 140.,
01780 &     173., 215., 260., 290., 302., 304., 309.,
01790 &     343., 421., 545., 667., 738., 735., 688., 628.,
01800 &     587., 572., 573., 538., 470., 375., 288.,
01810 &     232., 208., 237., 241., 276., 332., 386.,
01820 &     408., 373., 304., 234., 183., 154., 147., 157.,
01830 &     179., 207., 231., 249., 264., 280., 307.,
01840 &     358., 454., 578., 699., 749., 705., 633.,
01850 &     577., 557., 565., 582., 570., 517., 417.,
01860 &     324., 264., 237., 202., 201., 225., 258.,
01870 &     287., 293., 269., 229., 190., 160., 140.,
01880 &     130., 127., 129., 131., 133., 141., 156., 183.,
01890 &     226., 286., 360., 429., 478., 467., 418.,
01900 &     369., 351., 364., 403., 442., 450., 409.,
01910 &     341., 269., 223., 202., 173., 166., 177.,
01920 &     193., 207., 211., 202., 184., 162., 142.,
01930 &     126., 112., 101., 93., 87., 85., 89., 103.,
01940 &     128., 169., 222., 273., 308., 310., 281.,
01950 &     237., 204., 196., 214., 254., 303.,
01960 &     331., 322., 281., 235., 196., 173., 163., 147., 140.,
01970 &     141., 147., 157., 163., 162., 152., 133.,
01980 &     112., 92., 77., 69., 67., 70., 79., 97.,
01990 &     122., 153., 185., 205., 213., 200., 178.,
02000 &     155., 139., 137., 146., 167., 196., 223.,
02010 &     237., 235., 215., 186., 163., 133., 114.,
02020 &     101., 95., 96., 105., 115., 124., 121.,
02030 &     107., 88., 69., 57., 51., 52., 57., 69.,
02040 &     86., 108., 127., 137., 137., 128., 117.,
02050 &     106., 97., 92., 91., 95., 102., 115., 132.,
02060 &     150., 163., 164., 152., 133., 83., 74.,
02070 &     67., 63., 62., 66., 71., 77., 79., 74.,
02080 &     66., 56., 49., 45., 43., 46., 52., 61.,
02090 &     71., 78., 82., 81., 77., 71., 67., 64.,
02100 &     63., 64., 65., 69., 74., 81., 88., 92.,
02110 &     94., 90., 83., 59., 56., 53., 50., 48.,
02120 &     2*49., 50., 2*51., 50., 47., 43., 41.,
```

```
02130 &      40., 41., 43., 47., 52., 55.,
02140 &      2*57., 55., 52., 50., 49., 50., 53., 57.,
02150 &      60., 62., 64., 65., 2*64., 61., 59., 2*46.,
02160 &      45., 43., 41., 39., 3*37., 4*38., 2*37.,
02170 &      2*36., 38., 40., 42., 2*43., 42., 3*41.,
02180 &      43., 46., 49., 51., 53., 52., 51., 2*49.,
02190 &      47., 46., 4*39., 38., 36., 35., 34., 33.,
02200 &      2*32., 33., 4*34., 33., 2*34., 2*35., 36.,
02210 &      3*37., 38., 39., 40., 4*42., 41., 4*39.,
02220 &      2*36., 3*37., 36., 35., 33., 32., 4*31.,
02230 &      5*32., 31., 32., 33., 33., 34., 35.,
02240 &      6*36., 3*35., 2*34., 35., 36., 34., 35., 34., 35.,
02250 &      2*34., 2*33., 12*32., 2*33., 3*34., 3*35.,
02260 &      2*34., 33., 34., 2*33., 3*34., 37*32./
02270 *      COMPUTATION OF LONGITUDE VALUES
02280        M=1
02290        N=1
02300      1 IF (GLNG-LNG(M)) 4,3,2
02310 *      LONGITUDE NOT FOUND YET
02320      2 M=M+1
02330        GO TO 1
02340 *      EQUAL
02350      3 MM=M
02360        GO TO 5
02370 *      BRACKETED
02380      4 MM=M-1
02390        GO TO 5
02400 *      COMPUTATION OF LATITUDE VALUES
02410      5 IF (LAT(N)-GLAT) 8,7,6
02420 *      LATITUDE NOT FOUND YET
02430      6 N=N+1
02440        GO TO 5
02450 *      EQUAL
02460      7 IF (N .EQ. 1) GO TO 11
02470        NN=N
02480        IF(MM .EQ. 37) GO TO 10
02490        GO TO 9
02500 *      BRACKETED
02510      8 NN=N
02520        IF (MM .EQ. 37) GO TO 10
02530        GO TO 9
02540 *      INTERPOLATION
02550      9 SIGMA=STARS(MM,NN)+((STARS(MM+1,NN)-STARS(MM,NN))/
02560 &      (LNG(MM+1)-LNG(MM)))*(GLNG-LNG(MM))+((STARS(MM,NN-1)
02570 &      -STARS(MM,NN))/(LAT(NN-1)-LAT(NN)))*(GLAT-LAT(NN))
02580        RETURN
02590     10 SIGMA=STARS(37,NN)+((STARS(37,NN-1)-STARS(37,NN))/
02600 &      (LAT(NN-1)-LAT(NN)))*(GLAT-LAT(NN))
02610        RETURN
02620     11 SIGMA=27.
02630        RETURN
02640        END
```

```
$FORT THRESH1

SGLNG, SGLAT, GANG, DELTAF, ROLRTE, TCONST,      M1,M2,DELTAG .GE. 3.
=333.,0.,-29.,13000.,30.,.5,2.0,1.1,8.
```

ANGLE DEG.	BACKGROUND AMPS.	RMS NOISE AMPS.	RELATIVE THRESHOLDS AMPS.	W/SQ CM	MAGS.
0.	4.14E-12	1.31E-13	2.17E-12	1.86E-13	2.15
8.	3.83E-12	1.26E-13	1.61E-12	1.38E-13	2.47
16.	3.61E-12	1.22E-13	1.09E-12	9.29E-14	2.90
24.	3.53E-12	1.21E-13	8.89E-13	7.60E-14	3.12
32.	3.57E-12	1.22E-13	6.28E-13	5.37E-14	3.50
40.	3.66E-12	1.23E-13	4.72E-13	4.03E-14	3.81
48.	3.89E-12	1.27E-13	3.07E-13	2.62E-14	4.28
56.	4.58E-12	1.38E-13	-2.47E-13	-2.12E-14	9.99
64.	5.16E-12	1.47E-13	-5.49E-13	-4.69E-14	9.99
72.	6.13E-12	1.60E-13	-6.68E-13	-5.71E-14	9.99
80.	7.70E-12	1.79E-13	-1.53E-12	-1.31E-13	9.99
88.	9.65E-12	2.00E-13	-2.37E-12	-2.02E-13	9.99
96.	1.13E-11	2.17E-13	-2.16E-12	-1.85E-13	9.99
104.	9.94E-12	2.03E-13	1.35E-12	1.15E-13	2.67
112.	1.18E-11	2.22E-13	1.23E-12	1.06E-13	2.76
120.	1.89E-11	2.81E-13	-7.26E-12	-6.20E-13	9.99
128.	1.49E-11	2.49E-13	-3.59E-13	-3.07E-14	9.99
136.	1.15E-11	2.18E-13	1.06E-11	9.08E-13	0.42
144.	9.23E-12	1.96E-13	7.11E-12	6.08E-13	0.86
152.	7.53E-12	1.77E-13	5.24E-12	4.48E-13	1.19
160.	6.36E-12	1.63E-13	3.78E-12	3.23E-13	1.54
168.	5.64E-12	1.53E-13	2.76E-12	2.36E-13	1.89
176.	5.01E-12	1.44E-13	2.06E-12	1.76E-13	2.21
184.	4.52E-12	1.37E-13	1.86E-12	1.59E-13	2.32
192.	4.36E-12	1.35E-13	1.34E-12	1.15E-13	2.67
200.	4.28E-12	1.33E-13	9.27E-13	7.92E-14	3.07
208.	4.23E-12	1.33E-13	8.11E-13	6.93E-14	3.22
216.	4.31E-12	1.34E-13	6.63E-13	5.67E-14	3.44
224.	4.47E-12	1.36E-13	4.59E-13	3.92E-14	3.84
232.	4.75E-12	1.41E-13	3.08E-13	2.64E-14	4.27
240.	4.99E-12	1.44E-13	2.48E-13	2.12E-14	4.51
248.	5.28E-12	1.48E-13	2.84E-13	2.43E-14	4.36
256.	5.79E-12	1.55E-13	4.19E-14	3.58E-15	6.44
264.	6.90E-12	1.69E-13	-8.95E-13	-7.65E-14	9.99
272.	9.42E-12	1.98E-13	-2.51E-12	-2.14E-13	9.99
280.	1.46E-11	2.47E-13	-6.38E-12	-5.45E-13	9.99
288.	2.47E-11	3.21E-13	-1.30E-11	-1.11E-12	9.99
296.	4.26E-11	4.21E-13	-2.49E-11	-2.13E-12	9.99
304.	2.95E-11	3.50E-13	7.27E-14	6.21E-15	5.84
312.	1.91E-11	2.82E-13	2.92E-11	2.50E-12	-0.68
320.	1.52E-11	2.52E-13	1.51E-11	1.29E-12	0.04
328.	1.05E-11	2.09E-13	1.08E-11	9.26E-13	0.40
336.	7.67E-12	1.79E-13	8.74E-12	7.47E-13	0.64
344.	5.62E-12	1.53E-13	5.84E-12	4.99E-13	1.07
352.	4.82E-12	1.42E-13	3.52E-12	3.01E-13	1.62
360.	4.05E-12	1.30E-13	2.26E-12	1.93E-13	2.11

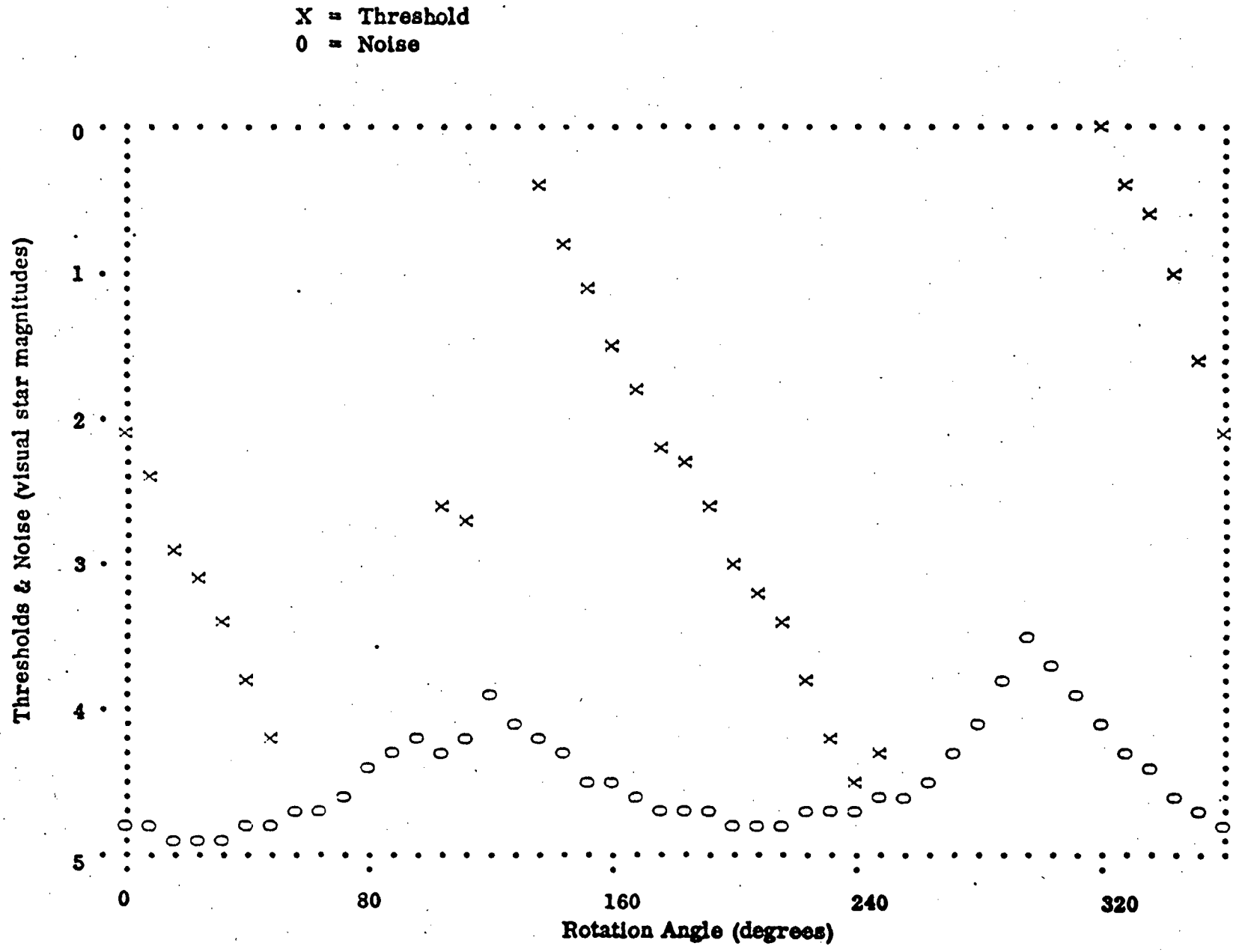
X = Threshold
0 = Noise
Thresholds & Noise (visual star magnitudes)
0
1
2
3
4
5
0
80
160
240
320
Rotation Angle (degrees)

Figure 50.

ANGLE	GAL. LONG.	GAL. LAT.
0.	307.1	38.2
8.	313.2	41.3
16.	320.3	43.5
24.	328.0	44.8
32.	336.0	44.9
40.	343.8	43.9
48.	351.1	41.9
56.	357.5	39.0
64.	2.9	35.3
72.	7.4	31.1
80.	10.9	26.3
88.	13.7	21.2
96.	15.7	15.9
104.	17.0	10.4
112.	17.8	4.8
120.	18.0	-0.9
128.	17.6	-6.5
136.	16.7	-12.1
144.	15.1	-17.6
152.	12.9	-22.9
160.	9.9	-27.8
168.	6.1	-32.4
176.	1.3	-36.6
184.	355.6	-40.0
192.	348.9	-42.7
200.	341.5	-44.4
208.	333.5	-45.0
216.	325.6	-44.5
224.	318.0	-42.9
232.	311.2	-40.4
240.	305.3	-37.0
248.	300.5	-33.0
256.	296.5	-28.5
264.	293.5	-23.5
272.	291.1	-18.3
280.	289.5	-12.8
288.	288.5	-7.3
296.	288.0	-1.6
304.	288.1	4.1
312.	288.8	9.7
320.	290.1	15.2
328.	292.0	20.6
336.	294.7	25.7
344.	298.1	30.5
352.	302.4	34.8
360.	307.7	38.6

PROGRAM STOP AT 1250

READY

$FORT THRESH1

SGLNG, SGLAT, GANG, DELTAF, ROLRTE, TCONST, M1,M2,DELTAG .GE. 3.
=333.,0.,-29.,500000.,30.,.047,2.0,1.1,8.

ANGLE DEG.	BACKGROUND AMPS.	RMS NOISE AMPS.	RELATIVE THRESHOLDS AMPS.	W/SQ CM	MAGS.
-0.	4.14E-12	8.14E-13	2.09E-12	1.78E-13	2.19
8.	3.83E-12	7.83E-13	2.01E-12	1.71E-13	2.24
16.	3.61E-12	7.60E-13	1.89E-12	1.62E-13	2.30
24.	3.53E-12	7.52E-13	1.87E-12	1.59E-13	2.31
32.	3.57E-12	7.56E-13	1.85E-12	1.58E-13	2.32
40.	3.66E-12	7.65E-13	1.85E-12	1.58E-13	2.32
48.	3.89E-12	7.88E-13	1.94E-12	1.66E-13	2.27
56.	4.58E-12	8.56E-13	2.02E-12	1.72E-13	2.23
64.	5.16E-12	9.09E-13	2.15E-12	1.84E-13	2.16
72.	6.13E-12	9.90E-13	2.40E-12	2.05E-13	2.04
80.	7.70E-12	1.11E-12	2.61E-12	2.23E-13	1.95
88.	9.65E-12	1.24E-12	3.07E-12	2.63E-13	1.77
96.	1.13E-11	1.35E-12	3.58E-12	3.06E-13	1.60
104.	9.94E-12	1.26E-12	3.78E-12	3.23E-13	1.55
112.	1.18E-11	1.38E-12	2.62E-12	2.24E-13	1.94
120.	1.89E-11	1.74E-12	4.09E-12	3.50E-13	1.46
128.	1.49E-11	1.54E-12	5.16E-12	4.41E-13	1.21
136.	1.15E-11	1.36E-12	4.15E-12	3.55E-13	1.44
144.	9.23E-12	1.22E-12	3.84E-12	3.28E-13	1.53
152.	7.53E-12	1.10E-12	3.22E-12	2.75E-13	1.72
160.	6.36E-12	1.01E-12	2.72E-12	2.33E-13	1.90
168.	5.64E-12	9.50E-13	2.60E-12	2.22E-13	1.95
176.	5.01E-12	8.95E-13	2.40E-12	2.05E-13	2.04
184.	4.52E-12	8.51E-13	2.22E-12	1.90E-13	2.12
192.	4.36E-12	8.35E-13	2.07E-12	1.77E-13	2.20
200.	4.28E-12	8.27E-13	2.09E-12	1.78E-13	2.19
208.	4.23E-12	8.23E-13	2.07E-12	1.77E-13	2.20
216.	4.31E-12	8.31E-13	2.05E-12	1.75E-13	2.21
224.	4.47E-12	8.45E-13	2.09E-12	1.79E-13	2.19
232.	4.75E-12	8.71E-13	2.16E-12	1.84E-13	2.16
240.	4.99E-12	8.93E-13	2.24E-12	1.91E-13	2.12
248.	5.28E-12	9.19E-13	2.30E-12	1.97E-13	2.08
256.	5.79E-12	9.63E-13	2.30E-12	1.97E-13	2.08
264.	6.90E-12	1.05E-12	2.57E-12	2.19E-13	1.97
272.	9.42E-12	1.23E-12	2.43E-12	2.08E-13	2.03
280.	1.46E-11	1.53E-12	3.48E-12	2.97E-13	1.64
288.	2.47E-11	1.99E-12	4.05E-12	3.46E-13	1.47
296.	4.26E-11	2.61E-12	7.82E-12	6.68E-13	0.76
304.	2.95E-11	2.17E-12	1.10E-11	9.37E-13	0.39
312.	1.91E-11	1.75E-12	7.02E-12	6.00E-13	0.87
320.	1.52E-11	1.56E-12	4.55E-12	3.89E-13	1.35
328.	1.05E-11	1.30E-12	4.27E-12	3.65E-13	1.41
336.	7.67E-12	1.11E-12	3.53E-12	3.01E-13	1.62
344.	5.62E-12	9.48E-13	2.21E-12	1.89E-13	2.13
352.	4.82E-12	8.78E-13	2.39E-12	2.05E-13	2.04
360.	4.05E-12	8.05E-13	2.16E-12	1.85E-13	2.15

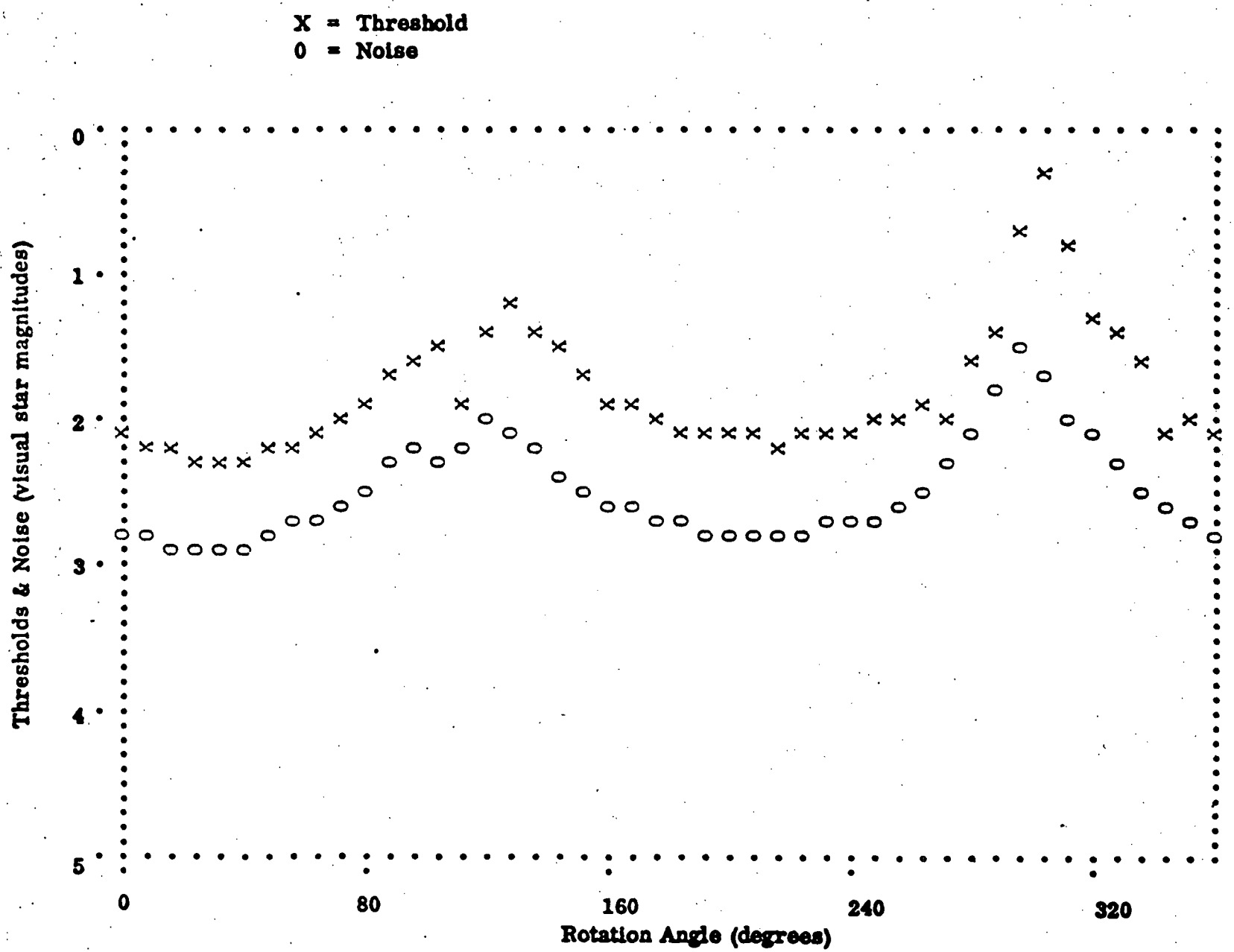
X = Threshold
0 = Noise
Thresholds & Noise (visual star magnitudes)
0
1
2
3
4
5
0
80
160
240
320
Rotation Angle (degrees)

Figure 51.

ANGLE	GAL. LONG.	GAL. LAT.
0.	307.1	38.2
8.	313.2	41.3
16.	320.3	43.5
24.	328.0	44.8
32.	336.0	44.9
40.	343.8	43.9
48.	351.1	41.9
56.	357.5	39.0
64.	2.9	35.3
72.	7.4	31.1
80.	10.9	26.3
88.	13.7	21.2
96.	15.7	15.9
104.	17.0	10.4
112.	17.8	4.8
120.	18.0	-0.9
128.	17.6	-6.5
136.	16.7	-12.1
144.	15.1	-17.6
152.	12.9	-22.9
160.	9.9	-27.8
168.	6.1	-32.4
176.	1.3	-36.6
184.	355.6	-40.0
192.	348.9	-42.7
200.	341.5	-44.4
208.	333.5	-45.0
216.	325.6	-44.5
224.	318.0	-42.9
232.	311.2	-40.4
240.	305.3	-37.0
248.	300.5	-33.0
256.	296.5	-28.5
264.	293.5	-23.5
272.	291.1	-18.3
280.	289.5	-12.8
288.	288.5	-7.3
296.	288.0	-1.6
304.	288.1	4.1
312.	288.8	9.7
320.	290.1	15.2
328.	292.0	20.6
336.	294.7	25.7
344.	298.1	30.5
352.	302.4	34.8
360.	307.7	38.6

PROGRAM STOP AT 1250

READY

```
$FORT THRESH1

SGLNG, SGLAT, GANG, DELTAF, ROLRTE, TCONST,     M1,M2,DELTAG .GE. 3.
=14.,-49.,-29.,13000.,30.,.047,2.0,1.1,8.
```

ANGLE DEG.	BACKGROUND AMPS.	RMS NOISE AMPS.	RELATIVE THRESHOLDS AMPS.	W/SQ CM	MAGS.
-0.	1.51E-11	2.51E-13	2.02E-12	1.73E-13	2.23
8.	1.48E-11	2.48E-13	2.05E-12	1.75E-13	2.21
16.	1.54E-11	2.53E-13	1.90E-12	1.62E-13	2.29
24.	1.60E-11	2.58E-13	1.85E-12	1.58E-13	2.32
32.	1.71E-11	2.67E-13	2.08E-12	1.77E-13	2.20
40.	1.79E-11	2.73E-13	2.23E-12	1.91E-13	2.12
48.	1.74E-11	2.69E-13	2.31E-12	1.98E-13	2.08
56.	1.78E-11	2.72E-13	2.52E-12	2.16E-13	1.99
64.	1.64E-11	2.62E-13	2.46E-12	2.10E-13	2.01
72.	1.47E-11	2.47E-13	2.33E-12	1.99E-13	2.07
80.	1.25E-11	2.28E-13	2.15E-12	1.84E-13	2.16
88.	1.03E-11	2.07E-13	1.88E-12	1.60E-13	2.31
96.	7.97E-12	1.82E-13	1.33E-12	1.14E-13	2.68
104.	7.26E-12	1.74E-13	1.28E-12	1.10E-13	2.72
112.	6.12E-12	1.60E-13	1.16E-12	9.91E-14	2.83
120.	5.20E-12	1.47E-13	9.81E-13	8.38E-14	3.01
128.	4.32E-12	1.34E-13	8.74E-13	7.47E-14	3.14
136.	3.54E-12	1.21E-13	6.87E-13	5.87E-14	3.40
144.	3.12E-12	1.14E-13	6.34E-13	5.42E-14	3.49
152.	2.65E-12	1.05E-13	5.11E-13	4.37E-14	3.72
160.	2.53E-12	1.03E-13	5.03E-13	4.30E-14	3.74
168.	2.38E-12	9.95E-14	4.45E-13	3.80E-14	3.87
176.	2.34E-12	9.87E-14	4.39E-13	3.75E-14	3.89
184.	2.34E-12	9.87E-14	4.24E-13	3.62E-14	3.92
192.	2.40E-12	9.98E-14	4.13E-13	3.53E-14	3.95
200.	2.45E-12	1.01E-13	4.54E-13	3.88E-14	3.85
208.	2.50E-12	1.02E-13	4.58E-13	3.92E-14	3.84
216.	2.45E-12	1.01E-13	4.41E-13	3.77E-14	3.88
224.	2.50E-12	1.02E-13	4.59E-13	3.93E-14	3.84
232.	2.65E-12	1.05E-13	4.47E-13	3.82E-14	3.87
240.	2.78E-12	1.08E-13	4.48E-13	3.83E-14	3.86
248.	3.02E-12	1.12E-13	4.83E-13	4.13E-14	3.78
256.	3.30E-12	1.17E-13	4.98E-13	4.25E-14	3.75
264.	3.65E-12	1.23E-13	5.45E-13	4.66E-14	3.65
272.	4.11E-12	1.31E-13	6.13E-13	5.24E-14	3.52
280.	4.40E-12	1.35E-13	6.54E-13	5.59E-14	3.45
288.	5.07E-12	1.45E-13	6.76E-13	5.78E-14	3.42
296.	5.67E-12	1.54E-13	7.59E-13	6.48E-14	3.29
304.	7.02E-12	1.71E-13	6.10E-13	5.22E-14	3.53
312.	9.06E-12	1.94E-13	9.09E-13	7.77E-14	3.10
320.	1.10E-11	2.14E-13	1.16E-12	9.95E-14	2.83
328.	1.48E-11	2.48E-13	1.26E-12	1.08E-13	2.74
336.	1.67E-11	2.64E-13	1.93E-12	1.65E-13	2.28
344.	1.63E-11	2.60E-13	2.21E-12	1.89E-13	2.13
352.	1.54E-11	2.53E-13	2.12E-12	1.81E-13	2.17
360.	1.51E-11	2.50E-13	2.05E-12	1.75E-13	2.21

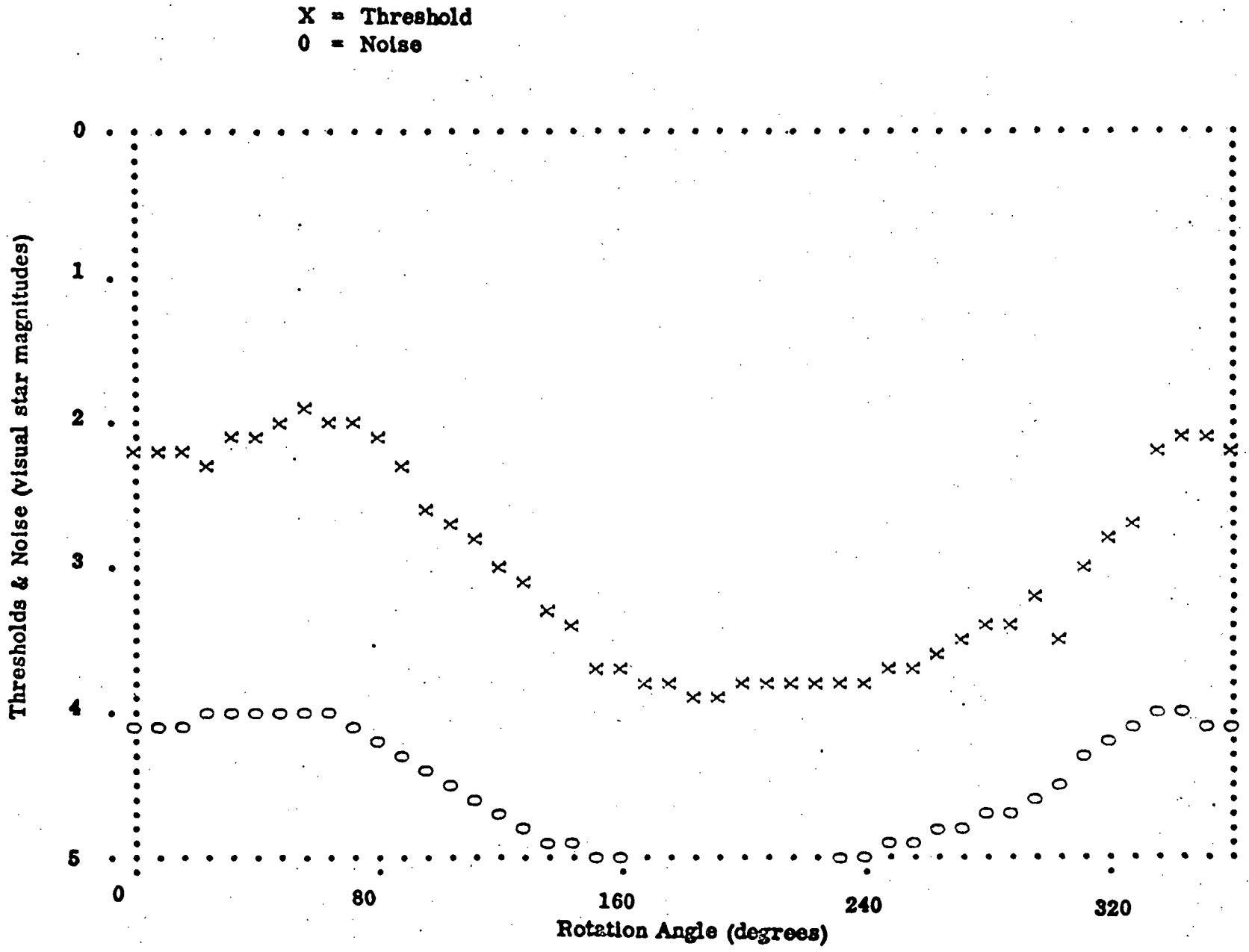
X = Threshold
0 = Noise
Thresholds & Noise (visual star magnitudes)
0
1
2
3
4
5
0
80
160
240
320
Rotation Angle (degrees)

Figure 52.

ANGLE	GAL. LONG.	GAL. LAT.
0.	353.7	-7.4
8.	359.2	-5.8
16.	4.8	-4.7
24.	10.5	-4.1
32.	16.1	-4.0
40.	21.8	-4.5
48.	27.4	-5.5
56.	32.9	-6.9
64.	38.3	-8.8
72.	43.5	-11.2
80.	48.6	-14.0
88.	53.5	-17.2
96.	58.2	-20.7
104.	62.7	-24.5
112.	67.1	-28.5
120.	71.4	-32.8
128.	75.6	-37.4
136.	79.7	-42.1
144.	83.9	-46.9
152.	88.0	-51.9
160.	92.3	-57.0
168.	97.0	-62.1
176.	102.2	-67.4
184.	98.8	-72.6
192.	89.4	-77.8
200.	70.9	-82.6
208.	19.0	-85.5
216.	321.1	-83.1
224.	300.3	-78.4
232.	290.2	-73.3
240.	285.0	-68.0
248.	290.4	-62.8
256.	295.1	-57.6
264.	299.4	-52.5
272.	303.6	-47.6
280.	307.7	-42.7
288.	311.9	-38.0
296.	316.0	-33.4
304.	320.3	-29.1
312.	324.7	-25.0
320.	329.2	-21.1
328.	333.9	-17.6
336.	338.8	-14.4
344.	343.8	-11.6
352.	349.0	-9.1
360.	354.4	-7.1

```
READY
$FORT THRESH1

SGLNG, SGLAT, GANG, DELTAF, ROLRTE, TCONST,      M1,M2,DELTAG .GE. 3.
=14.,-49.,-29.,13000.,30.,.5,2.0,1.1,8.
```

ANGLE DEG.	BACKGROUND AMPS.	RMS NOISE AMPS.	RELATIVE THRESHOLDS AMPS.	W/SQ CM	MAGS.
0.	1.51E-11	2.51E-13	3.28E-12	2.81E-13	1.70
8.	1.48E-11	2.48E-13	2.58E-12	2.21E-13	1.96
16.	1.54E-11	2.53E-13	1.72E-12	1.47E-13	2.40
24.	1.60E-11	2.58E-13	7.07E-13	6.04E-14	3.37
32.	1.71E-11	2.67E-13	4.12E-13	3.52E-14	3.95
40.	1.79E-11	2.73E-13	4.19E-13	3.58E-14	3.94
48.	1.74E-11	2.69E-13	2.07E-12	1.77E-13	2.20
56.	1.78E-11	2.72E-13	2.58E-12	2.21E-13	1.96
64.	1.64E-11	2.62E-13	3.20E-12	2.73E-13	1.73
72.	1.47E-11	2.47E-13	5.21E-12	4.45E-13	1.20
80.	1.25E-11	2.28E-13	5.78E-12	4.94E-13	1.08
88.	1.03E-11	2.07E-13	5.95E-12	5.08E-13	1.05
96.	7.97E-12	1.82E-13	5.87E-12	5.01E-13	1.07
104.	7.26E-12	1.74E-13	4.14E-12	3.54E-13	1.45
112.	6.12E-12	1.60E-13	2.85E-12	2.43E-13	1.85
120.	5.20E-12	1.47E-13	2.93E-12	2.50E-13	1.82
128.	4.32E-12	1.34E-13	2.52E-12	2.15E-13	1.99
136.	3.54E-12	1.21E-13	2.30E-12	1.97E-13	2.09
144.	3.12E-12	1.14E-13	1.73E-12	1.48E-13	2.39
152.	2.65E-12	1.05E-13	1.45E-12	1.24E-13	2.59
160.	2.53E-12	1.03E-13	1.04E-12	8.91E-14	2.95
168.	2.38E-12	9.95E-14	7.13E-13	6.09E-14	3.36
176.	2.34E-12	9.87E-14	6.10E-13	5.21E-14	3.53
184.	2.34E-12	9.87E-14	4.69E-13	4.01E-14	3.81
192.	2.40E-12	9.98E-14	3.73E-13	3.19E-14	4.06
200.	2.45E-12	1.01E-13	3.30E-13	2.82E-14	4.20
208.	2.50E-12	1.02E-13	3.42E-13	2.93E-14	4.16
216.	2.45E-12	1.01E-13	4.47E-13	3.82E-14	3.87
224.	2.50E-12	1.02E-13	4.17E-13	3.56E-14	3.94
232.	2.65E-12	1.05E-13	3.22E-13	2.75E-14	4.22
240.	2.78E-12	1.08E-13	1.97E-13	1.69E-14	4.76
248.	3.02E-12	1.12E-13	1.31E-13	1.12E-14	5.20
256.	3.30E-12	1.17E-13	2.51E-14	2.15E-15	7.00
264.	3.65E-12	1.23E-13	-5.69E-14	-4.86E-15	9.99
272.	4.11E-12	1.31E-13	-1.64E-13	-1.40E-14	9.99
280.	4.40E-12	1.35E-13	-7.46E-14	-6.37E-15	9.99
288.	5.07E-12	1.45E-13	-2.16E-13	-1.85E-14	9.99
296.	5.67E-12	1.54E-13	-4.83E-13	-4.13E-14	9.99
304.	7.02E-12	1.71E-13	-1.03E-12	-8.76E-14	9.99
312.	9.06E-12	1.94E-13	-2.35E-12	-2.01E-13	9.99
320.	1.10E-11	2.14E-13	-2.54E-12	-2.17E-13	9.99
328.	1.48E-11	2.48E-13	-4.09E-12	-3.49E-13	9.99
336.	1.67E-11	2.64E-13	-3.84E-12	-3.28E-13	9.99
344.	1.63E-11	2.60E-13	1.03E-12	8.79E-14	2.96
352.	1.54E-11	2.53E-13	3.65E-12	3.12E-13	1.58
360.	1.51E-11	2.50E-13	3.31E-12	2.83E-13	1.69

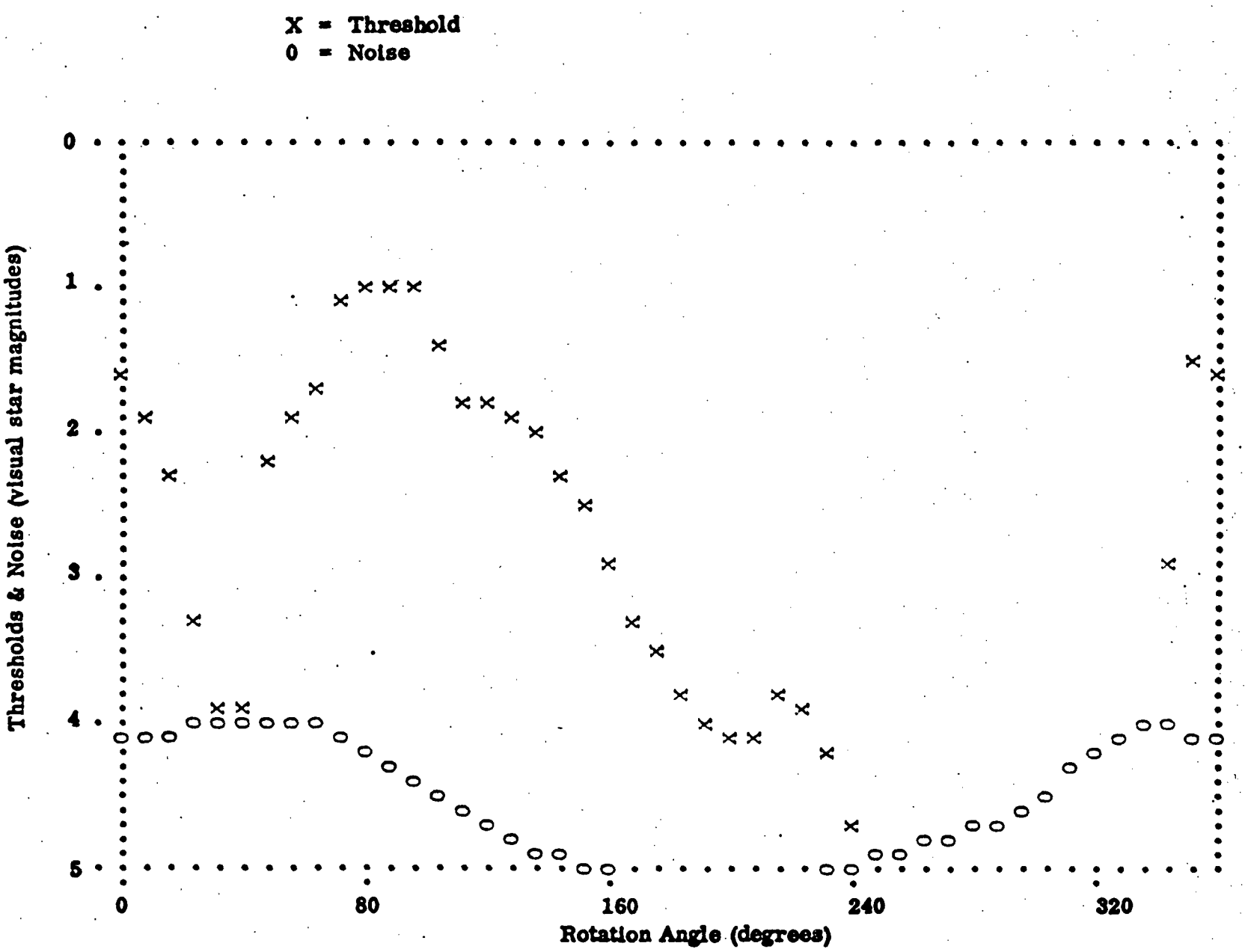
X = Threshold
0 = Noise
Thresholds & Noise (visual star magnitudes)
0
1
2
3
4
5
0
80
160
240
320
Rotation Angle (degrees)

Figure 53.

ANGLE	GAL. LONG.	GAL. LAT.
0.	353.7	-7.4
8.	359.2	-5.8
16.	4.8	-4.7
24.	10.5	-4.1
32.	16.1	-4.0
40.	21.8	-4.5
48.	27.4	-5.5
56.	32.9	-6.9
64.	38.3	-8.8
72.	43.5	-11.2
80.	48.6	-14.0
88.	53.5	-17.2
96.	58.2	-20.7
104.	62.7	-24.5
112.	67.1	-28.5
120.	71.4	-32.8
128.	75.6	-37.4
136.	79.7	-42.1
144.	83.9	-46.9
152.	88.0	-51.9
160.	92.3	-57.0
168.	97.0	-62.1
176.	102.2	-67.4
184.	98.8	-72.6
192.	89.4	-77.8
200.	70.9	-82.6
208.	19.0	-85.5
216.	321.1	-83.1
224.	300.3	-78.4
232.	290.2	-73.3
240.	285.0	-68.0
248.	290.4	-62.8
256.	295.1	-57.6
264.	299.4	-52.5
272.	303.6	-47.6
280.	307.7	-42.7
288.	311.9	-38.0
296.	316.0	-33.4
304.	320.3	-29.1
312.	324.7	-25.0
320.	329.2	-21.1
328.	333.9	-17.6
336.	338.8	-14.4
344.	343.8	-11.6
352.	349.0	-9.1
360.	354.4	-7.1

READY

$FORT THRESH1

SGLNG, SGLAT, GANG, DELTAF, ROLRTE, TCONST, M1,M2,DELTAG .GE. 3.
=311.,34.,-29.,160000.,30.,.047,2.0,1.1,8.

ANGLE DEG.	BACKGROUND AMPS.	RMS NOISE AMPS.	RELATIVE THRESHOLDS AMPS.	W/SQ CM	MAGS.
-0.	2.59E-12	3.64E-13	9.95E-13	8.50E-14	3.00
8.	2.39E-12	3.50E-13	1.05E-12	8.94E-14	2.94
16.	2.27E-12	3.41E-13	9.44E-13	8.07E-14	3.05
24.	2.21E-12	3.36E-13	9.55E-13	8.17E-14	3.04
32.	2.35E-12	3.47E-13	8.99E-13	7.69E-14	3.11
40.	2.38E-12	3.49E-13	9.26E-13	7.91E-14	3.08
48.	2.37E-12	3.48E-13	9.26E-13	7.92E-14	3.08
56.	2.50E-12	3.58E-13	9.35E-13	7.99E-14	3.06
64.	2.67E-12	3.70E-13	9.73E-13	8.32E-14	3.02
72.	2.98E-12	3.90E-13	1.03E-12	8.79E-14	2.96
80.	3.32E-12	4.13E-13	1.01E-12	8.61E-14	2.98
88.	3.90E-12	4.47E-13	1.17E-12	1.00E-13	2.82
96.	4.81E-12	4.96E-13	1.29E-12	1.11E-13	2.71
104.	5.71E-12	5.41E-13	1.48E-12	1.27E-13	2.56
112.	7.02E-12	5.99E-13	1.79E-12	1.53E-13	2.36
120.	7.51E-12	6.20E-13	1.90E-12	1.63E-13	2.29
128.	7.89E-12	6.35E-13	2.03E-12	1.73E-13	2.22
136.	7.55E-12	6.22E-13	1.82E-12	1.55E-13	2.34
144.	8.64E-12	6.65E-13	1.83E-12	1.57E-13	2.33
152.	1.04E-11	7.30E-13	6.87E-13	5.87E-14	3.40
160.	1.94E-11	9.97E-13	2.24E-12	1.92E-13	2.11
168.	2.51E-11	1.13E-12	5.42E-12	4.63E-13	1.16
176.	2.37E-11	1.10E-12	4.69E-12	4.01E-13	1.31
184.	2.43E-11	1.12E-12	4.85E-12	4.15E-13	1.27
192.	2.38E-11	1.10E-12	4.61E-12	3.94E-13	1.33
200.	2.45E-11	1.12E-12	5.05E-12	4.32E-13	1.23
208.	2.33E-11	1.09E-12	4.67E-12	3.99E-13	1.32
216.	2.27E-11	1.08E-12	4.47E-12	3.82E-13	1.36
224.	2.32E-11	1.09E-12	4.21E-12	3.60E-13	1.43
232.	2.47E-11	1.13E-12	4.31E-12	3.69E-13	1.40
240.	2.78E-11	1.19E-12	4.36E-12	3.72E-13	1.39
248.	3.69E-11	1.38E-12	3.96E-12	3.39E-13	1.50
256.	4.56E-11	1.53E-12	5.09E-12	4.35E-13	1.22
264.	3.22E-11	1.28E-12	8.22E-12	7.03E-13	0.70
272.	2.37E-11	1.10E-12	5.97E-12	5.10E-13	1.05
280.	1.59E-11	9.03E-13	4.91E-12	4.20E-13	1.26
288.	1.06E-11	7.38E-13	3.15E-12	2.70E-13	1.74
296.	7.83E-12	6.33E-13	2.35E-12	2.01E-13	2.06
304.	6.84E-12	5.92E-13	2.07E-12	1.77E-13	2.20
312.	5.33E-12	5.23E-13	1.73E-12	1.48E-13	2.39
320.	4.53E-12	4.81E-13	1.57E-12	1.34E-13	2.50
328.	3.85E-12	4.44E-13	1.37E-12	1.17E-13	2.65
336.	3.36E-12	4.15E-13	1.26E-12	1.08E-13	2.74
344.	3.01E-12	3.93E-13	1.14E-12	9.78E-14	2.85
352.	2.71E-12	3.73E-13	1.09E-12	9.33E-14	2.90
360.	2.57E-12	3.63E-13	1.01E-12	8.62E-14	2.98

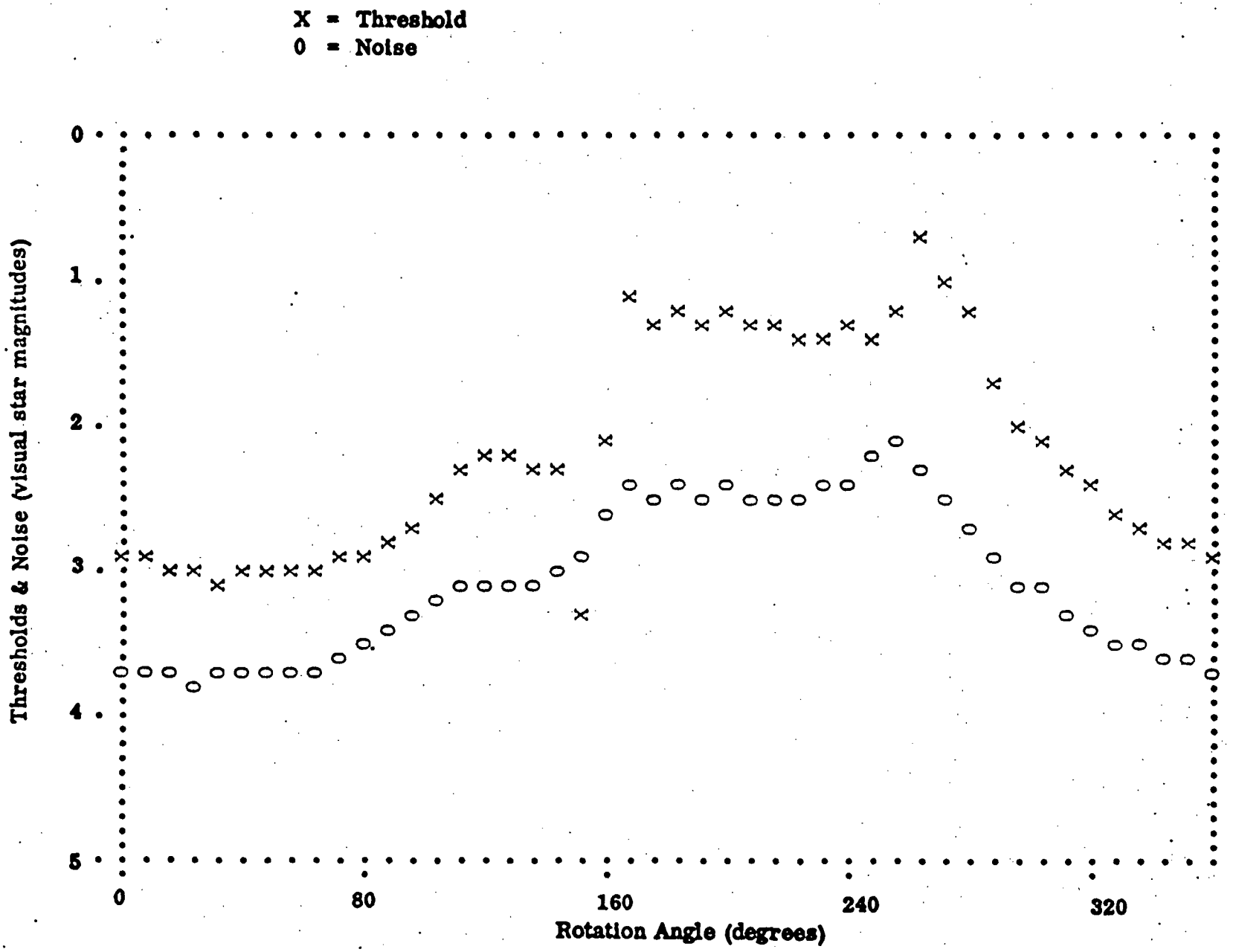
X = Threshold
0 = Noise
Thresholds & Noise (visual star magnitudes)
0
1
2
3
4
5
0
80
160
240
320
Rotation Angle (degrees)

Figure 54.

ANGLE	GAL. LONG.	GAL. LAT.
0.	255.7	65.1
8.	261.1	70.4
16.	272.1	75.1
24.	292.9	78.3
32.	322.2	78.8
40.	345.8	76.1
48.	358.8	71.6
56.	5.3	66.5
64.	8.4	61.0
72.	9.5	55.3
80.	9.6	49.7
88.	8.8	44.0
96.	7.5	38.4
104.	5.7	33.0
112.	3.5	27.6
120.	0.9	22.4
128.	358.0	17.5
136.	354.8	12.7
144.	351.2	8.3
152.	347.3	4.2
160.	343.1	0.4
168.	338.4	-2.9
176.	333.5	-5.7
184.	328.3	-7.9
192.	322.8	-9.6
200.	317.1	-10.6
208.	311.4	-11.0
216.	305.6	-10.7
224.	299.9	-9.8
232.	294.4	-8.2
240.	289.2	-6.0
248.	284.2	-3.2
256.	279.5	-0.0
264.	275.2	3.7
272.	271.3	7.7
280.	267.6	12.1
288.	264.4	16.8
296.	261.4	21.8
304.	258.8	26.9
312.	256.6	32.3
320.	254.7	37.7
328.	253.3	43.3
336.	252.5	48.9
344.	252.4	54.6
352.	253.4	60.2
360.	256.2	65.8

$FORT THRESH1

SGLNG, SGLAT, GANG, DELTAF, ROLRTE, TCONST, M1,M2,DELTAG .GE. 3.
=311.,34.,-29.,13000.,30.,.5,2.0,1.1,8.

ANGLE DEG.	BACKGROUND AMPS.	RMS NOISE AMPS.	RELATIVE THRESHOLDS AMPS.	W/SQ CM	MAGS.
0.	2.59E-12	1.04E-13	8.99E-13	7.68E-14	3.11
8.	2.39E-12	9.97E-14	7.76E-13	6.64E-14	3.27
16.	2.27E-12	9.71E-14	7.54E-13	6.44E-14	3.30
24.	2.21E-12	9.59E-14	5.93E-13	5.07E-14	3.56
32.	2.35E-12	9.89E-14	3.12E-13	2.67E-14	4.26
40.	2.38E-12	9.95E-14	2.43E-13	2.08E-14	4.53
48.	2.37E-12	9.93E-14	4.19E-13	3.58E-14	3.94
56.	2.50E-12	1.02E-13	3.28E-13	2.80E-14	4.20
64.	2.67E-12	1.05E-13	1.55E-13	1.33E-14	5.02
72.	2.98E-12	1.11E-13	2.01E-14	1.71E-15	7.24
80.	3.32E-12	1.18E-13	-1.32E-13	-1.13E-14	9.99
88.	3.90E-12	1.27E-13	-3.39E-13	-2.90E-14	9.99
96.	4.81E-12	1.41E-13	-7.89E-13	-6.75E-14	9.99
104.	5.71E-12	1.54E-13	-1.03E-12	-8.81E-14	9.99
112.	7.02E-12	1.71E-13	-1.26E-12	-1.08E-13	9.99
120.	7.51E-12	1.77E-13	-7.51E-13	-6.42E-14	9.99
128.	7.89E-12	1.81E-13	2.68E-13	2.29E-14	4.42
136.	7.55E-12	1.77E-13	1.13E-12	9.63E-14	2.86
144.	8.64E-12	1.90E-13	4.32E-13	3.69E-14	3.90
152.	1.04E-11	2.08E-13	-1.57E-12	-1.35E-13	9.99
160.	1.94E-11	2.84E-13	-9.09E-12	-7.77E-13	9.99
168.	2.51E-11	3.23E-13	-1.17E-11	-9.98E-13	9.99
176.	2.37E-11	3.14E-13	-5.57E-13	-4.76E-14	9.99
184.	2.43E-11	3.18E-13	3.48E-12	2.98E-13	1.64
192.	2.38E-11	3.15E-13	2.88E-12	2.46E-13	1.84
200.	2.45E-11	3.19E-13	2.71E-12	2.31E-13	1.91
208.	2.33E-11	3.11E-13	3.48E-12	2.98E-13	1.64
216.	2.27E-11	3.07E-13	4.67E-12	4.00E-13	1.32
224.	2.32E-11	3.11E-13	2.98E-12	2.54E-13	1.81
232.	2.47E-11	3.21E-13	8.56E-13	7.32E-14	3.16
240.	2.78E-11	3.40E-13	-1.46E-12	-1.25E-13	9.99
248.	3.69E-11	3.92E-13	-8.63E-12	-7.37E-13	9.99
256.	4.56E-11	4.35E-13	-1.36E-11	-1.16E-12	9.99
264.	3.22E-11	3.66E-13	1.10E-11	9.36E-13	0.39
272.	2.37E-11	3.14E-13	2.39E-11	2.05E-12	-0.46
280.	1.59E-11	2.58E-13	1.83E-11	1.56E-12	-0.17
288.	1.06E-11	2.10E-13	1.49E-11	1.27E-12	0.06
296.	7.83E-12	1.81E-13	8.99E-12	7.68E-13	0.60
304.	6.84E-12	1.69E-13	4.75E-12	4.06E-13	1.30
312.	5.33E-12	1.49E-13	3.37E-12	2.88E-13	1.67
320.	4.53E-12	1.37E-13	3.13E-12	2.67E-13	1.75
328.	3.85E-12	1.27E-13	2.16E-12	1.85E-13	2.15
336.	3.36E-12	1.18E-13	1.74E-12	1.49E-13	2.39
344.	3.01E-12	1.12E-13	1.37E-12	1.17E-13	2.65
352.	2.71E-12	1.06E-13	1.13E-12	9.69E-14	2.86
360.	2.57E-12	1.03E-13	9.14E-13	7.81E-14	3.09

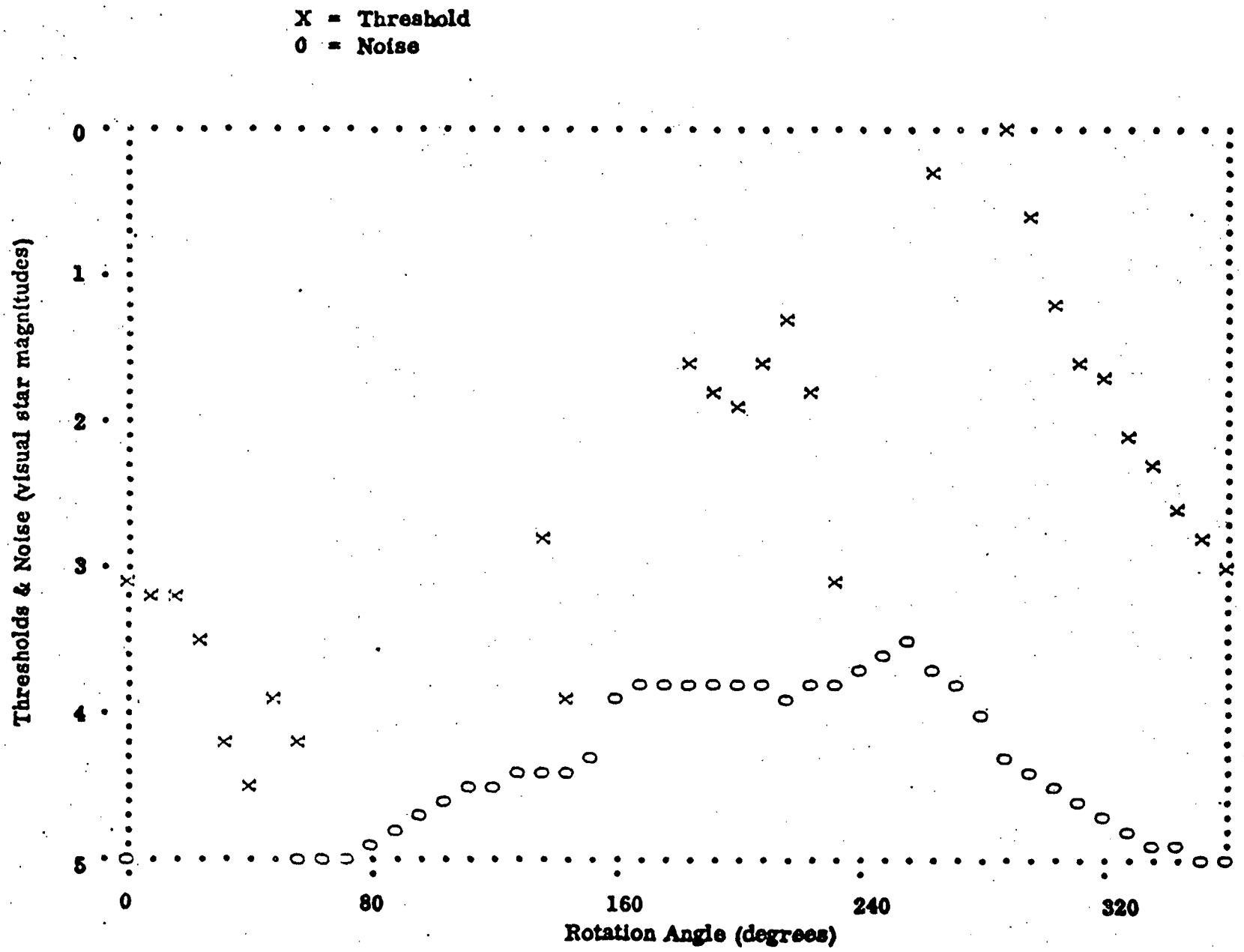
X = Threshold
0 = Noise
Thresholds & Noise (visual star magnitudes)
0
1
2
3
4
5
0
80
160
240
320
Rotation Angle (degrees)

Figure 55.

ANGLE	GAL. LONG.	GAL. LAT.
0.	255.7	65.1
8.	261.1	70.4
16.	272.1	75.1
24.	292.9	78.3
32.	322.2	78.8
40.	345.8	76.1
48.	358.8	71.6
56.	5.3	66.5
64.	8.4	61.0
72.	9.5	55.3
80.	9.6	49.7
88.	8.8	44.0
96.	7.5	38.4
104.	5.7	33.0
112.	3.5	27.6
120.	0.9	22.4
128.	358.0	17.5
136.	354.8	12.7
144.	351.2	8.3
152.	347.3	4.2
160.	343.1	0.4
168.	338.4	-2.9
176.	333.5	-5.7
184.	328.3	-7.9
192.	322.8	-9.6
200.	317.1	-10.6
208.	311.4	-11.0
216.	305.6	-10.7
224.	299.9	-9.8
232.	294.4	-8.2
240.	289.2	-6.0
248.	284.2	-3.2
256.	279.5	-0.0
264.	275.2	3.7
272.	271.3	7.7
280.	267.6	12.1
288.	264.4	16.8
296.	261.4	21.8
304.	258.8	26.9
312.	256.6	32.3
320.	254.7	37.7
328.	253.3	43.3
336.	252.5	48.9
344.	252.4	54.6
352.	253.4	60.2
360.	256.2	65.8

C. HAND CALCULATION OF STAR BACKGROUNDS AND THRESHOLDS

The graphical results presented in the previous section were first calculated by hand and are presented below. In order to simplify the calculations, a rather crude approximation to the actual star distribution was assumed. The model was crude in the sense that a mean star background was determined for a given galactic latitude and this value was then used for all galactic longitudes, as well as positive and negative values of that latitude (Allen, 1964). Thus, the model assumed that the star background was independent of galactic longitude and that $\pm$ values of a given galactic latitude presented the same background. The more exact sky map shown in Figure 48 of the report shows that these assumptions would introduce inaccuracies in the analyses, e.g., rapid or local variations in background would not be considered.

Figures 56, 57, and 58 depict the absolute background and threshold variation which may be encountered at three points (same as in Section B of this appendix). As is indicated on the figures, the threshold was calculated for three values of the active filter multiplication factor (1.1, 1.2 and 1.3). Also, the instantaneous threshold was determined from the background which was presented to the instrument 0.5 sec earlier. Each cycle was arbitrarily chosen to begin (i.e., $t = 0$) when the instrument's optical axis crossed the ecliptic; the resulting galactic latitude variation is shown to aid in determining the abolute point of observation.

Figures 59, 61, and 63 illustrate the relative threshold variation corresponding to the cases discussed above. This relative threshold was found by obtaining the difference between the absolute threshold and the absolute background (see Figures 56, 57, and 58) and converting it to a visual magnitude. Regions where the background exceeds the threshold are denoted by vertical lines. Finally, stars which exceed the threshold, and can be used for calibration purposes, are also shown. Following each of the latter three curves, the computerized equivalent (from Section B) for the one case of active filter multiplication constant equal to 1.1 is shown for comparison (Figures 60, 62, and 64).

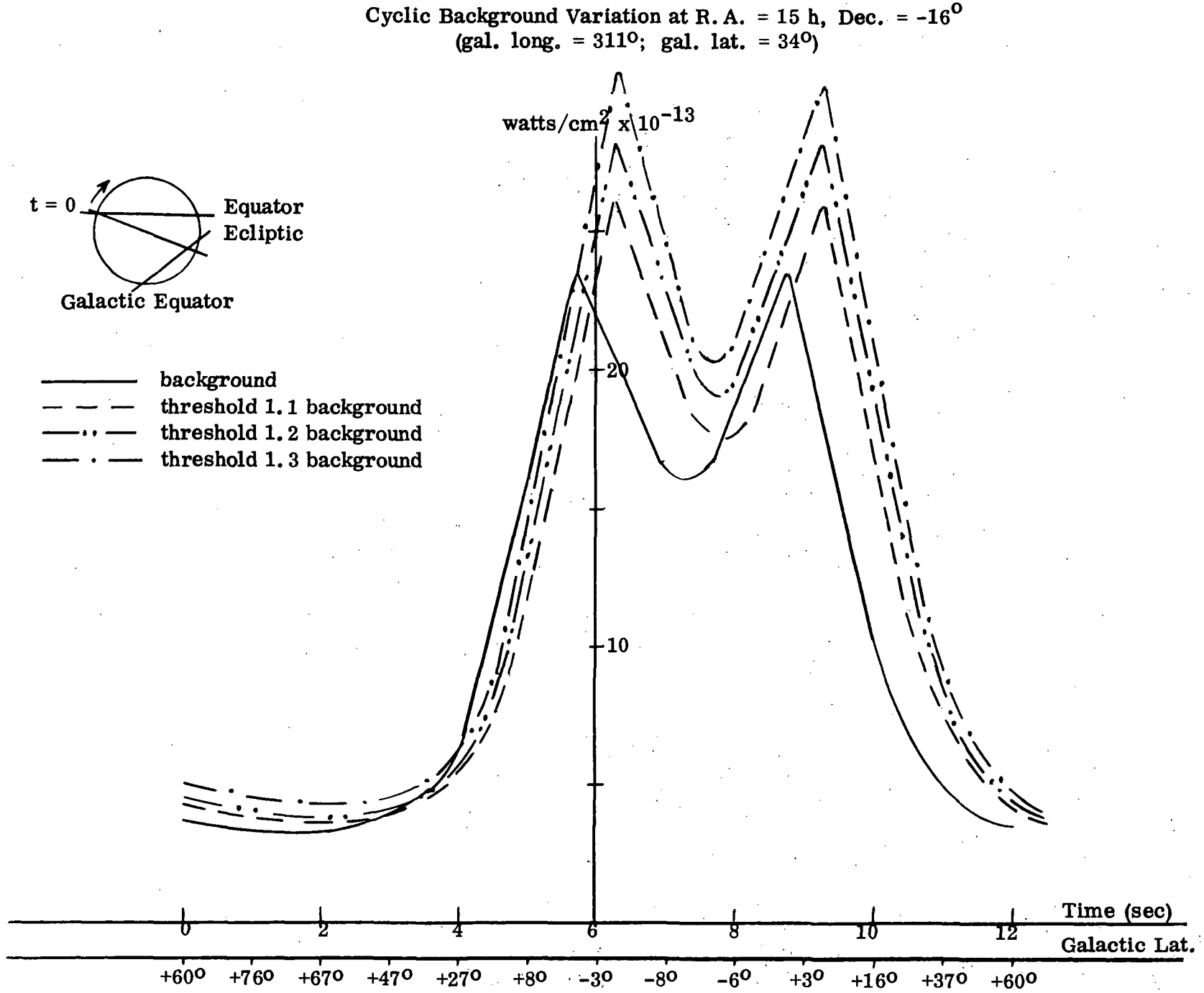
Cyclic Background Variation at R. A. = 15 h, Dec. = -16°
(gal. long. = 311°; gal. lat. = 34°)
watts/cm² x 10⁻¹³
t = 0
Equator
Ecliptic
Galactic Equator
background
threshold 1.1 background
threshold 1.2 background
threshold 1.3 background
20
10
0
2
4
6
8
10
12
Time (sec)
Galactic Lat.
+60°
+76°
+67°
+47°
+27°
+8°
-3°
-8°
-6°
+3°
+16°
+37°
+60°

Figure 56

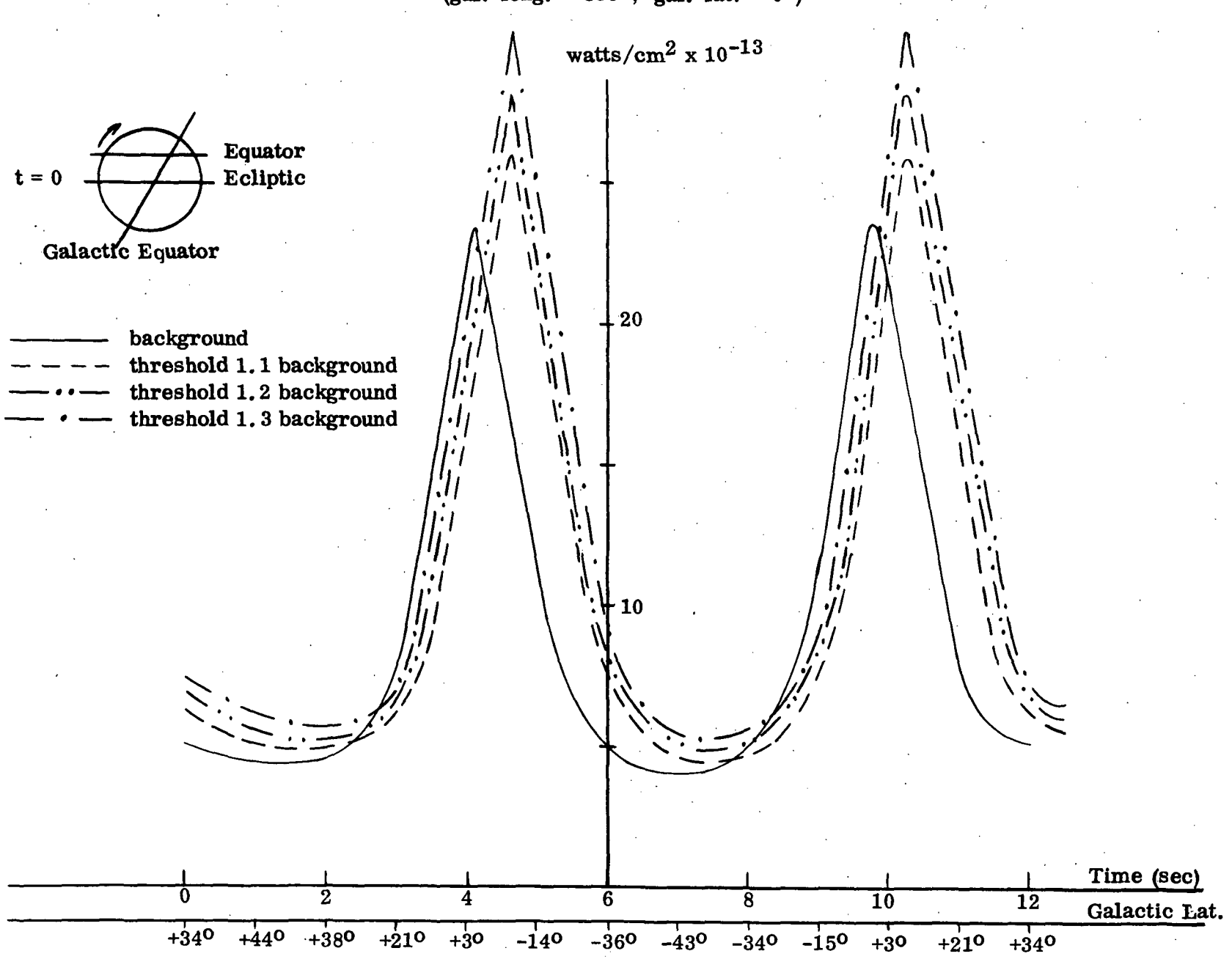
(gal. long. = 333°; gal. lat. = 0°)
watts/cm² x 10⁻¹³
20
10
t = 0
Equator
Ecliptic
Galactic Equator
background
threshold 1.1 background
threshold 1.2 background
threshold 1.3 background
Time (sec)
0
2
4
6
8
10
12
Galactic Lat.
+34°
+44°
+38°
+21°
+3°
-14°
-36°
-43°
-34°
-15°
+3°
+21°
+34°

Figure 57.

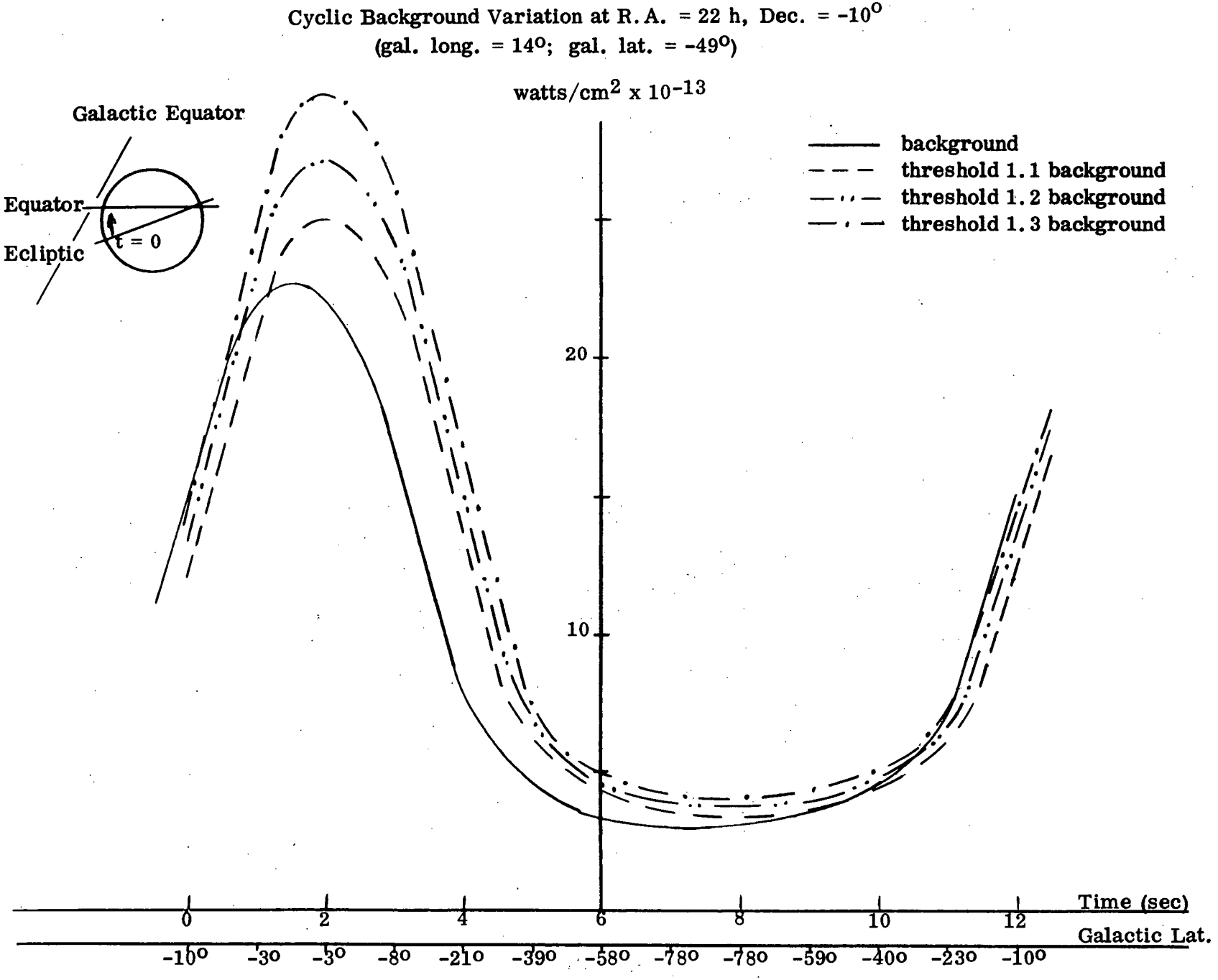
Cyclic Background Variation at R.A. = 22 h, Dec. = -10°
(gal. long. = 14°; gal. lat. = -49°)
watts/cm² x 10⁻¹³
Galactic Equator
Equator
Ecliptic
t = 0
background
threshold 1.1 background
threshold 1.2 background
threshold 1.3 background
20
10
0
2
4
6
8
10
12
Time (sec)
-10°
-3°
-3°
-8°
-21°
-39°
-58°
-78°
-78°
-59°
-40°
-23°
-10°
Galactic Lat.

Figure 58.

Cyclic Threshold Variation at R. A. = 15 h, Dec. = -16°
(gal. long. = 311°; gal. lat. = 34°)

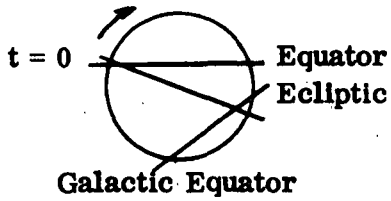

— — — threshold 1.1 background
— · · — threshold 1.2 background
— · — threshold 1.3 background

Apparent Visual Magnitude, m_v

-1
0
+1
+2
+3
+4
+5

(Arcturus)
(Alphecca)
(ηBoo)
(ε Vir)
(αCen)
(β Cen)

Background Above Threshold

0 2 4 6 8 10 12 Time (sec)

Galactic Lat.

+60° +76° +67° +47° +27° +8° -3° -8° -6° +3° +16° +37° +60°

Figure 59.

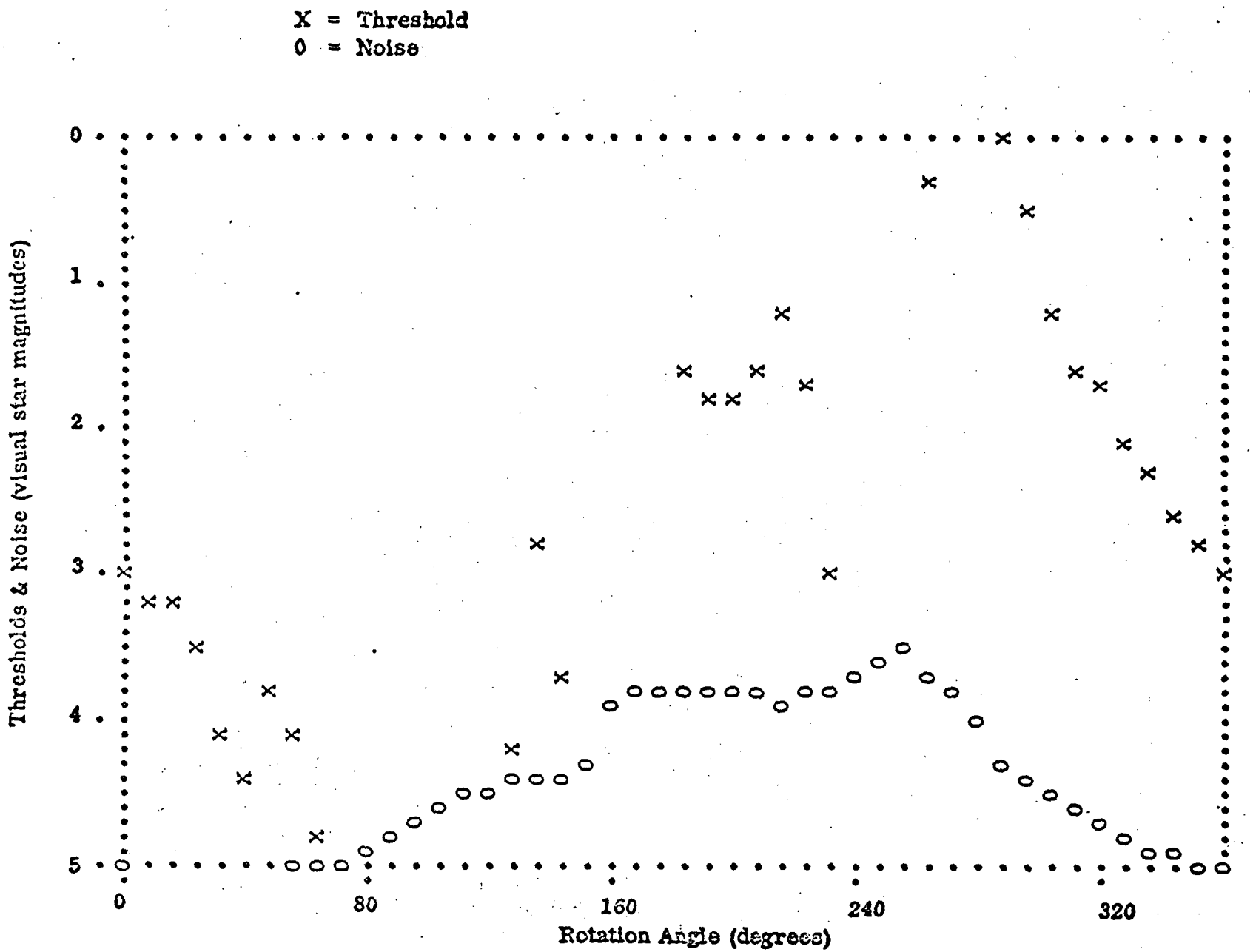
X = Threshold
0 = Noise
Thresholds & Noise (visual star magnitudes)
0
1
2
3
4
5
0
80
160
240
320
Rotation Angle (degrees)

Figure 60.

Cyclic Threshold Variation at R. A. = 18 h, Dec. = -20°
(gal. long. = 333°; gal. lat. = 0°)

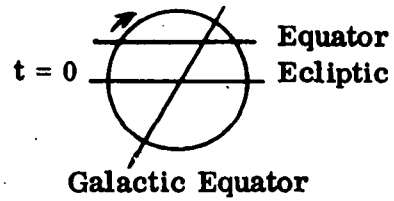

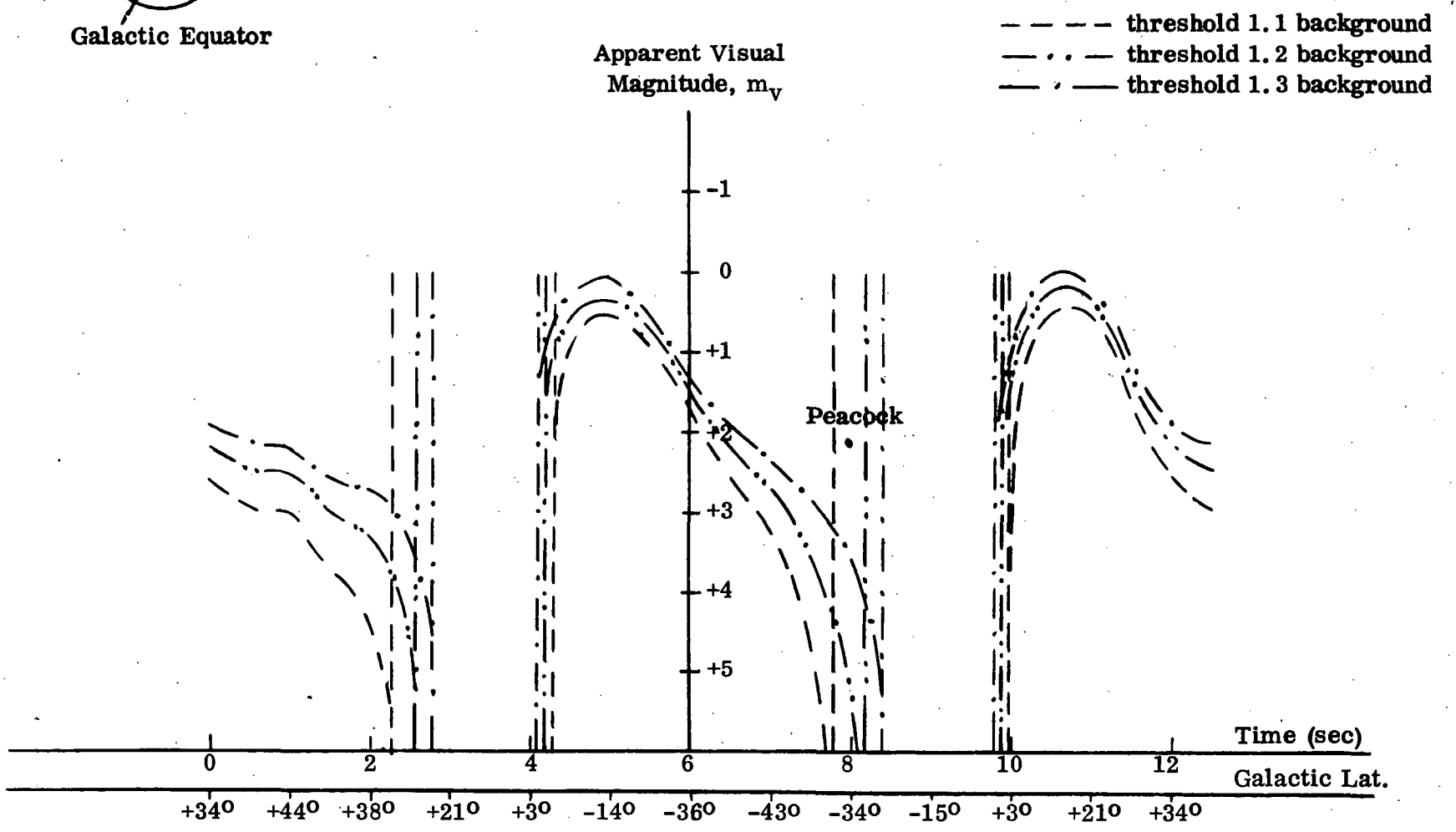

Figure 61.

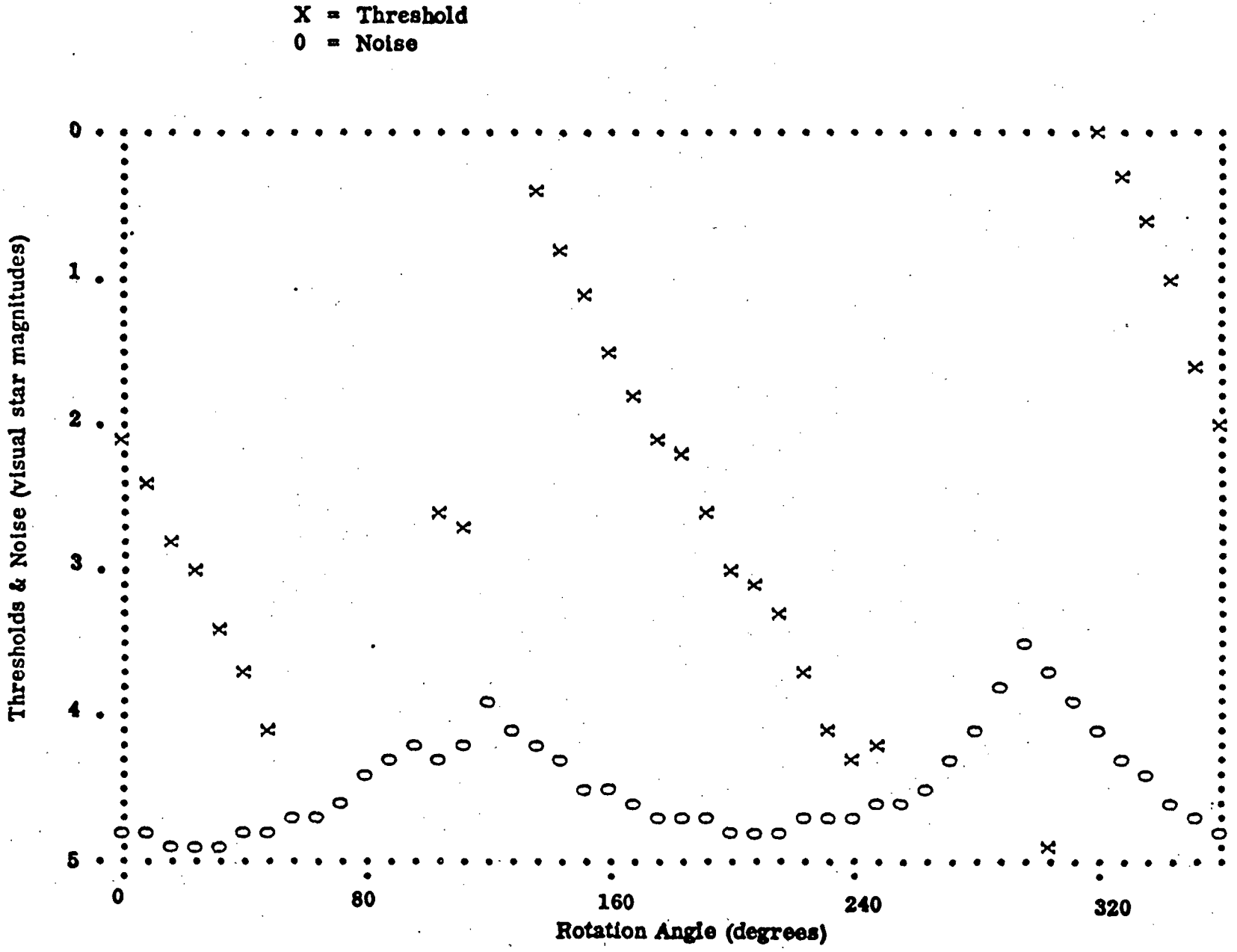
X = Threshold
0 = Noise
Thresholds & Noise (visual star magnitudes)
0
1
2
3
4
5
0
80
160
240
320
Rotation Angle (degrees)

Figure 62.

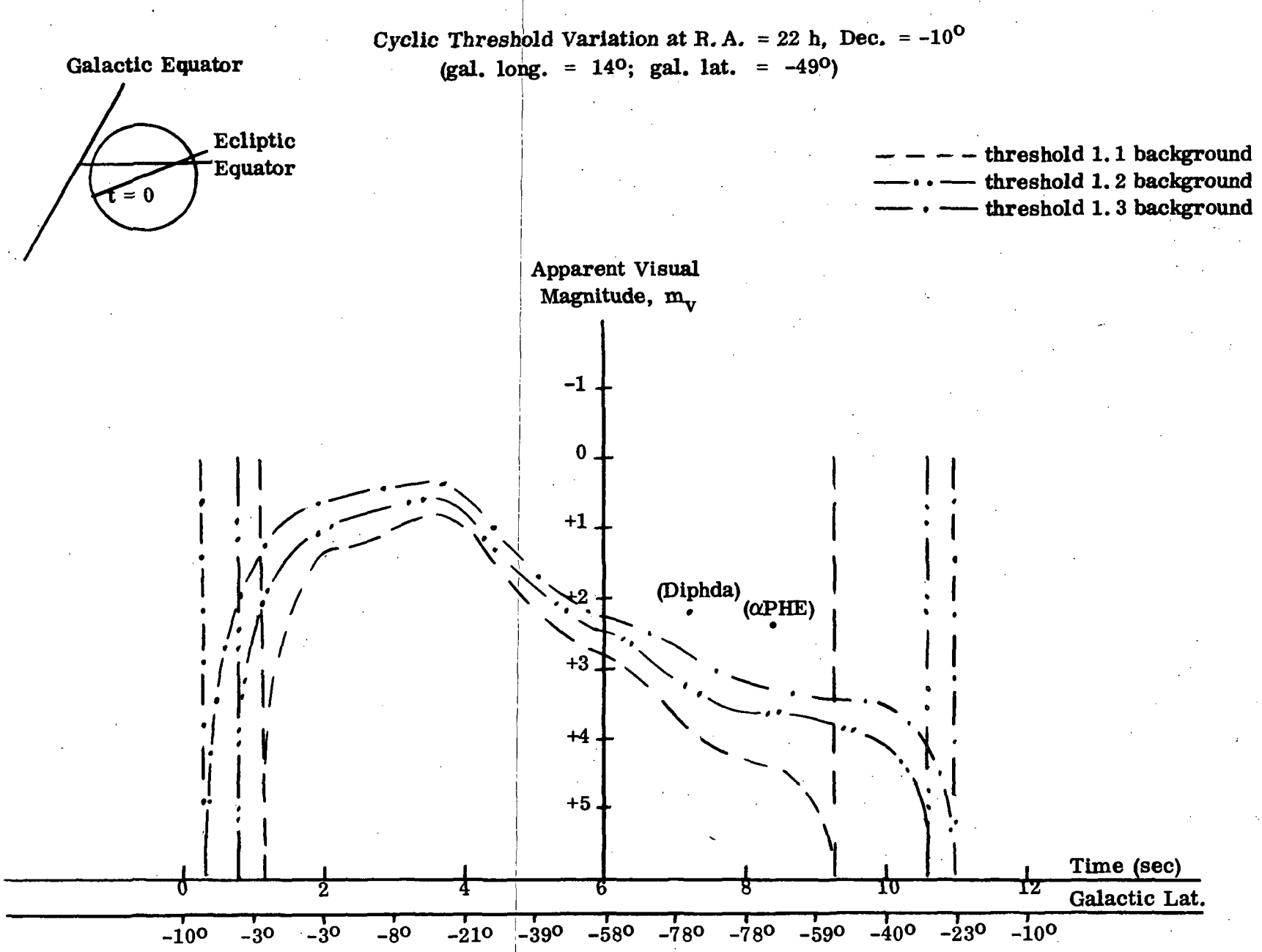
Cyclic Threshold Variation at R. A. = 22 h, Dec. = -10°
(gal. long. = 14°; gal. lat. = -49°)
Galactic Equator
Ecliptic
Equator
t = 0
threshold 1.1 background
threshold 1.2 background
threshold 1.3 background
Apparent Visual
Magnitude, m_v
-1
0
+1
+2
+3
+4
+5
(Diphda)
(αPHE)
Time (sec)
0
2
4
6
8
10
12
Galactic Lat.
-10°
-3°
-3°
-8°
-21°
-39°
-58°
-78°
-78°
-59°
-40°
-23°
-10°

Figure 63.

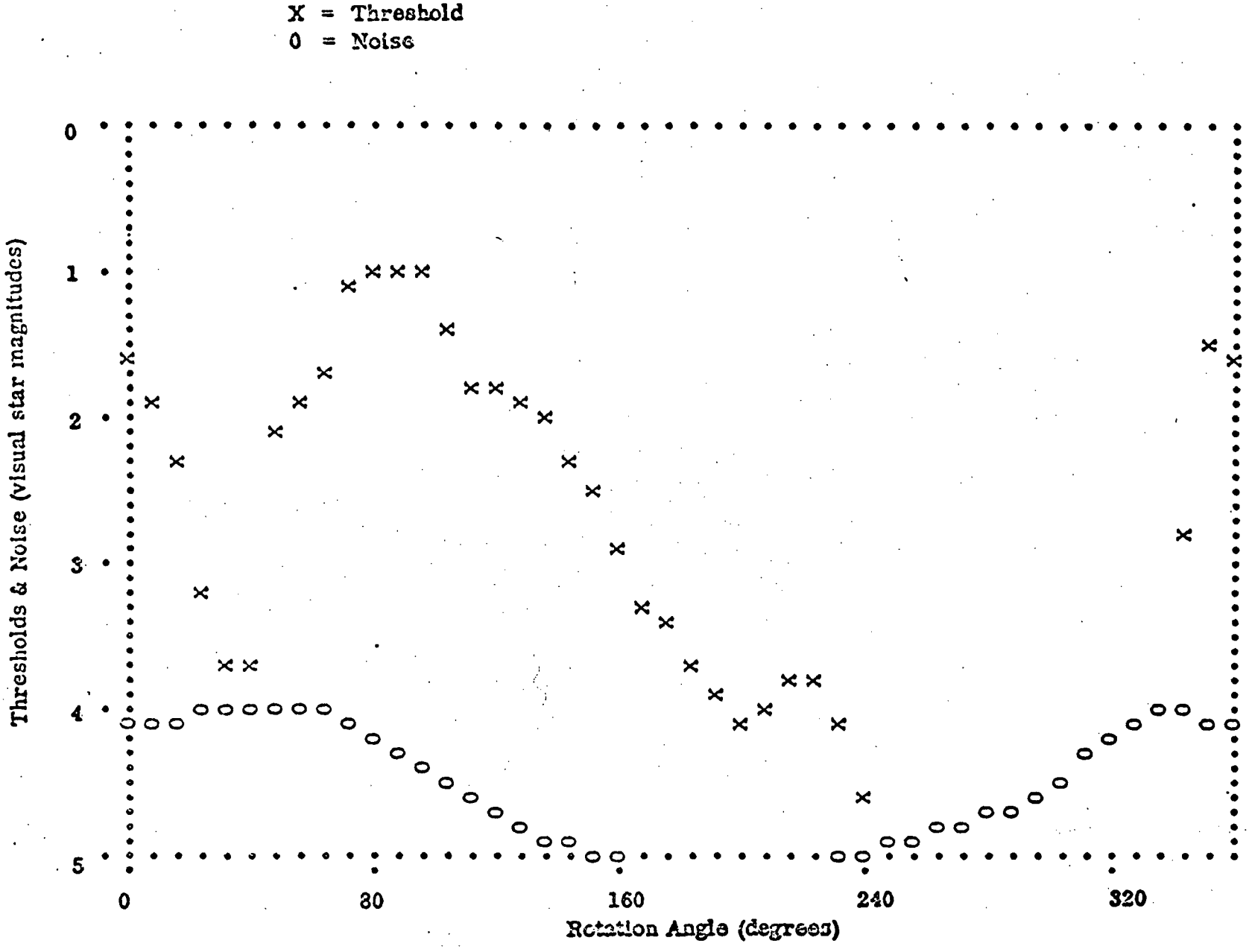
X = Threshold
0 = Noise
Thresholds & Noise (visual star magnitudes)
0
1
2
3
4
5
0
80
160
240
320
Rotation Angle (degrees)

Figure 64.

REFERENCES

1. Allen, C. W., Astrophysical Quantities (U. of London Press, London, 1964).

2. Chandra, S., et al, 1970, Meteoroid Hazard In Deep Space, Final Report on Contract NAS 9-8104 to Manned Spacecraft Center, Houston, Texas, Space Sciences Laboratory, General Electric Company.

3. Grenda, R., Neste, S., Soberman, R. K., 1969, COSPAR Space Research IX, pp. 95-101, North-Holland Publishing Company, Amsterdam.

4. McCracken, D. C., "A Guide to FORTRAN IV Programming" (John Wiley & Sons, New York, 1965).

5. Kuiper, G. P., 1961, "Limits of Completeness", Planets and Satellites, ed. by G. P. Kuiper and B. M. Middlehurst, (U. of Chicago Press, 580-590).

6. Meteoroid Environmental Model-1969: NASA Space Vehicle Design Criteria, NASA SP-8013.

7. Newkirk, G., Jr., 1967, The Optical Environment of Manned Spacecraft, Plan. and Space Science., Vol. 15, pp. 1267-1285.

8. Roach, F. E. and Megill, L. R., "Integrated Starlight Over the Sky", Astrophys. J. 133, 228-242 (1961).

9. Space Defense Center Satellite Catalog (Space Objects Identification Catalog); Also referred to as Space Track Data Base, HQNORAD, NOSD. Obtained from Ent AFB.

10. Watson, F. G., "Reflectivity and Color of Meteorites", Proc. Nat. Acad. of Science 24, 532-537 (1938).